PAVEMENT RESEARCH
at the
WASHINGTON STATE UNIVERSITY
TEST TRACK

VOLUME FOUR

EXPERIMENTAL RING NO. 4: A STUDY OF UNTREATED, SAND ASPHALT, AND ASPHALT CONCRETE BASES

Report to the Washington Department of Highways
on Research Project Y-993

by

Milan Krukar and John C. Cook

Highway Research Section
College of Engineering Research Division
Washington State University
Pullman, Washington
August 1970

In Cooperation with
U. S. Department of Transportation
Federal Highway Administration

The Washington State Highway Commission
Department of Highways
and
The Asphalt Institute

(Highway Research Section Publication H-31)

ACKNOWLEDGMENTS

The Highway Research staff wishes to thank the Washington Highway Department for their financial and technical support. There were many Highway Department staff personnel from Olympia who helped; particularly the following: Carl E. Minor, then Assistant Director for Planning and Research; Roger V. LeClerc, Materials Engineer; Mrs. Willa Mylroie, Special Assignments and Research Engineer; and Tom R. Marshall, Special Assignments Engineer. Art Sinclair, Materials Engineer from District 6, Spokane, was also involved in the project.

Continual financial and technical support was given the project by the Asphalt Institute, College Park, Maryland. Particular acknowledgment and thanks are given to the following individuals of that organization: J. E. Buchanan, then President; John M. Griffith, Director of Research and Development; and R. Ian Kingham, Staff Engineer. Provision of funds and expert technical knowledge from men such as these has helped immensely.

Appreciation is recorded to Ron Trolle, Sales Engineer with the Chevron Asphalt Company, for continued help, interest and advice on the project.

Thanks go to the secretaries, Judy Benes and Annette Waylett, who helped in typing and editing the rough drafts. The following Washington State University students contributed to the preparation of this report by helping with the tabulation and evaluation of the data and with drafting: Ted Rees, John Harrison, Al Badal, Dale Barr, Don Averill and Chuck Cooper. Some of the latter drawings were done by Louis E. Krukar.

Last but not least, a word of appreciation to Jack E. Schaefer, Leadman, who ran the test track and was responsible for construction inspection, maintenance, and data accumulation, to Bob Bureau of the Electrical Engineering Section who worked with instrumentation, and to the personnel in the College of Engineering Research Division photography laboratory who were responsible for the photographs.

The staff also wishes to put on record the excellent cooperation that was received from the contractor, United Paving Company, Inc. Dave Shardlow, United Paving plant superintendent, and his crew were very helpful.

TABLE OF CONTENTS

	Page
ACKNOWLEDGMENTS	ii
LIST OF TABLES	v
LIST OF FIGURES	vii
ABSTRACT	xiii
INTRODUCTION	1
EXPERIMENTAL DESIGN	2
Materials	3
Subgrade	3
Crushed Surfacing Top Course	7
Sand	7
Asphalt Concrete Base Class "F" Aggregate	11
Asphalt Concrete Class "B" Aggregate	13
Construction	13
Pre-Conditioning	13
Subgrade	16
Crushed Surfacing Top Course Base--Untreated (Sections 9-12)	19
Sand-Asphalt Bases (Sections 1-4)	19
Class "F" Asphalt Concrete Bases (Sections 5-8)	21
Class "B" Asphalt Concrete Wearing Course (All Sections)	23
Shoulders	25
Comments	25
Instrumentation	25
Measurement of Moisture	28
Temperature Measurements	29
Iron-constantan thermocouples	29
Thermograph	29
Stress Measurements	30
WSU pressure cells	30
WSU strain gage pressure cells	30
Strain Measurements	30
Strain gages (subgrade)	30
Strain gages (bases and surfaces)	31
Deflection Measurements	32
Dynamic deflection measurements	32
Rebound deflection measurements	32

Page

Read-Out Equipment 32

PERFORMANCE OF TEST RING #4 33

Testing Periods 33
Testing Conditions 34

Design Thickness 34
Speed 34
Environmental Conditions 37

Experimental Results 38

Section Failures 38
Fall period (1968) 38
Spring period (1969) 38
Failure pattern 43
Discussion of Failures 46

Load Response Characteristics 100

Temperature Variables 100
Moisture Contents 100
Static Deflections 101
Dynamic Deflections 105
Strain Gage Data 120
Stress Data 146

Discussion of Results 160
Comparison With Other Rings 166

CONCLUSIONS 167

Major Conclusions 167
Minor Conclusions 168

PRACTICAL IMPLICATIONS FROM THE TEST RINGS TO DATE 169

REFERENCES 172

APPENDIX A 176

APPENDIX B 178

LIST OF TABLES

Table		Page
1	Types, Sections and Thicknesses of Ring #4	4
2	Optimum Density and Moisture for Subgrade Material	8
3	Soil Characteristics and Classification	8
4	California Bearing Ratio (CBR) Test on Palouse Silt Subgrade Soil	9
5	Final Subgrade Densities and Moisture Content	20
6	Table of Base Course Densities, Ring #4	20
7	Mix Design Requirements	22
8	Location of Instruments Along Center Line	27
9	Depth of LVDT Holes	32
10	Core Thicknesses and Densities	35
11	Weekly Ambient Temperatures and Precipitation, Ring #4, 1968-69	39
12	Section Condition Progress Report	41
13	Ring #4 Pavement Performance Summary, Fall and Spring Periods	42
14	Typical Benkelman Beam Rebound Measurements-- Thin Sections	47
15	Moisture Content After Breakup of Untreated Base, Fall 1968	89
16	Spring Moisture Contents in the Untreated Bases	89
17	Crushed Surfacing Top Course Sizes After Failure	91
18	Moisture Contents in the Subgrade & Degree of Saturation . .	92
19	Permanent Pavement Deformation Depths After 177,501 Wheel Load Applications	95
20	Permanent Pavement Deformation Depths After 247,128 Wheel Load Applications	96

Table		Page
21	Pavement Failure Span (PFS)	98
22	Equivalent Thicknesses	99
23	Summary of Fall 1968 Benkelman Beam Rebound Deflections, Ring #4	103
24	Summary of Spring 1969 Benkelman Beam Rebound Deflections, Ring #4	104
25	Summary of Summer 1969 Benkelman Beam Rebound Deflections, Ring #4	106
26	Summary of LVDT Deflection Maximum Measurements, Ring #4	107
27	Summary of Maximum Longitudinal and Transverse Strain Gage Measurements, Ring #4	128
28	Summary of Maximum Measured Vertical Stresses	153
29	Equivalencies Based on Rings #2, #3, and #4	165
30	Equivalencies in Terms of UTB	165

LIST OF FIGURES

Figure		Page
1	Permanent Structures and Pavement Sections, Test Ring No. 4	4
2	Schematic Profile for Ring #4	5
3	Typical Cross-Section of Pavement Structure	6
4	Density - Moisture Curves	8
5	Combined Gradation Curve for Crushed Surfacing Top Course, Untreated Sections 9-12 and Shoulders	10
6	Maximum Density Curve, Crushed Surfacing Top Course	10
7	Gradation Curve for Sand-Asphalt Base Sections 1-4	12
8	Gradation Curve for the Class "F" Asphalt Concrete Base Aggregate, ACB Sections 5-8	12
9	Combined Gradation Curve for Asphalt Concrete Class "B" Aggregate, All Sections	14
10	Depth and Extent of the Excavation for Removal of the "Weak" Area by Sections 11 and 12	15
11	Huber Blade Dozer Spreading the Subgrade Soil	17
12	Spreading the Silt by Hand and Compacting with a Pneumatic Rubber-Tired Roller	17
13	Hand Working and Screeding of the Subgrade to Final Elevation by the Contractor's Crew	18
14	Section 4, Sand-Asphalt Base	18
15	Surface Transverse Tension Cracks on Top of the Sand-Asphalt Base in Section 4	24
16	Appearance of the Surface of the Class "F" Asphalt Concrete Base After Compaction	24
17	Instrumentation for Section 7	26
18	Speed Versus Time (Expressed in Wheel Load Repetitions)	36
19	Appearance of Section 9 After 16,641 Wheel Loads	48

Figure		Page
20	Overall Appearance of Section 9 at "Ultimate Failure" After 36,681 Wheel Loads	48
21	Close-Up View of the Failed Area of Section 9 After 36,681 Wheel Loads	49
22	Overall View of Section 10 After 82,470 Wheel Loads	50
23	Close-Up View of the Cracks Around LVDT Gage #7 After 82,470 Wheel Loads in Section 10	51
24	"Ultimate Failure" in Half of Section 10 at 104,187 Wheel Loads	51
25	View of Section 10 at 143,370 Wheel Loads After Test Track Closed for Winter	52
26	Overall View of the Extent of Transverse Cracks in Section 11 After 82,470 Wheel Loads	53
27	Permanent Deformation of About 3/4 Inches in Section 11 After 104,187 Wheel Loads	54
28	Appearance of Section 11 Just After the Test Track Was Closed for the Winter at 143,370 Wheel Loads	54
29	Overall View of Section 12 Showing the Extent of Cracking After 82,470 Wheel Loads	55
30	Close-Up View of Section 12	55
31	Appearance of Section 12 After 104,187 Wheel Loads	56
32	Overall View of Section 12 After End of Fall Testing Period After 143,370 Wheel Loads	56
33	Close-Up View of Section 12 After 143,370 Wheel Loads	57
34	Permanent Settlement of Section 12 After 211,065 Wheel Loads	57
35	Final Appearance of Section 12 After 247,128 Wheel Loads	58
36	Transverse Cracks Around Construction Joint in Section 5 After 82,470 Wheel Loads	58
37	Close-Up View of Section 5 After 143,370 Wheel Loads	59
38	Appearance of Section 5 After 143,370 Wheel Loads	59
39	Close-Up View of Transverse Cracks in Section 5 at 143,370 Wheel Loads	60
40	Overall View of "Ultimate Failure" in Section 5 After 144,660 Wheel Loads	60

Figure

Page

41 Close-Up View of the "Ultimate Failure" in Section 5 61

42 Continued Failure of Asphalt Concrete Overlay in Section 5 After 170,700 Wheel Loads 61

43 Appearance of Section 1 After 143,370 Wheel Loads 62

44 Continued Permanent Deformation in Section 1 After 146,265 Wheel Loads 62

45 Close-Up View of the Transverse Cracks in Section 1 After 146,265 Wheel Loads 63

46 Permanent Deformation of Section 1 After 154,170 Wheel Loads . 63

47 Close-Up View of Cracks in Section 1 After 154,170 Wheel Loads 64

48 "Ultimate Failure" Due to Punching Shear in Section 1 After 157,020 Wheel Loads 64

49 Close-Up View of Section 1 at "Ultimate Failure" 65

50 Appearance of Section 6 After 143,370 Wheel Loads 65

51 Appearance of Section 6 After 157,473 Wheel Loads 66

52 Close-Up View of Section 6 After 157,473 Wheel Loads 66

53 Continued Deterioration of Section 6 After 158,031 Wheel Loads 67

54 Close-Up View of Section 6 After 158,031 Wheel Loads 67

55 "Ultimate Failure" at Section 6 at 158,235 Wheel Loads 68

56 Appearance of Section 2 Prior to Resumption of Testing in Spring at 143,370 Wheel Loads 68

57 Failure in the Transition Zone Between Sections 1 and 2 at 158,031 Wheel Loads 69

58 Continued Deterioration of the Transition Zone Between Sections 1 and 2 at 158,235 Wheel Loads 69

59 Close-Up of the Permanent Deformation in Section 2 After 158,235 Wheel Loads 70

60 Continued Deformation of Section 2 at 162,774 Wheel Loads . . 70

61 Appearance of Section 2 at "Ultimate Failure" After 164,790 Wheel Loads 71

Figure		Page
62	Appearance of the First Lift of SAB in Section 2	72
63	Appearance of Area of Section 2 Nearest Section 3 After 164,790 Wheel Loads	73
64	Excavation of Section 2 Showing First Layer of SAB	73
65	Appearance of Section 7 at 143,370 Wheel Loads Prior to Resumption of Testing in the Spring	74
66	Appearance of Section 7 After 162,774 Wheel Loads	74
67	Continued Deterioration of Section 7 at 170,700 Wheel Loads .	75
68	Close-Up View of Section 7 at 170,700 Wheel Loads	75
69	"Ultimate Failure" at 171,168 Wheel Loads in Section 7 . . .	76
70	Close-Up View of the Section 7 "Ultimate Failure" in Punching Shear	76
71	Appearance of Section 3 Prior to Resumption of Testing in Spring After 143,370 Wheel Loads	77
72	Deformation of Section 3 After 162,774 Wheel Loads	77
73	"Ultimate Failure" in Section 3 at 177,501 Wheel Loads . . .	78
74	Continued Rutting of the Asphalt Concrete Overlay in Section 3 After 211,065 Wheel Loads	78
75	Appearance of Section 4 After 143,370 Wheel Loads	79
76	Permanent Deformation Over LVDT #3 of Section 4 After 177,501 Wheel Loads	79
77	Appearance and Depth of Ruts in Section 4 After 211,065 Wheel Loads	80
78	Appearance of Section 4 With Section 3 in Background After 247,128 Wheel Loads and End of Experiment	80
79	Appearance of Section 4 With Section 5 in Foreground After 247,128 Wheel Loads	81
80	Appearance of Section 8 After 143,370 Wheel Loads	81
81	Deformation of Section 8 After 177,501 Wheel Loads	82
82	Continued Deformation of Section 8 After 211,065 Wheel Loads	82
83	Appearance of Section 8 After the Experiment was Ended After 247,128 Wheel Loads	83

Figure

Page

84 Location of Benkelman Rebound Measurements 108

85 Benkelman Beam Rebound Deflections Vs. Wheel Loads 109

86 Pavement Temperature Vs. Benkelman Beam Deflection 110

87 Dimensions of Dual Tires 113

88-95 Dynamic Deflection Vs. Lateral Distance

88 Shallow LVDT, Section 2 114
89 Deep LVDT, Section 2 114
90 Shallow LVDT, Section 4 115
91 Deep LVDT, Section 4 115
92 Deep LVDT, Section 4 116
93 Shallow LVDT, Section 7 117
94 Shallow LVDT, Deep LVDT, Section 10 118
95 Shallow LVDT, Deep LVDT, Section 10 119

96 Dynamic Deflection Ratio Vs. Wheel Loads 121

97 Dynamic Deflection Vs. Speed for LVDT #4 121

98-102 Strain Vs. Lateral Distance

98 Transverse, Surface, Section 1 122
99 Longitudinal, Surface, Section 1 122
100 Longitudinal, Bottom of Base, Section 2 123
101 Transverse, Bottom of Base, Section 2 124
102 Longitudinal, Surface, Section 2 125

103-104 Strain Vs. Wheel Load

103 Longitudinal, Bottom of Base, Section 2 126
104 Longitudinal, Top of Base, Section 4 126

105-114 Strain Vs. Lateral Distance

105 Longitudinal, Surface, Section 3 132
106 Transverse, Surface, Section 3 132
107 Transverse, Section 4 133
108 Transverse, Section 4 133
109 Longitudinal, Section 4 134
110 Transverse, Section 4 134
111 Longitudinal, Section 4 134
112 Transverse, Section 4 134
113 Longitudinal, Section 4 135
114 Longitudinal, Section 4 135

115-116 Compressive Strain Vs. Temperature

115 Longitudinal, Section 4 136
116 Longitudinal, Section 4 136

Figure		Page
117	Maximum Strain Vs. Depth	137
118-124	Strain Vs. Lateral Distance	
118	Longitudinal, Surface, Section 5	138
119	Transverse, Surface, Section 5	138
120	Longitudinal, Surface, Section 6	139
121	Longitudinal, Section 7	140
122	Longitudinal, Section 7	140
123	Transverse, Section 7	140
124	Transverse, Section 7	140
125	Strain Vs. Wheel Loads	141
126-137	Strain Vs. Lateral Distance	
126	Longitudinal, Surface, Section 9	144
127	Transverse, Surface, Section 9	144
128	Longitudinal, Bottom of Base, Section 10	145
129	Transverse, Bottom of Base, Section 10	145
130	Longitudinal, Bottom of Base, Section 10	145
131	Transverse, Bottom of Base, Section 10	145
132	Longitudinal, Section 12	147
133	Transverse, Section 12	147
134	Longitudinal, Section 12	148
135	Transverse, Section 12	149
136	Transverse, Section 12	150
137	Longitudinal, Section 12	151
138	Maximum Strain Vs. Depth	152
139-144	Stress Vs. Lateral Distance	
139	Section 4	154
140	Section 7	154
141	Section 4	155
142	Section 7	156
143	Section 8	157
144	Section 10	157

ABSTRACT

Three different kinds of base material of varying base thicknesses were tested at the Washington State University Test Track on Ring #4 during the fall of 1968 and the spring of 1969. Twelve 18-foot test sections consisting of 4.5, 7.0, 9.5 and 12 inches of untreated crushed rock surfacing top course base; 2.0, 4.0, 6.0 and 8.0 inches of sand-asphalt base; and 0.0, 2.0, 3.5 and 5.0 inches of Class "F" asphalt concrete base, covered by a uniform 3.0-inch thick Class "B" asphalt concrete wearing course were tested during this period. The pavement structure was built on a clay-silt subgrade soil.

Instrumentation consisted of moisture tensiometers, strain gages, pressure cells, LVDT gages and thermocouples for measuring moisture, strain, stress, dynamic deflections and temperatures. Benkelman beam readings were taken.

The testing revealed that the fall failure modes were different from the spring failures. The fall failure pattern started from transverse cracks in the thin sections which developed into alligator cracking patterns. These cracks appeared after a period of cold weather and heavy rains followed by a warming trend. Thermal and mechanical loads in conjunction with adverse environmental conditions during construction and prior to and during the fall testing period were believed to be responsible for the early fall failures on the thin sections. The spring failures were very rapid and sudden and were due to environmental factors which led to highly saturated subgrade, thus resulting in poor bearing capacity. Punching shear was the failure mode. The thickest sections survived without cracks but developed severe rutting.

Comparison of the results with those obtained from Rings #3 and #4, show that they were similar in many respects. This indicates that the test track is capable of replicating results and is a reliable research instrument.

Equivalencies were developed for the different materials. On this basis the Class "F" asphalt concrete base was superior to the sand-asphalt and untreated crushed rock bases in that order.

Maximum values for static and dynamic deflections, strains and stresses for different times and temperatures were developed. The lateral position of the dual tires with respect to the gage severely affected the strain, stress and deflection values. Temperature also caused variations in the measurements.

Spring instrument readings for static and dynamic deflections, strain and stress show values as much as 2 to 4 times of those obtained in the fall. Spring subgrade conditions probably were responsible for these differences.

Ring #4 series operational time was half that of Ring #3 and about the same as Ring #2. Ring #4 sustained about a quarter of the wheel load applications of Ring #3. Construction and testing environmental conditions were inferior to those for Ring #3, although they were similar for Ring #2 and hence contributed to the lower test period. This points out that environmental factors are very important in pavement life.

EXPERIMENTAL PAVEMENT RING NO. 4

INTRODUCTION

Experimental pavement Ring #4, the second ring built under contract Y-993 and the fourth ring built since the project started, was the last of three rings of a continuing pavement experiment designed to test bases constructed from different materials varying in thicknesses in order to study their relative strengths and determine their relative equivalencies. Rings #1 and #2 were part of contract Y-651; Rings #3 and #4 were part of contract Y-993. Both contracts were with the Washington Highway Department.

Each ring consisted of 12 sections constructed from three different base materials which were subdivided into four sections of varying base thicknesses, the exception being Ring #1 which had six. Crushed rock base was used as the standard control for comparison purposes; sand asphalt and Class "F" asphalt concrete were the other base materials tested in Ring #4. Cement treated, emulsion treated, asphalt treated, special screened non-fractured aggregate and asphalt concrete treated base material were tested in previous rings.

The three rings were constructed during the summer and tested under different environmental conditions--fall and spring. Ring #2 was constructed in the summer of 1966 and tested during the fall of 1966 and spring of 1967; Ring #3, built in the summer of 1967, was tested in the fall of 1967 and spring of 1968; Ring #4 was constructed in the summer of 1968 and was tested during the fall of 1968 and the spring of 1969. Ring #1 was built in the summer of 1964 and was tested from 1965 to 1966. This report is concerned

with a description and the experimental results contained from Ring #4. The results from Rings #1, #2 and #3 were reported in References (1), (2) and (3) respectively.*

This project was conceived and initiated by the Highway Research Section, College of Engineering Research Division, Washington State University. Financing was a joint undertaking among the University, the Washington State Highway Commission, Department of Highways, the Bureau of Public Roads of the Federal Highway Administration, Department of Transportation, as a HRP federal aid research project, and the Asphalt Institute, which also provided professional guidance in design, planning, and evaluation of results.

EXPERIMENTAL DESIGN

The 260-foot test track centerline circumference limits the number of test sections that can be tested at any one time. Experience suggests that twelve 18-foot test sections separated by 3.7-foot transition zones would provide the necessary length without causing or being affected by boundary conditions. This division permits testing of three base types at four thickness levels in any one-ring experiment. The inclusion of several thicknesses of each base type was considered necessary for proper evaluation of the performance of several base types. The degree of thickness was chosen to provide estimated pavement lives of several hundred up to two million wheel load applications of 10,000 pounds. The actual load per set of duals, however, is 10,600 pounds.

---

*Figures in parentheses refer to specific reports in the References.

The subgrade, surfacing and other variables were kept constant, while base types and thickness were varied. A subbase was not used so as to keep the pavement layers at a minimum and to simplify the theoretical analysis of the system.

A random distribution of base types of varying thicknesses might have been preferable (4), but time, costs and the ease of construction dictated that sections of same base types be grouped together. Random distribution would have required more hand labor which would cost more,and more importantly, would have prevented the contractor from being able to use standard construction equipment.

The location and dimensions of the pavement sections of Ring #4 are shown in Figure 1. The crushed stone sections were moved 120° from their position in Ring #3 and 240° from those in Ring #2. This was done to identify any effect of boundary conditions due to subgrade variations and cut and fill location. The base types and thicknesses are listed in Table 1. The thicknesses of the sections and transition zones are shown schematically in Figure 2. The subgrade soil, type A-6 (10), a clay-silt, was common to all sections. Figure 3 shows a typical cross-section of the pavement structure.

Materials

Subgrade

The subgrade soil, a clay-silt A-6 (10) known locally as Palouse silt, was the same type as used in Rings #1, #2 and #3, and is described in Reference (1). This soil, a loess, covers a wide area in southeastern Washington and is remarkably similar in properties although the clay-silt proportions may vary from area to area and from location to location. The

PLAN VIEW

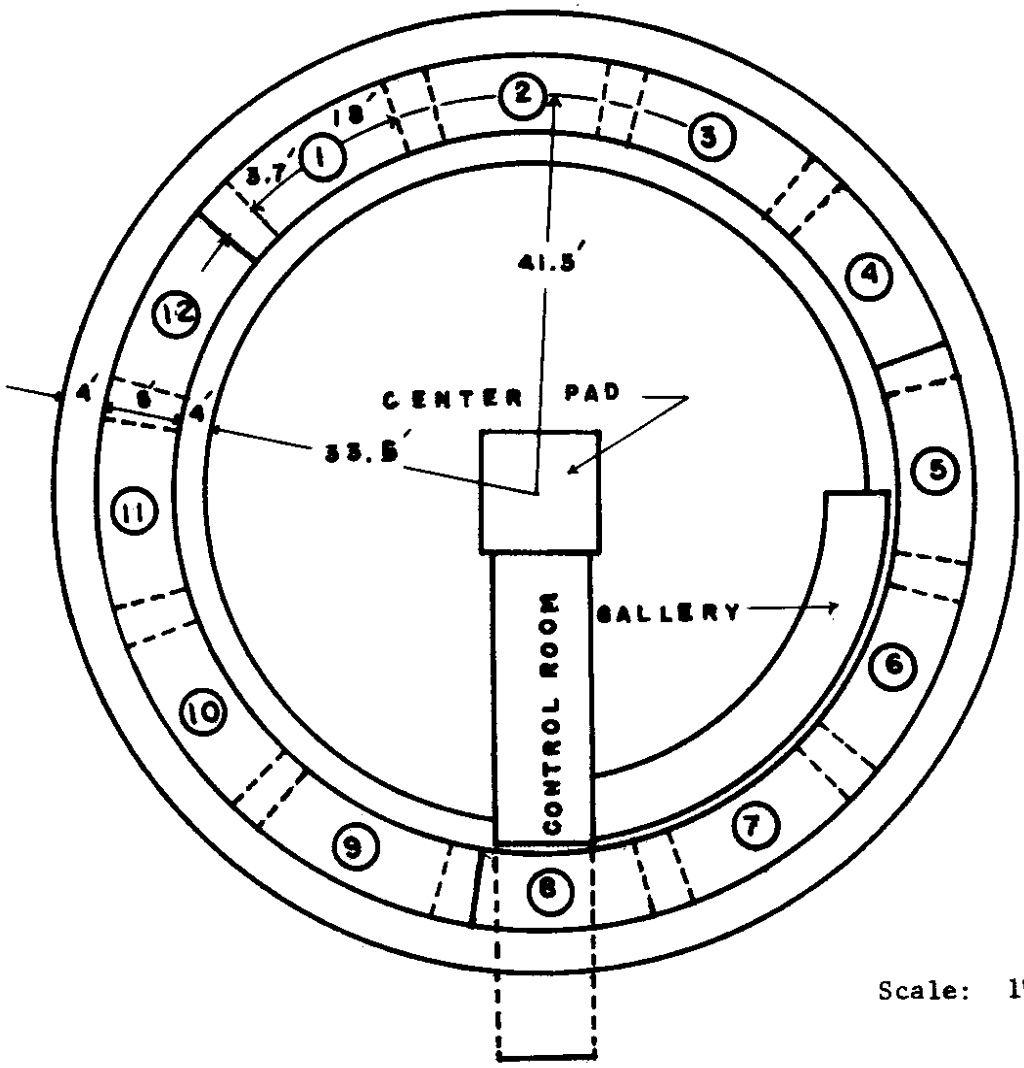

FIGURE 1. PERMANENT STRUCTURES AND PAVEMENT SECTIONS
TEST RING NO. 4

TABLE 1: TYPES, SECTIONS AND THICKNESSES OF RING #4

Type of Base	Sections	Thickness Levels--Inches			
		A	B	C	D
Crushed Surfacing Top Course	9 - 12	4.5	7.0	9.5	12.0
Cl "F" Asphalt Concrete	5 - 8	0.0	2.0	3.5	5.0
Sand Asphalt	1 - 4	2.0	4.0	6.0	8.0
Wearing Course-- Class "B" Asphalt	All Sections	3.0			

Highway Research Section
Washington State University
June 1970

FIGURE 2. SCHEMATIC PROFILE FOR RING #4

Sections 1-4 - Sand-Asphalt Base (SAB)
Sections 5-8 - Class "F" Asphalt Concrete Base (ACB)
Sections 9-12 - Untreated Crushed Surfacing Top Course Base (UTB)

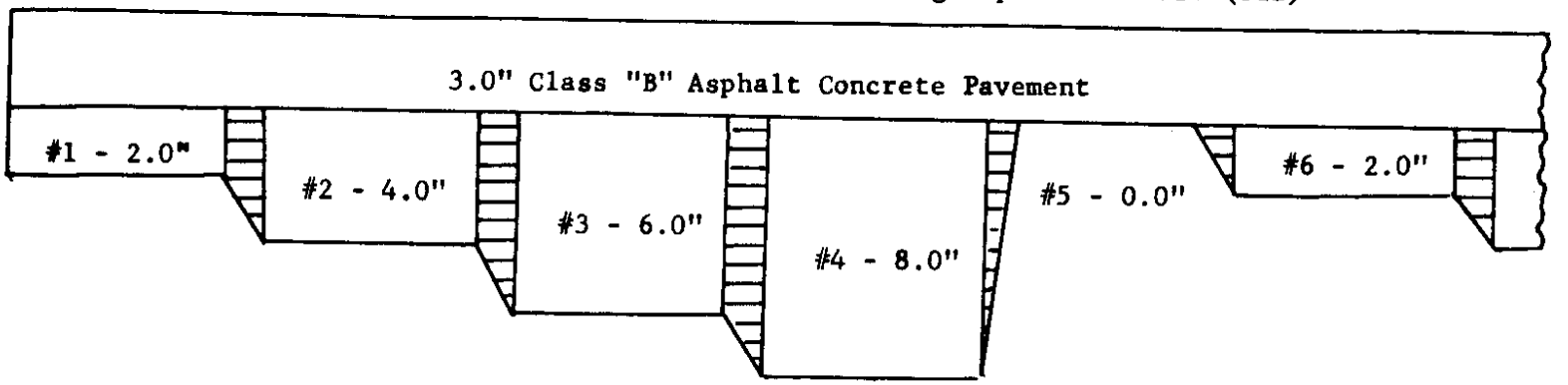

A-6 (10) Soil

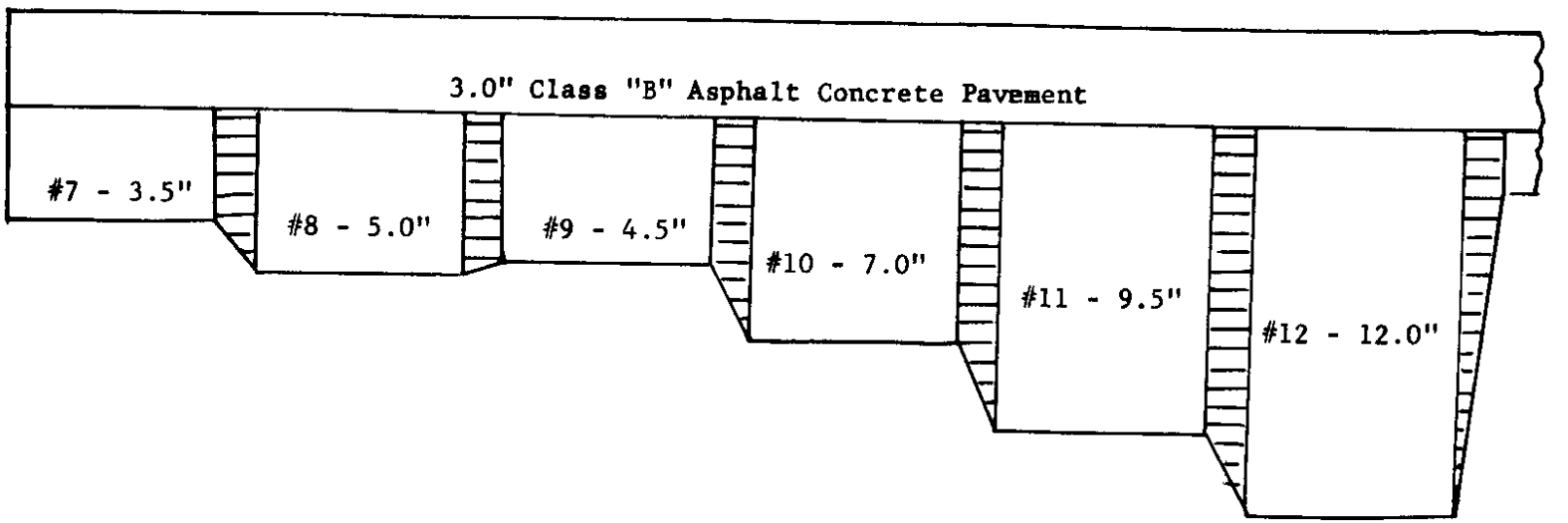

A-6 (10) Soil

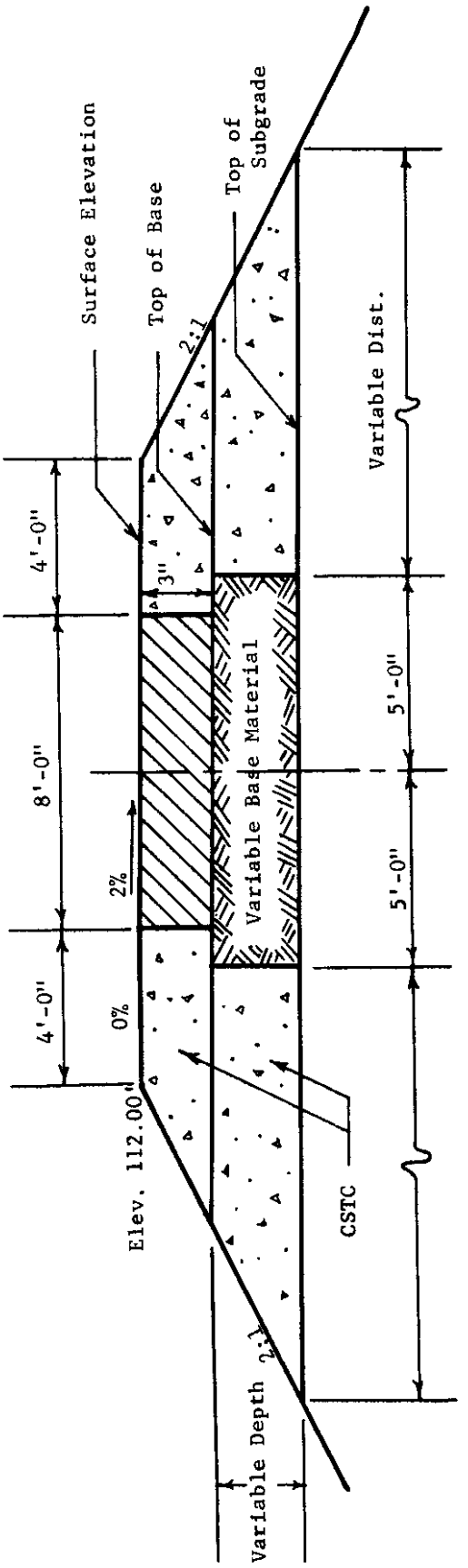

FIGURE 3. TYPICAL CROSS-SECTION OF PAVEMENT STRUCTURE

Rings 2, 3 and 4

soil moisture-density relationship curves are shown in Figure 4 and Table 2. Characteristics and classifications are shown in Table 3. Table 4 shows the results obtained from a series of tests run by the Asphalt Institute on the Palouse silt subgrade samples (5). The results are similar to other work done at Washington State University. Some of the soil came from the contractor's local pit and the curve is also shown in Figure 4. The slight difference in density may be attributed to a difference in the clay contents of the two silts or to testing variance.

Crushed Surfacing Top Course

The basaltic aggregate came from the Halpin Pit located between Pullman, Washington and Moscow, Idaho on the Moscow-Pullman Highway and owned by the contractor, United Paving Company, Inc. The rock met Washington Highway Department specifications for crushed surfacing top course (6). This rock was used for the untreated bases in sections 9 to 12 and for the shoulders. Figure 5 shows the gradation curve for this aggregate while Figure 6 represents the maximum computerized density curve which can be obtained with this aggregate.

Sand

The sand for the sand-asphalt bases came from the Nesbitt Pit located in the Spokane area and owned by the contractor, United Paving Company, Inc. This was shipped to Pullman and stockpiled at the contractor's local plant. This source is a fine-grained, glacial lake deposit of clean, almost white sand. This sand was hot-mixed with asphalt and laid as base in sections 1 to 4. The sand met all the required specifications (7) as shown in Figure 7.

Although sand is fairly common in the state of Washington, the Washington Highway Department has not made use of it for hot-mixed asphalt bases for

FIGURE 4. DENSITY - MOISTURE CURVES
(Subgrade Soil Characteristics)

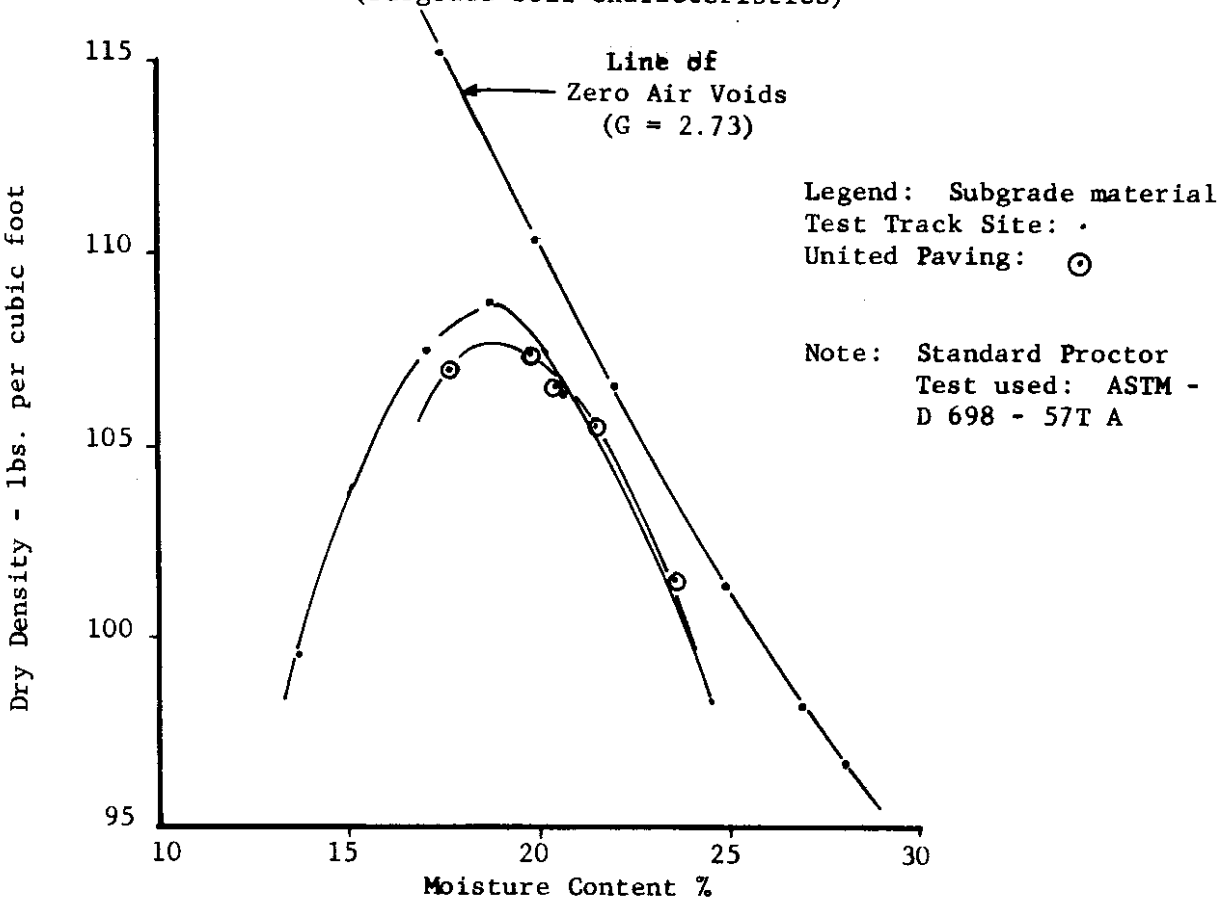

TABLE 2: OPTIMUM DENSITY AND MOISTURE
FOR SUBGRADE MATERIAL

Source	Max. Optimum Dry Density	Optimum Moisture
Test Track	108.8	18.8
United Paving	107.8	18.8

TABLE 3: SOIL CHARACTERISTICS AND CLASSIFICATION

Soil	Specific Gravity S.G.	Liquid Limit L.L.	Plastic Limit P.L.	Plasticity Index P.I.	Highway Res., Board Class.	Airfield Classification
Clay-silt	2.73	34.9	20.2	14.7	A - 6 (10)	CL

Stabilometer "R" Value = 16
pH Factor = 6.1

TABLE 4: CALIFORNIA BEARING RATIO (CBR) TEST ON PALOUSE SILT SUBGRADE SOIL

Water Content (%)	Dry Density (lb./cu.ft.)	CBR (%)	Swell (%)	Water Content After Soaking (%)
		SERIES 1		
13.0	105.1	4.6	2.4	20.2
16.4	108.0	9.2	0.8	18.9
19.3	105.8	2.8	0.3	19.9
		SERIES 2		
13.0	114.0	13.5	1.5	16.4
16.4	112.5	7.5	0.5	17.3
19.3	106.6	2.2	0.4	19.6

NOTE: Specimens soaked 4 days, 10 lb. surcharge weight.

Series 1 compaction: 10 lb. hammer, 18 in. drop, 5 layers, 12 blows per layer (12,200 ft.-lb./ft.^{3}).

Series 2 compaction: 10 lb. hammer, 18 in. drop, 5 layers, 29 blows per layer (26,400 ft.-lb./ft.^{3}).

(After Kallas)

FIGURE 5. COMBINED GRADATION CURVE FOR CRUSHED SURFACING TOP COURSE UNTREATED SECTIONS 9-12 AND SHOULDERS

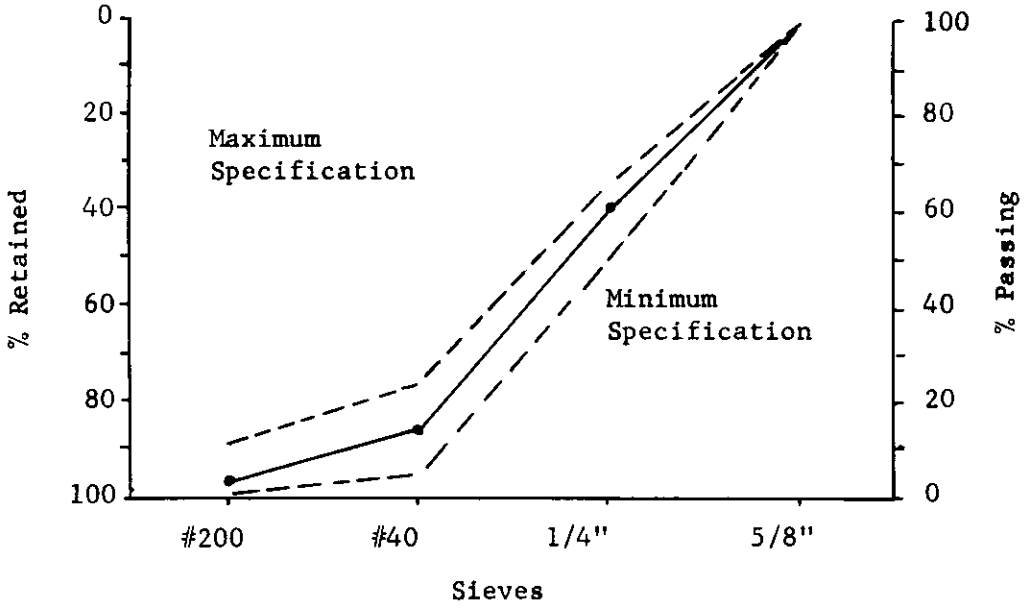

FIGURE 6. MAXIMUM DENSITY CURVE CRUSHED SURFACING TOP COURSE

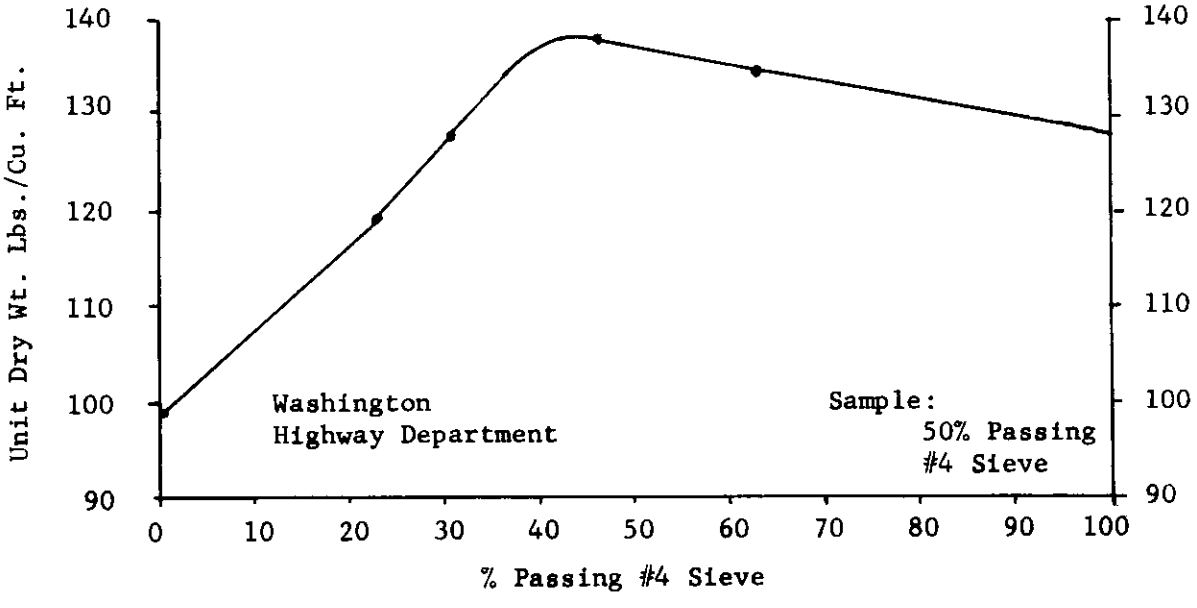

highways. Some of the western Washington counties (for example, Pacific County) are planning to use their extensive resources of ocean beach and glacial sands for hot-mixed sand-asphalt bases in county roads. Other states have used sand for hot-mixed sand-asphalt bases in their highway systems (8). The Asphalt Institute, which was involved in the Colorado Test Road Project (8), was interested in studying sand-asphalt base behavior under test track conditions. Therefore, the sponsors decided to include sand-asphalt bases as one of the base materials for study.

Asphalt Concrete Base Class "F" Aggregate

The Washington Highway Department specifications for aggregate to be used for Class "F" asphalt concrete have wide limits and require a minimum of 50% fresh fractured surfaces (6). These specifications were designed to take advantage of the many glacial deposits of aggregate found in the state of Washington, which have many variations in gradation and fractures. The contractor, United Paving Company, Inc., supplied a basaltic aggregate which met all the specifications and was 100% fractured, but was considered to be too "good" for the experiment. The Washington Highway Department wanted a lower grade of aggregate for the asphalt concrete Class "F" bases. A compromise was reached by mixing the special screened non-fractured aggregate with United Paving's Class "F" aggregate on a 60%-40% basis. The special aggregate was used in Rings #2 and #3 for the special asphalt treated bases (2, 3). There was a remaining stockpile at the test track site. This gave a fracture percentage of about 72%; the reason for the high fracture percentage was that some of the large screened non-fractured aggregate was screened off to meet specifications (6, 7). Figure 8 shows the specification and gradation of this aggregate.

FIGURE 7. GRADATION CURVE FOR SAND-ASPHALT BASE SECTIONS 1-4

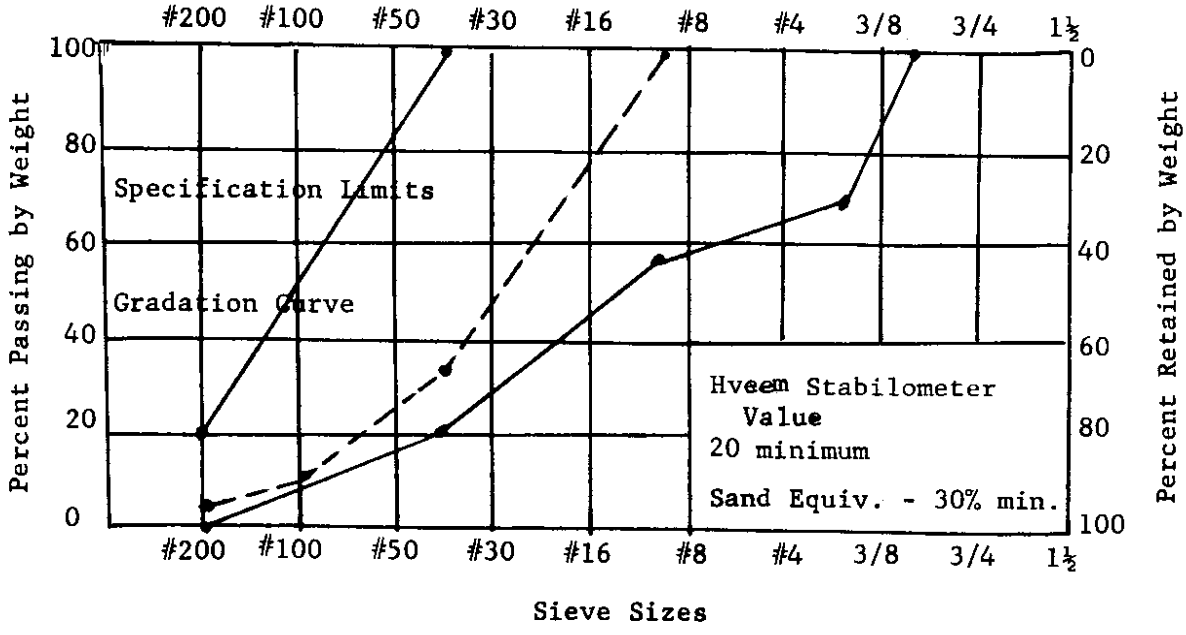

FIGURE 8. GRADATION CURVE FOR THE CLASS "F" ASPHALT CONCRETE BASE AGGREGATE - ACB SECTIONS 5-8

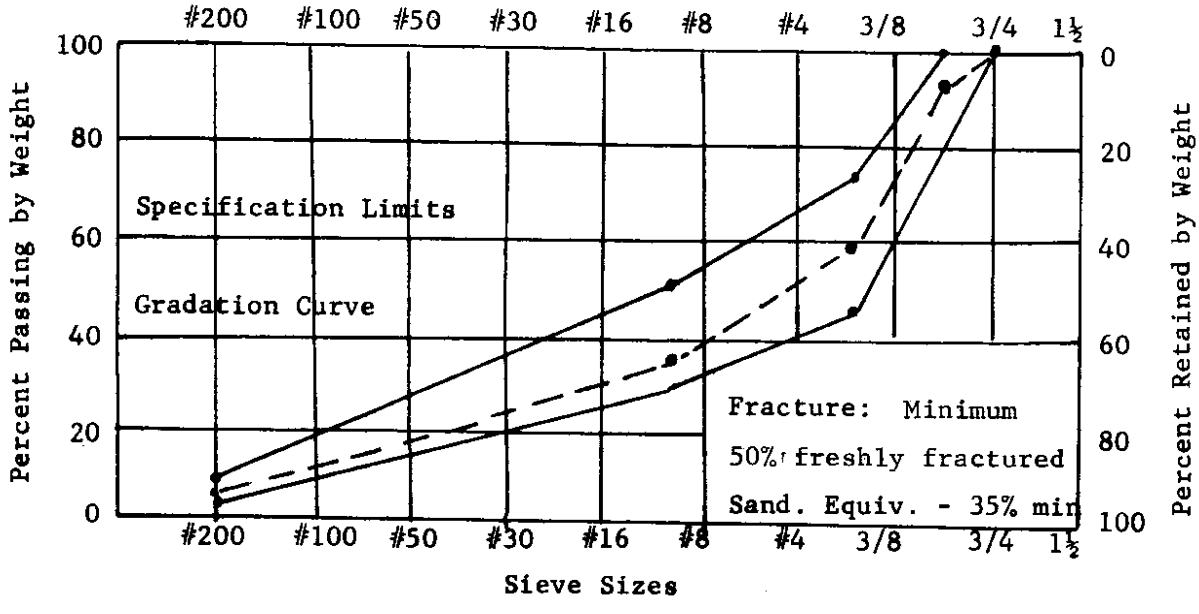

Asphalt Concrete Class "B" Aggregate

This aggregate came from the United Paving's Pullman Quarry and was checked and blended to meet Washington State Highway specifications (6). This is basalt rock similar to the crushed surfacing top course. The combined gradation curve is shown in Figure 9.

Construction

Pre-Conditioning

Construction began on August 8, 1968 by United Paving Company, Inc. of Pullman, Washington which was the only bidder on the project. The existing pavements, treated bases and crushed rock were removed, and the subgrade was excavated from elevation 112.0 feet to 110.5 feet. The remaining subgrade was scarified and processed. At this time, wet, unseasonable weather arrived causing a delay of several weeks. Actual work on the subgrade did not begin until after September 3 when sunshine appeared thus allowing the drying of the subgrade.

Work again commenced on scarifying and processing of the subgrade. A full-loaded 37,500-lb. truck was used to check the section for "weak" areas. Fresh Palouse silt was obtained from the United Paving Pit and was used to build up the grade to a rough elevation. A "weak" or "soft" spot developed on the outside edge of sections 11 and 12. This was excavated to a depth of 5 feet, approximate elevation of 105.0 feet and filled with Palouse silt (Figure 10). The excavation revealed that this area was covered with black organic material, which was formed when a large dairy farm was located in this area (9).

FIGURE 9. COMBINED GRADATION CURVE FOR ASPHALT CONCRETE CLASS "B" AGGREGATE - ALL SECTIONS

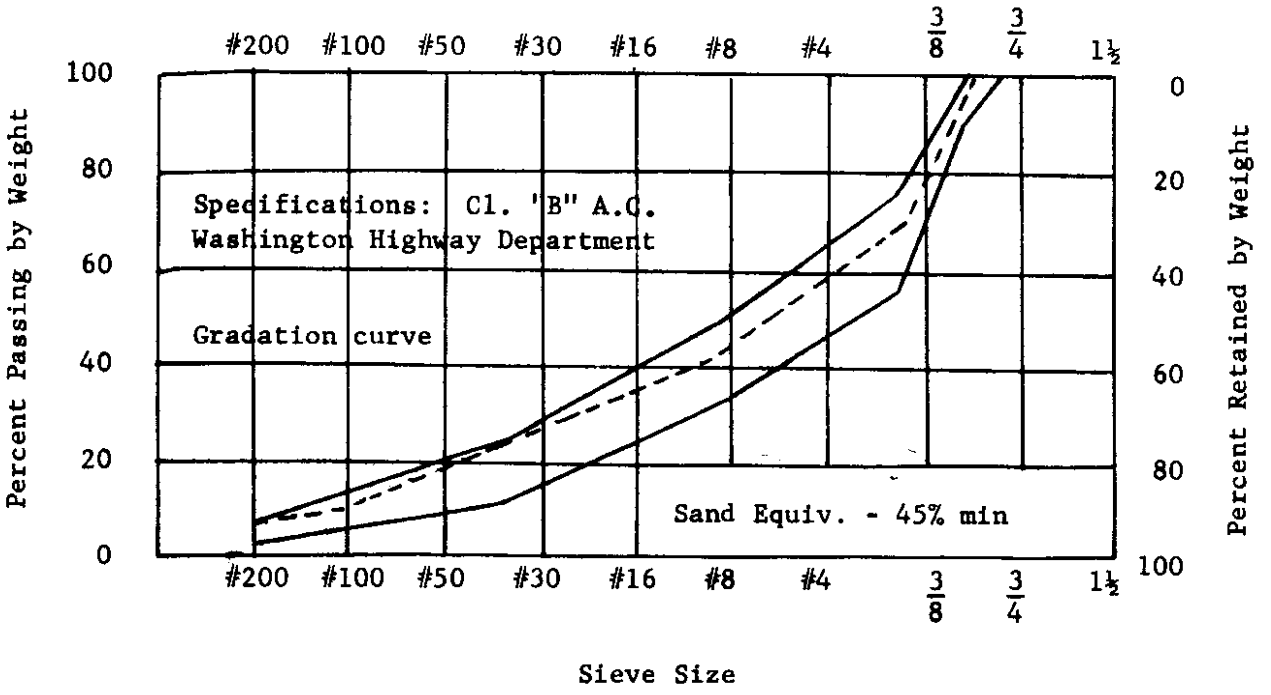

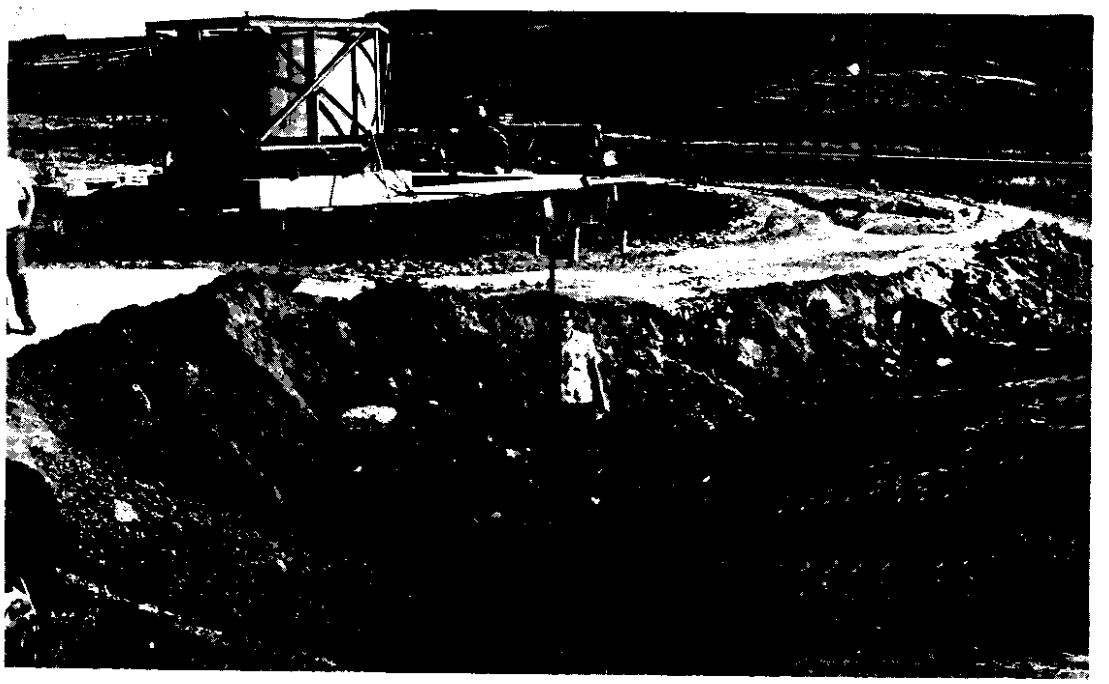

FIGURE 10. THIS SHOWS THE DEPTH AND EXTENT OF THE EXCAVATION FOR REMOVAL OF THE "WEAK" AREA BY SECTIONS 11 AND 12. NOTE THE BLACK, ORGANIC SOIL AT BOTTOM OF THE EXCAVATION.

Subgrade

The subgrade was brought up in 6-inch lifts, spread by a Huber blade dozer, and compacted by a pneumatic rubber-tired, smooth steel wheel, and steel vibratory rollers (Figures 11 and 12). Density was checked by nuclear methods. It was noticed that as construction progressed, the lifts became progressively dryer. This was due to the favorable warm weather which lasted for about two weeks, long enough to prepare the subgrade.

The subgrade was brought up to the final rough grade; that is, each group of sections 1-4, 5-8 and 9-12. Then each section was cut to a final grade elevation. The contractor tried to speed up this grading by setting up 1" x 4" forms, 14 feet apart and then working the area by means of hand shoveling and screeding to the exact elevation as shown in Figure 13. Then the forms were removed and the whole area was compacted. Table 5 shows the final densities and moisture contents; the final column shows how well 95% of specified density was achieved. This method of working the subgrade seems to have required as much time and labor as did the hand-labor final grade construction procedure used for Ring #3.

On September 11, the subgrade was finished and instrumentation began immediately, which was finished on the afternoon of September 13. The weather looked threatening and all of the subgrade was covered with 20-foot wide sheets of visqueen. This was necessary as rain did not allow work to continue until September 24 when the visqueen was removed. It was found that some parts of the subgrade were wet even though visqueen was used; these were parts of sections 5, 9 and 12. No work was allowed, and the subgrade was exposed to the sun for the rest of the week. Inspection revealed that the subgrade was in good shape and it was decided to go ahead and start laying base on September 27.

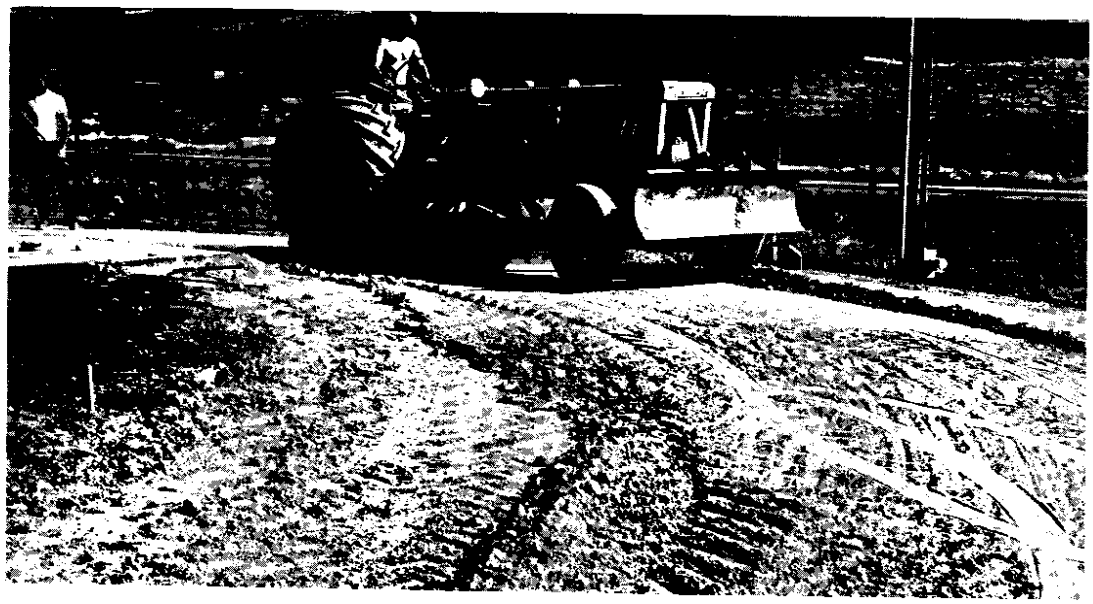

FIGURE 11. HUBER BLADE DOZER SPREADING THE SUBGRADE SOIL. NOTE THE DRY APPEARANCE OF THE SILT.

FIGURE 12. SPREADING THE SILT BY HAND AND COMPACTING WITH A PNEUMATIC RUBBER-TIRED ROLLER.

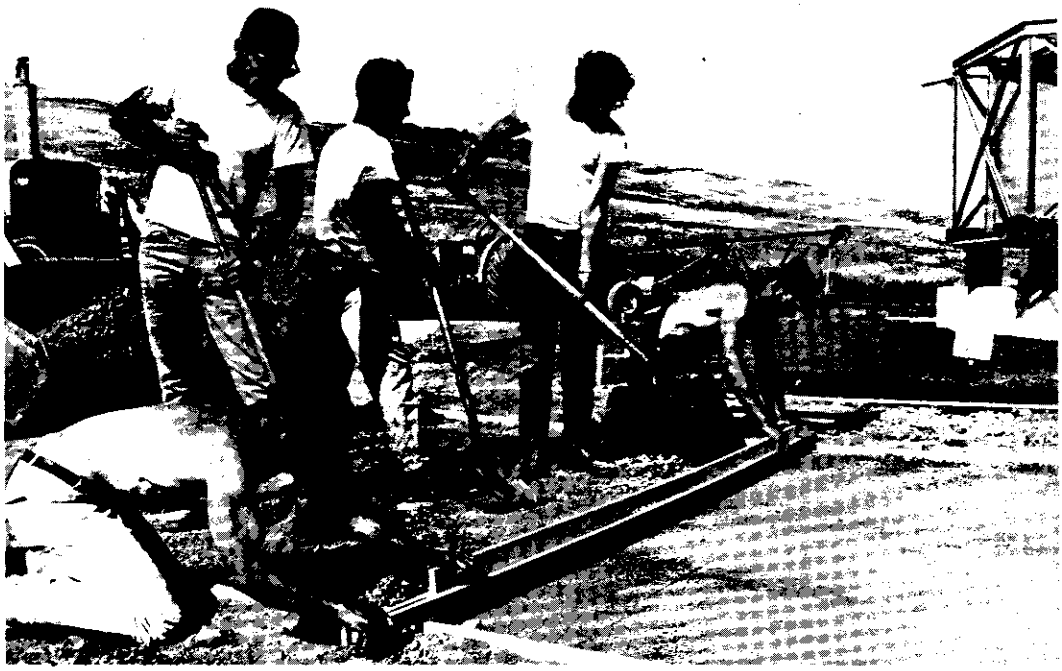

FIGURE 13. HAND WORKING AND SCREEDING OF THE SUBGRADE TO FINAL ELEVATION BY THE CONTRACTOR'S CREW. THE FORMS WERE SET TO CORRECT GRADE PRIOR TO FINAL GRADING.

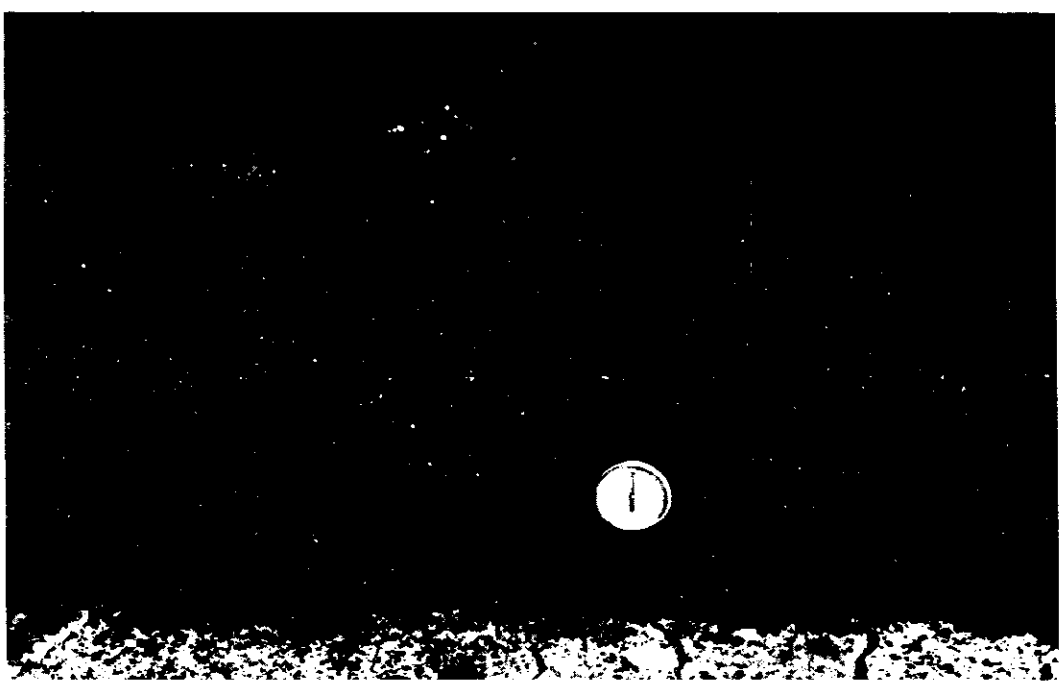

FIGURE 14. SECTION 4, SAND-ASPHALT BASE. NOTE THE APPEARANCE OF THE FIRST LIFT. THE TEMPERATURE IS BEING CHECKED FOR PROPER COMPACTION CONTROL.

Crushed Surfacing Top Course Base--Untreated (Sections 9-12)

On the morning of September 27, crushed rock base was laid in sections 9-12 in three lifts. The crushed rock was processed in the United Paving yard using a grader and was trucked to the test track site. A Blaw-Knox paver was used to lay the crushed rock base in three lifts. The deepest sections were laid first; that is, sections 12 and 11, and these were compacted with steel and pneumatic rubber-tired rollers. The second lift was then laid in sections 12, 11 and 10, and then rolled to desired density which was checked by nuclear density equipment. The final lift was laid in all sections (12-9) and then compacted. The grade was checked by rod and level and by straight edge. High and low spots were cut and filled respectively. Table 6 shows the density achieved. The measured moisture content was 5.7%.

Sand-Asphalt Bases (Sections 1-4)

Laying of the sand-asphalt base with a Blaw-Knox paver in three lifts commenced on the afternoon of September 27. The sand came from United Paving's Nesbitt Pit in Spokane; 5.0% of 85-100 penetration asphalt was used. Construction techniques followed were those recommended by Washington State Highway specifications (7) and the Asphalt Institute (11).

The first lift was 4.0 inches loose depth and was laid in sections 4 and 3 at 1 p.m. The temperature of the mix was 250° F. (See Figure 14, page 18). After passes with steel and pneumatic-tired rollers, the desired minimum density was achieved. The edges of the base were not rolled until the mix had sufficiently cooled so that edge breakdown did not occur.

The second lift was 4.0 inches loose depth and was laid in sections 4, 3 and 2 at 3:05 p.m. The mix temperature was 195° F. Density was achieved by means of steel and pneumatic-tired rollers. The steel roller was used first, followed by the pneumatic roller, and then the steel roller again.

TABLE 5: FINAL SUBGRADE DENSITIES AND MOISTURE CONTENT

Section	Wet Density lb/ft^3	Dry Density lb/ft^3	Moisture Content		Percent Compaction of 95% Required Density
			lb/ft^3	%	
1	119.7	103.5	16.2	15.7	101.8
2	113.7	98.3	15.4	15.7	96.7
3	113.5	98.9	14.6	14.8	97.2
4	113.5	98.4	15.1	15.3	96.8
5	123.0	107.3	15.7	14.6	105.5
6	125.5	109.2	16.3	14.9	107.4
7	120.5	103.0	17.5	17.0	101.3
8	115.0	100.0	15.0	15.0	98.3
9	120.5	105.1	15.4	14.7	103.3
10	114.0	98.0	16.0	16.3	96.4
11	121.0	102.8	18.2	17.7	101.1
12	114.7	99.1	15.6	15.7	97.4
Mean	117.9	102.0	15.9	15.6	100.3

TABLE 6: TABLE OF BASE COURSE DENSITIES, RING 4

Date	Base Material	Section Number	Nuclear Density (lb/ft^3)	Laboratory Density (lb/ft^3)	Compaction % Laboratory
10-3-68	Cl "B"	1-12	147.5	156.0	94.6
9-27-68	S.A.B.	1	111.2	128.1	87.8
	S.A.B.	2	112.2	128.1	87.6
	S.A.B.	3	113.1	128.1	88.3
9-27-68	S.A.B.	4	117.7	128.1	91.7
9-28-68	No Base	5	--	--	--
	A.C.B.	6	143.8	156.0	92.2
	A.C.B.	7	145.1	156.0	93.0
9-28-68	A.C.B.	8	148.8	156.0	95.4
9-27-68	U.T.B.	9	--	--	--
	U.T.B.	10	143.0	137.5	104.0
	U.T.B.	11	141.9	137.5	103.2
9-27-68	U.T.B.	12	141.9	137.5	103.2

The final lift was placed on all sections at 4:55 p.m.; the mix temperature was 212° F. Rolling operations were started immediately. On the final lift, 4½ passes were made with the pneumatic roller and 8½ passes with the Galion steel roller. One roller pass is a complete trip forward and backward. One pass was later made with the large steel roller.

Nuclear density equipment was used to check density and to indicate when and where additional compaction was necessary. In the absence of previous records of sand asphalt nuclear readings, the manufacturer's curve was used. The edges were compacted only after the rest of the base had reached compaction. It was noticed that after mix temperature had cooled down the steel roller had a tendency to induce tension surface cracks due either to the lateral twisting of the roller or the coolness of the surface (see Figure 15, page 24). No tack coat was applied between the layers as the layer surfaces were clean. When the sections were cored during the fall, it was noticed that the layers separated indicating that tacking might have been desirable. Cores taken in the summer of 1969 did not separate and had to be split apart for testing. The densities achieved are shown in Table 6.

Class "F" Asphalt Concrete Bases (Sections 5-8)

At 8:55 a.m. on Saturday, September 28, laying of the Class "F" asphalt treated base was begun. Table 7 (page 22) shows the mix design. The first lift was laid in sections 8 and 7 in loose depths of 4 and 2-3/4 inches respectively. The mix temperature was 270° F. At 9:05 a.m., when the mix temperature was 260° F, 3 passes were made with the steel roller and a density of 142 pounds per cu. ft. was achieved. At 9:30 a.m. and after 4 more passes with the steel roller and a temperature of 225° F in section 8 and 185° F in section 7, the density was 145.1 pounds per cu. ft. At 9:45 a.m., 4 passes were made with the pneumatic rubber-tired roller along with 4 more passes with

TABLE 7: MIX DESIGN REQUIREMENTS

Sieves--% Passing	Untreated Base (C.S.T.C.)		Sand-Asphalt Base (S.A.B.)		Asphalt Concrete Base Cl "F"		Asphalt Concrete Cl "B" Pavement	
	Specified	In Place	Specified	From Extraction	Specified	From Extraction	Specified	From Extraction
2" Square								
1" Square								
3/4" Square			100	100	100	100		
5/8" Square	100	100					100	100
1/2" Square					80-100	93	90-100	100
1/4" Square	50-65	60	70-100	100	45-75	59	55-75	70
U. S. No. 4		50						
U. S. No. 10		32	55-100	100	30-50	36	32-48	44
U. S. No. 40	5-23	13	20-100	33			11-24	25
U. S. No. 80						9	6-15	14
U. S. No. 100		7		9				13
U. S. No. 200	10 max.	4	0-20	3	2-8	5	3-7	7
Sand Equivalent % Min.	40		30		45		45	
% Fractures	75	100			50	72	75	100
Penetration Grade A.C.			85-100	85-100	85-100	85-100	85-100	85-100
Amount of A.C. %			5.0	5.3	5.5	5.8	5.3	6.1
Wt. Per Cu. Ft. of Mix	137.5	142.3	128.1	113.5	156.0	146.6	156.0	147.5

the steel roller. The density was now 147.2 and the temperature 215°F. Density in section 7 could not be accurately measured by the nuclear asphalt equipment because of the thin layer of asphalt.

A tack coat was applied and the second lift was laid in sections 8-6 at 10:35 a.m. The mix temperature was 190°F. A total of 10 passes with the pneumatic rubber-tired roller and 5 passes with the small steel roller were made on the main part of the bases. Figure 16 shows the appearance of the Class "F" asphalt concrete base after compaction. A total of 6 passes with the steel roller were made on the edges. The densities achieved are shown in Table 6 (page 20). The low reading in section 6 is probably due to the thin lift causing an inaccurate nuclear gage reading.

Class "B" Asphalt Concrete Wearing Course (All Sections)

After the instruments were installed, a tack coat of SS-1 was applied to all sections on the morning of October 2. Laying of the first lift of 1-3/4-inch thickness started at 2:00 p.m. The temperature of the Class "B" mix in the truck was 285°F and 265°F as placed 10 minutes later. Laying began in section 4 and proceeded counter-clockwise. (The numbering of the sections is clockwise.) Compaction was easily achieved by means of the pneumatic rubber-tired and steel rollers, 10 passes with each type roller. The steel roller was used only in sections 4 to 1.

The second lift was laid October 3 at 8:55 a.m. after an application of tack coat. The mix temperature was 360°F. It was a sunny morning with a cool west wind blowing; the ambient temperature range being 31°-70°F. This cooled off the asphalt mix rather rapidly. Paving was initiated from section 4 and proceeded counter-clockwise. A cold joint may have resulted in transition zone between sections 4 and 5 due to the cold wind. Compaction was achieved

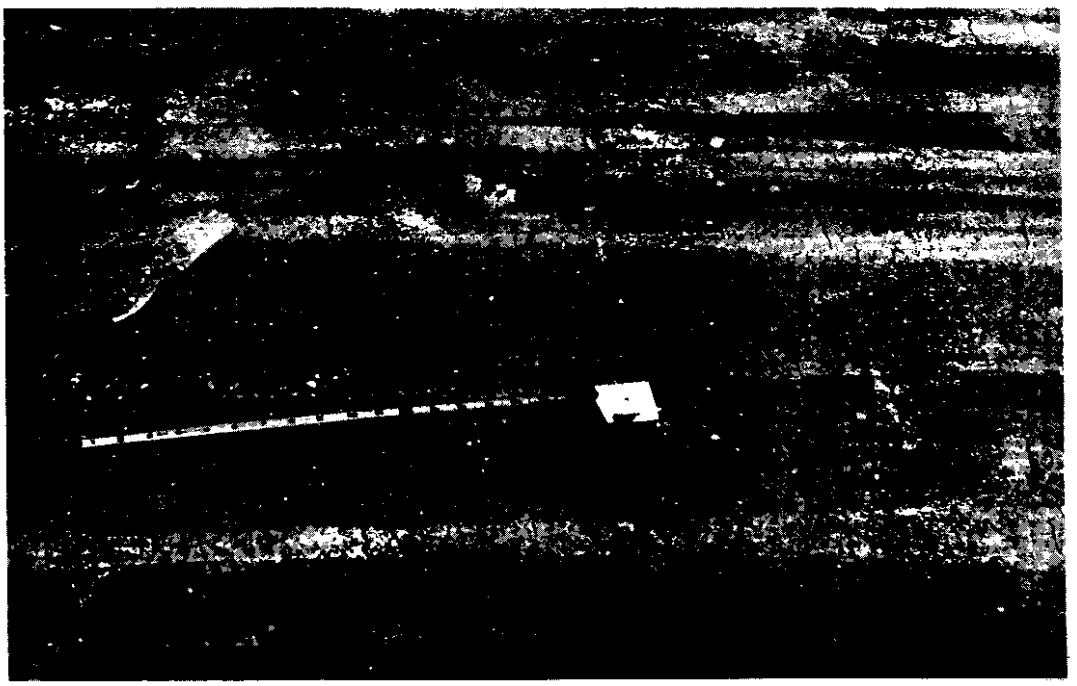

FIGURE 15. SURFACE TRANSVERSE TENSION CRACKS ON TOP OF THE SAND-ASPHALT BASE IN SECTION 4. THIS WAS PROBABLY CAUSED BY THE ACTION OF THE STEEL ROLLER ON A COOLED-DOWN MIX.

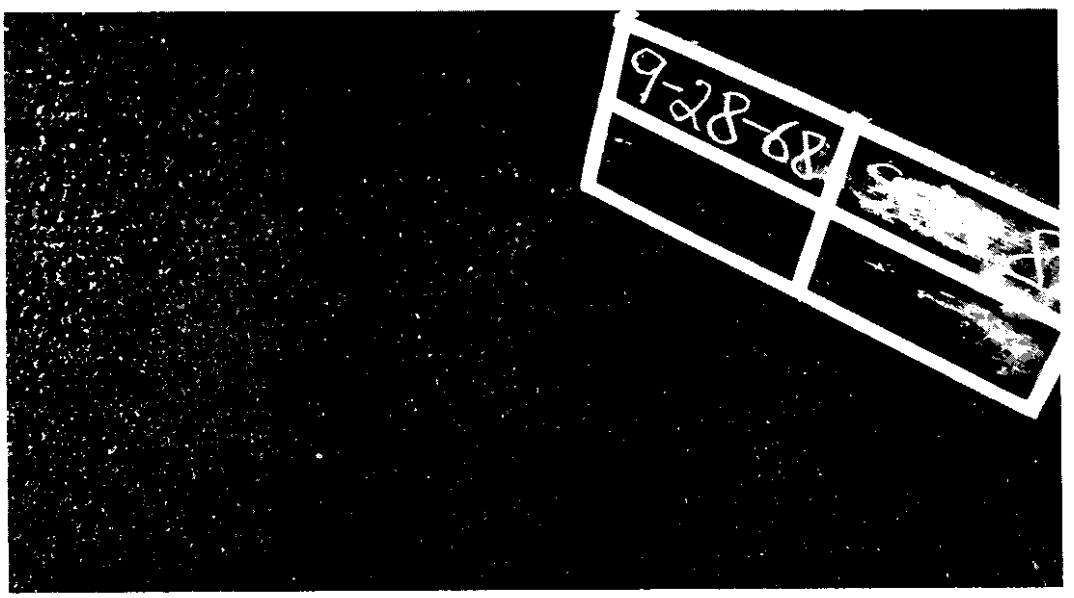

FIGURE 16. APPEARANCE OF THE SURFACE OF THE CLASS "F" ASPHALT CONCRETE BASE AFTER COMPACTION.

by means of rubber-tired and steel rollers. Much hand work was done to try to achieve a smooth, level wearing course. Table 6 (page 20) shows the surface densities and Table 7 shows the mix design.

Shoulders

Shoulders of crushed surfacing top course aggregate from the Halpin pit were put in place on October 7 and 8. These were graded to the proper grade and elevation and compacted to specifications similar to those for the crushed surfacing top course base sections 9-12 (7). A waterproofing tack coat was sprayed on the inside shoulders and ditch.

Comments

The weather during the time of construction was rather unfavorable. Work had to be done between periods of bad weather in order to have Ring #4 built before the really bad weather set in and so that testing could start in the fall of 1968. Otherwise, testing would have had to wait until 1969. The contractor, United Paving Company, Inc. of Pullman, Washington, cooperated to the best of their ability and was ready to work whenever permitted by the weather.

Instrumentation

Instruments to measure stresses, strains, temperature, dynamic deflection and moisture were installed in the different layers of the pavement structure in similar positions as was done at the San Diego County Experimental Base Project (12), following the recommendations of Materials and Research Development (13). Figure 17 shows the depth and the location of some of the instruments in one section; the positioning of the instruments was similar for the other sections. Table 8 shows the type of instrumentation installed and their location in the various sections. All the instruments, with the exception of

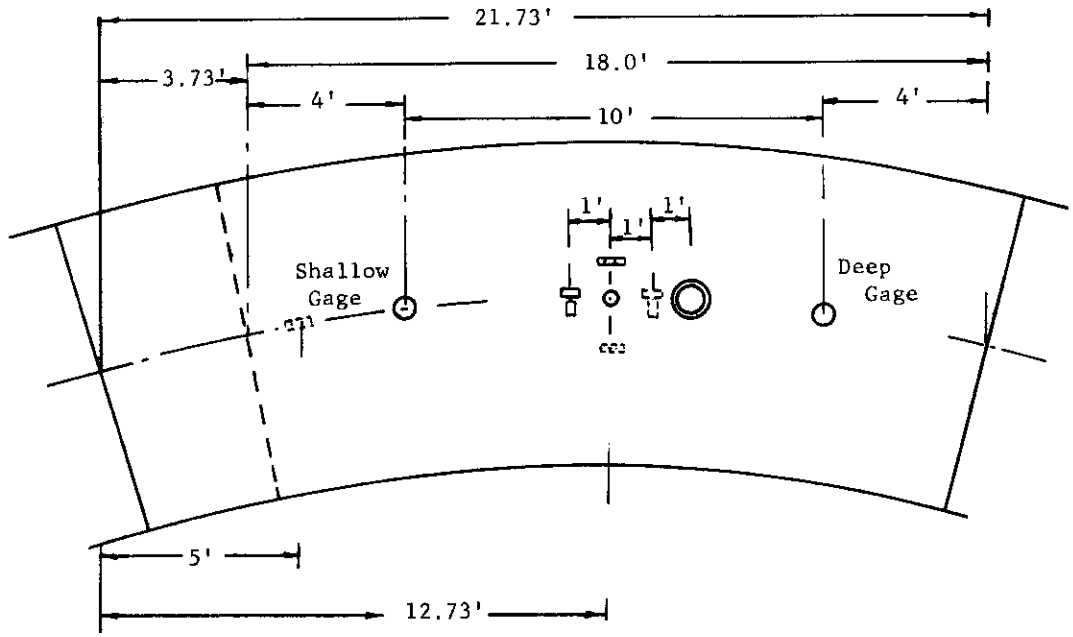

LEGEND

WSU Cell

Pressure Cell

Strain Gage

LVDT

Moisture Cell

Thermocouple

FIGURE 17. INSTRUMENTATION FOR SECTION 7
Class "F" ACB

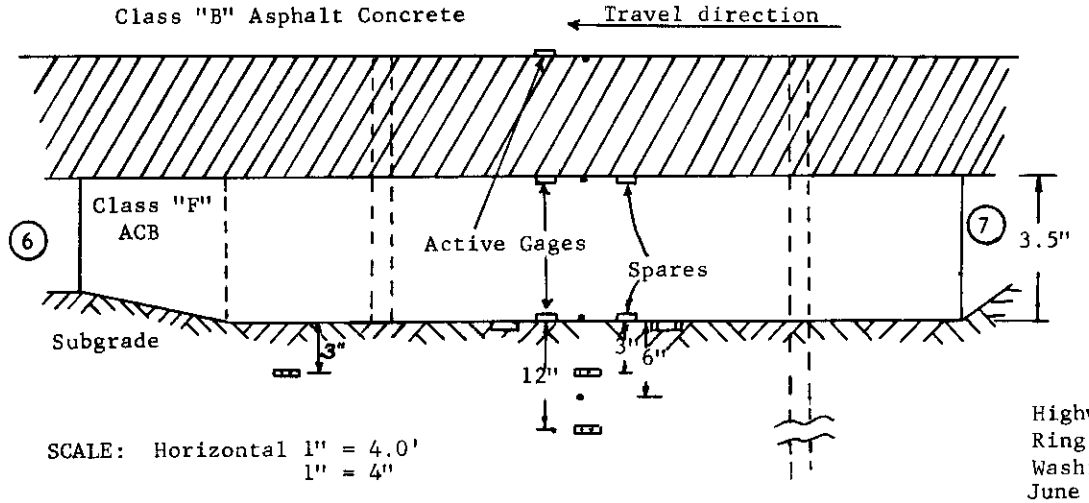

SCALE: Horizontal 1" = 4.0'
1" = 4"

Highway Research Section
Ring No. 4 Y-993
Washington State University
June 1970 M. Krukar

TABLE 8: LOCATION OF INSTRUMENTS ALONG CENTER LINE

Type of Instrument	Subgrade		Base	Surface
	Below	On Top	On Top	On Top
	Sections	Sections	Sections	Sections
Moisture Tensiometers[a]	2,7,8,10,11	---	---	---
WSU Hydraulic Cell	---	7,8	---	---
WSU Strain Gage Cell	---	2,4,7,8, 10,12	---	---
Thermocouples	1-12	1-12	1-12	1-12
Strain Gages[b]	---	2,4,7,10, 12	2,4,7,8, 10,12	1-12
LVDT[c]	---	---	---	2,4,7,10

[a] Only one moisture tensiometer was installed in these sections.

[b] The strain gages were installed in pairs; one longitudinal to the direction of travel and the other transverse. Spares were also installed except on the surface.

[c] One shallow and one deep LVDT gage was installed on each of these sections to measure the pavement structure and system dynamic deflections respectively.

the WSU hydraulic cells and the moisture probes, were wired into permanent junction boxes. The cables from these boxes were connected to an amplifier, manual switching panel and recorder. The thermocouples were wired directly into an automatic Honeywell recorder. All of the instruments, with exception of the thermocouples, were manually switched when readings were desired. Static deflections were taken with a Benkelman beam.

Measurement of Moisture

The moisture in the subgrade during construction was measured by nuclear methods. Five moisture tensiometer probes were installed to measure the amount and movement of water in the silt subgrade. These probes work on the principle that moisture tension between the soil particles causes soil suction. Porous ceramic cups filled with water are attached by long capillary-like copper tubing to a Bourdon dial gage. As the surrounding soil dries out, tension within the water film draws the water from the porous cup. This suction registers in centibars on the Bourdon gage. High readings on the dial indicate dry soil.

Several moisture probes were calibrated in the laboratory on the wetting cycle. The calibration graphs for these probes exhibit a hysteresis effect; one curve for the drying cycle and another for the wetting cycle (14). The previous reports (2, 3) showed typical calibration curves obtained for the Palouse silt.

The probes were installed in holes bored with an auger. Twenty-four hours before installation, the ceramic cups were saturated with de-aired distilled water. The ceramic probes were installed in pre-wetted holes in a vertical position to make filling and removal of air bubbles easier. They were then filled with distilled water and purged. The copper leads were laid on top of

the subgrade and were protected during construction. All leads were placed so the gages would be on the outside shoulders of the track to facilitate reading.

Five moisture probes were installed in this ring because these were the only ones which were undamaged from Ring 3. Unfortunately, due to the late start in testing, frost came early and damaged the Bourdon gages so that no data was obtained.

Temperature Measurements

Iron-constantan thermocouples: Forty-eight Pall Trinity Micro iron-constantan thermocouples type 20-J-TF were installed in four different positions in each section: top of wearing course, top of base, bottom of base, and 6 inches below subgrade. Each conductor was insulated with extruded Teflon with an overall insulation of extruded Teflon. The ends were bared, sanded clean, crimped together, fused and then dipped in a casing full of epoxy for water-proofing. The thermocouples were then hooked up to permanent junction boxes from which leads were connected to a direct-reading automatic modified 48-point Honeywell recorder. Each thermocouple reading took 1½ minutes. No problems developed with this system.

Thermograph: A two-pen, semi-automatic recording Belfort Instrument Thermograph (one for recording daily air temperature and the other for soil) was installed outside the test track. The recorder had to be wound up every 7 days; the charts were released every 7 days. This instrument recorded temperature continuously for the duration of the test.

Stress Measurements

WSU pressure cells: These cells were similar to those used in Rings #1 and #2, and were calibrated in an air pressure chamber. They were placed in sections 7 and 8 on top of the subgrade. A hole was dug in the compacted subgrade and leveled with fine silica sand. The cell was then put in flush with the subgrade elevation and covered with a layer of fine silica sand to protect the bed from pressure points. The system was connected to a manometer board in the tunnel. Operational difficulties with purging resulted in obtaining very little useful data.

WSU strain gage pressure cells: Six pressure cells with strain gages were installed in sections 2, 4, 7, 8, 10 and 12. These pressure cells are similar to other types of strain gage cells; their diameter is 7 inches and 3/4-inch thick. Four were working and recording after installation. Calibration was done in an air pressure chamber. Installation procedure was similar to that used for the WSU pressure cells. These cells were connected to a Brüel and Kjaer switching panel, a Brush amplifier and recorder.

Strain Measurements

Shinkoh polyester SR-4 P#20 strain gages were used for the measurement of strain. Strain gages in longitudinal and transverse positions were installed on the surfaces, bases and subgrades as shown in Figure 17.

Strain gages (subgrade): Extensometers were used for installing strain gages in loose material, such as the subgrade and crushed rock. They were installed in sections 2, 4, 7, 10 and 12. The extensometer design is basically the same as those used in Ring #2. More care was taken in the waterproofing and protection of the leads. They were placed in a strained position and longitudinal and transverse position in the subgrade and covered with a thin

layer of asphalt concrete. In addition to extensometer, strain gages were installed on 11" x 7" asphalt shingle roofing, which were then installed in subgrade in sections 2, 4, 7 and 10. This was done to compare strain readings. It was felt that asphalt shingles had a modulus of elasticity more in keeping with that of the treated bases, and that the extensometers gave lower strain readings than anticipated (15).

Strain gages (bases and surfaces): Extensometers were used in placement of strain gages on top of the untreated base (sections 10 and 12). For mounting on the asphalt and emulsion bases, the surface was prepared by filling it with a silicone seal to level the surface and give consistency of strain to the gage. After curing, the surface was sanded where necessary and the gage and mounting blocks were epoxied, then connected to Belden strain gage wire. A tack coat of SS-1 emulsified asphalt was applied and covered with fine asphalt concrete mix. Several of these strain gages mounted on asphalt shingles were placed and installed on top of bases in sections 4, 10 and 12. This was done for comparison with extensometers and regular strain gages. These were protected in the same manner as previously mentioned.

Strain gages were installed on all sections on the surface. Grooves using dowels were made in the Class "B" asphalt concrete wearing course during compaction. The asphalt surface was ground down and sanded; the gages were epoxied under pressure with standard gage epoxy. A rubberized paint was used for waterproofing and protecting the strain gages. Then a BLH Barrier E, a patch-type instant waterproofing, was stuck over the gages. Although it was easy to apply, the tires had a tendency to distort the patching which destroyed the strain gages. It was found that patching material did not work well on the test track surface under the tire loads.

Deflection Measurements

Dynamic deflection measurements: Four short 585 DT-100 and four long 585 DT-500 Sanborn Linear Variable Differential Transformers (LVDT) gages were installed. The short LVDT's measured deflection of the pavement structure; that is, the wearing course and base with respect to the subgrade. The long gages measured the dynamic displacement of the total pavement system. Holders for the gages were constructed at the Research Division's machine shop.

Four deep and four shallow holes were diamond drilled through the asphalt wearing course and bases to the final depth placement of the gages and holders (see Table 9). The gages, which were calibrated before and after installation to insure proper readings, were then connected to the junction boxes which are permanently connected to a switching panel and recorder.

Rebound deflection measurements: These were measured with a Soiltest Benkelman beam at 5 fixed locations per section, longitudinally spaced 2½ feet apart (lettered from A to E) to obtain an average deflection value.

TABLE 9: DEPTH OF LVDT HOLES

Section	Shallow (In.)	Deep (Ft.-In.)
2	7.0	14 - 11.5
4	11.0	14 - 2.5
7	6.5	16 - 2.0
10	10.0	15 - 7.5

Read-out Equipment

A Brush amplifier with input boxes for strains and LVDT gages was utilized. Several manual switching panels were made by the Electrical Sciences Section,

WSU, to work with the B & K switcher. The system was manually operated and each strain gage, pressure cell and LVDT was individually switched into the system. The strain gages had to be balanced before read-out.

A Honeywell 24-point recorder, modified to take 48 readings, was used to record thermocouples automatically, one reading every 1.5 minutes. A semi-automatic Belford Thermograph was used to record daily air and soil temperatures.

PERFORMANCE OF TEST RING #4

Testing Periods

Full time testing began November 6, 1968, after several trial runs to test the reliability of the instruments. Testing was suspended on December 3, 1968, due to the advent of winter and after 143,370 wheel loads and 47,790 revolutions had been applied. Testing was done on a 7-day, 16-hour basis whenever possible. Appendix A shows how many wheel loads were applied each day during the testing periods.

Signs of distress appeared in all the untreated base sections 9 to 12, and in section 5 which had no base. No signs of distress except for minor rutting were observed in the remaining sections. Section 9 and part of section 10, 4.5 and 7.0 inches of untreated base respectively, were declared to have failed (10).

A constant speed of 20 mph was maintained up to 115,878 wheel loads; on November 24, the speed was reduced to 15 mph which was maintained until the end of the fall testing period.

Testing resumed on April 2 and continued until August 9 when the experiment was declared ended. At this time a total of 247,128 wheel loads and 82,376 revolutions had been applied; of these, 103,758 wheel loads had been applied during the spring and summer.

Sections 1, 2, 3, 6, 7, 10 and 11 with 2, 4 and 6 inches of sand-asphalt base, 2.0 and 3.5 inches of Class "F" asphalt-concrete base and 7.0 and 9.5 inches of untreated base respectively were declared failed in "ultimate failure"; the remaining sections 4, 8 and 12 have 8.0 inches of sand-asphalt base, 5.0 inches of Class "F" asphalt-concrete bases and 12.0 inches of untreated base respectively were declared failed due to severe rutting. Section 12 had a thin asphalt-concrete overlay (16, 17).

Speed during this period of testing was 10 mph and was slowed down when various sections started to fail.

Testing Conditions

Design Thickness

Special care was taken during construction to ensure that the proper specified base and wearing course thicknesses would be achieved. The subgrade was brought to the desired elevation and was checked by rod and level. It was still difficult to achieve the proper thickness due to the tight radius and the contractor's paving equipment. Cores were drilled before and after testing and thicknesses were checked along with densities. Table 10 shows the measured thicknesses and the deviations from design thicknesses. Densities of the cores were also measured and compared to laboratory and nuclear densities.

Speed

Speed was one of the variables which was kept as constant as possible during the testing period. This was kept at 20 mph until the break-up of the sections required reduction of speed for protection of the apparatus. Figure 18 shows speed versus wheel load applications. The figure illustrates that as the number of wheel loads increased, the speed was reduced. The graph

TABLE 10: CORE THICKNESSES AND DENSITIES

Sect.	Type	Design Thickness (in.)	Core Thickness (in.)	Deviation From Design (in.)	Ave. Nuclear Density lbs/cu.ft.	Core Density lbs/cu.ft.	Laboratory Density lbs/cu.ft.	Minimum Spec. Den. lbs/cu.ft.	Dev. From Min. Spec. Lab Density lbs/cu.ft.
1-12	CL "B" A.C.	3.0	3.16[1]	+0.16	147.5	146.3[3]	156.0	145.0[4]	+1.3
1	S.A.B.	2.0	2.03[2]	+0.03	111.2	115.5	128.1	108.9[5]	+6.6
2	S.A.B.	4.0	4.28[2]	+0.28	112.2	117.2	128.1	108.9	+8.3
3	S.A.B.	6.0	5.94[2]	-0.06	113.1	118.1	128.1	108.9	+9.2
4	S.A.B.	8.0	8.19[2]	+0.19	117.7	115.7	128.1	108.9	+8.8
6	CL "F" A.C.	2.0	2.12[2]	+0.12	143.8	144.6	156.0	145.0[6]	-0.4
7	CL "F" A.C.	3.5	3.69[2]	+0.19	145.1	146.8	156.0	145.0	+1.8
8	CL "F" A.C.	5.0	5.16[2]	+0.16	148.8	150.4	156.0	145.0	+5.4

[1] Average from 37 cores.

[2] Average from 4 cores.

[3] Average from 5 cores.

[4] This is 93% of the maximum laboratory density.

[5] This is 85% of maximum laboratory density.

[6] This is 93% of maximum laboratory density.

FIGURE 18. SPEED VERSUS TIME (EXPRESSED IN WHEEL LOAD REPETITIONS)

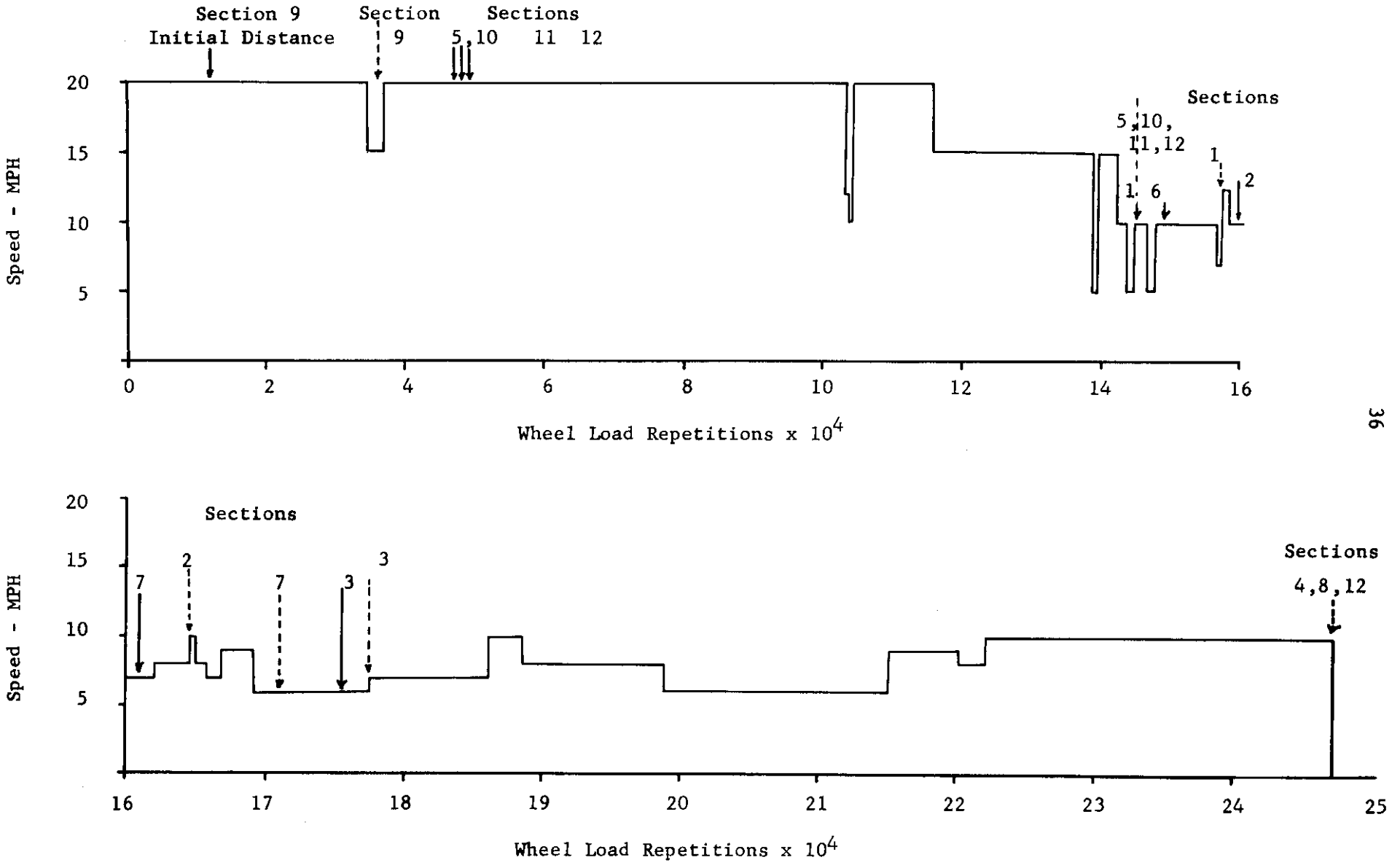

illustrates that the reduction in speed was definitely correlated with distress in the various sections.

Environmental Conditions

The testing pavement center is open to all the elements of weather, and hence is subject to all the variable effects caused by a changing environment.

All testing was done during a total of some 72 days--22 days in November-December, 1968 and 50 days in April-August 1969. In actual hours of running time, this amounted to a total of 311.5 hours--129.5 hours in the fall and 182.0 hours in spring and summer.

Table 11 shows the amounts of precipitation that occurred during the operations of Ring #4; this table also shows the weekly high and low air temperatures, and the temperature variations.

The table shows that experimental Ring #4 experienced large amounts of rain during the construction months of September and October. Rain and some snow were also heavy during the fall testing months of November and December. This was a period of steadily decreasing ambient temperatures.

The period during which the test track was idle (from December to the end of March), was one of the severest winters in the Palouse area in some 30 years. During the days of December 29, 30 and 31, this area was one of the coldest in the nation. This winter period also brought heavy snowfall.

The month of April, when testing resumed, was wet. The rest of the testing period was dry with steadily rising ambient temperatures. After the middle of May, the daily low temperatures seemed to have stabilized while the daily high temperatures kept on increasing until about the middle of July.

The significance of these temperature and precipitation differences results in the division of the two testing periods into three time and

temperature zones. The fall period from November to December, 1968 was wet and cold with an 8-10 degree variation between the maximum and minimum temperatures. The 1969 testing period can probably be divided into two periods--a spring period from April to May, and a summer period from June to August. The spring period was relatively wet with rising daily temperatures. The summer period was dry with large variations in daily high and low temperatures, usually of the magnitude of 25 to 40 degrees (see Table 11).

Experimental Results

Section Failures

Fall Period (1968): Several sections started to show signs of distress and ultimately failed during this period. Signs of distress in the form of transverse cracks appeared at 12,000 wheel load repetitions in section 9 with 4.5 inches of UTB; "ultimate failure" occurred at 36,681 wheel loads. Initial distress then occurred in sections 5 and 10, having 0.0 and 7.0 inches of UTB respectively. Distress occurred in sections 11 and 12, having 9.5 and 12.0 inches of UTB respectively at 47,391 and 49,104 wheel loads respectively. Testing ceased after 143,370 wheel load repetitions. Only section 9 had been declared failed and was removed. The remaining sections showing distress were not removed until spring testing began (see Tables 12 and 13).

The fall period was a period of wet weather and falling temperatures. Environmental conditions probably contributed significantly to the early distress of the untreated base sections.

Spring Period (1969): Sections continued to develop signs of distress, and section failures increased at an accelerated pace. Sections 5, 10, 11 and 12, which showed signs of distress in the fall, were declared failed and were removed soon after testing resumed; that is, at 144,600 wheel loads. The

TABLE 11: WEEKLY AMBIENT TEMPERATURES AND PRECIPITATION
RING NO. 4, 1968-69

Month	Week	Average Ambient Temperatures °F			Total Precipitation Inches	
		Maximum	Minimum	Variation		
September 1968	26-1	75.9	51.6	24.3	0.17	
	2-8	79.1	48.9	30.2	0	
	9-15	74.3	50.0	24.3	0.99	
	16-22	54.9	41.1	13.8	1.85	
	23-30	72.9	45.9	27.0	0	
October 1968	1-5	62.4	36.2	26.2	0	
	6-12	53.4	39.0	14.4	1.62	
	13-19	50.6	34.9	15.7	0.41	
	20-26	55.3	39.2	16.1	0.35	
	27-2	55.3	36.6	18.7	0.44	
November 1968	3-9[1]	43.3	33.3	10.0	0.90	
	10-16	40.4	31.9	8.5	0.88	
	17-23	46.6	34.1	12.5	0.98	
	24-30	41.1	32.3	8.8	0.46	
					Rain	Snow
December 1968	1-7[2]	40.9	29.1	11.8	0.73	3.2
	8-14	42.6	30.0	12.6	0.85	-
	15-21	31.7	20.7	11.0	0.58	3.5
	22-28	36.4	23.3	13.1	1.03	12.5
	29-31	2.3	-24.7	27.0	0.60	8.5
January 1969	1-4	28.8	6.3	22.5	0.20	0.5
	5-11	35.6	27.7	7.9	1.85	13.5
	12-18	32.4	19.7	12.7	0.64	6.6
	19-25	24.7	2.9	21.8	0.35	6.2
	26-31	23.0	1.0	22.0	0.78	12.5
February 1969	1-7	32.7	20.4	12.3	0.11	1.5
	8-14	38.6	26.3	12.3	0.52	3.5
	15-21	35.3	26.1	9.2	-	-
	22-28	38.3	25.1	13.2	0.07	0.3

[1] Testing started on November 5, 1968.

[2] Testing was stopped temporarily on December 3, 1968.

TABLE 11 CONTINUED:

Month	Week	Average Ambient Temperatures °F			Total Precipitation Inches
		Maximum	Minimum	Variation	
March 1969	1-7	39.4	27.9	11.5	0.23
	8-14	34.3	20.0	14.3	-
	15-21	49.7	33.9	15.8	0.53
	22-28	52.7	33.3	19.4	0.22
	29-31	60.3	40.7	19.6	0.05
April 1969	1-7[3]	48.6	36.0	12.6	0.35
	8-14	55.6	36.0	19.6	0.57
	15-21	57.6	37.6	20.0	0.35
	22-30	57.7	37.6	20.1	1.49
May 1969	1-7	54.0	35.3	18.7	-
	8-14	75.9	45.7	30.2	-
	15-21	64.4	43.3	21.1	-
	22-28	73.7	53.7	20.0	-
	29-31	66.0	44.0	22.0	-
June 1969	1-7	81.6	53.6	28.0	0.07
	8-14	79.1	49.6	29.5	-
	15-21	83.0	48.6	34.4	-
	22-30	62.8	46.3	16.5	0.93
July 1969	1-7	72.4	46.4	26.0	-
	8-14	78.9	50.6	28.3	-
	15-21	82.3	42.9	39.4	-
	22-31	85.7	49.1	36.6	-
August 1969	1-7	80.4	43.1	37.3	0.05
	8-14[4]	83.9	48.0	35.9	-
	15-21	81.7	48.9	32.8	-
	22-31	80.0	47.1	32.9	-

[3] Testing resumed on April 2, 1969.

[4] The experiment was declared ended on August 9, 1969.

TABLE 12: SECTION CONDITION PROGRESS REPORT

Base Type	Section	Base Thickness (Inches)	First Appearance of Distress		Section Declared Failed		Condition at 247,128 Wheel Loads
			Wheel Loads	Date	Wheel Loads	Date	
Sand-Asphalt (SAB)	1	2.0	144,660	04-04-69	157,020	05-20-69	Replaced
	2	4.0	159,789	05-26-69	164,790	05-28-69	Replaced
	3	6.0	175,620[1]	06-18-69	177,501	06-20-69	Section continued to rut despite overlay
	4	8.0	175,620[1]	06-18-69	247,128	08-09-69	Excessive surface deformation
CL "F" Asphalt Concrete (ACB)	5	0.0	47,391	11-16-68	144,660	04-04-69	Replaced
	6	2.0	148,887	04-29-69	158,235	05-22-69	Replaced
	7	3.5	161,262	05-27-69	171,168	06-06-69	Replaced
	8	5.0	175,620[1]	06-18-69	247,128	08-09-69	Excessive surface deformation
Crushed Surfacing Top Course (UTB)	9	4.5	12,000	11-08-68	36,681	11-10-68	Replaced
	10	7.0	47,391	11-16-68	144,660	04-04-69	Replaced
	11	9.5	48,000	11-16-68	144,660	04-04-69	Replaced
	12	12.0	49,104	11-16-68	247,128[2]	08-09-69	Excessive surface deformation

[1] Distress for these sections was rutting, while for the rest it was the start of initial cracking.

[2] This section had an asphalt concrete overlay for improvement of riding qualities just after start of spring testing.

TABLE 13: RING 4 PAVEMENT PERFORMANCE SUMMARY
FALL & SPRING PERIODS

Base Type	Section	Base Thickness (In.)	First Appearance of Cracking				Section Failure			
			Date	Wheel Load Applications			Date	Wheel Load Applications		
				Fall	Spring	Total		Fall	Spring	Total
Sand Asphalt Base (S.A.B.)	1	2.0	4-4-69	1	1,290	144,660	5-20-69	143,370	13,650	157,020
	2	4.0	5-26-69	1	16,419	159,789	5-28-69	143,370	21,420	164,790
	3	6.0	6-18-69	1	32,250[4]	175,620	6-20-69	143,370	34,131[5] 69,621[6]	177,501[5] 247,128[6]
	4	8.0		1			8-9-69	143,370	103,758	247,128
Cl "F" Asphalt Concrete Base (A.C.B.)	5	0.0	11-16-68	47,991		47,391	4-4-69	143,370	1,290	144,660
	6	2.0	4-29-69	1	5,517	148,887	5-22-69	143,370	14,865	158,235
	7	3.5	5-27-69	1	17,892	161,262	6-6-69	143,370	27,798	171,168
	8	5.0		1			8-9-69	143,370	103,758	247,128
Crushed Surfacing Top Course Untreated (U.T.B.)	9	4.5	11-8-68	12,000		12,000	11-10-68	36,681		36,681
	10	7.0	11-16-68	47,391		47,391	11-20-68	104,187[2]		104,187[2]
	11	9.5	11-16-68	48,000		48,000	4-4-69 4-4-69	143,370 143,370	1,290 1,290	144,660 144,660
	12	10.0	11-16-68	49,104		49,104	4-4-69 8-9-69	143,370	1,290[3] 102,468[6]	144,660[3] 247,128[6]

[1]
[2]Section did not crack or fail in the time period indicated.
[3]One-half section 10 was removed.
[4]This section was overlaid with 1-1 1/2" of hot asphalt concrete mix.
[5]Section started to rut very badly.
[6]An asphalt concrete overlay 1 1/2-2 1/2" deep was put on this section.
Wheel loads applied with overlay.

exception was section 12 which was overlaid with asphalt concrete. Distress appeared in sections 1, 6, 2, 7 and 3 in that order at 144,660; 148,887; 159,789; 161,252 and 175,620 wheel loads respectively (Tables 12 and 13).

Sections 1, 2, 3, 5, 6, 7, 10 and 11 were declared failed during this period. Section 3 was declared failed when deep ruts of over 2-inch depth occurred and had to be overlaid with asphalt concrete. At the end of the period only sections 4 and 8 did not have any cracks. The remaining sections 4, 8 and 12, the latter having an asphalt concrete overlay, were badly rutted. Testing was halted at 247,128 wheel loads.

The spring period can be divided into a spring period characterized by rising temperatures with precipitation and a summer period characterized by high temperatures and dry hot weather (Table 11).

Failure pattern: The failure patterns of the sections in Rings #2, #3 and #4 for the two periods had enough similarity so that a general failure pattern could be established. Pavement distress seemed to follow this pattern:

1. Ruts start to develop.
2. Visible flexing of the pavement section.
3. The appearance of a few transverse cracks of varying lengths and the pumping of mud through them. Since pumping depends upon wetness, cracking and pumping may or may not occur simultaneously, depending upon environmental conditions.
4. The transverse cracks lengthen and increase in frequency with or without pumping.
5. The appearance of a longitudinal crack along the wheel path center with some noticeable permanent pavement subsidence and pumping. Pumping may or may not increase depending upon the weather.
6. Alligator cracking appearance and more settlement.
7. Longitudinal cracks appear at edge of the wheel path, with extensive subsidence of the traveled part of the pavement. The untraveled part of the pavement may bulge.

8. It becomes necessary to fill in the distressed sections to keep the frame from dragging. At this point the section is declared failed.

This is the usual distress pattern although there may be variations and omissions, depending upon the time period. During the fall period, the first two patterns were not as evident as in the spring period. This may be due to the pavement temperature differences. During the spring, steps 5 and 6 were often by-passed, and instead a sudden longitudinal shear failure often occurred either on the inside or outside edge of the dual tires. As mentioned before, pumping of mud was a function of the environment. The different distress steps are shown in Figures 19-33, 36 and 37 for the fall period and Figures 34, 35 and 38-83 for the spring period.

In the fall, the failure pattern usually followed these steps:

1. Some visible flexing of the pavement section along with some settlement.

2. The appearance of a few transverse cracks of varying lengths and the pumping of mud through them. Since pumping depends upon wetness, cracking and pumping may or may not occur simultaneously, depending upon environmental conditions.

3. The transverse cracks lengthen and increase in frequency with or without pumping.

4. The appearance of a longitudinal crack along the wheel path center with some noticeable permanent pavement subsidence and pumping. Pumping may or may not increase depending upon the weather.

5. Alligator cracking appearance and more settlement.

6. Longitudinal cracks appear at edge of the while path with extensive subsidence of the traveled part of the pavement. The untraveled part of the pavement may bulge.

7. It becomes necessary to fill in the distress sections to keep the frame from dragging. At this point the section is declared failed.

In the spring, the failure pattern differed somewhat and usually followed these steps:

1. Ruts start to develop.

2. Very visible flexing of the pavement.

3. The appearance of a few transverse cracks of varying lengths and the pumping of mud through them. Since pumping depends upon wetness, cracking and pumping may or may not occur simultaneously, depending upon environmental conditions.

4. The transverse cracks lengthen and increase in frequency with or without pumping.

5. Longitudinal shear cracks appear at the edge of the dual tires. some alligator cracking pattern may occur, but is not fully developed.

6. Extensive settlement occurs followed by a longitudinal shear crack on the inside or outside edge of dual tires. The untraveled part of the pavement may bulge. Often this step does not occur throughout the pavement section but is localized.

7. It becomes necessary to fill in the distressed section to keep the frame from dragging. At this point the section is declared failed. For the thickest sections, steps 1 and 2 may occur with the ruts becoming so pronounced that testing cannot continue.

Discussion of Section Failures

Contrasts between fall and spring failures were evident. Table 12 (p. 41) was rearranged into Table 13 to show the number of wheel applications for the different time periods, the time of first distress and failure. These tables also show the amount of wheel loads needed to cause "ultimate" failure after the first appearance of cracking. "Ultimate" failure, as used here, means that the failure of the pavement was beyond practical limits reached in regular highway usage. In other words, on a regular highway the pavement would have been repaired long before the "ultimate" failure point was ever reached. Usually, when the skids on the loading arms started to drag on the pavement edge, "ultimate" failure was declared to have occurred. "Ultimate" failure is shown in Figures 20, 21, 24, 35, 40, 41, 48, 49, 55, 61, 69, 70, 73, 79 and 83.

Visible pavement deflection of over 0.09 inches and permanent deformation of about 1/8-inch depth usually preceded the appearance of transverse cracks in the fall period. The cracks usually started in weak areas located by Benkelman beam rebound measurements. Each section was divided into 5 areas spaced 2½ feet apart which were lettered from A to E as shown in Figure 84 (p. 108); rebound measurements were always taken at each marked line. Relatively higher readings pin-pointed the location where the first signs of distress would appear. Table 14 gives an indication of the size of these deflections prior to initial cracking for sections 1, 5 and 9. The relatively higher readings found in Lines A, C and A in sections 1, 5 and 9 respectively indicate a variance and a zone of weakness. Initial distress usually started at these points as shown in Figures 19, 36 and 44 on pages 48, 58 and 62 respectively.

Transverse cracks in section 9 with 4.5 inches of untreated base appeared with unexpected rapidity at 12,000 wheel loads around area A which was

(Text continued on page 84.)

TABLE 14: TYPICAL BENKELMAN BEAM REBOUND MEASUREMENTS-THIN SECTIONS
(Prior To Initial Cracking)

SECTION:		1	5	9
TYPE AND DEPTH:		2.0" SAB	0.0" Cl. "F" ACB	4.5" UTB
Wheel Loads Prior To Initial Cracks:		430,370	25,000	390
Temperature °F	Air:	56	47	45
	*Pavement:	70	49	52
Line		Benkelman Beam Measurements-Inches	Benkelman Beam Measurements-Inches	Benkelman Beam Measurements-Inches
A		0.168	0.049	0.117
B		0.135	0.049	0.108
C		0.108	0.052	0.095
D		0.113	0.045	0.112
E		0.097	0.046	0.060
AVERAGE		0.124	0.048	0.099
Date & Time		03-31-69 2:30 pm	10-09-68 11 am	11-06-68 1 pm
COMMENTS:		Transverse cracks started on Line A and worked themselves towards Line E.	Transverse cracks started at construction joint and at Line C which worked towards B and D.	Transverse cracks started in Line A and then worked towards B, C, and D.

*For sections 1 and 5, this was an average temperature of top of pavement surface, top of base and bottom of base; for section 9, this was an average of top of pavement surface and bottom of pavement.

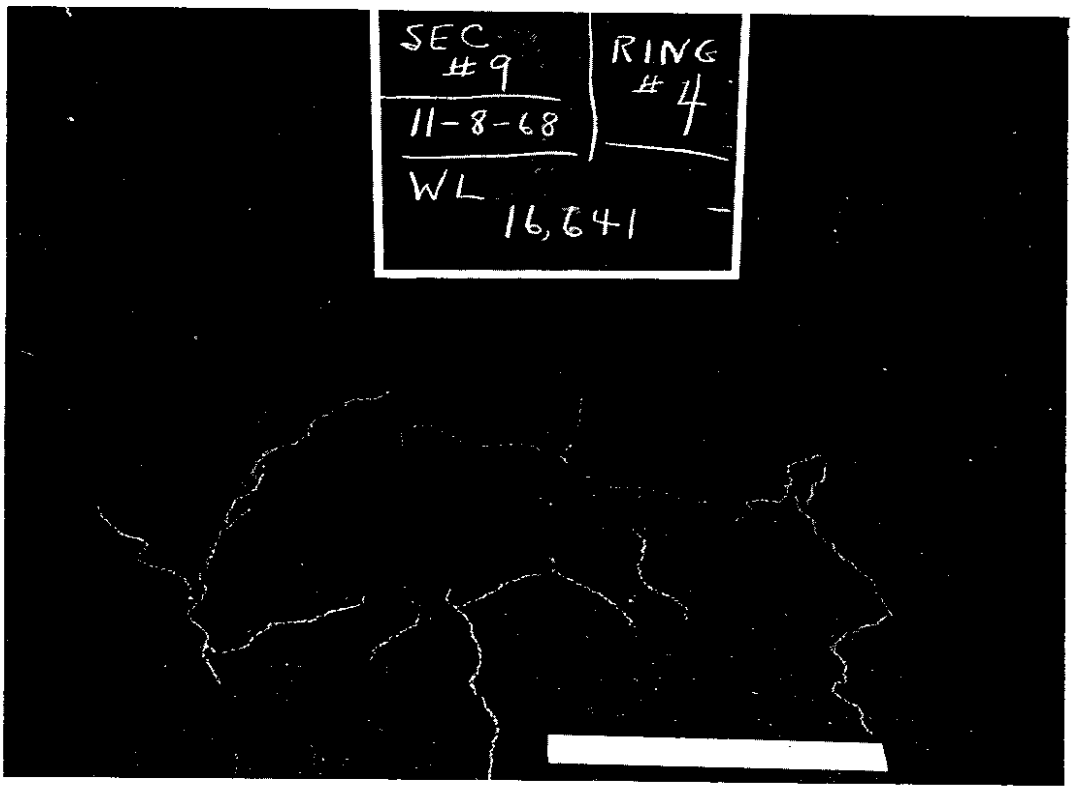

FIGURE 19. APPEARANCE OF SECTION 9, 4.5 INCHES OF UTB, AFTER 16,641 WHEEL LOADS. NOTE THE START OF ALLIGATOR CRACKING PATTERN. NOVEMBER 8, 1968-- LOCATION WAS AROUND LINES A AND B.

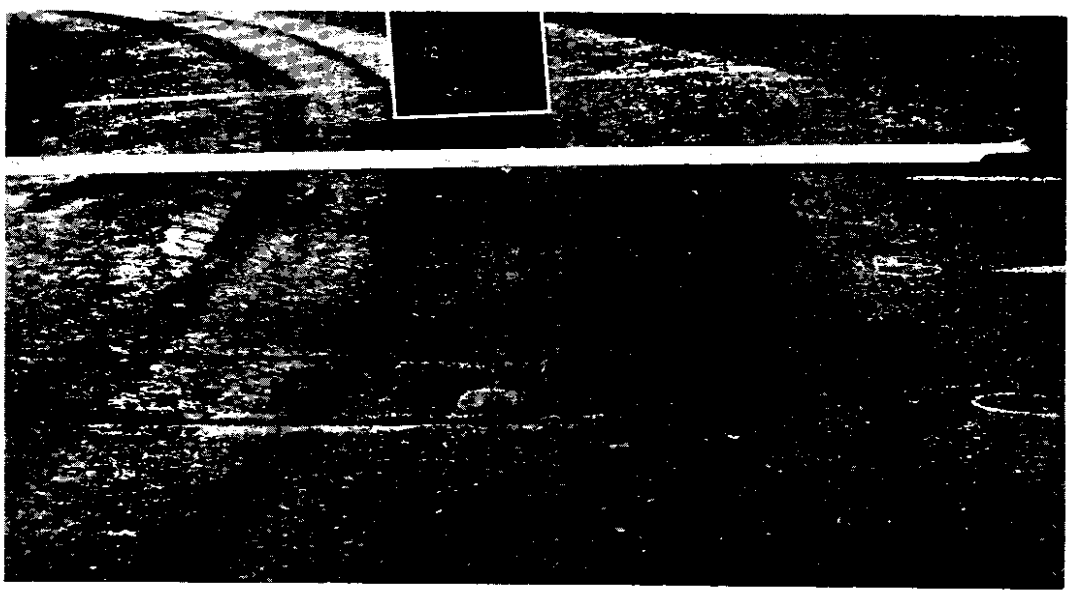

FIGURE 20. OVERALL APPEARANCE OF SECTION 9 AT "ULTIMATE FAILURE" AFTER 36,681 WHEEL LOADS. NOTE THE PERMANENT DEFORMATION IN THE WHEEL PATH. NOVEMBER 12, 1968.

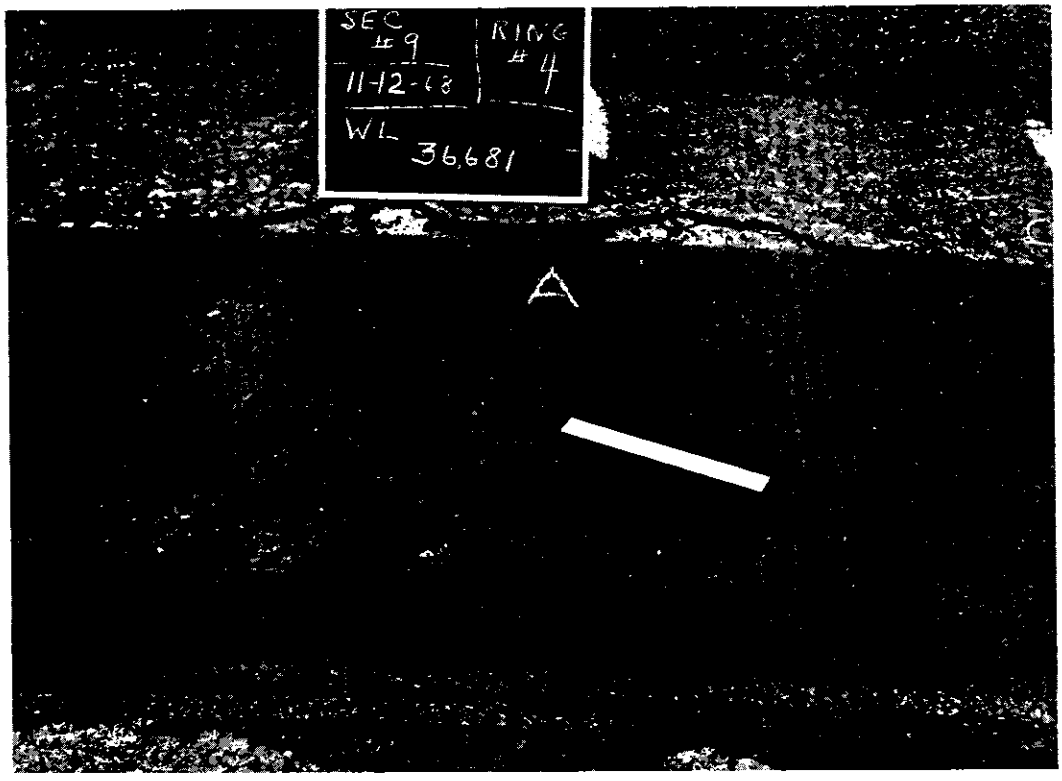

FIGURE 21. CLOSE-UP VIEW OF THE FAILED AREA OF SECTION 9, AFTER 36,681 WHEEL LOADS, NOVEMBER 12, 1968. NOTE THE LONGITUDINAL SHEAR FAILURE CRACKS ALONG BOTH EDGES OF THE WHEEL PATH, ALLIGATOR CRACKING PATTERN.

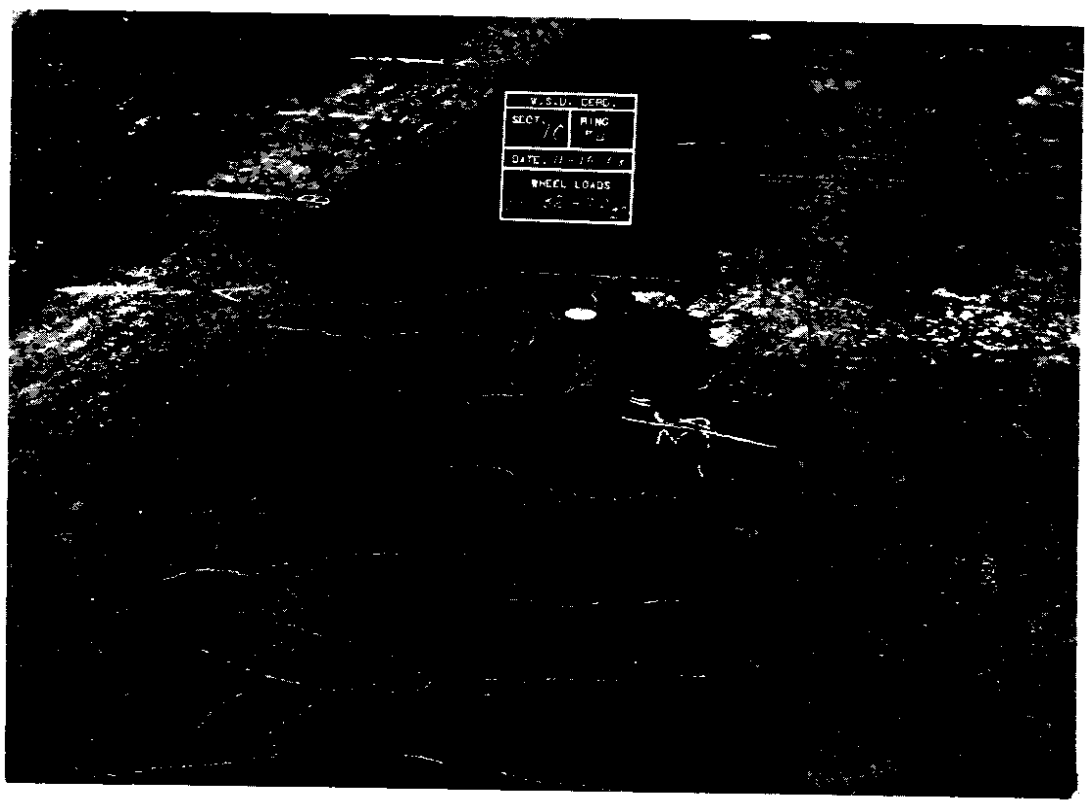

FIGURE 22. AN OVERALL VIEW OF SECTION 10, 7.0 INCHES OF UTB, AFTER 82,470 WHEEL LOADS ON NOVEMBER 18, 1968. NOTE THE TRANSVERSE CRACKS ESPECIALLY IN THE BOTTOM HALF OF THE PICTURE.

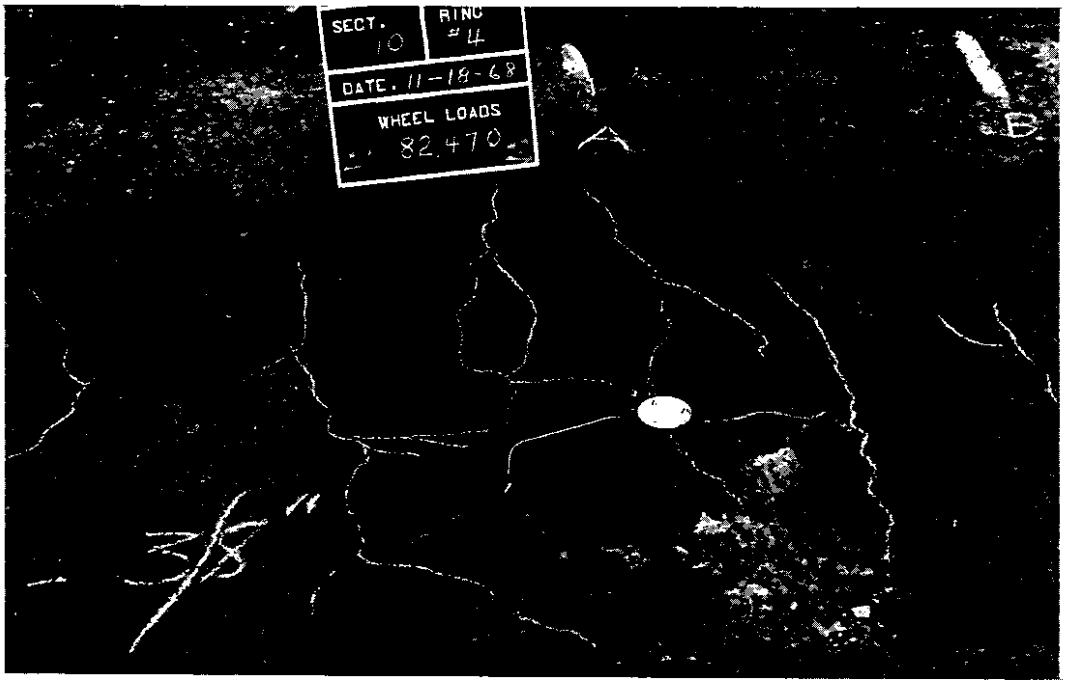

FIGURE 23. A CLOSE-UP VIEW OF THE CRACKS AROUND LVDT GAGE #7 AFTER 82,470 WHEEL LOADS IN SECTION 10.

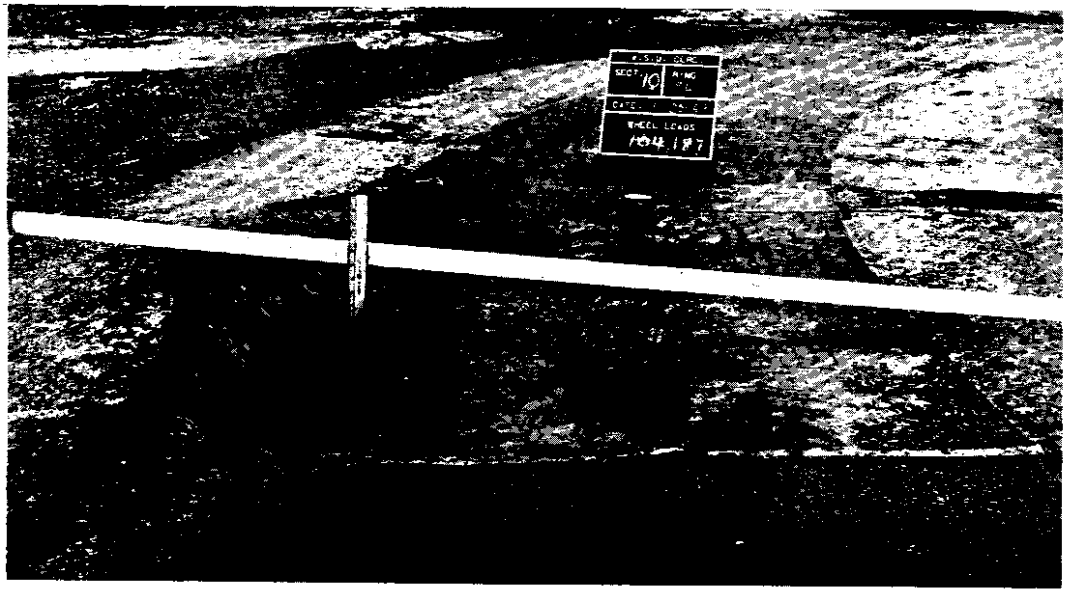

FIGURE 24. "ULTIMATE FAILURE" IN HALF OF SECTION 10 AT 104,187 WHEEL LOADS. THIS PART WAS REMOVED AND THE OTHER HALF OF THE SECTION WAS LEFT.

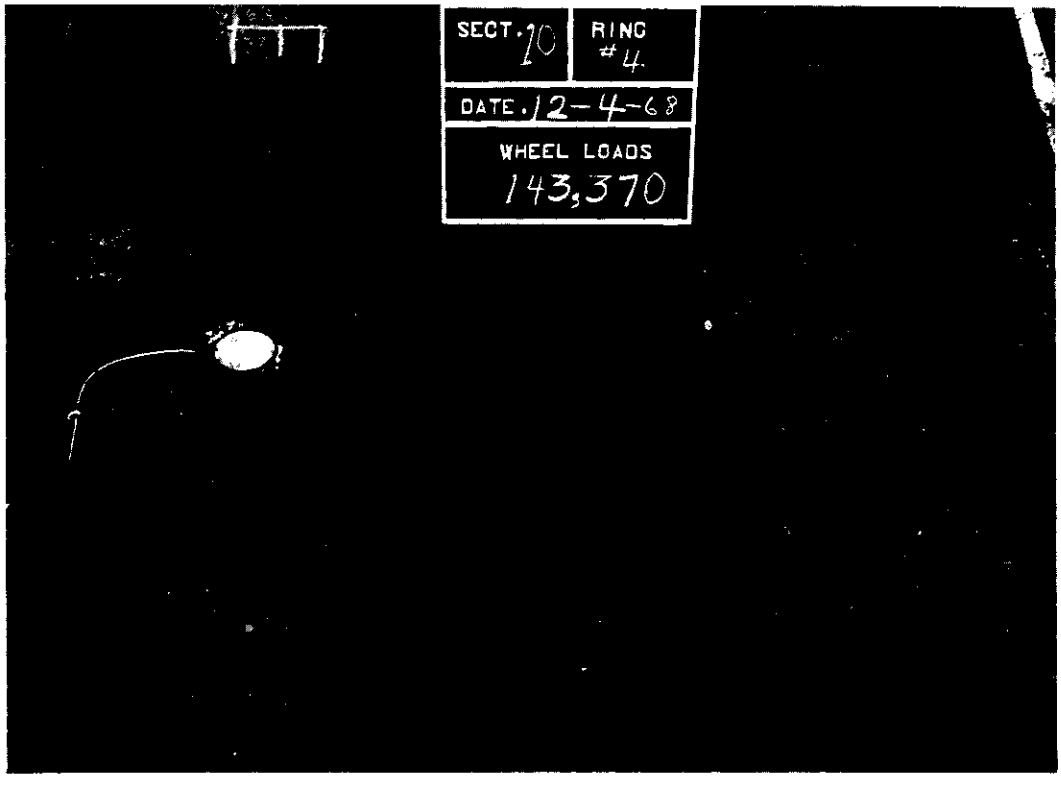

FIGURE 25. A VIEW OF SECTION 10 AT 143,370 WHEEL LOADS ON DECEMBER 4, 1968, AFTER THE TEST TRACK WAS CLOSED FOR THE WINTER. NOTE THE ALLIGATOR CRACKING PATTERN BEING FORMED. THIS FAILED IN THE SPRING AFTER AN ADDITIONAL 1,290 WHEEL LOADS.

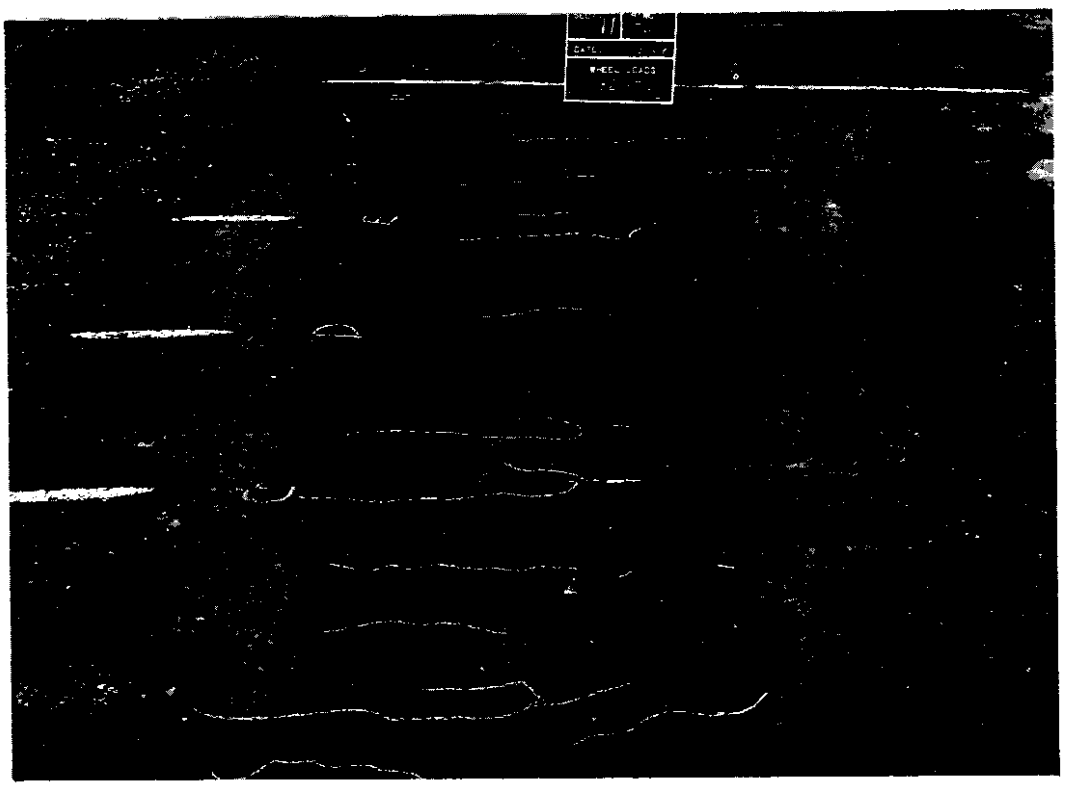

FIGURE 26. AN OVERALL VIEW OF THE EXTENT OF TRANSVERSE CRACKS IN SECTION 11, 9.5 INCHES OF UTB, AFTER 82,470 WHEEL LOADS-- NOVEMBER 18, 1968.

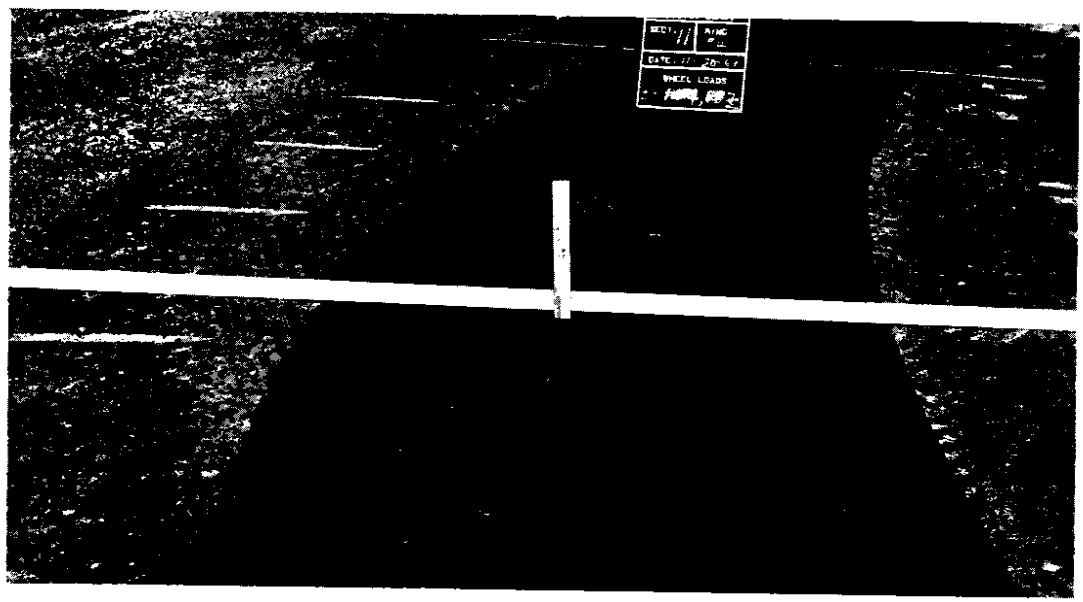

FIGURE 27. PERMANENT DEFORMATION OF ABOUT 3/4 INCHES IN SECTION 11 AFTER 104,187 WHEEL LOADS-- NOVEMBER 20, 1968. THE LIGHTING DOES NOT SHOW UP THE CRACKS.

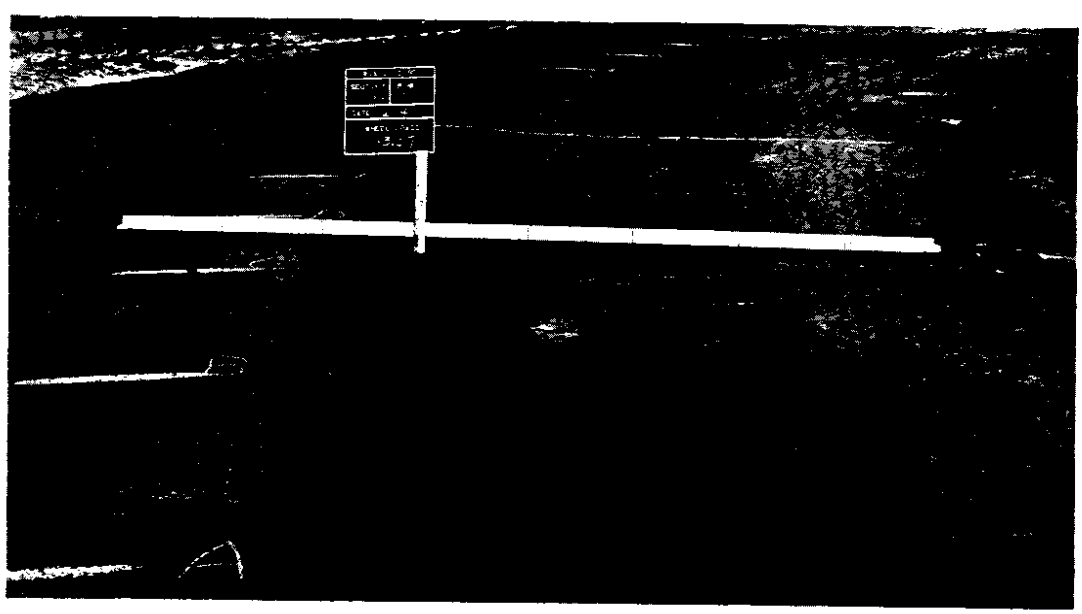

FIGURE 28. APPEARANCE OF SECTION 11 JUST AFTER THE TEST TRACK WAS CLOSED FOR THE WINTER AT 143,370 WHEEL LOADS-- DECEMBER 4, 1968. NOTE THE EXTENT OF THE CRACKING, BOTH LONGITUDINAL AND ALLIGATOR, AND THE DEPTH OF THE PERMANENT SETTLEMENT. THIS SECTION FAILED IN SPRING AFTER AN ADDITIONAL 1,290 WHEEL LOADS.

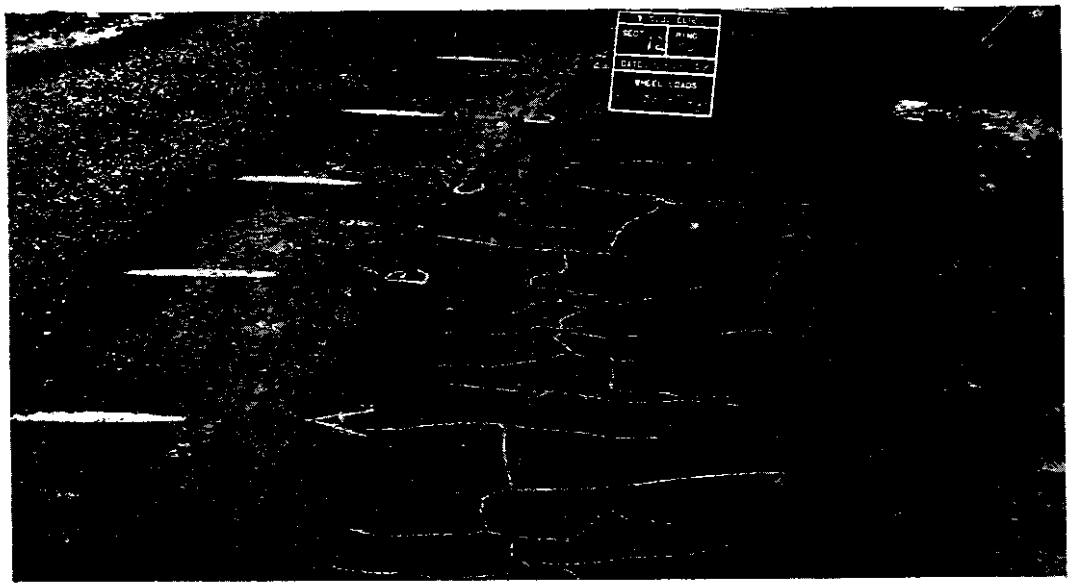

FIGURE 29. AN OVERALL VIEW OF SECTION 12, 12.0 INCHES OF UTB, SHOWING THE EXTENT OF THE CRACKING AFTER 82,470 WHEEL LOADS-- NOVEMBER 18, 1968.

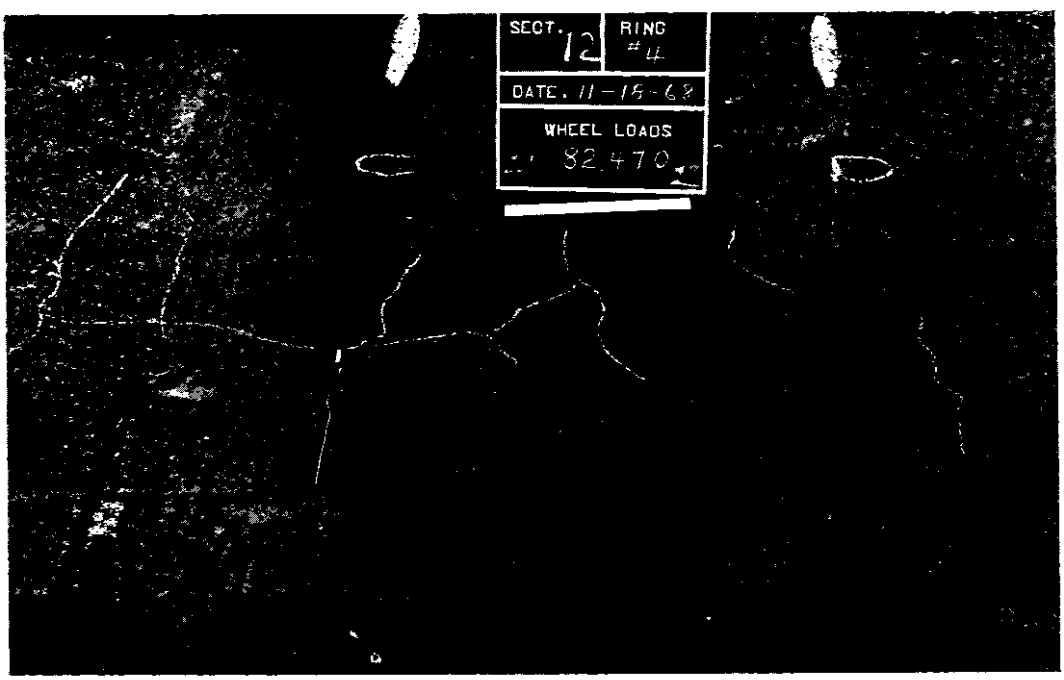

FIGURE 30. A CLOSE-UP VIEW OF SECTION 12. NOTE THE BEGINNING OF THE FORMATION OF AN ALLIGATOR CRACKING PATTERN.

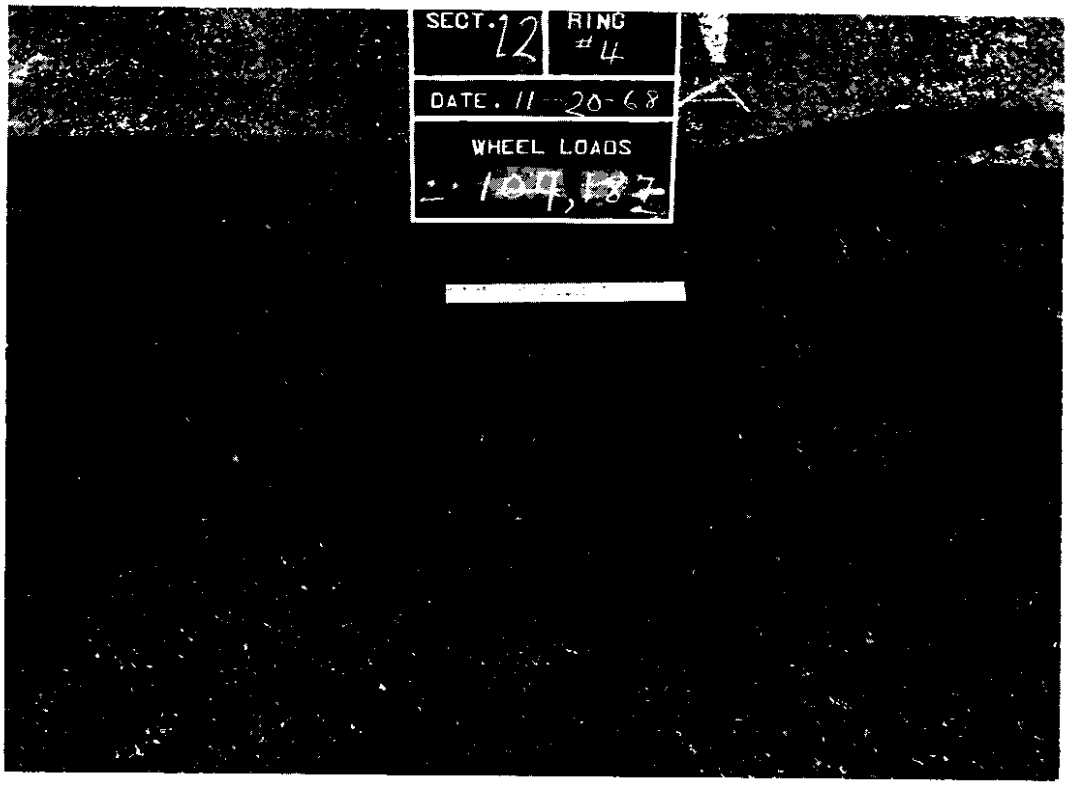

FIGURE 31. APPEARANCE OF SECTION 12 AFTER 104,187 WHEEL LOADS ON NOVEMBER 20, 1968. NOTE THE CRACKS IN THE PAVEMENT.

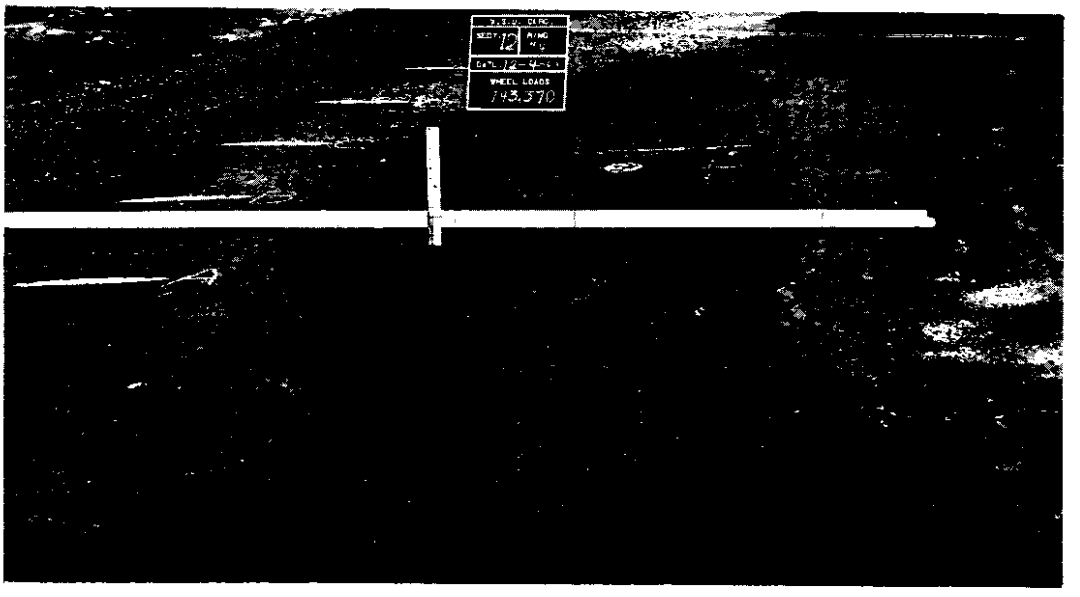

FIGURE 32. AN OVERALL VIEW OF SECTION 12 AFTER THE END OF FALL TESTING PERIOD AFTER 143,370 WHEEL LOADS-- DECEMBER 4, 1968. NOTE THE EXTENT OF THE LONGITUDINAL AND ALLIGATOR CRACKS AND THE DEPTH OF PERMANENT SETTLEMENT.

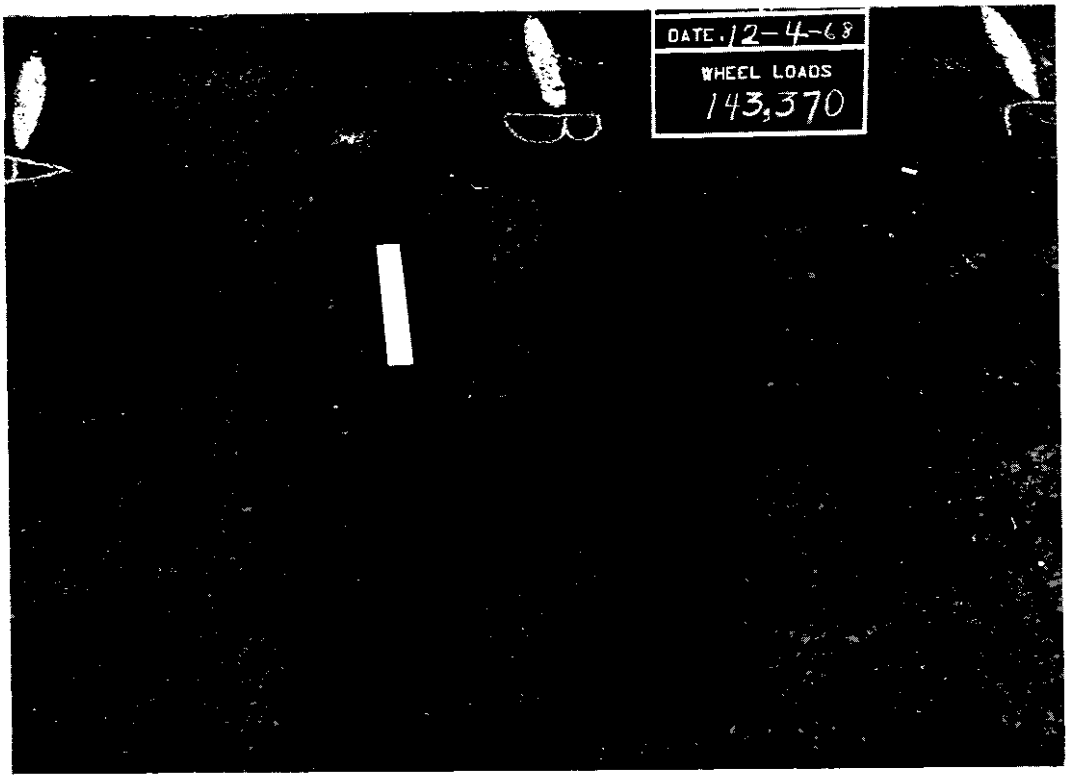

FIGURE 33. A CLOSE-UP VIEW OF SECTION 12 AFTER 143,370 WHEEL LOADS SHOWING THE ALLIGATOR CRACKING PATTERN AND THE LONGITUDINAL EDGE SHEAR CRACK ON THE OUTSIDE.

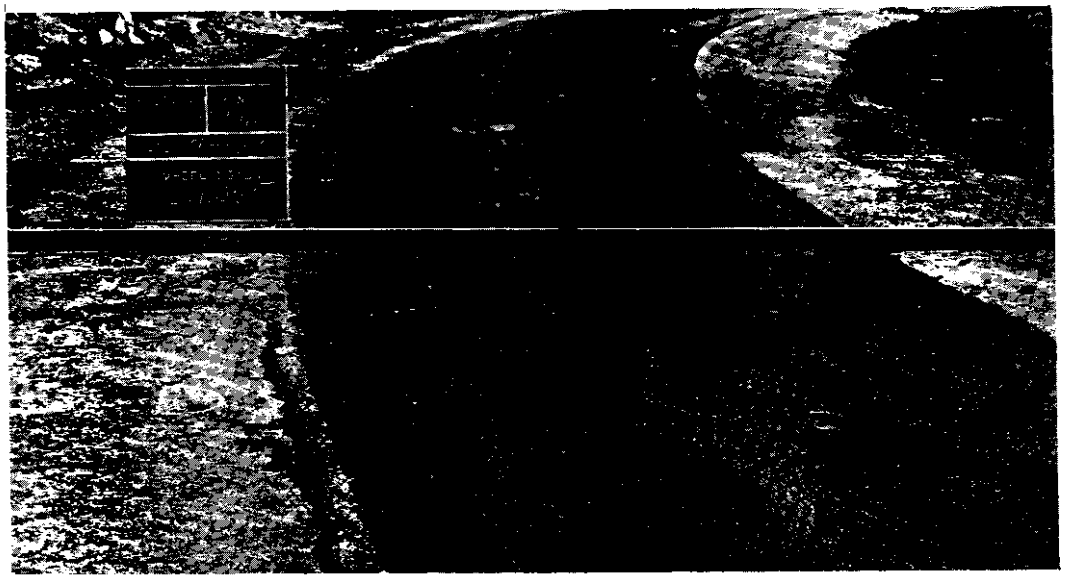

FIGURE 34. PERMANENT SETTLEMENT OF SECTION 12, WITH ASPHALT CONCRETE OVERLAY, AFTER 211,065 WHEEL LOADS ON JULY 18, 1969. NOTE THE RUTS.

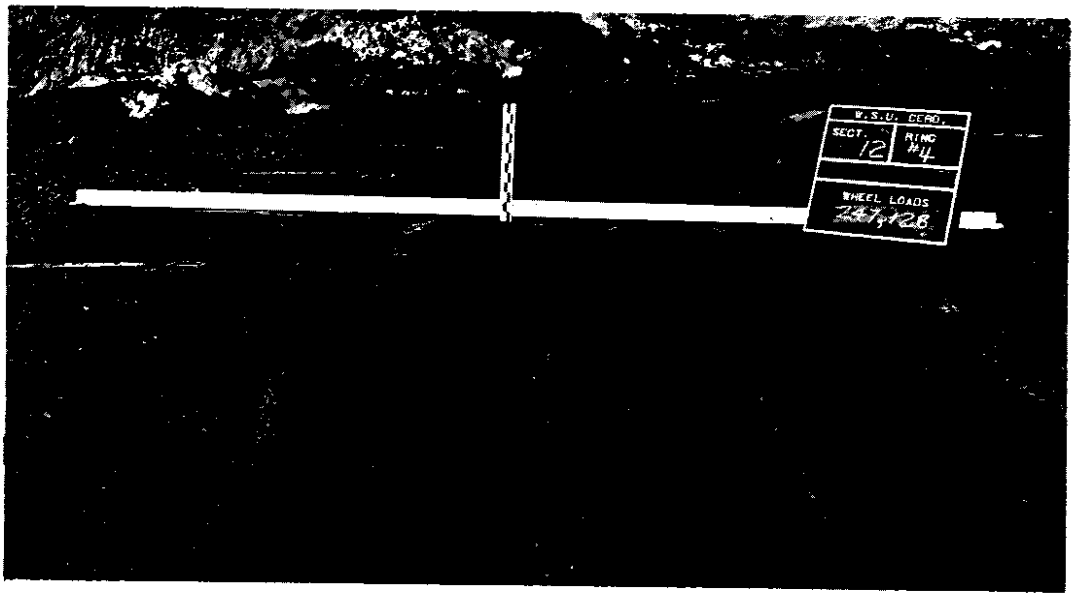

FIGURE 35. FINAL APPEARANCE OF SECTION 12 AFTER 247,128 WHEEL LOADS. NOTE THE RUTTING AND DEPTH OF PERMANENT DEFORMATION.

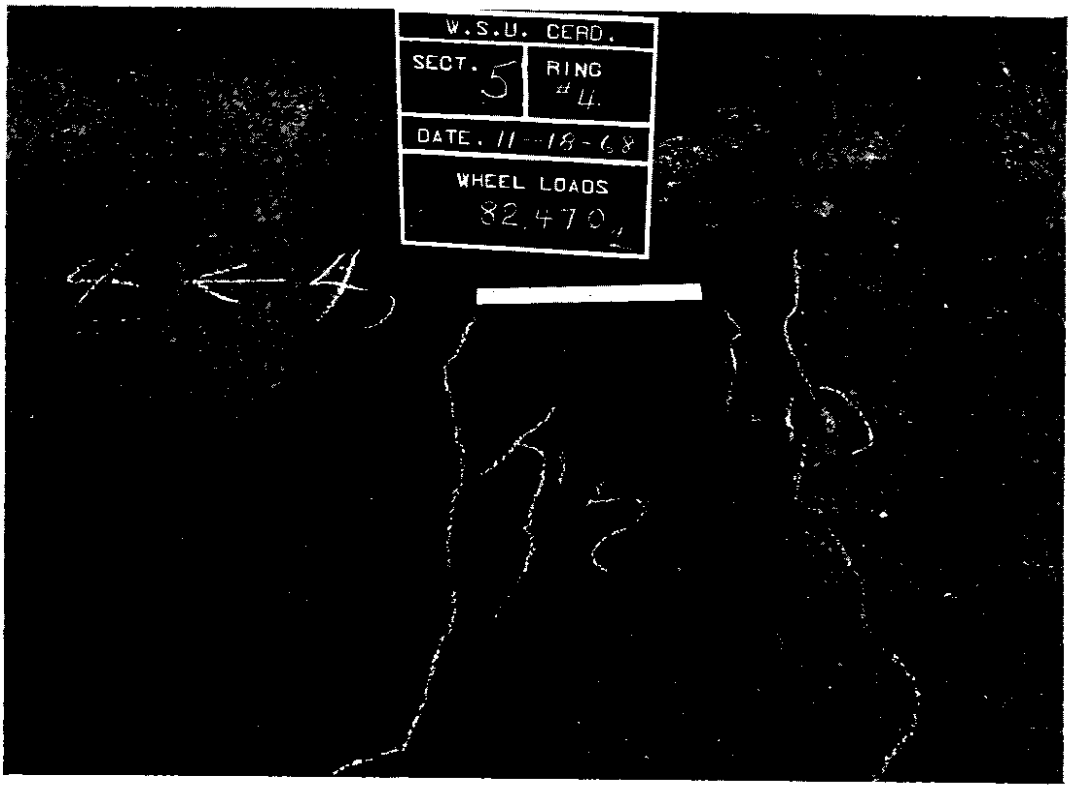

FIGURE 36. TRANSVERSE CRACKS AROUND CONSTRUCTION JOINT IN SECTION 5, 0.0 INCHES OF BASE AFTER 82,470 WHEEL LOADS--NOVEMBER 18, 1968.

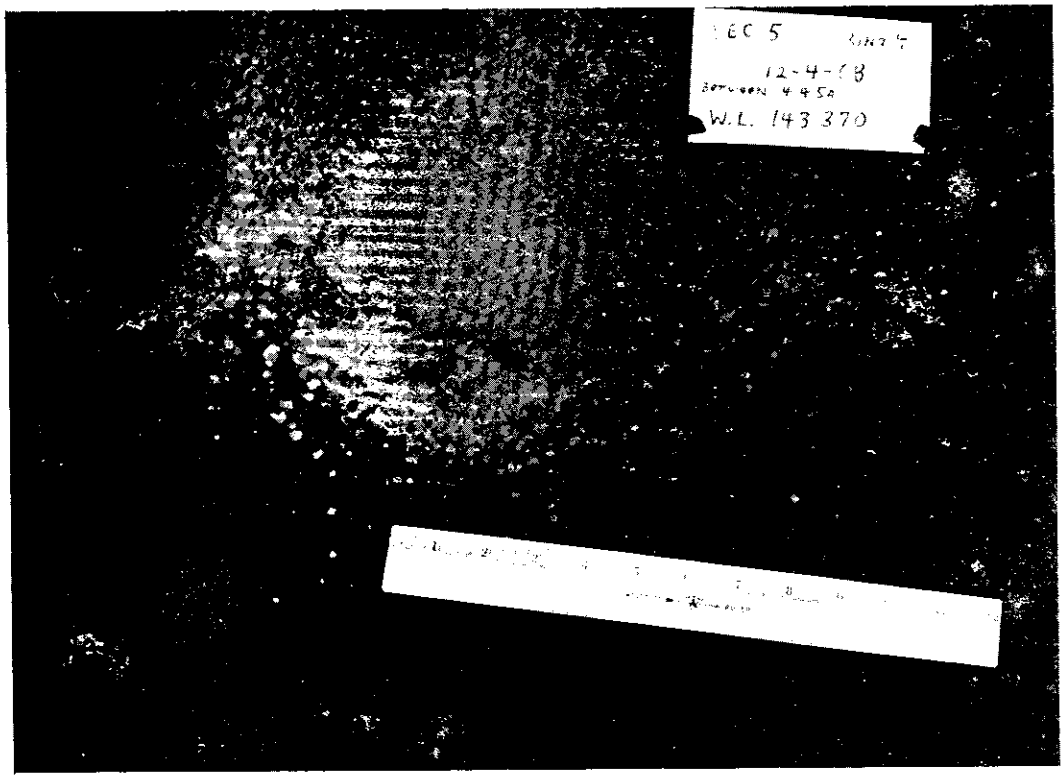

FIGURE 37. CLOSE-UP VIEW OF SECTION 5 AFTER 143,370 WHEEL LOADS TAKEN ON DECEMBER 4, 1968 JUST AFTER THE TEST TRACK WAS CLOSED FOR WINTER. NOTE THE TRANSVERSE CRACKS AND THE PUMPING OF SILT THROUGH ONE OF THE CRACKS.

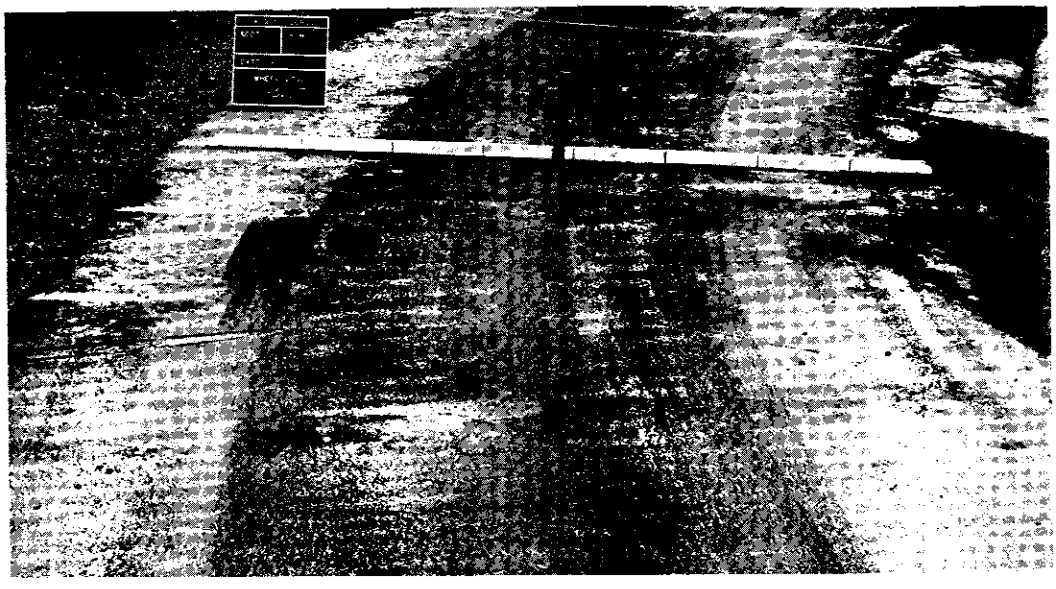

FIGURE 38. APPEARANCE OF SECTION 5 AFTER 143,370 WHEEL LOADS ON APRIL 2, 1969 PRIOR TO RESUMPTION OF TESTING IN THE SPRING. NOTE THE DEPTH OF PERMANENT SETTLEMENT AND THE TRANSVERSE CRACKS IN THE FOREGROUND AT THE JUNCTION OF THE CONSTRUCTION START AND END OF THE CLASS "B" ASPHALT CONCRETE PAVEMENT.

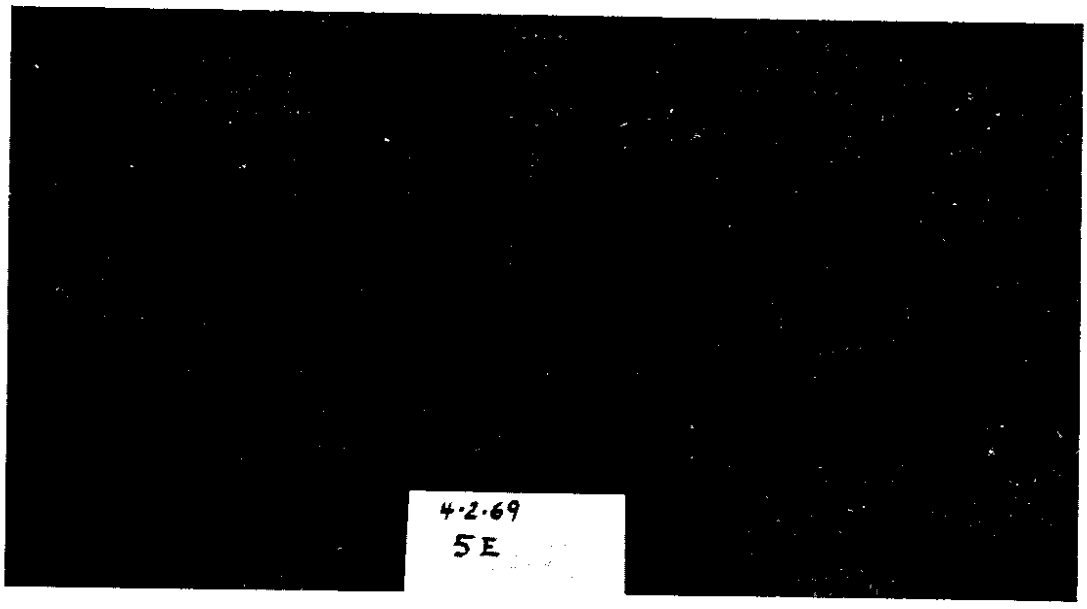

FIGURE 39. CLOSE-UP VIEW OF TRANSVERSE CRACKS IN SECTION 5 AT 143,370 WHEEL LOADS PRIOR TO RESUMPTION OF TESTING IN THE SPRING OF 1969.

FIGURE 40. OVERALL VIEW OF "ULTIMATE FAILURE" IN SECTION 5 AFTER 144,660 WHEEL LOADS ON APRIL 4, 1969. NOTE THE EXTENT OF THE LONGITUDINAL SHEAR FAILURE AND THE DEPTH OF PERMANENT DEFORMATION.

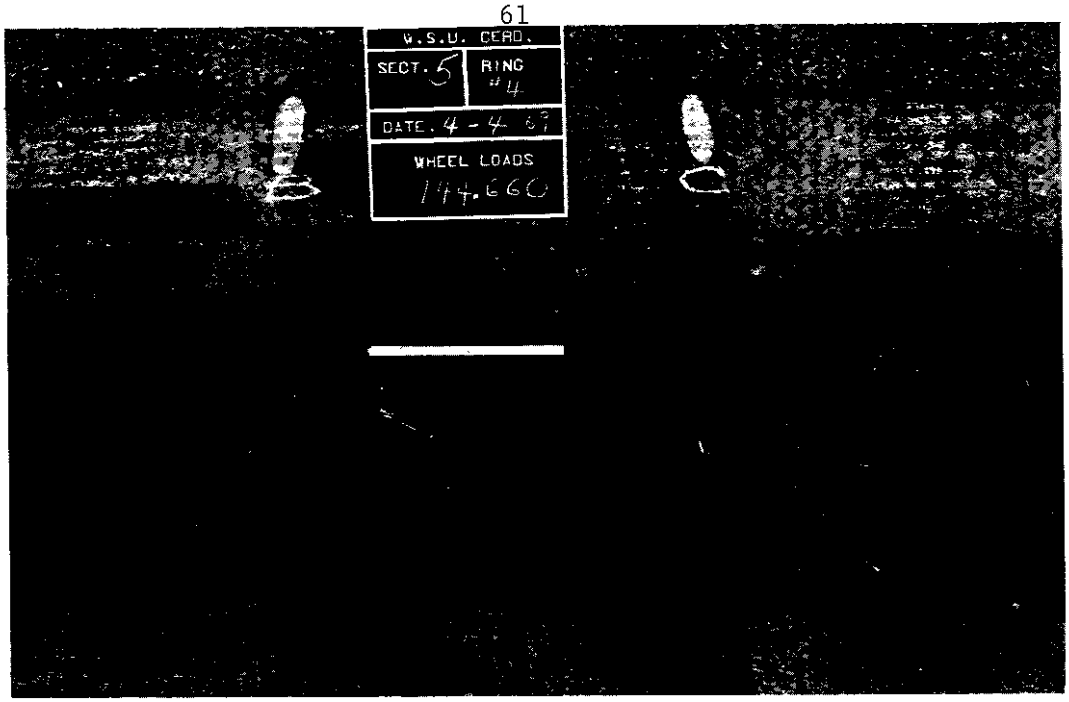

FIGURE 41. CLOSE-UP VIEW OF THE "ULTIMATE FAILURE" IN SECTION 5.

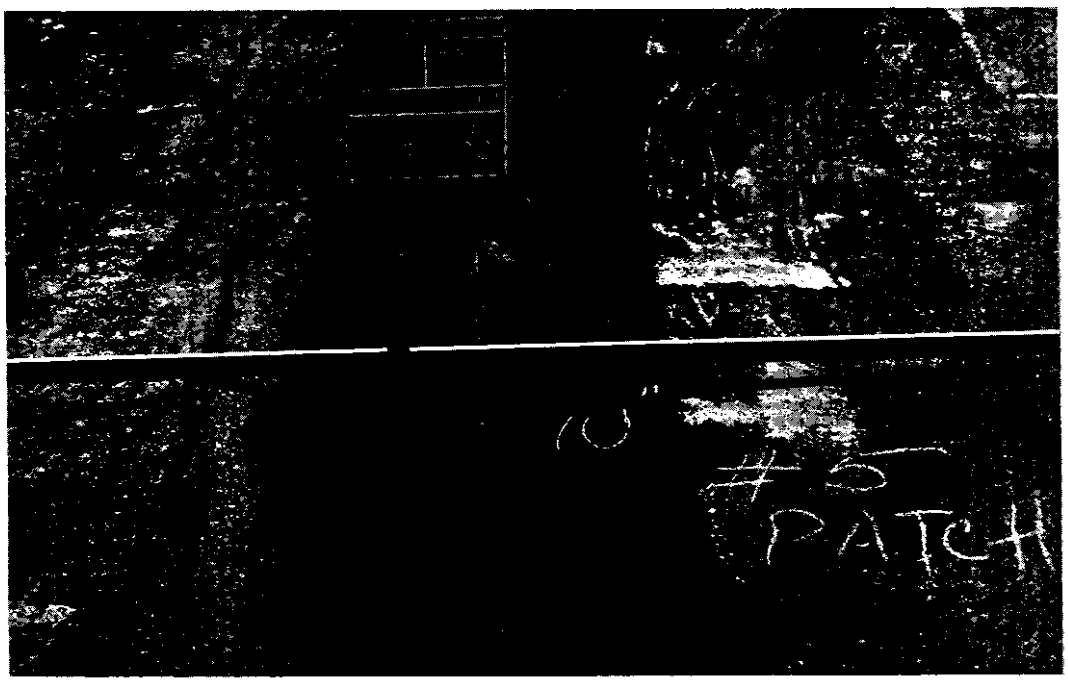

FIGURE 42. CONTINUED FAILURE OF THE 10-INCH ASPHALT CONCRETE OVERLAY IN SECTION 5 AFTER 170,700 WHEEL LOADS-- JUNE 6, 1969. NOTE DEPTH OF PERMANENT DEFORMATION.

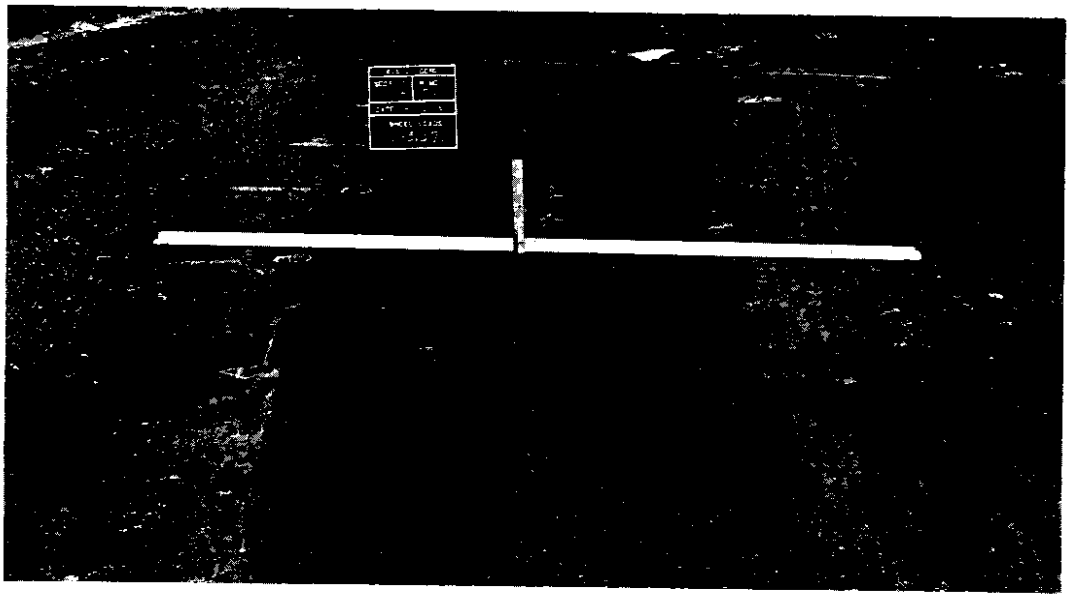

FIGURE 43. APPEARANCE OF SECTION 1, 2.0 INCHES OF SAB, AFTER 143,370 WHEEL LOADS ON APRIL 2, 1969 PRIOR TO START OF SPRING TESTING. NOTE THE DEPTH OF PERMANENT DEFORMATION.

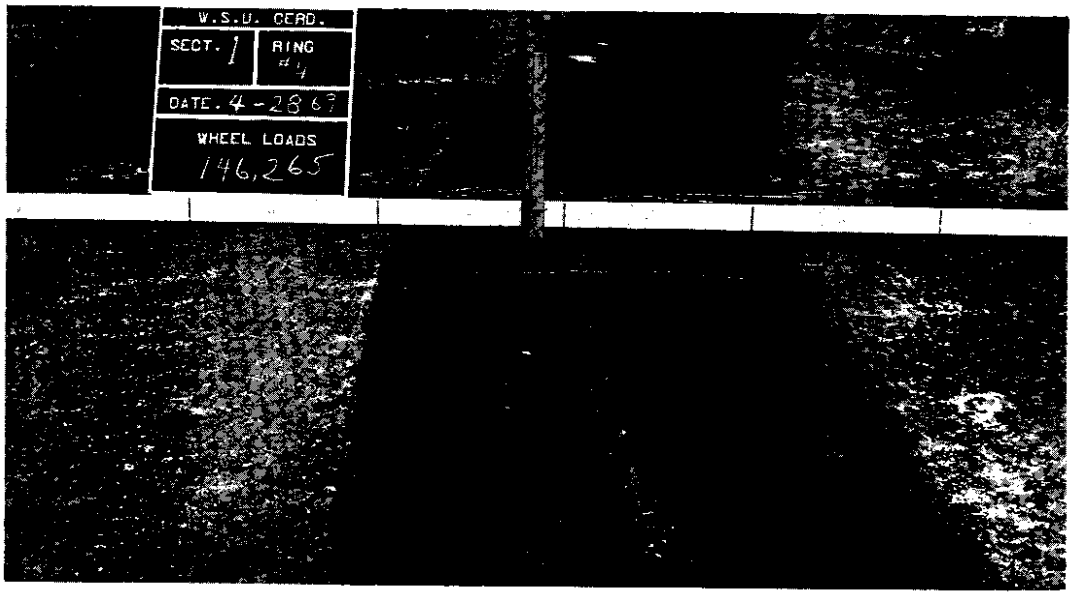

FIGURE 44. CONTINUED PERMANENT DEFORMATION IN SECTION 1 AFTER 146,265 WHEEL LOADS ON APRIL 27, 1969. NOTE THE TRANSVERSE CRACKS. TIME LAG BETWEEN FIGURES 43 AND 44 DUE TO OTHER SECTION REPAIR.

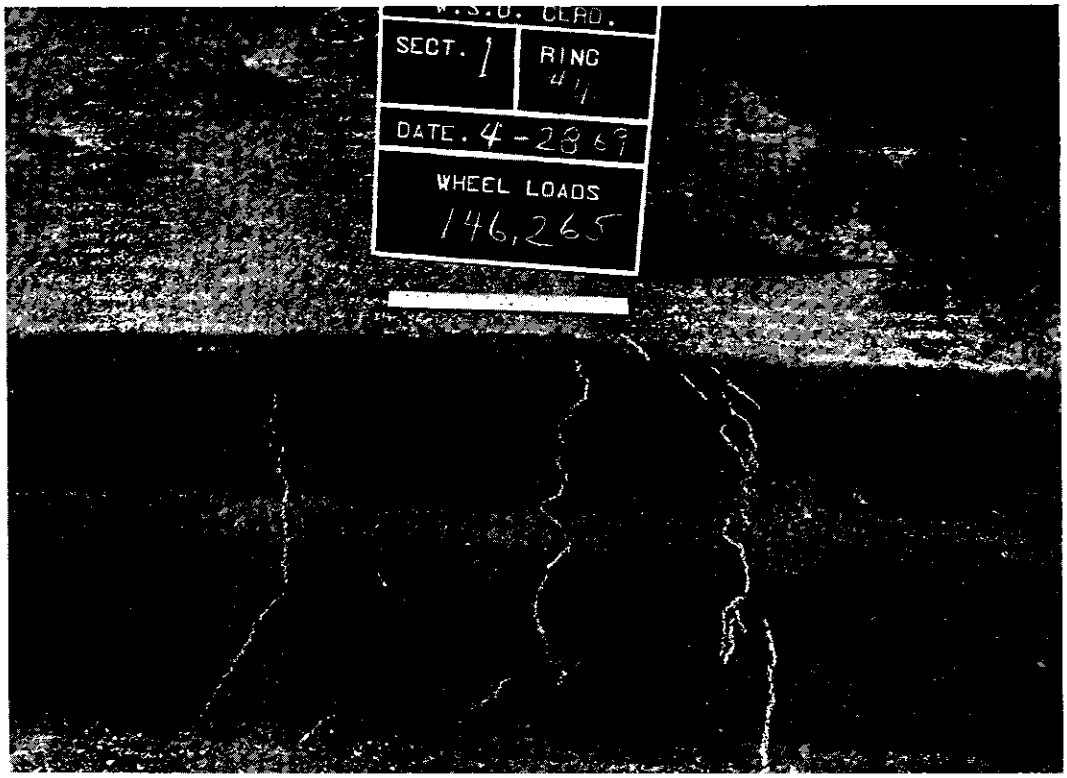

FIGURE 45. CLOSE-UP VIEW OF THE TRANSVERSE CRACKS IN SECTION 1 AFTER 146,265 WHEEL LOADS.

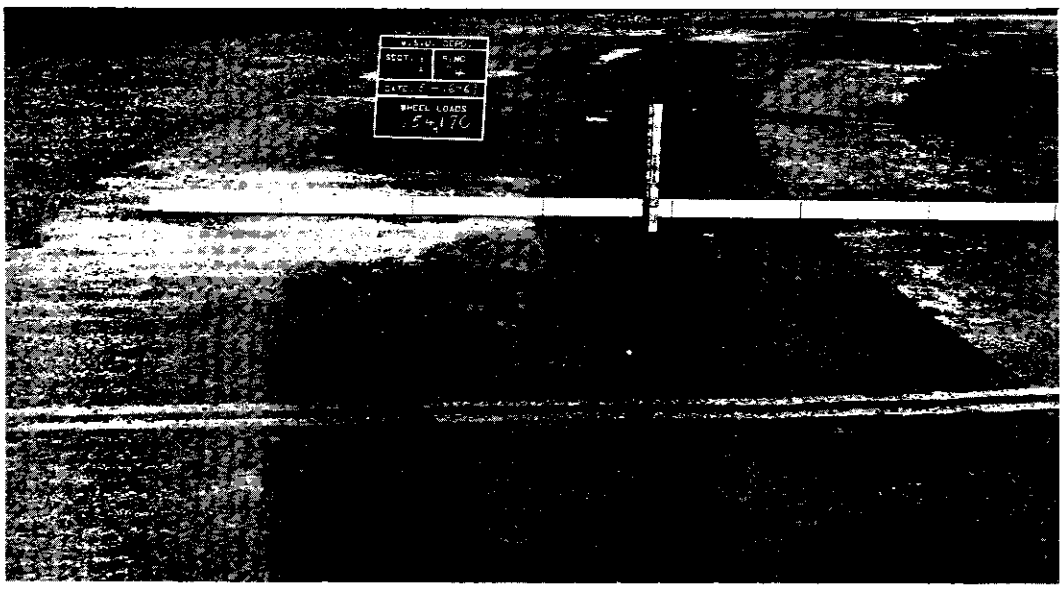

FIGURE 46. PERMANENT DEFORMATION OF SECTION 1 AFTER 154,170 WHEEL LOADS ON MAY 16, 1969. NOTE DEPTH OF DEFORMATION.

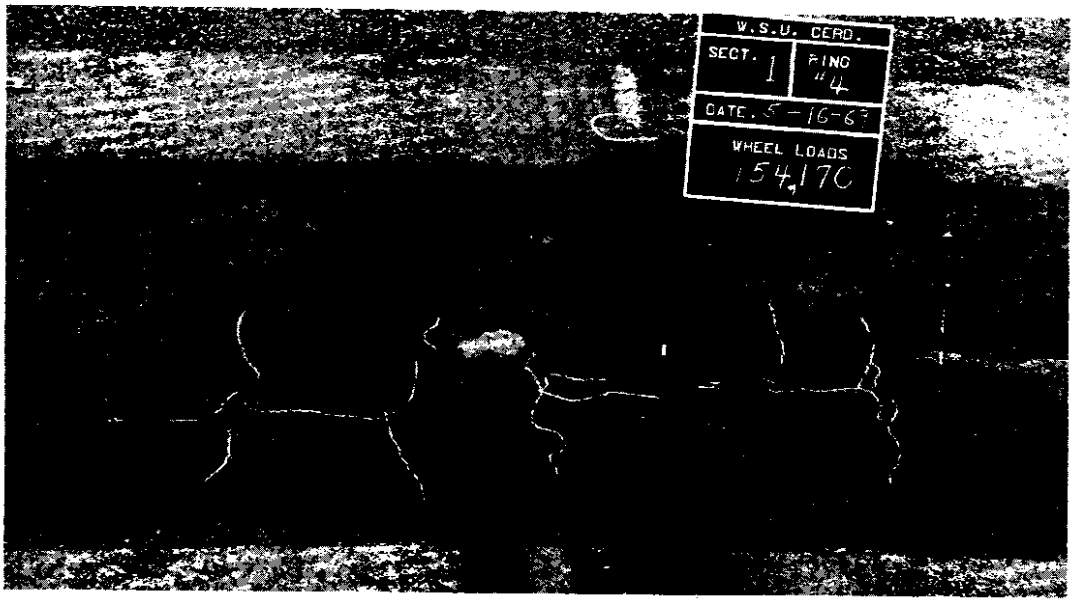

FIGURE 47. CLOSE-UP VIEW OF THE CRACKS IN SECTION 1 AFTER 154,170 WHEEL LOADS. THE CRACKS ARE STARTING TO INCREASE IN SCOPE.

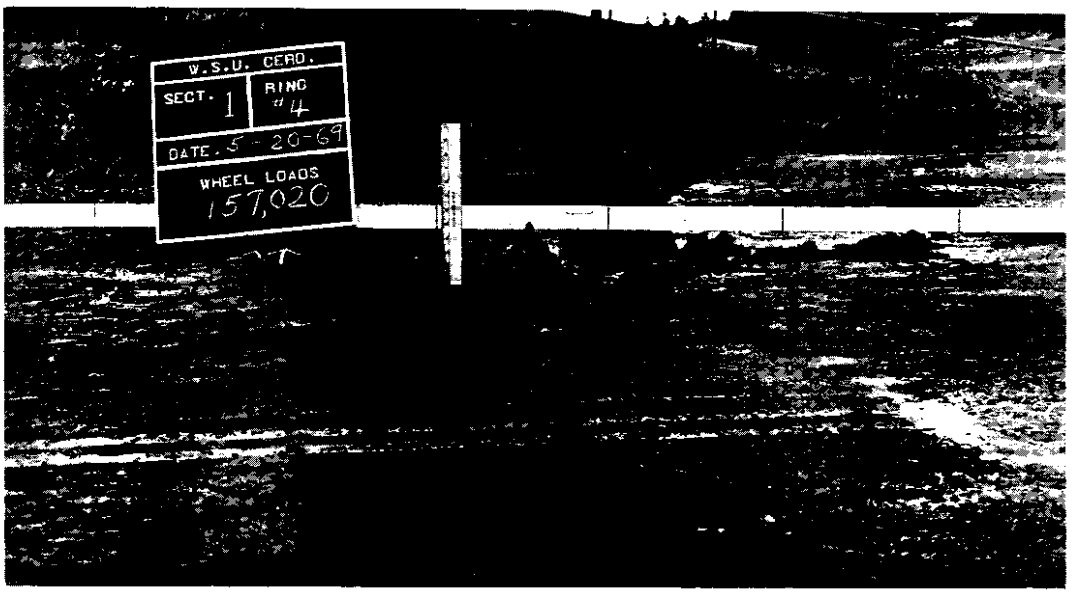

FIGURE 48. "ULTIMATE FAILURE" DUE TO PUNCHING SHEAR IN SECTION 1 AFTER 157,020 WHEEL LOADS ON MAY 20, 1969. NOTE DEPTH OF DEFORMATIONS.

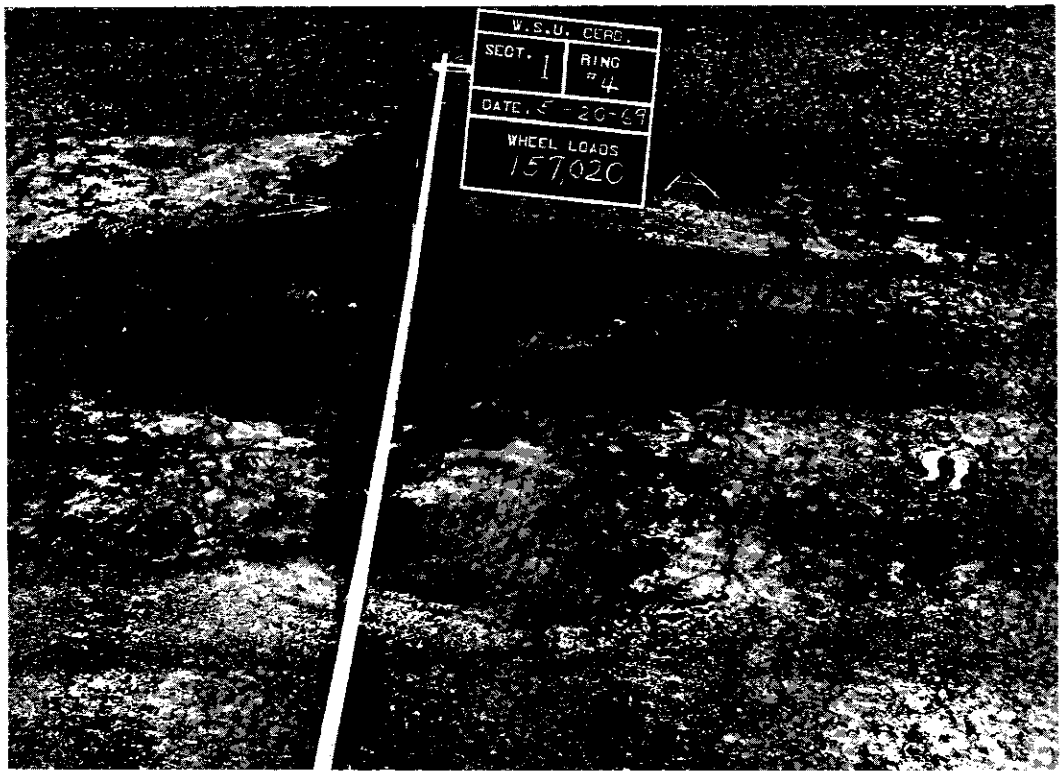

FIGURE 49. CLOSE-UP VIEW OF SECTION 1 AT "ULTIMATE FAILURE."

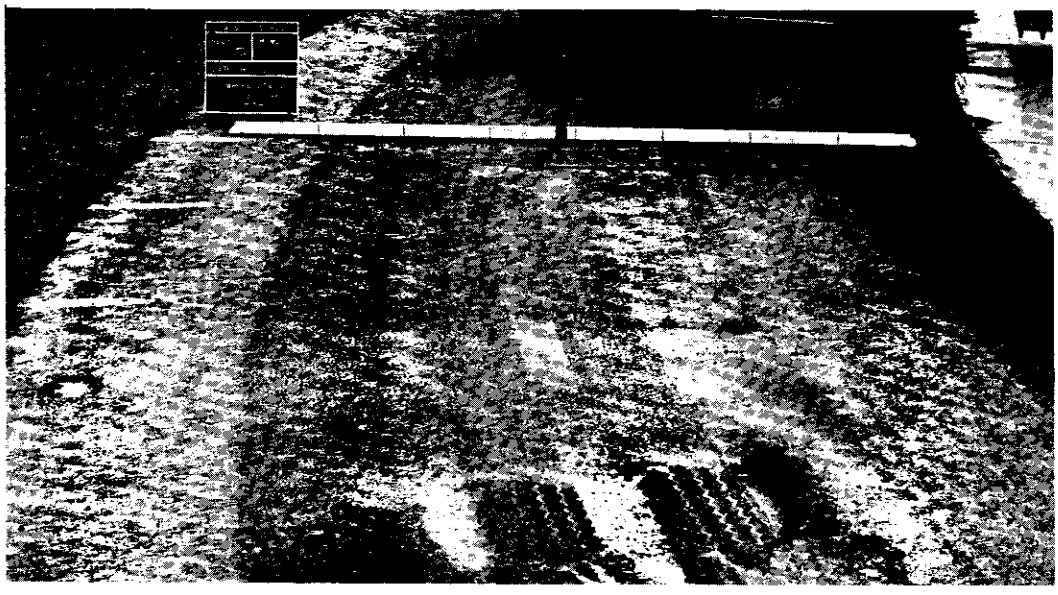

FIGURE 50. APPEARANCE OF SECTION 6, 2.0 INCHES OF CLASS "F" ASPHALT CONCRETE BASE AFTER 143,370 WHEEL LOADS PRIOR TO RESUMPTION OF TESTING IN THE SPRING.

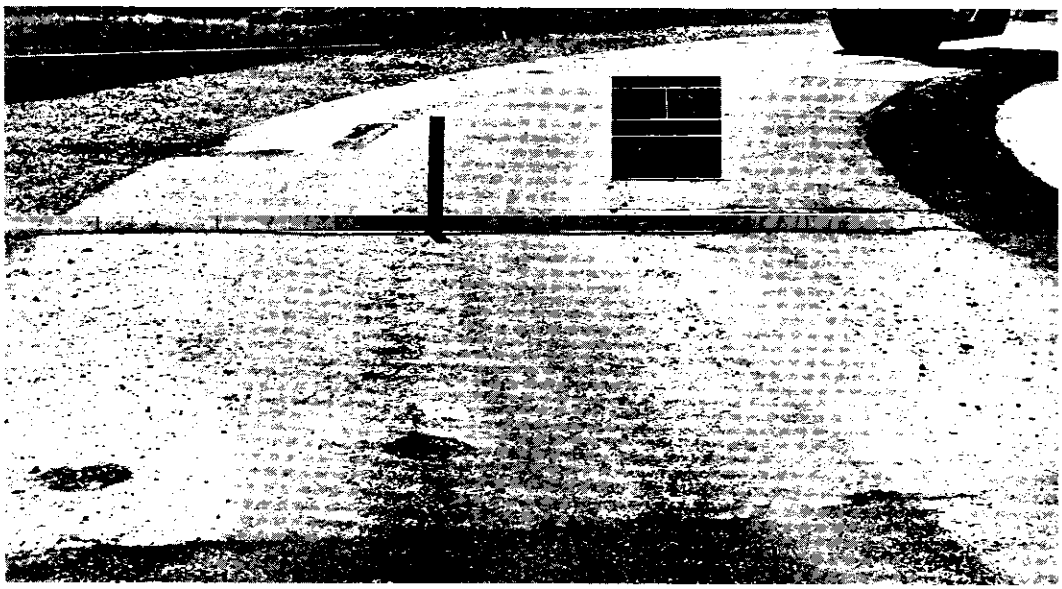

FIGURE 51. APPEARANCE OF SECTION 6 AFTER 157,473 WHEEL LOADS ON MAY 22, 1969. NOTE DEPTH OF PERMANENT DEFORMATION.

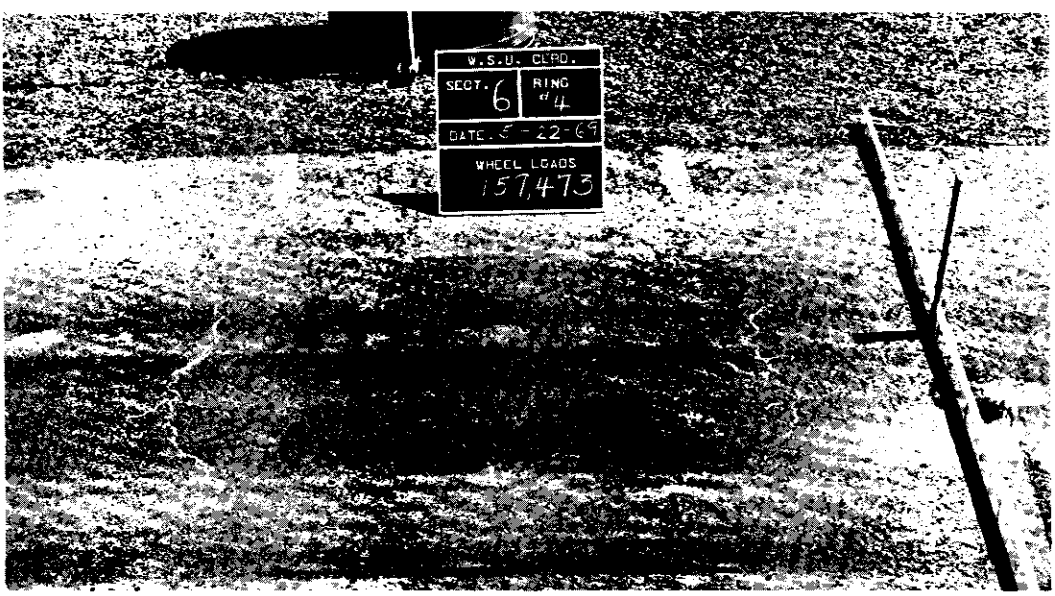

FIGURE 52. CLOSE-UP VIEW OF SECTION 6 AFTER 157,473 WHEEL LOADS. NOTE THE TRANSVERSE CRACKS.

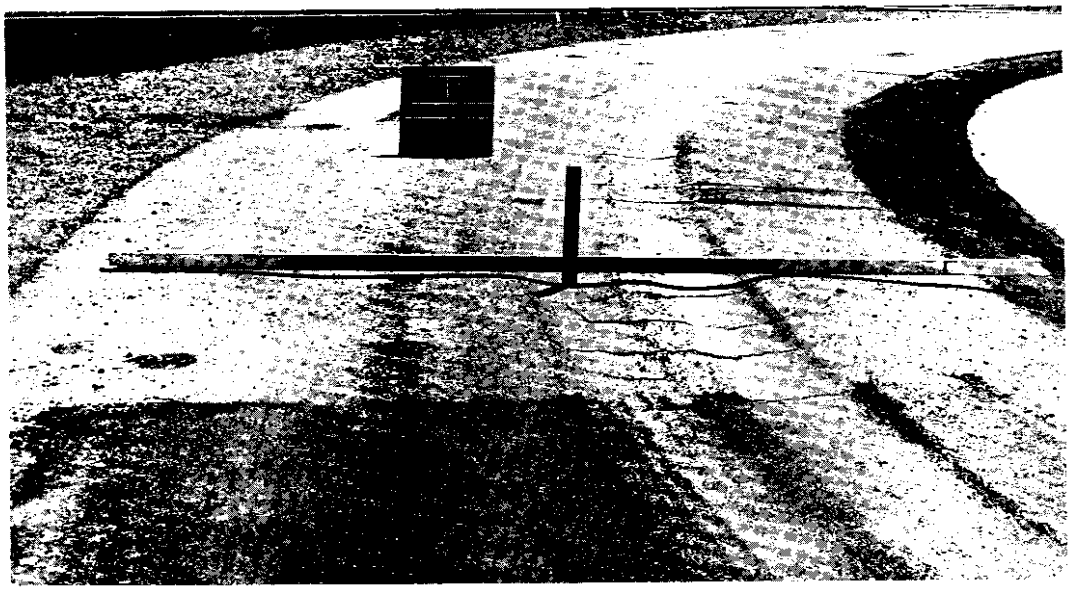

FIGURE 53. CONTINUED DETERIORATION OF SECTION 6 AFTER 158,031 WHEEL LOADS ON MAY 22, 1969. NOTE THE DEPTH OF THE RUTTING AND THE TRANSVERSE CRACKS.

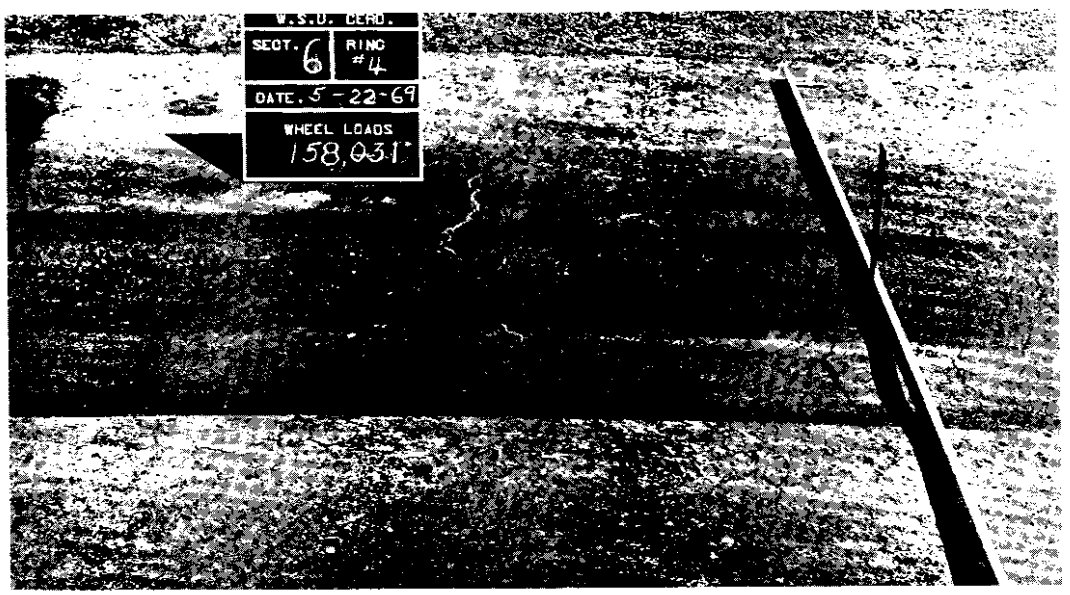

FIGURE 54. CLOSE-UP VIEW OF SECTION 6 AFTER 158,031 WHEEL LOADS. NOTE THE WIDTH OF TRANSVERSE CRACKS AND THE FORMATION OF LONGITUDINAL CRACKS AT THE EDGES OF PATH.

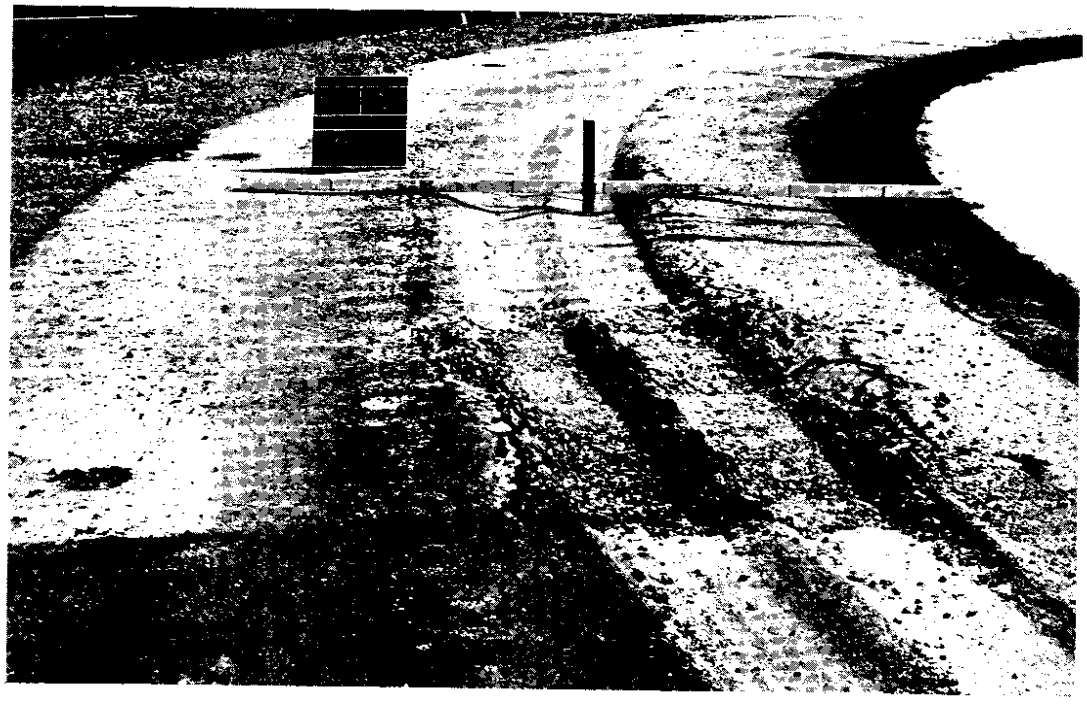

FIGURE 55. "ULTIMATE FAILURE" AT SECTION 6 AT 158,235 WHEEL LOADS--
MAY 22, 1969. NOTE THE DEPTH OF THE PERMANENT DEFORMATION.

FIGURE 56. APPEARANCE OF SECTION 2, 4.0 INCHES OF SAB, PRIOR TO
RESUMPTION OF TESTING IN SPRING AT 143,370 WHEEL LOADS.

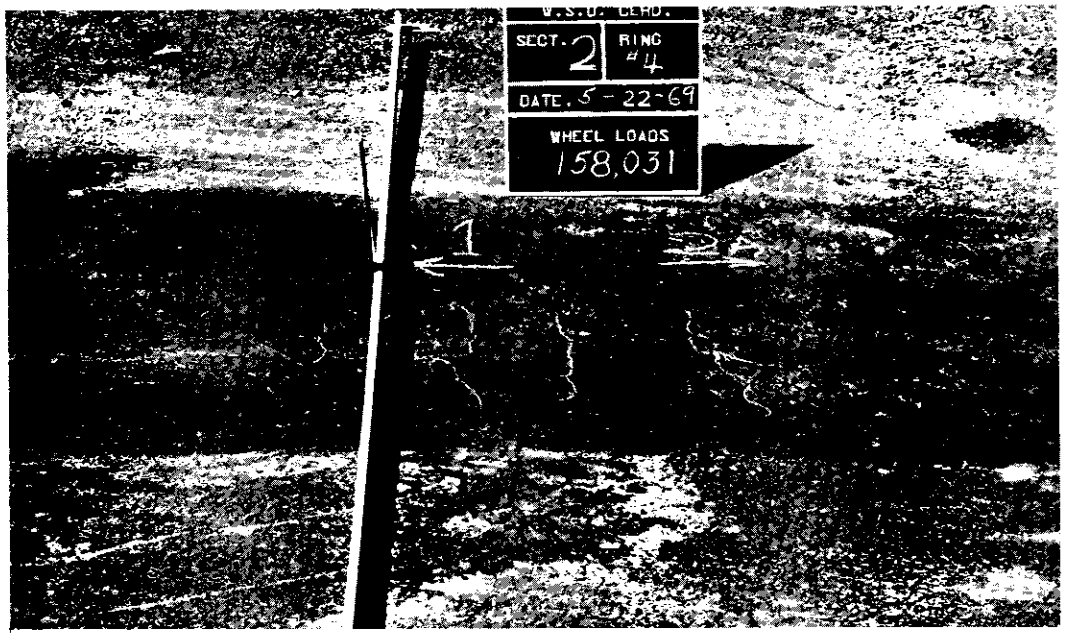

FIGURE 57. FAILURE IN THE TRANSITION ZONE BETWEEN SECTIONS 1 AND 2 AT 158,031 WHEEL LOADS--MAY 22, 1969.

FIGURE 58. CONTINUED DETERIORATION OF THE TRANSITION ZONE BETWEEN SECTIONS 1 AND 2, AT 158,235 WHEEL LOADS--MAY 22, 1969. NOTE THE RUT DEPTH IN THE BACKGROUND.

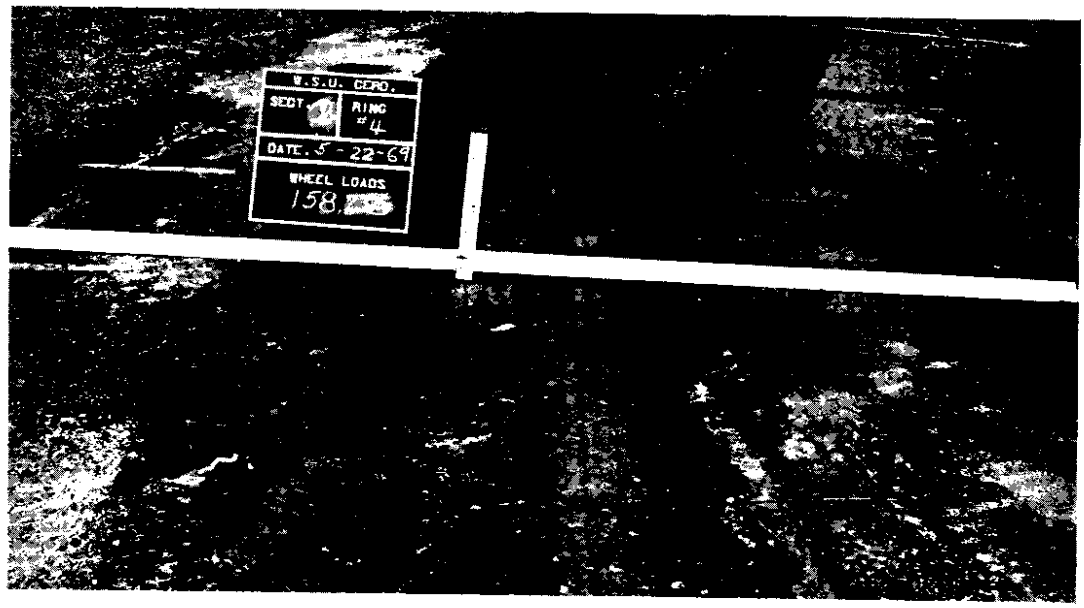

FIGURE 59. CLOSE-UP OF THE PERMANENT DEFORMATION IN SECTION 2 AFTER 158,235 WHEEL LOADS.

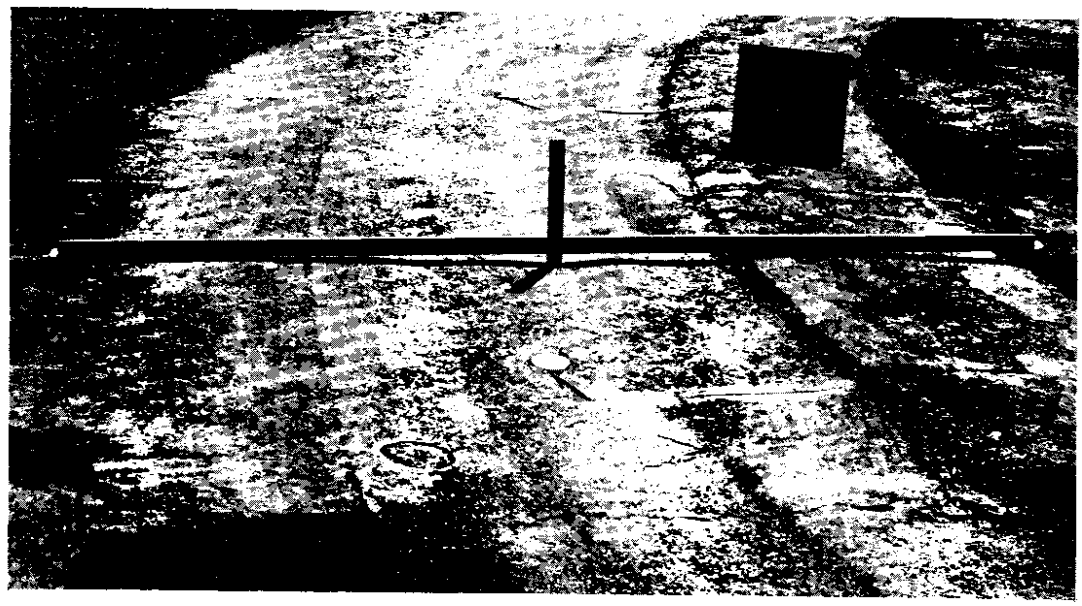

FIGURE 60. CONTINUED DEFORMATION OF SECTION 2 AT 162,774 WHEEL LOADS--MAY 28, 1969. NOTE APPEARANCE OF SECTION.

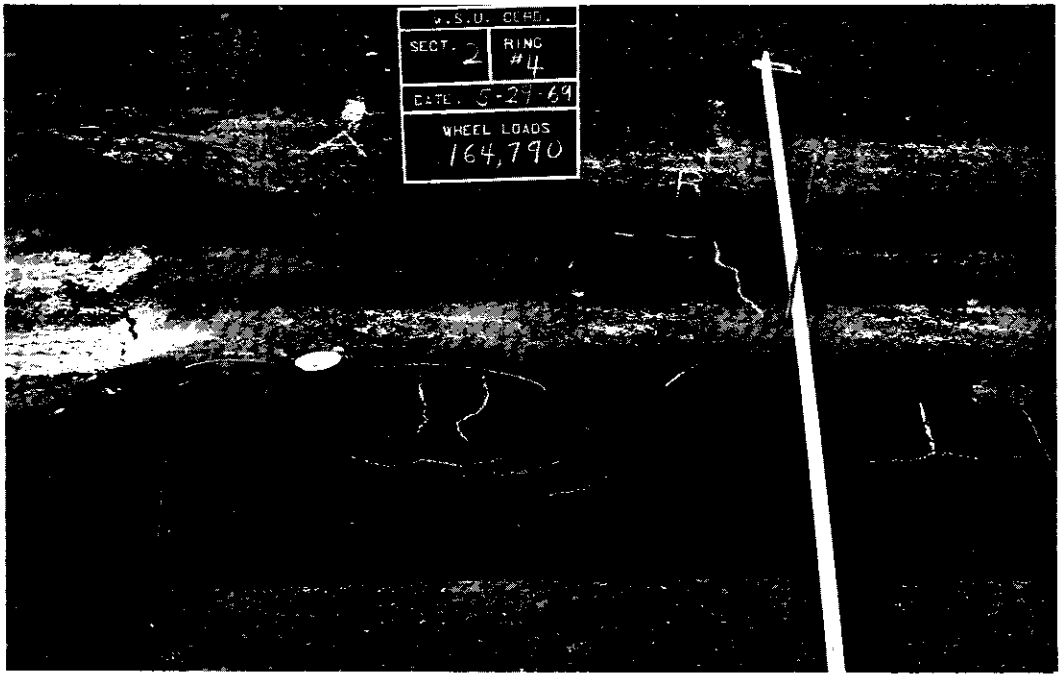

FIGURE 61. APPEARANCE OF SECTION 2 AT "ULTIMATE FAILURE" AFTER 164,790 WHEEL LOADS--MAY 29, 1969. THIS IS THE END NEAREST TO SECTION 1.

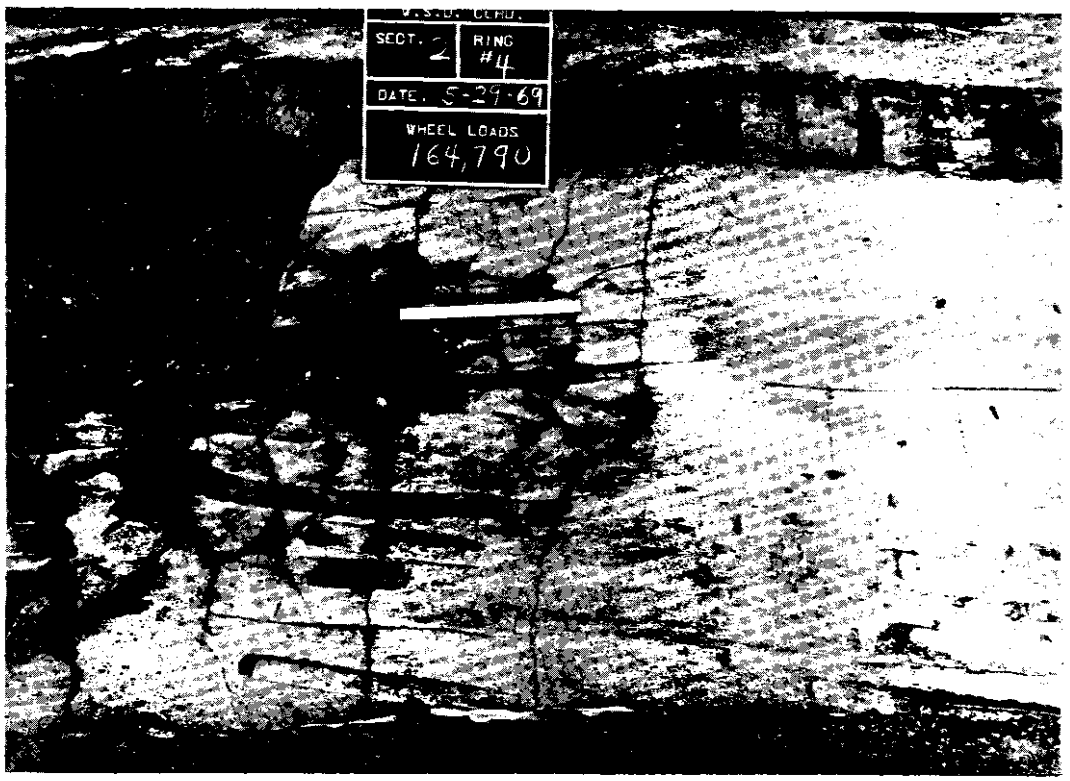

FIGURE 62. APPEARANCE OF THE FIRST LIFT OF SAB IN SECTION 2. THE LEFT SIDE IS NEAR SECTION 1. NOTE HOW THE BASE HAS BEEN CRACKED THROUGH, AND HOW THE BASE HAS FOLLOWED THE DEFORMATION OF THE SUBGRADE.

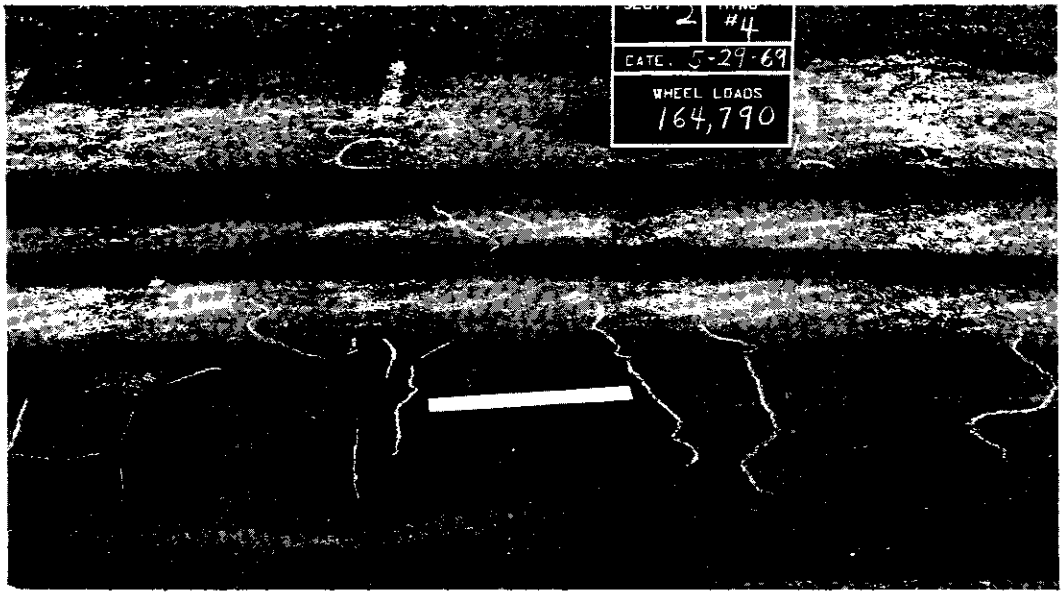

FIGURE 63. APPEARANCE OF THE AREA OF SECTION 2 NEAREST SECTION 3 AFTER 164,790 WHEEL LOADS. NOTE THE TRANSVERSE CRACKS.

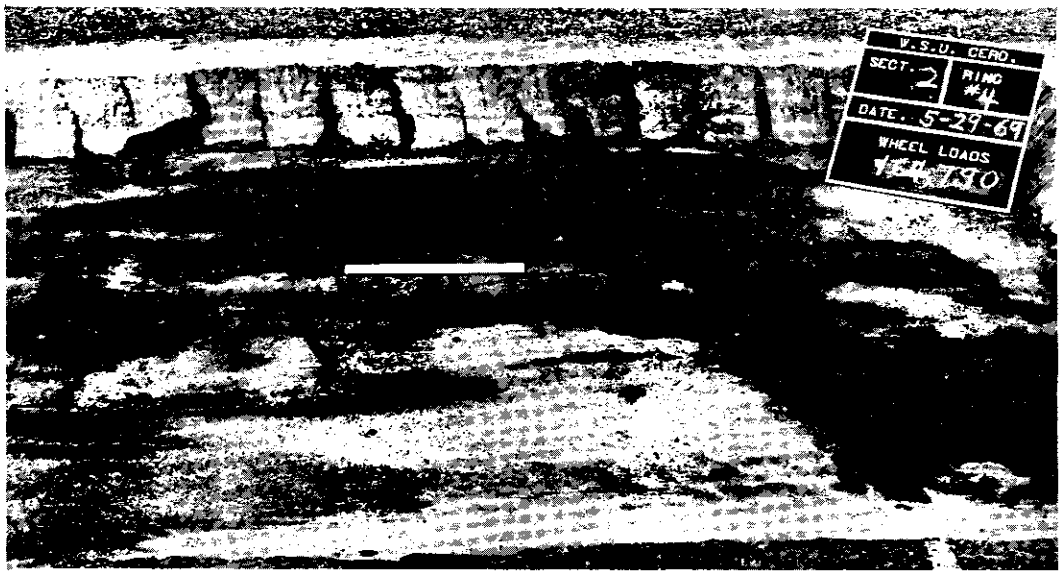

FIGURE 64. EXCAVATION OF SECTION 2 SHOWING THE FIRST LAYER OF SAB. NOTE THE CRACKS AND THE WAY THE SAND-ASPHALT BASE MIRRORS THE SUBGRADE DEFORMATION.

FIGURE 65. APPEARANCE OF SECTION 7, 3.5 INCHES OF ACB, AT 143,370 WHEEL LOADS PRIOR TO RESUMPTION OF TESTING IN THE SPRING.

FIGURE 66. APPEARANCE OF SECTION 7 AFTER 162,774 WHEEL LOADS ON MAY 28, 1969. NOTE THE TRANSVERSE CRACKS AND THE DEPTH OF DEFORMATION.

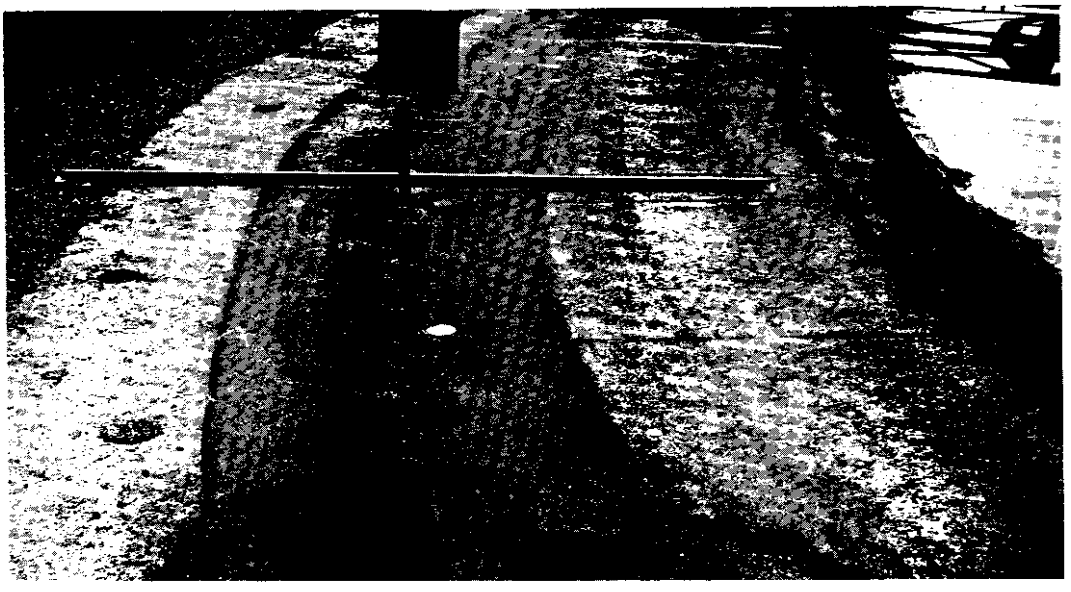

FIGURE 67. CONTINUED DETERIORATION OF SECTION 7 AT 170,700 WHEEL LOADS--JUNE 6, 1969. NOTE THE DEPTH OF RUTS AND THE CRACKS.

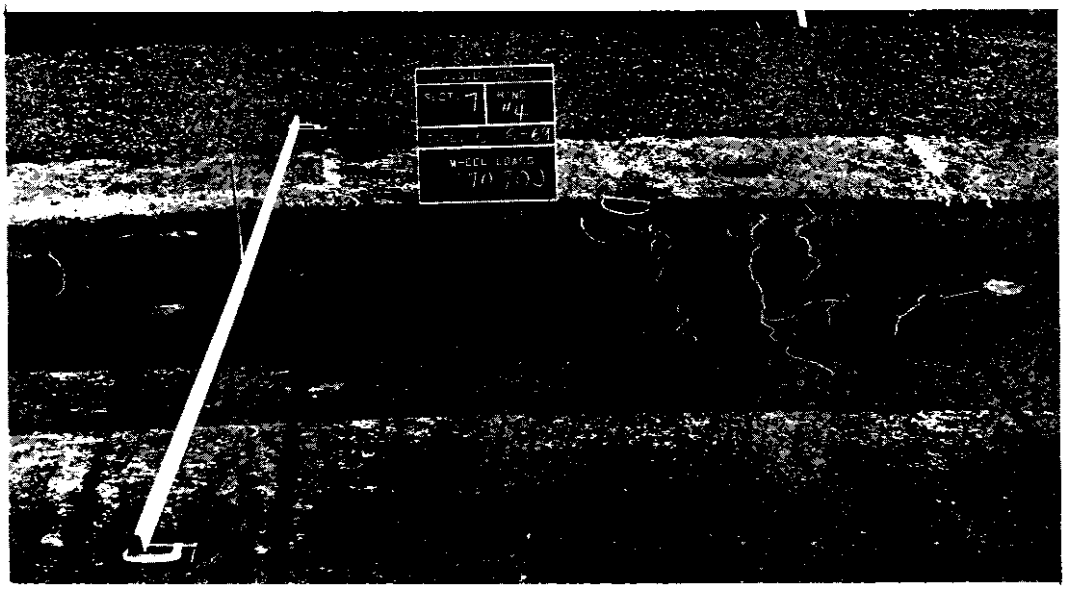

FIGURE 68. CLOSE-UP VIEW OF SECTION 7 AFTER 170,700 WHEEL LOADS. NOTE THE EXTENT OF THE TRANSVERSE CRACKS.

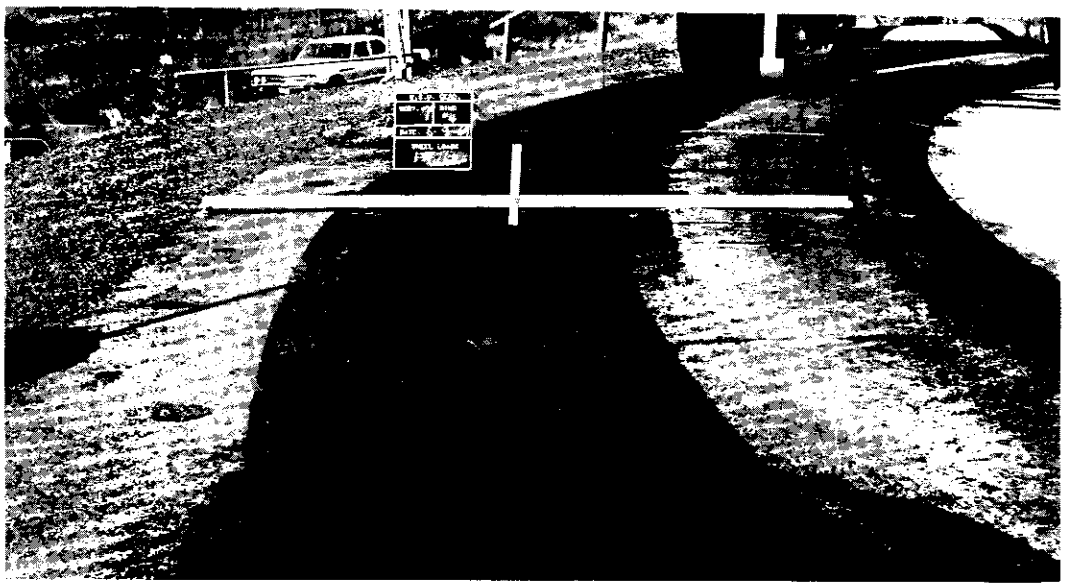

FIGURE 69. "ULTIMATE FAILURE" AT 171,168 WHEEL LOADS IN SECTION 7. NOTE THE DEPTH OF THE RUTS AND THE EXTENT OF THE FAILURE. NOTE HOW THE PLUG IN THE FOREGROUND HAS BEEN FORCED UPWARD.

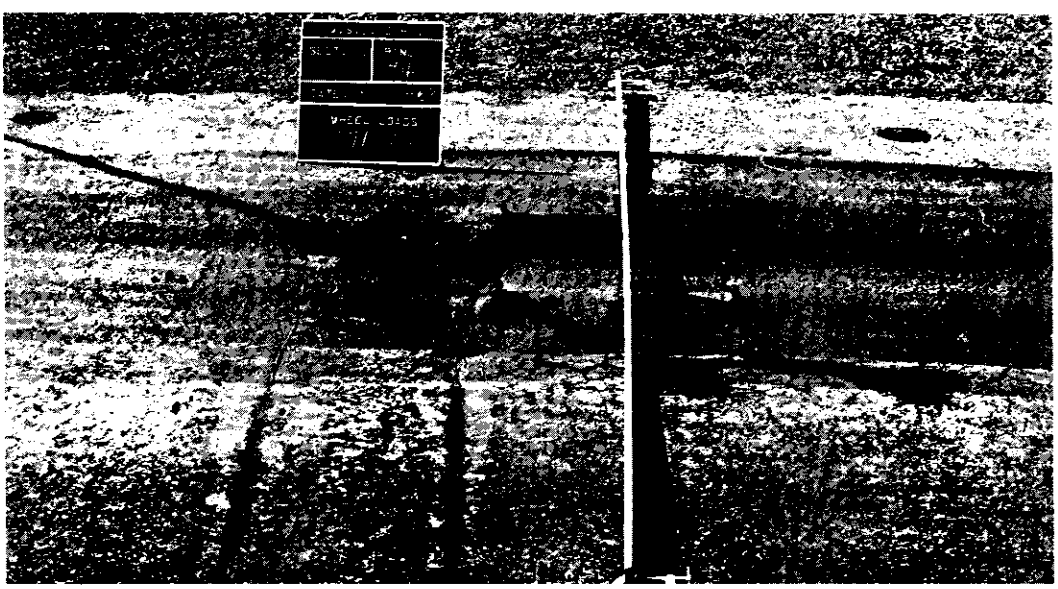

FIGURE 70. CLOSE-UP VIEW OF THE SECTION 7 "ULTIMATE FAILURE" IN PUNCHING SHEAR.

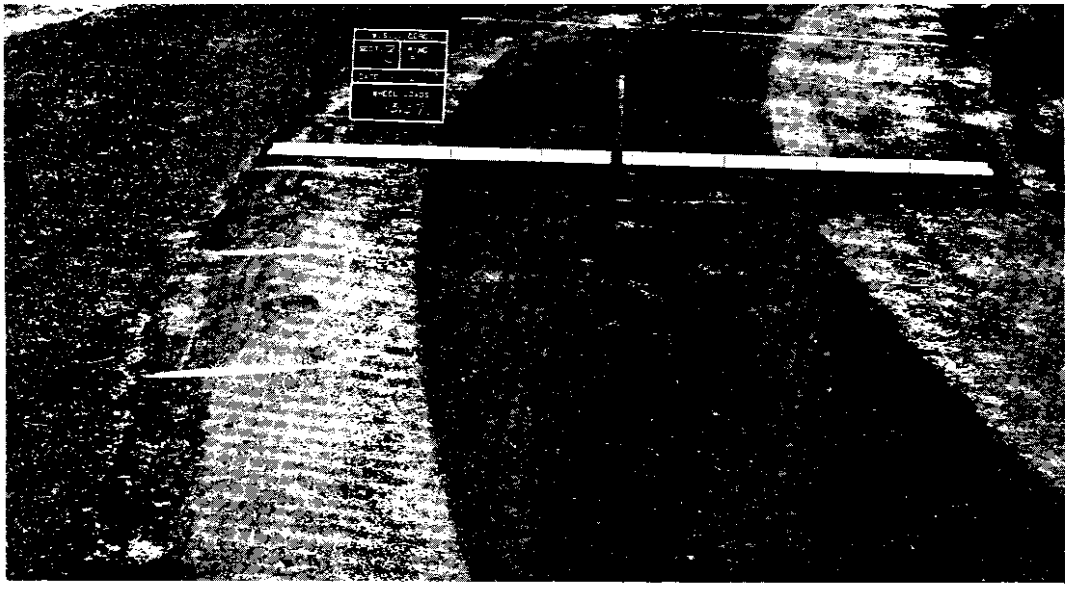

FIGURE 71. APPEARANCE OF SECTION 3, 6.0 INCHES OF SAB, PRIOR TO RESUMPTION OF TESTING IN SPRING AFTER 143,370 WHEEL LOADS--APRIL 2, 1969.

FIGURE 72. DEFORMATION OF SECTION 3 AFTER 162,774 WHEEL LOADS--MAY 28, 1969. NOTE THE EXTENT OF DEFORMATION. CRACKS IN THE TRANSITION ZONE BETWEEN SECTIONS 2 AND 3 ARE VISIBLE IN THE FOREGROUND.

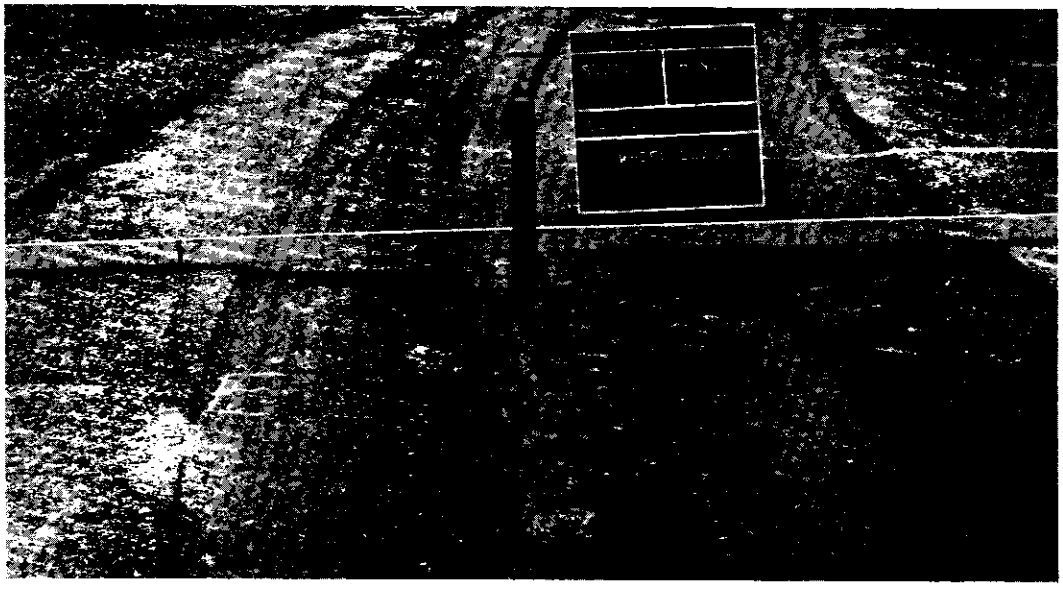

FIGURE 73. "ULTIMATE FAILURE" IN SECTION 3 AT 177,501 WHEEL LOADS ON JUNE 19, 1969. NOTE THE DEPTH AND EXTENT OF THE PERMANENT DEFORMATION. NO CRACKS WERE VISIBLE.

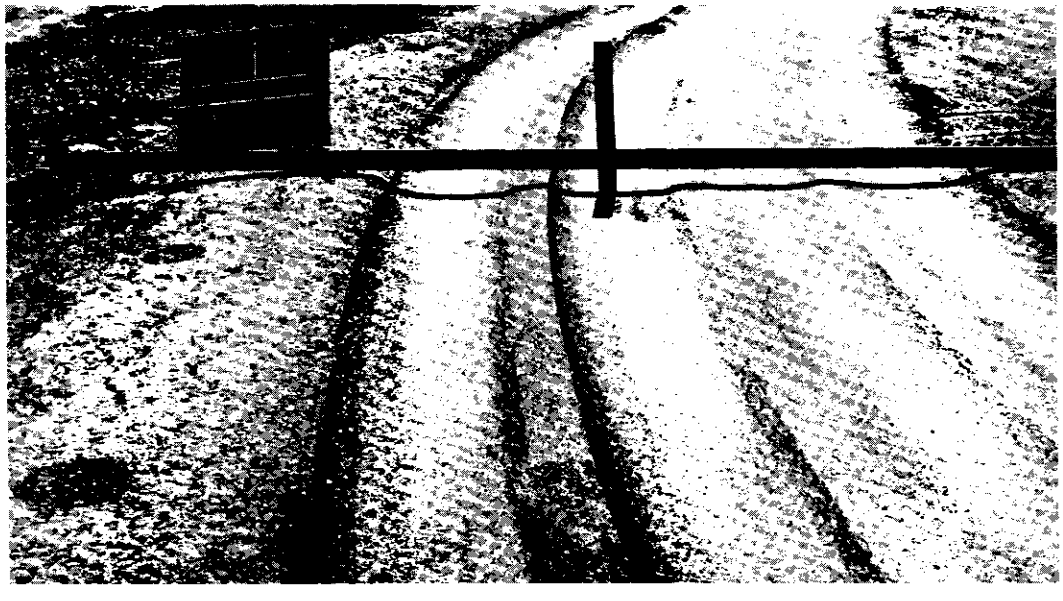

FIGURE 74. CONTINUED RUTTING OF THE ASPHALT CONCRETE OVERLAY IN SECTION 3 AFTER 211,065 WHEEL LOADS--JULY 18, 1969. NOTE DEPTH OF PAVEMENT DEFORMATION.

FIGURE 75. APPEARANCE OF SECTION 4, 8.0 INCHES OF SAB, AFTER 143,370 WHEEL LOADS AND PRIOR TO SPRING TESTING.

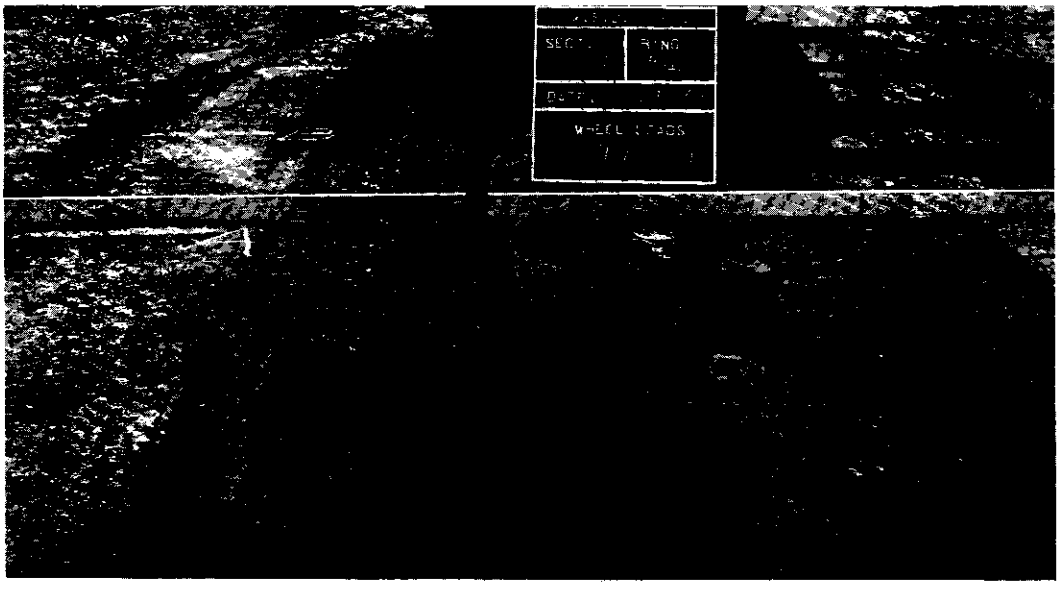

FIGURE 76. PERMANENT DEFORMATION OVER LVDT #3 OF SECTION 4 AFTER 177,501 WHEEL LOADS ON JUNE 19, 1969. NOTE THE EXTENT OF THE DEFORMATION.

FIGURE 77. APPEARANCE AND DEPTH OF RUTS IN SECTION 4 AFTER 211,065 WHEEL LOADS--JULY 18, 1969.

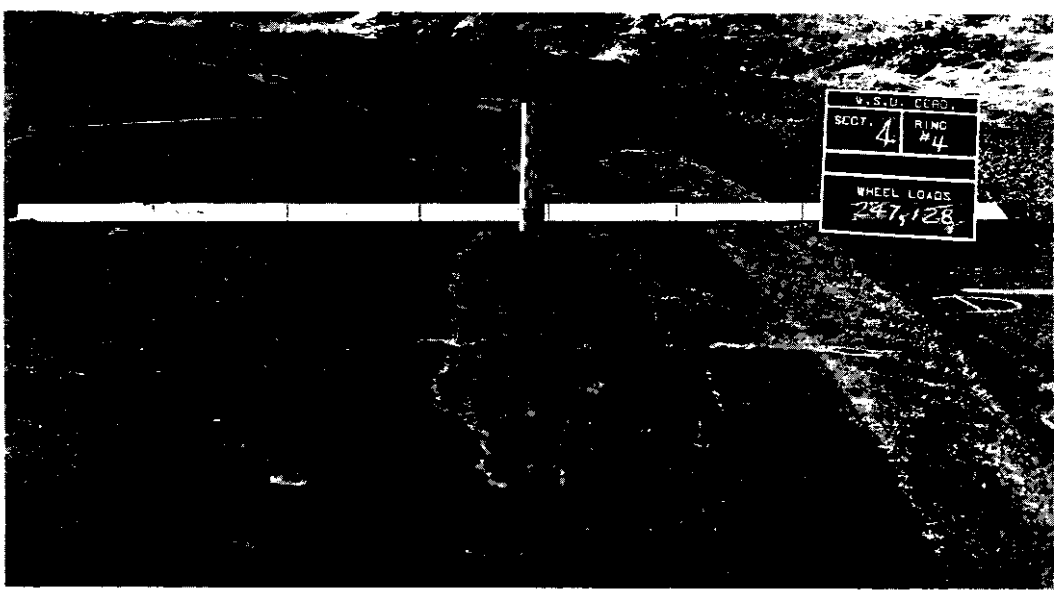

FIGURE 78. APPEARANCE OF SECTION 4 WITH SECTION 3 IN THE BACKGROUND AFTER 247,128 WHEEL LOADS AND THE END OF THE EXPERIMENT. NOTE THE DEPTH OF THE RUTTING.

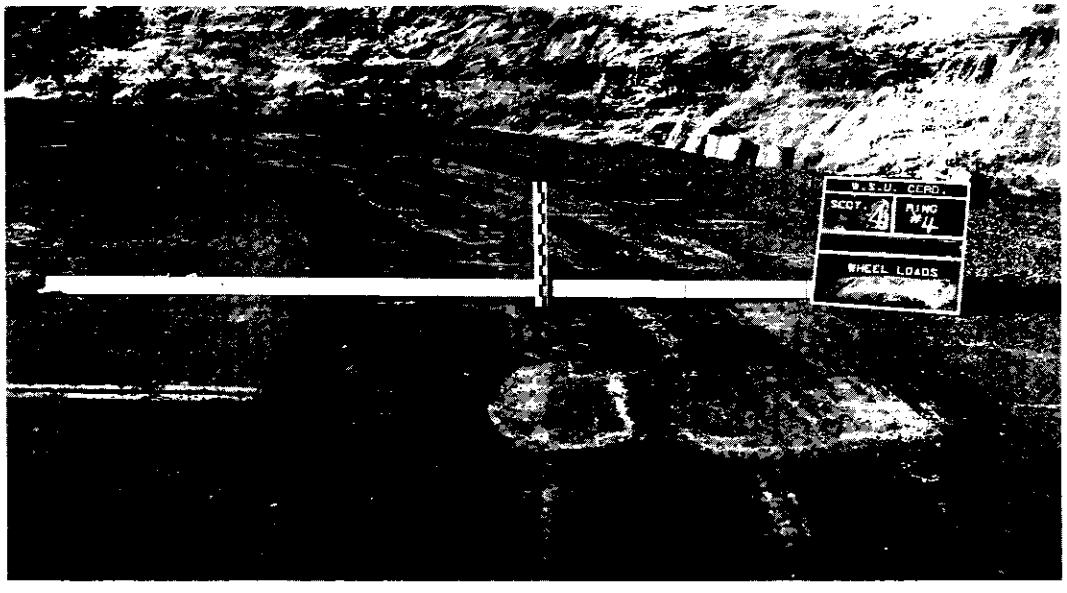

FIGURE 79. APPEARANCE OF SECTION 4 WITH SECTION 5 IN THE FOREGROUND AFTER 247,128 WHEEL LOADS. NOTE THE DEPTH OF RUTS.

FIGURE 80. APPEARANCE OF SECTION 8, 5.0 INCHES OF CLASS "F" ACB, AFTER 143,370 WHEEL LOADS AND PRIOR TO START OF SPRING TESTING.

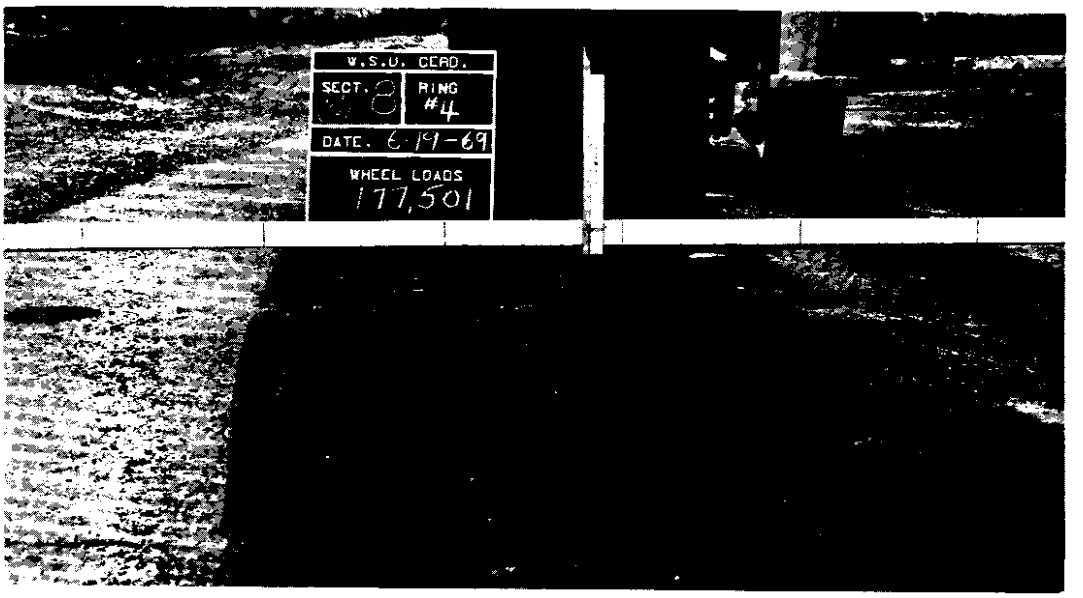

FIGURE 81. DEFORMATION OF SECTION 8 AFTER 177,501 WHEEL LOADS ON JUNE 19, 1969. NOTE THE DEPTH AND EXTENT OF DEFORMATION.

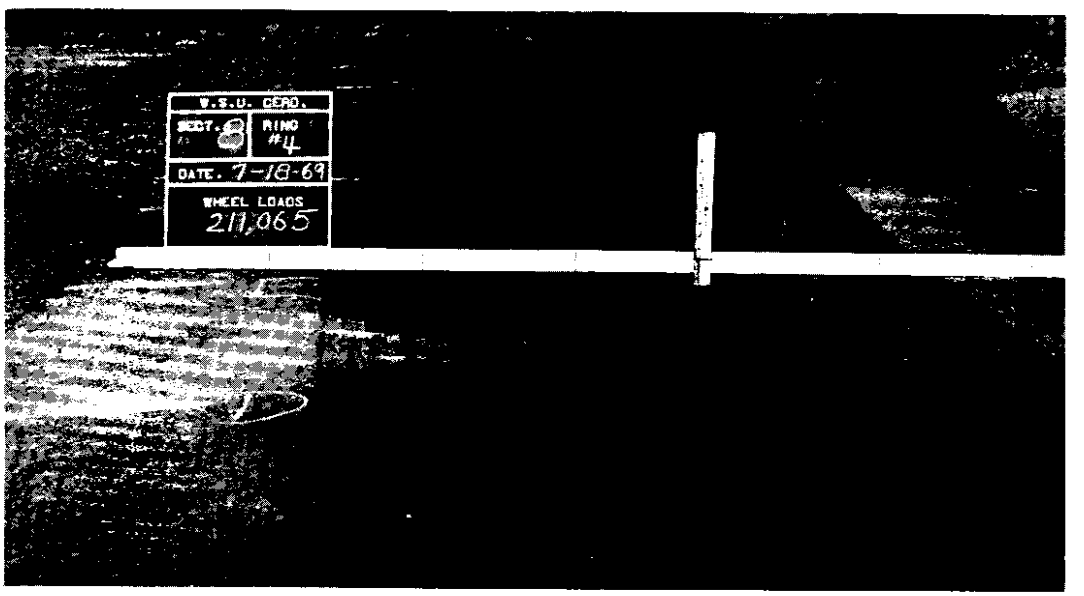

FIGURE 82. CONTINUED DEFORMATION OF SECTION 8 AFTER 211,065 WHEEL LOADS ON JULY 18, 1969. NOTE THE INCREASED DEPTH AND EXTENT OF RUTTING.

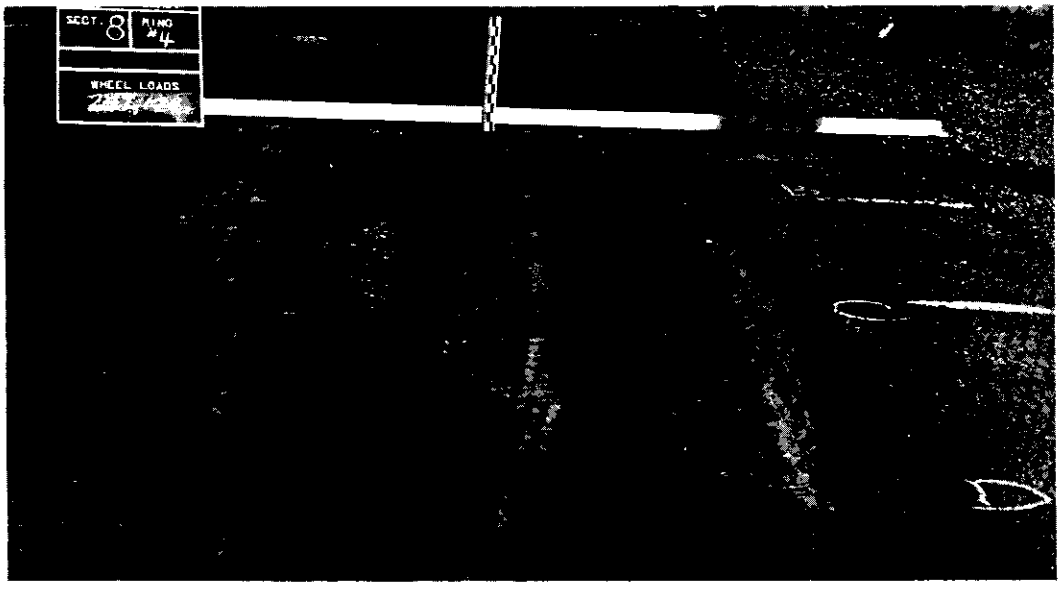

FIGURE 83. APPEARANCE OF SECTION 8 AFTER THE EXPERIMENT WAS ENDED AFTER 247,128 WHEEL LOADS. NOTE DEPTH OF THE RUTS.

predicted by Benkelman beam rebound measurements (Table 14, p. 47). The cracks continued to increase in this spot and began to form an alligator pattern (Figure 19). Permanent settlement continued to increase. Longitudinal shear cracks appeared along the edges of the wheel path causing a collapse of the pavement in the wheel path (Figure 20). Figure 21 shows the close-up of this area and the large alligator cracking pattern. Settlement of pavement exceeded 3 inches and "ultimate" failure was declared (Figures 20-21). This section was removed after 36,681 wheel loads.

On the same day, November 16, 1968, transverse cracks appeared in the remaining untreated base sections 10, 11 and 12 with 7.0, 9.5 and 12.0 inches of untreated base, respectively, at 47,391, 48,000 and 49,104 wheel loads respectively. Transverse cracks appeared in section 10 at line A which then continued to increase and work towards line E (Figures 22 and 23). The end closest to section 9 (lines A and B) continued to deteriorate at a faster rate than the remaining part of the section. "Ultimate" failure occurred at this end of the section with a permanent settlement of over 7.0 inches. Figure 24 (p. 51) shows this phenomena and the fact that punching shear failure occurred. This part of the section was removed and replaced with 8-10 inches of asphalt concrete. The other half of the section continued in service until spring; Figure 25 shows the appearance of this section at the end of the fall testing period. Transverse cracks were evident throughout this section.

Transverse cracks appeared in section 11 at line C and rapidly developed in lines D, E, A and B in that order. Transverse cracks were soon evident throughout the section as shown in Figure 26. With accumulated wheel loads, the section continued to deteriorate with a permanent settlement of 3/4 inches occurring as shown in Figure 27. Alligator cracking pattern followed by a

longitudinal shear crack along the wheel path edges formed. The collapse of the pavement in the wheel path caused permanent deformation greater than 2 inches (Figure 28). This section was not declared failed as the skid had not started to drag.

Transverse cracks in section 12 occurred in line B and then moved towards lines A, C, D and E in that order. The transverse cracks developed into alligator cracks as shown in Figures 29 and 30. The figures show that cracking was more extensive in the areas around A and B and less extensive in D and E. As the wheel loads accumulated, the cracks increased (Figure 31). Eventually longitudinal shear edge cracks occurred thus causing a collapse of the pavement in the wheel path and a permanent settlement of 1-3/4 to 2 inches (Figure 32, p. 56). The Figures 32 and 33 show that this was localized in the extensively cracked area (A to C). Since the skid was not dragging, "ultimate" failure was not declared.

Also on November 16, 1968, transverse cracks at 47,391 wheel loads appeared in section 5 (no base). These occurred in the transition zone between sections 4 and 5, and then in line C as predicted by Benkelman beam deflection measurements. Figures 36 and 37 show the transverse cracks in this zone; the latter figure shows the pumping of mud through one of the cracks. Figure 38 shows the appearance of the section 5 at the end of fall testing and the amount of permanent settlement that occurred. Ruts were about 1/4 inch deep. Figure 39 shows the extent of cracking in area around D and E. This section was intact at the end of fall testing.

At the end of fall testing all the untreated base sections had suffered some distress. Section 9 and part of section 10 had been removed. Examination and tests on the crushed rock and silt were quite revealing as shown in

Table 15 (p. 89). The untreated base was quite saturated having moisture contents of over 7.8%. This was quite an increase over the moisture content of the crushed rock during construction.

The subgrade moisture was also above optimum. Table 15 shows that moisture content decreased with depth. Screen analysis of the crushed rock revealed no excessive fines and that the rock was within specifications.

Environment may have had a large effect on the fall performance of this ring. During the October period there was much rain and snow. The rain must have soaked through the shoulders and saturated the crushed rock base. This, in turn, penetrated into the subgrade, and is shown by the fact that moisture contents decreased with depth. When testing started in November, Benkelman beam deflections showed that subgrade support was rather poor for the untreated sections. The cold and wet November month may have contributed to the rapidity of the development of cracks. It is interesting to note that it snowed on November 13, the day before cracks appeared in sections 5, 10, 11 and 12. The rapidity of the development of cracks and failure of untreated sections indicates that the high moisture content of the untreated crushed rock apparently led to almost complete saturation of the subgrade and an eventual loss of support, and hence, failure. Environmental conditions of cold, rain and snow accelerated the process. The thicker crushed rock sections were able to give some support to the pavement before the occurrence of distress.

The transverse crack which occurred in section 5 was due to construction as it occurred at a joint of Class "B" asphalt concrete pavement. In the construction section of this report, it was mentioned that paving of the second lift occurred during a cold wind. By the time paving was finished, one part of the junction was cold while the other was hot thus forming a

weak plane. The other transverse cracks were tension cracks which were caused by flexure of the pavement due to wheel loads. The silt subgrade gave good support during this period.

The failures in the fall were different from those in the spring. The failure mode followed was that as outlined in the previous sections, although rutting and visible pavement deflections were not as evident or prominent as during the spring. Deflections were usually less than in the spring, although this was not as evident in this ring as in the previous ones (2, 3). The number of wheel load applications to reach "ultimate" failure was large as compared to the spring period as shown in Table 21.

The failures which occurred in the remaining uncracked sections in the spring were very rapid. Once initial cracking appeared, "ultimate" failure occurred very rapidly as shown in Table 21 and Figures 43 to 73 (pages 62 to 78).

Differences between failures occurring during the two periods were noticeable. Shear cracks occurred at the edge of the wheel path during the spring period as shown in Figures 40 and 41. The alligator cracking pattern was not as fully developed as in the sections which failed in the fall and frequently never developed as shown in Figures 40, 41, 49, 53, 54, 58, 69 and 70. Failure in the fall was slower and progressive, following the failure mode steps mentioned before. The spring failure bypassed some of the failure mode steps and occurred rapidly and spectacularly. Pavement deflections were evident and large with pronounced rutting just before the appearance of cracking as shown in Figures 43, 48, 53, 58, 59, 60, 67, 69, 73, 74, 77 and 81.

As soon as testing resumed in the spring, 5, 10, 11 and 12, the sections which were cracked during the fall became progressively worse. Longitudinal

punching shear failure occurred in section 5 (no base) very rapidly as shown in Figures 39 to 41. Failure, preceded by extreme deflections and rutting, occurred in the wheel path. As the wheel moved outward, there was lateral shoving of the subgrade and base causing uplift of the pavement. This section was removed and replaced with 8 to 10 inches of asphalt concrete mix. Figure 42 shows that the thick overlay was not sufficient to stop failure of the subgrade.

The untreated sections 10, 11 and 12 were declared failed soon after testing resumed and were replaced with asphalt overlay; section 12 was overlaid with 1½ to 2 inches of asphalt concrete.

Excavations of sections 10 and 11 reveal that very little degradation of the crushed surfacing top course occurred. After testing, the material was within the Washington Highway Department specifications as shown in Table 17. Moisture contents in the crushed surfacing top course were high, the bottom half of the crushed rock base having 1.7 to 2.5% moisture contents higher than those in the top half. This is shown in Table 16. Generally, the subgrade moisture contents under the untreated bases decreased with depth. This is shown in Table 18 (p. 92). In section 5, the subgrade moisture contents paralleled those found in sections 10 and 11, although they seemed to be slightly higher. A comparison of moisture contents in the untreated bases for the fall and spring periods showed that there did not seem to be significant differences as shown in Tables 15, 16 and 18, although moisture with depth in the subgrade did increase in the spring. The degree of saturation of the subgrade was higher than in the fall. One reason for the high moisture contents in the bottom half of the untreated bases and the top of the subgrade was moisture probably penetrated through the cracked sections and saturated the bases and subgrade. The crushed rock may have acted as a reservoir thus increasing the subgrade saturation.

TABLE 15: MOISTURE CONTENT AFTER BREAKUP OF UNTREATED BASE-FALL 1968

		Moisture Content-%		
		Section 9 4.5" UTB		Section 10 7.0" UTB
Material	Depth (In.)	B	D	A
UTB	Mid Depth	10.0	7.8	8.4
Subgrade	0*	29.2	29.2	27.8
	6	25.6	24.5	25.6
	12	24.4	25.1	23.1
	18	22.0	21.1	22.3

*Measured from top of subgrade.

TABLE 16: SPRING MOISTURE CONTENTS IN THE UNTREATED BASES

	% Moisture Content		
Material CSTC	Sect. 10	Sect. 11	
	D & E	A & B	E
Top Half	6.7	7.5	7.0
Bottom Half	8.4	10.0	9.4
Average	7.6	8.8	8.2

The sections which developed initial distress and the "ultimate" failure in the spring testing period can be divided into the thin base and thick base sections. The thin base sections; that is, sections 1, 2, 6 and 7 with 2.0, 4.0 inches of sand-asphalt base and 2.0 and 3.5 inches of Class "F" asphalt concrete base respectively, followed the classic spring failure pattern as observed in rings 2, 3 and 4. The thick sections 3, 4, 8 and 12, with 6.0 and 8.0 inches of sand-asphalt base, and 5.0 inches of Class "F" asphalt concrete base and 12 inches of untreated base respectively, did not develop cracks (except for section 12 in the fall) but skipped several steps and developed severe rutting.

Sections 1, 6, 2 and 7 developed initial distress in the following order. Rutting and excessive deflection developed in section 1 as shown in Figure 43, followed with more rutting and then transverse cracks (Figures 44 and 45). The rutting became more severe causing curvature of the wheel path which then caused longitudinal tension cracks to appear (Figures 46 and 47). Failure was then usually very rapid with poorly developed or no alligator cracking appearing. Figures 48 and 49 show the "ultimate" failure in punching shear at which testing was halted. This failure seems to be due to highly saturated subgrade conditions caused by spring conditions (Table 18.) The base may have been inadequate in strength to withstand the extreme deflections thus failing in tension and fatigue.

Initial distress next appeared in section 6 and followed a similar pattern. Figures 50 to 55 show the progressive failures history of this section. Figure 53 (p. 67) shows that rutting was localized in the path of the dual tires and increased with longitudinal tension surface cracks appearing along the dual tire edge path. This eventually sheared causing a collapse of the

TABLE 17. CRUSHED SURFACING TOP COURSE SIZES AFTER FAILURE

Screen Size	Percent Passing				
	Specifications WHD - CSTC	Section 10:7.0" UTB		Section 11"9.5" UTB	
		Top	Bottom	Top	Bottom
5/8	100	100	100	100	100
1/4	50 - 65	62.5	60	52.4	64.4
#4		50	50	42.9	51.1
#10		28.3	31.5	21.4	28.4
#20		13.1	19.3	11.5	16.2
#40	5 - 24	8.0	12.8	8.1	10.7
#200	10 Max.	3.2	3.7	3.1	4.2

TABLE 18: MOISTURE CONTENTS IN THE SUBGRADE AND DEGREE OF SATURATION--SPRING BREAKUP

Depth Inches	Percent Moisture Content						
	Section 10 7.0" UTB	Section 11 9.5" UTB	Section 5 0" ATB	Section 1 2.0" SAB	Section 2 4.0" SAB	Section 6 2.0" ATB	Section 7 3.5" ATB
	E	A&B E	A D	C	A	A D&E	C
0	26.3	27.5 27.3	29.5 24.6	29.3	28.9	24.4 22.9	28.6
6	27.1	26.4 26.9	26.7 26.7	27.7	28.5	27.2 27.1	29.0
12	28.4	20.3 23.1	25.7 25.1	29.1	25.3	30.4 28.8	27.2
18	22.0	24.3 22.3	24.2 25.7	28.0	22.9	-- 25.7	25.8
	Degree of Saturation						
0	95.1	96.0 96.2	99.6 92.4	99.2	98.5	92.4 88.5	97.9
6	96.2	95.1 95.5	95.2 95.3	96.7	97.9	96.3 96.2	98.8
12	97.9	86.9 90.6	94.1 94.5	98.8	94.5	100.0 98.5	96.2
18	87.7	92.4 90.5	92.4 94.3	97.5	90.5	-- 94.8	94.8

pavement (Figure 55). At this point the rut depth exceeded 2 inches and testing was halted to replace this section. Examination of the subgrade as shown in Table 18 revealed that the subgrade was highly saturated which probably contributed to the subgrade failure.

Figures 56 to 64 show the history of the failure of section 2 as it progressed through the respective stages. The failure pattern was similar to that of sections 1 and 6. The interesting thing about these figures is that failure was uneven in this section. Failure was more severe near section 1 (line A) than by section 3 (line E) (Figures 60, 61 and 63). When this section was excavated, the bottom layer of sand-asphalt was completely cracked and deformed in the severe failed part of the section (line A-B); this is shown in Figures 61 and 62. The excavation of the less severely failed part of the section (lines C-E), as shown in Figure 63, revealed that the bottom sand-asphalt layer was cracked and was deformed so that it duplicated the surface rutting (Figure 64). This means that the subgrade was deformed and that cracks developed at the bottom and worked upward through the layers. Subgrade moisture contents (Table 18) also show that the soil was almost completely saturated which probably resulted in lower subgrade wearing strength which reduced subgrade support. The degree of saturation of the subgrade increased from 57-63% at construction to 90-97% in the spring.

Figures 65 to 70 show progress of failure in section 7. This was similar to sections 1, 2 and 6 and followed the failure mode steps mentioned previously. Excavation of the section also showed that the subgrade was highly saturated thus weakening the bearing capacity of the subgrade and contributing to the failure of the section.

Rutting was the cause of failure for the remaining thick sections. The ruts progressed as the wheel loads accumulated. Figures 34 and 35 show the extent of rutting on section 12 after it was resurfaced with an asphalt concrete

overlay. Tables 19 and 20 (p. 95) show the depth of the ruts. Figures 71 to 74 show the rutting as it progressed in section 3. Ruts of over 2½ inches developed without any visible cracking. Figure 74 (p. 78) shows that even with an asphalt concrete overlay the deformation continued. Figures 75 to 79 show how the ruts progressed with accumulated wheel loads in section 4 (p. 79). Figures 80 to 83 show the rutting with accumulated wheel loads in section 8. The extent and depth of ruts are shown in the individual photographs; Tables 19 and 20 give the depth of the ruts in the wheel paths of the sections.

These sections to date have not been excavated. It is hoped that in the future, sections will be cut through with a diamond saw and the extent and depth of the ruts for the individual layers and subgrade will be studied. If the results from Ring 3 are any criteria, the ruts probably extend into the subgrade and examination of the bottom layer of the bases will probably reveal that cracks have started to develop. Further study is needed.

The difference in modes of failure between the fall and spring periods is probably due to the difference in environmental conditions. An interesting observation came out of the adjustment of the LVDT gages prior to testing. Adjustments had to be made which indicated that the pavements had risen by 1/16 to 1/8 of an inch. This seems to indicate that the pavements were uplifted during the winter. This may explain why such rapid failures occurred. Differential recompaction of the highly saturated subgrade from the transversed part of the pavement to the non-transverved part may have occurred, causing localized stresses at the edge of the wheel track thereby bringing about a punching shear situation. The semi-rigidity of the sand-asphalt and Class "F" asphalt treated bases may have changed the rate of failure. The

TABLE 19. PERMANENT PAVEMENT DEFORMATION DEPTHS AFTER 177,501 WHEEL LOAD APPLICATIONS

Section:	3*			4			8			12**		
Material:	6.0 inches SAB Rut Depth-Inches			8.0 inches SAB Rut Depth-Inches			5.0 inches ACB Rut Depth-Inches			12.0 inches UTB Rut Depth-Inches		
Line	1'inside ℄	℄	1'outside ℄	1'inside ℄	℄	1'outside ℄	1'inside ℄	℄	1'outside ℄	1'inside ℄	℄	1'outside ℄
A	1-3/8	1-1/8	1/2	3/8	11/16	11/16	3/8	5/8	1/2	0	1/4	1/4
B	1-3/8	1-1/4	3/4	3/8	11/16	5/8	1/2	1/2	9/16	1/4	1/2	7/16
C	1-1/2	1-7/16	15/16	7/16	13/16	3/4	1/4	11/16	3/4	1/8	3/8	5/16
D	1-7/16	1-1/2	1	1/8	5/8	11/16	1/4	11/16	3/4	1/4	3/8	3/8
E	1-1/8	1-3/16	3/4	3/16	9/16	1/2	3/8	13/16	3/4	1/2	11/16	1/2
Deepest Rut	2-1/16" outside E, 6" outside ℄			13/16 ℄ Line C			13/16 ℄ Line E			1" Line E, 6" inside ℄		

*At "ultimate" failure
**With overlay

TABLE 20. PERMANENT PAVEMENT DEFORMATION DEPTHS AFTER 247,128 WHEEL LOAD APPLICATIONS

Section:	3*			4			8			12*		
Material:	6.0 inches SAB			8.0 inches SAB			5.0 inches ACB			12.0 inches UTB		
	Rut Depth-Inches			Rut Depth-Inches			Rut Depth-Inches			Rut Depth-Inches		
Line	1'inside ℄	℄	1'outside ℄	1'inside ℄	℄	1'outside ℄	1'inside ℄	℄	1'outside ℄	1'inside ℄	℄	1'outside ℄
A	7/8	1-1/16	5/8	3/4	7/8	7/16	5/8	3/8	3/8	1/4	1/2	7/16
B	3/4	1-1/16	1/2	9/16	3/4	11/16	5/8	1/2	1/4	3/8	5/8	7/16
C	3/4	7/8	3/8	3/4	13/16	13/16	5/8	5/8	1/4	3/8	5/8	3/8
D	1-1/8	1-1/2	3/4	9/16	5/8	5/8	1/8	3/8	1/4	7/16	5/8	7/16
E	1-1/8	15/16	3/4	1/2	11/16	5/8	1/8	1/4	0	1/4	3/8	0
Deepest Rut	1-5/16" Line E, ℄			1-3/8, 6" outside ℄ Line C			3/4", Lines A & C, 8" outside ℄ and 6" outside ℄ respectively			7/8", Lines C & D, 6" inside ℄ for both		

*With overlay

fact that section 12 with 12 inches of untreated base did not reach "ultimate" failure even when cracked indicates that the structure of its base enables it to follow the compaction and contours of subgrade (16).

The concept of "Pavement Failure Span" (PFS) was originally brought out in the report of Ring #2 and was used in Ring #3 (3); it is shown in Table 21. The table shows that for some sections almost as many wheel applications were needed to cause initial cracking as were needed to reach "ultimate" failure. The table shows that the more rigid pavement sections (1-4 and 6-8) did not have large pavement failure spans. It is interesting to note that the sections which cracked in the spring had lower pavement failure spans. The untreated sections in all three rings had higher pavement failure spans than the treated base sections. Contributing factors should be considered in evaluation of PFS. These factors are type and thickness of base, environmental conditions of temperature and moisture at time of testing. In addition, "ultimate" failure point is somewhat arbitrary. The researchers believe that the concept does indicate a relationship of interest which may have possible uses in maintenance planning.

The equivalency thickness is shown in Table 22. The equivalencies obtained for the fall period of 1968 are based on the thinnest surviving sections. The 1969 spring equivalencies are based on the thickest section that failed during this period.

TABLE 21: PAVEMENT FAILURE SPAN (PFS)[1]

Base Type	Section	Base Thickness (Inches)	Wheel Load Applications: Initial Cracks WL_I	Wheel Load Applications: At Failure WL_F	Wheel Load Applications: Initial to Failure WL_F-WL_I	PFS	Time Period
Sand-Asphalt	1	2.0	144,660	157,020	12,360	8.5	Spring
	2	4.0	159,789	164,790	5,001	3.1	Spring
SAB	3	6.0	175,620[2]	177,501	1,881	1.1	Spring
	4	8.0	175,620[2]	247,128	28,492	16.2	Spring
CL "F" Asphalt Concrete	5	0.0	47,391	144,660	97,269	205.2	Fall-Spring
	6	2.0	148,887	158,235	9,348	6.3	Spring
ACB	7	3.5	161,262	171,168	9,906	6.1	Spring
	8	5.0	175,620[2]	247,128	71,508	40.7	Spring
Crushed Surfacing Top Course	9	4.5	12,000	36,681	24,681	205.7	Fall
	10	7.0	47,391	104,187[3]	56,796	119.8	Fall
				144,660	97,269	205.2	Fall-Spring
UTB	11	9.5	48,000	144,660	96,660	201.4	Fall-Spring
	12	12.0	49,104	144,660[4]	95,556	194.6	Fall-Spring
				247,128[5]	198,024	403.3	Fall-Spring

1 $$P.F.S. = \frac{\text{Wheel Load Applications (Failure-Initial)}}{\text{Wheel Load Applications to First Sign of Cracking}} = \frac{WL_F - WL_I}{WL_I} \times 100$$

2 Distress for these sections was rutting.

3 One-half of section 10 was removed and overlaid.

4 This section was overlaid with an asphalt concrete mix.

5 Includes the wheel loads applied on the asphalt concrete overlay.

TABLE 22: EQUIVALENT THICKNESSES
(3.0" of Class "B" A.C. Wearing Course)

Base Type	Fall 1968 Period[1]		Spring 1968 Period[2]	
	Base Thickness	In Terms of ATB	Base Thickness	In Terms of ATB
Crushed Surfacing Top Course (CSTC) Untreated (UTB)	9.50	4.75	12.0	2.40
Sand-Asphalt (SAB)	2.00	1.00	8.0	1.60
CL "F" Asphalt Concrete (ACB)	2.00	1.00	5.0	1.00

1 The thinnest sections which survived during this period.

2 Thickest sections which failed during this time.

Load Response Characteristics

Temperature Variables

Weather during the fall testing period of 1968 can be described as miserable. During the construction of Ring 4 work could be done only between breaks in the bad weather. Testing started during a cold and wet period. The month of November was rainy with snow; ambient temperatures were falling and frequently were below freezing. The fall testing period can be characterized as a period of low falling temperatures with much rain and some snow (see Table 11). The pavement temperatures were low during this period and frequently were below freezing.

During the 1969 spring period, air, pavement and soil temperatures in April and the early part of May were fairly consistent. The temperatures slowly began to rise after May and soon reached typical summer values. The month of April was wet; thereafter the testing period was dry with little rain. The 1969 testing period can be subdivided into spring and summer testing periods. Temperatures probably affected the strain, stress and deflection readings. The high summer temperatures may have contributed to the surfacing rutting of the thick experimental sections.

Moisture Contents

Although moisture tensiometers were installed in the subgrade, the cold weather along with freezing temperatures damaged the gages so that no meaningful moisture data was obtained.

The moisture contents of the Palouse silt subgrade during construction were on the dry side. This probably changed rapidly because of the heavy rainfall during October and November. The rain probably penetrated into the

subgrade and untreated bases through the outside untreated shoulders and through natural moisture movement. Probably by the time the testing started the subgrade was partially saturated. Table 15 seems to indicate this and shows that although moisture contents decreased with depth, they were above optimum. The amount of moisture from seepage of rain through cracks is unknown.

The heavy snowfall during the winter resulted in an almost completely saturated subgrade. Samples taken from the failed sections as shown in Table 18 show that moisture contents were higher than in the fall and had penetrated deeply into the subgrade. The degree of saturation in the spring ranged from 90-100%; during construction the degree of saturation ranged from 55-64%.

High moisture contents in the subgrade and bases during both fall and spring periods indicate that moisture played an important role in the failures of the sections. The fact that moisture contents were above those during construction and above optimum during the two testing periods implies that the subgrade bearing strength was weakened which could have led to the early failures of the untreated bases in the fall and the rapid failures during the spring testing period.

Static Deflections

*Benkelman beam rebound measurements using the Canadian Good Roads Association procedure (18) were taken at five selected intervals per section as shown in Figure 84. This was done to check the homogeneity of the test pavement section and to obtain a better rebound average for that test section.

Rebound measurements were taken at the start of testing and continued throughout the testing period in the fall and spring. Pavement temperatures were obtained from thermocouples in the pavements and were averaged out for the pavement system. The average pavement temperature for the sand-asphalt

*See appendix B

and Class "F" asphalt concrete bases was the average of the top of pavement and the top and bottom of the base; for the untreated, the pavement temperature was the average of the top and bottom of the Class "B" asphalt concrete pavement. Some typical Benkelman beam rebound readings are shown on Table 14. No temperature corrections were made for the deflection measurements.

Table 23 shows the Benkelman beam rebound measurements with accompanying pavement temperatures obtained during the fall of 1968. The table shows that the untreated base sections had unusually high deflection readings. When these readings are compared to those from Ring #3, these untreated sections in Ring #4 seem to indicate different subgrade conditions than were present during the fall of 1967. All the sections show higher than usual readings probably indicating the effect of adverse environmental conditions prior to and during the testing period. Cracks seem to have started after deflections of over 0.050 inches had been measured. The table also shows that as pavement temperatures decreased, deflections also decreased.

Table 24 shows the Benkelman beam rebound measurements for April to June 1969. Deflection readings were 2 to 4 times greater than those measured in the fall. This is probably due to the existence of a highly saturated subgrade thus causing a loss of support. Cracks seemed to have occurred after deflection measurements of 0.10 inches had been reached. Table 25 data are Benkelman beam rebound deflections for July and August and seem to show that the maximum deflection readings had occurred and that the readings were starting to decrease. Figure 85 shows the same effect. This may indicate that the subgrade may have reached its limit of deformation for the surviving sections and thus began to stabilize.

TABLE 23: SUMMARY OF FALL 1968 BENKELMAN BEAM REBOUND DEFLECTIONS - RING #4

Date:		11 - 06		11 - 09		11 - 16		11 - 19		
Wheel Loads x 1000:		0.4		25.0		49.1		91.2		
Section Type	Thickness (Inches)	Pavement Temp. °F	Deflect. In.	Pavement Temp. °F	Deflect. In.	Pavement Temp. °F	Deflect. In.	Pavement Temp. °F	Deflect. In.	
1 SAB	2.0	50	0.044	46	0.041	27	0.029	43	0.036	
2	4.0	49	0.033	46	0.035	28	0.021	44	0.026	
3	6.0	50	0.023	47	0.023	29	0.018	44	0.022	
4	8.0	51	0.023	46	0.021	30	0.014	44	0.017	
5 ACB	0.0	52	0.043	49	0.048	36	0.042	45	0.043	cracked
6	2.0	51	0.048	47	0.049	30	0.033	43	0.039	
7	3.5	52	0.041	46	0.043	31	0.026	43	0.038	
8	5.0	52	0.030	47	0.033	33	0.018	44	0.026	
9 UTB[1]	4.5	52	0.099	45	0.122	--	--	--	--	
10	7.0	51	0.054	45	0.073	30	0.068	34	0 099	
11	9.5	54	0.052	46	0.074	31	0.074	35	0.086	cracked
12	12.0	53	0.058	46	0.075	29	0.080	35	0.094	

[1] Pavement temperature is based on the average between top and bottom temperatures of the Class "B" asphalt concrete pavement.

TABLE 24: SUMMARY OF SPRING 1969 BENKELMAN BEAM REBOUND DEFLECTIONS - RING #4

Date:		03 - 31		05 - 22		05 - 26		06 - 02		06 - 12		06 - 13		06 - 16		06 - 27	
Wheel Loads x 1000:		143.4		157.0		158.2		164.8		171.2		173.5		174.9		194.9	
Section & Type	Thickness (Inches)	PT °F	Defl. In.	PT °F	Defl. In.	PT °F	Defl. In.	PT °F	Defl. In.	PT °F	Defl. In.	PT °F	Defl. In.	PT °F	Defl. In.	PT °F	Defl. In.
1 SAB	2.0	70	0.124														
2	4.0	68	0.079	76	0.129	72	0.163										
3	6.0	69	0.065	78	0.101	72	0.177	74	0.177	81	0.124	80	0.165	83	0.171	73	0.136[2]
4	8.0	68	0.063	79	0.088	72	0.097	78	0.101	77	0.124	82	0.107	81	0.112	77	0.103
5 ACB	0.0	68	0.207														
6	2.0	71	0.128	83	0.159[3]												
7	3.5	69	0.103	79	0.119	73	0.147	77	0.144[3]								
8	5.0	66	0.088	79	0.104	74	0.108	80	0.126	78	0.138	80	0.130	85	0.130	79	0.113
9 UTB[1]	4.5																
10	7.0	72	0.154														
11	9.5	74	0.136														
12	12.0	72	0.100	83	0.072[2]	73	0.086	82	0.069	77	0.079	78	0.078	102	0.085	83	0.077

[1] Pavement temperature is based on the average temperature between top and bottom temperatures of the Class "B" asphalt concrete pavement.
[2] An asphalt concrete overlay was put on these sections.
[3] Transverse cracks were present.

An interesting experiment was conducted during July 14-15. Benkelman beam rebound measurements were taken on sections 4, 8 and 12 during a 24-hour period in an attempt to study the effects of temperature on pavement rebound. By chance, the time taken was a day when the air temperature dropped from a high of 74°F to a low of 33°F during this 24-hour period. Figure 86, page 110, shows the variation of deflection with pavement temperature. All three sections exhibit a hysteresis effect which may be due to the fact that this experiment was run on Monday after a weekend of no testing and the locked-in stresses and strains had no chance to be released. One study suggests that plastic movement in the asphalt mix may be responsible (19). This points out some of the difficulties of trying to correct deflection for temperature effects.

Dynamic Deflections

Dynamic deflections were measured by Sanborn Linear Variable Displacement Transformers (LVDT) in sections 2, 4, 7 and 10 (4.0 and 8.0 inches of sand-asphalt base, 3.5 inches of Class "F" asphalt concrete base and 7.0 inches of untreated base, respectively) during the period when strain gage readings were taken and during a continuous time period. The deep LVDT gages measured movement of the pavement system including subgrade; the shallow gages measured movement of the surface and base layers only. It was found after installation that the deep LVDT gage in section 7 was defective and hence no deep deflections were obtained from this gage. Some dynamic deflections were taken in conjunction with Benkelman beam measurements to check out the deep LVDT gages and installations. The correlation appeared good.

TABLE 25: SUMMARY OF SUMMER 1969 BENKELMAN BEAM REBOUND DEFLECTIONS - RING #4

Date:		07 - 10		07 - 15		07 - 24		07 - 28		08 - 21	
Wheel Loads x 1000:		202.8		205.8		216.2		220.8		247.1	
Section & Type	Thickness (Inches)	PT °F	Defl. In.	PT °F	Defl. In.	PT °F	Defl. In.	PT °F	Defl. In.	PT °F	Defl. In.
1 SAB	2.0										
2	4.0										
3	6.0	82	0.144[2]	60	0.123	86	0.125	100	0.126	101	0.098
4	8.0	81	0.113	68	0.098	86	0.101	109	0.081	86	0.073
5 ACB	0.0										
6	2.0										
7	3.5										
8	5.0	85	0.137	70	0.105	91	0.123	111	0.111	92	0.086
9 UTB[1]	4.5										
10	7.0										
11	9.5										
12	12.0	108	0.077[2]	61	0.056	88	0.061	110	0.055	92	0.043

[1] Pavement temperature is based on the average between top and bottom temperatures of the Class "B" asphalt concrete pavement.
[2] These sections had an asphalt concrete overlay.

TABLE 26: SUMMARY OF LVDT DEFLECTION MAXIMUM MEASUREMENTS
RING #4

Section	LVDT	Position	Period	Deflection Under Tires Inches	Deflection ℄ Duals Inches	Average Pavement Temp. °F	Speed mph
2	1	Shallow	Nov.	0.0009	0.0005	42	15
			Spring	0.044	0.042	86	10
	2	Deep	Nov.	0.030	0.016	42	20
			Spring	0.123	0.120	86	10
4	3	Shallow	Nov.	0.0009	0.0009	44	20
			Spring	0.0056	-	94	10
			Summer	0.007	-	98	8
	4	Deep	Nov.	0.036	-	42	20
			Spring	0.036	-	94	10
			Summer	0.071	0.071	93	8
7	5	Shallow	Nov.	0.0037	0.0013	43	20
			Spring	0.0026	-	63	10
10	7	Shallow	Nov.	0.015	-	40	15
	8	Deep	Nov.	0.079	-	33	15
			Dec.	0.179	-	33	15

FIGURE 84. LOCATION OF BENKELMAN REBOUND MEASUREMENTS

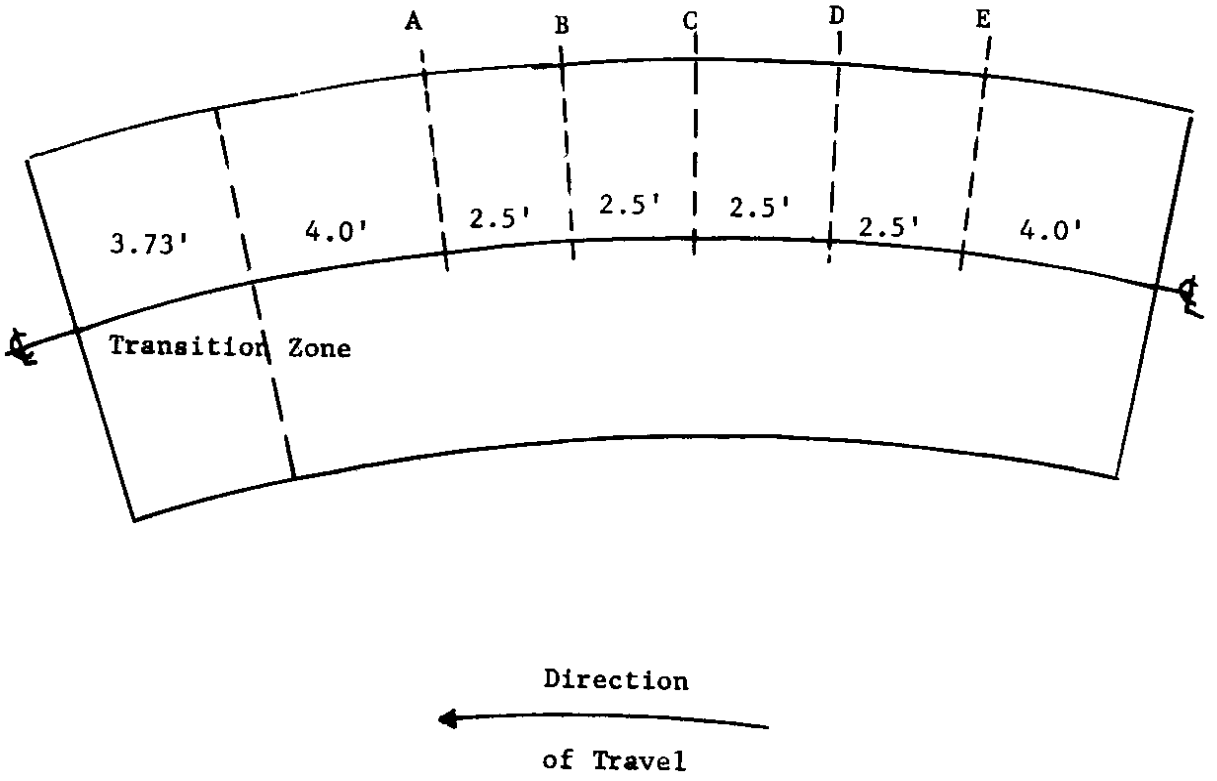

FIGURE 85. BENKELMAN BEAM REBOUND DEFLECTIONS VS. WHEEL LOADS

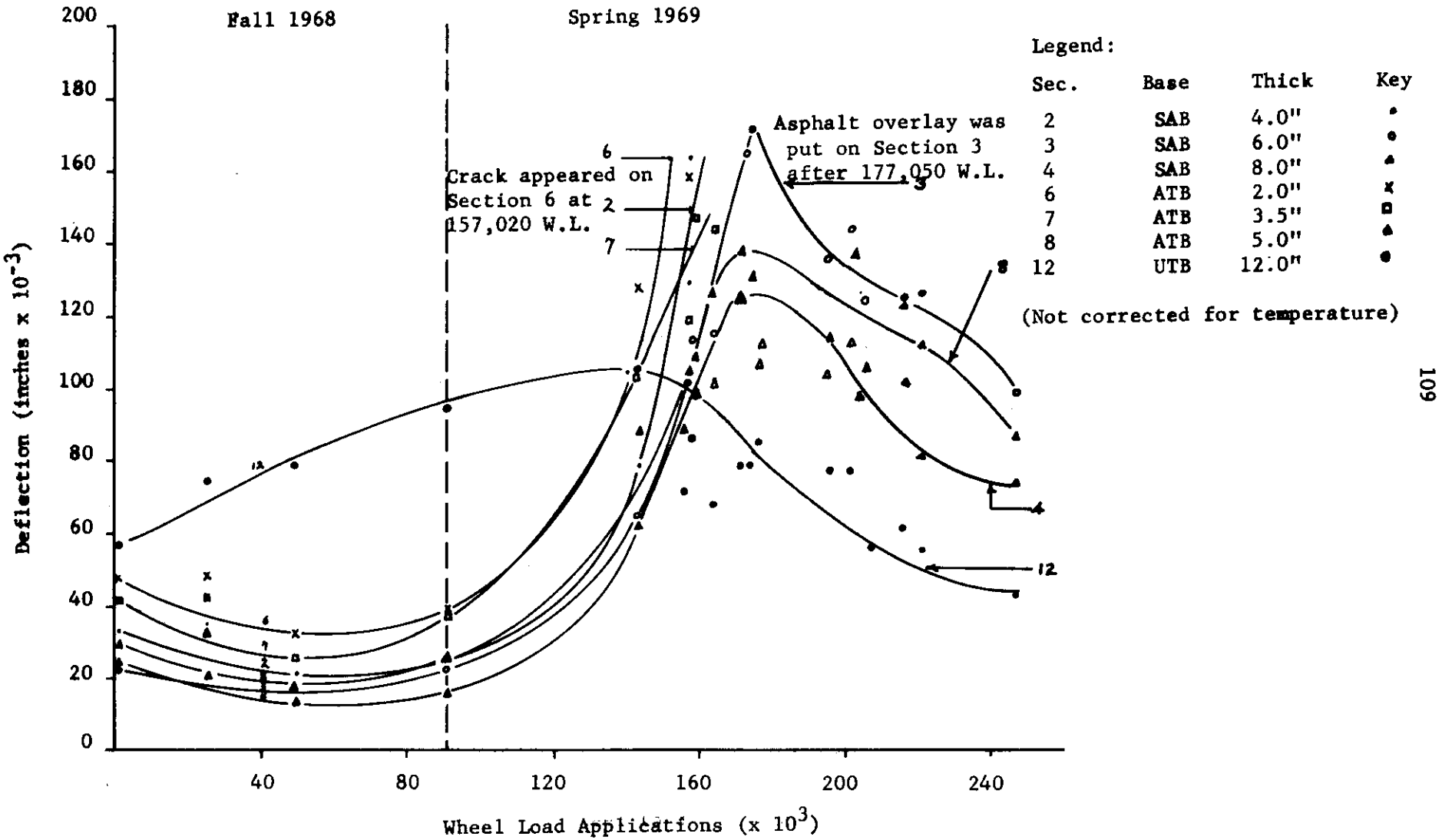

FIGURE 86. PAVEMENT TEMPERATURE VS. BENKELMAN BEAM DEFLECTION (24-Hour Period)

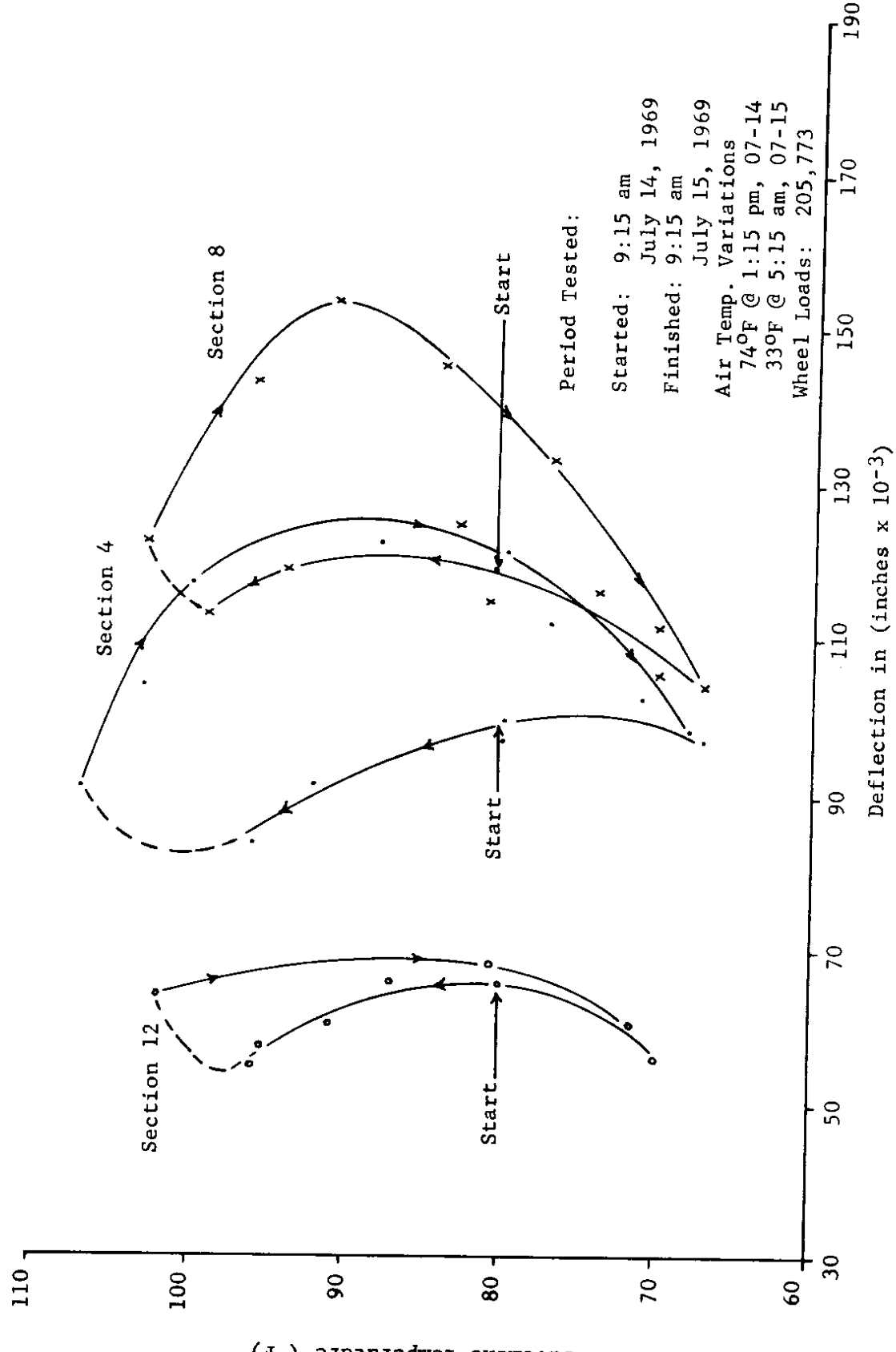

Note: Line 'A' & C temperatures combined in each section.

In previous rings, the fall testing period was divided into two periods. This was not done for Ring #4 as the temperature and the environmental conditions were rather uniform. By the end of the fall period most of the LVDT gages were not operational. Figure 87 is included since the position of the dual tires plays a very important role in affecting the value of deflections, strains and stresses (15, 20, 21).

Figures 88 and 89 show the deflection variations with transverse distance at a speed of 15 mph for LVDT #1 and LVDT #2 in section 2. Temperature effects were ignored since there was not a wide range. Table 26 (p.107) shows that the maximum readings occurred while one of the tires was over the gage. The figures and the table show that the dynamic deflections were very low in the fall and that the pavement structure wearing course plus base deflections measured by LVDT #1 were very low with respect to the total pavement system which was measured by LVDT #2. During the fall period, deflections occurring within the pavement system were only 3.3% of the total pavement system; this ratio is called the dynamic deflection ratio. In the spring, the dynamic deflections increased by some 8 times for the pavement structure but stayed about the same for the total pavement system. Thirty-six percent of the deflections occurred within the pavement structure. This would indicate that whole pavement structures may become more flexible under wheel load applications in a wet environment. The fact that the pavement structure deflection increased with respect to the subgrade by some 30% seems to indicate that the pavement was taking up more of the load and the subgrade less. The mode of failure shown in Figures 56-64 is an indication that the subgrade was displaced because the pavement structure was unable to continue taking the wheel load applications.

The deflection data for 8.0-inch sand-asphalt base is shown in Figures 90 to 91 (p. 115) and in Table 26 (p. 107). The thick base reduced the amount of deflections being taken by the pavement structure. Only 2.5% of the dynamic deflections were taken by the pavement structure. The cold temperature probably had quite a bit to do with this small ratio. In the spring, the dynamic deflection ratio increased to 15.5% and then decreased to 10%. The thick base reduced dynamic deflections within the pavement structure while protecting the subgrade from the wheel load effects. It appears that the sand-asphalt base is not as stiff as regular asphalt concrete base and hence may deform more readily to wheel load applications without cracking. This may have occurred in section 3 which had extremely deep ruts without cracking as shown in Figures 71 to 74.

Not much can be written about the deflections in section 7 since only the shallow LVDT #5 was working. Figure 93 shows a typical curve for this gage. Table 26 shows that dynamic deflections did not increase in the spring but this was due to the shallow gages which had to be adjusted frequently.

Dynamic deflections in section 10, 7.0 inches of untreated base, were high thus indicating that conditions were different in this section. Some 18% of the dynamic deflections were taken up by the pavement structure. Figures 94 and 95 (p. 118-119) show the variations of dynamic deflections with lateral distance and show the effect of temperature on the readings. After cracking occurred, dynamic deflections increased perhaps indicating that that pavement was now acting as separate slabs rather than one continuous beam. Figure 25 (p. 52) shows that pavement was cracked by the LVDT thus the gage may have been measuring slab action.

FIGURE 87. DIMENSIONS OF DUAL TIRES

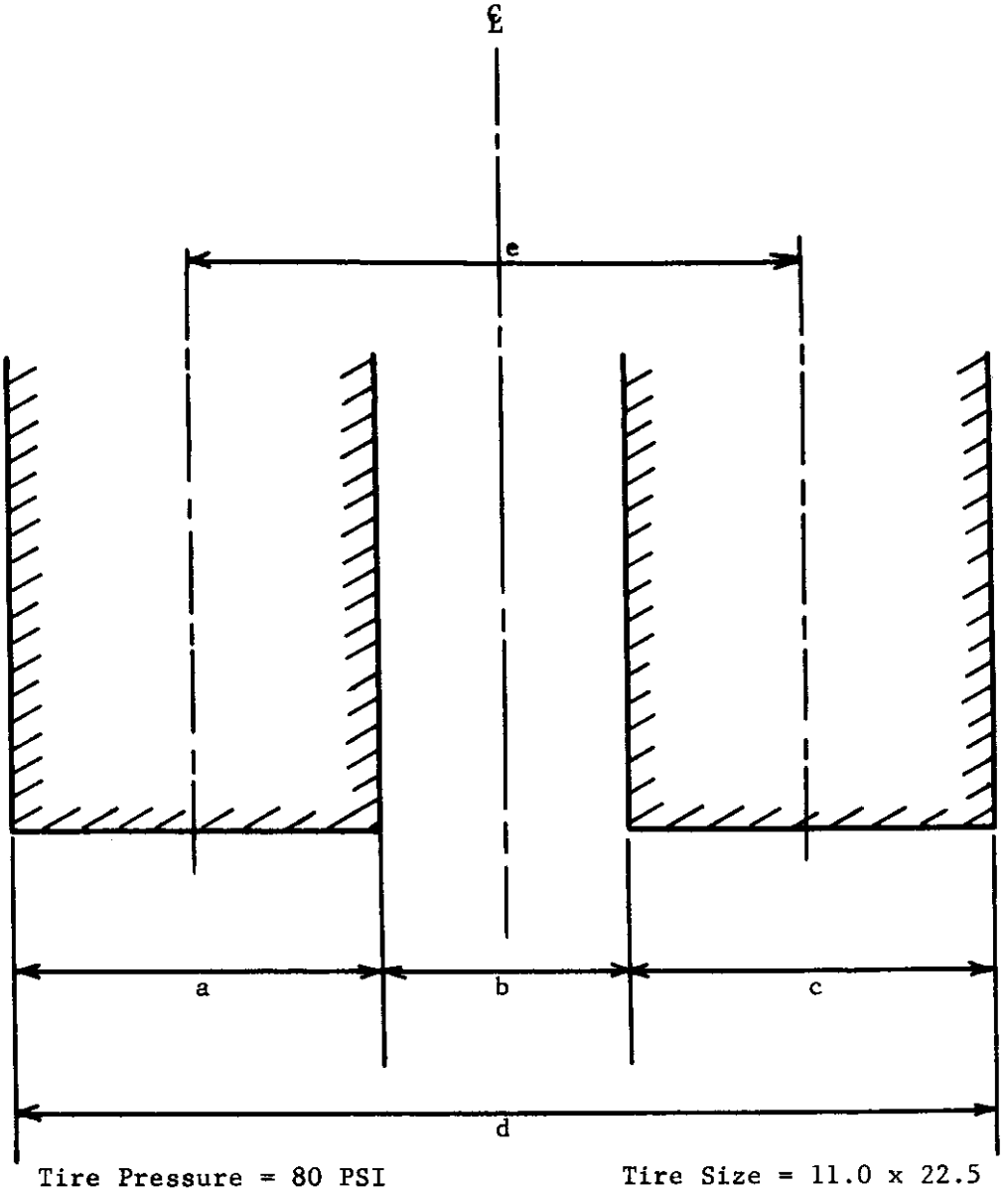

Tire Pressure = 80 PSI
Length of Tire = 11 "
a = c = 7.75" = 0.65'
b = 5.25" = 0.43'
d = 20.75" = 1.73'
d/2 = 10.37" = 0.86'
e = 13.0"

Tire Size = 11.0 x 22.5
Wheel Load = 5300 lbs.
Dual Load = 10,600 lbs.
Single Axle Load = 21,200 lbs.
Contact Area/Tire = 85.25 sq. in.

Scale: 1" = 4.0"

FIGURE 88. DYNAMIC DEFLECTION VS. LATERAL DISTANCE

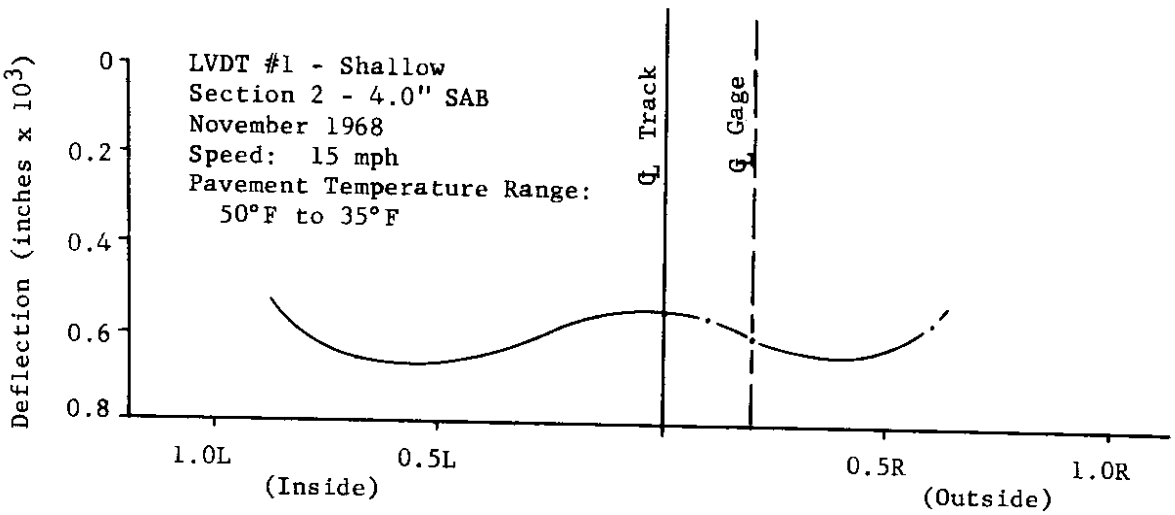

Distance to Duals (ft.)
LVDT #1
(Duration: November 4, 1968 to May 22, 1969)

FIGURE 89. DYNAMIC DEFLECTION VS. LATERAL DISTANCE

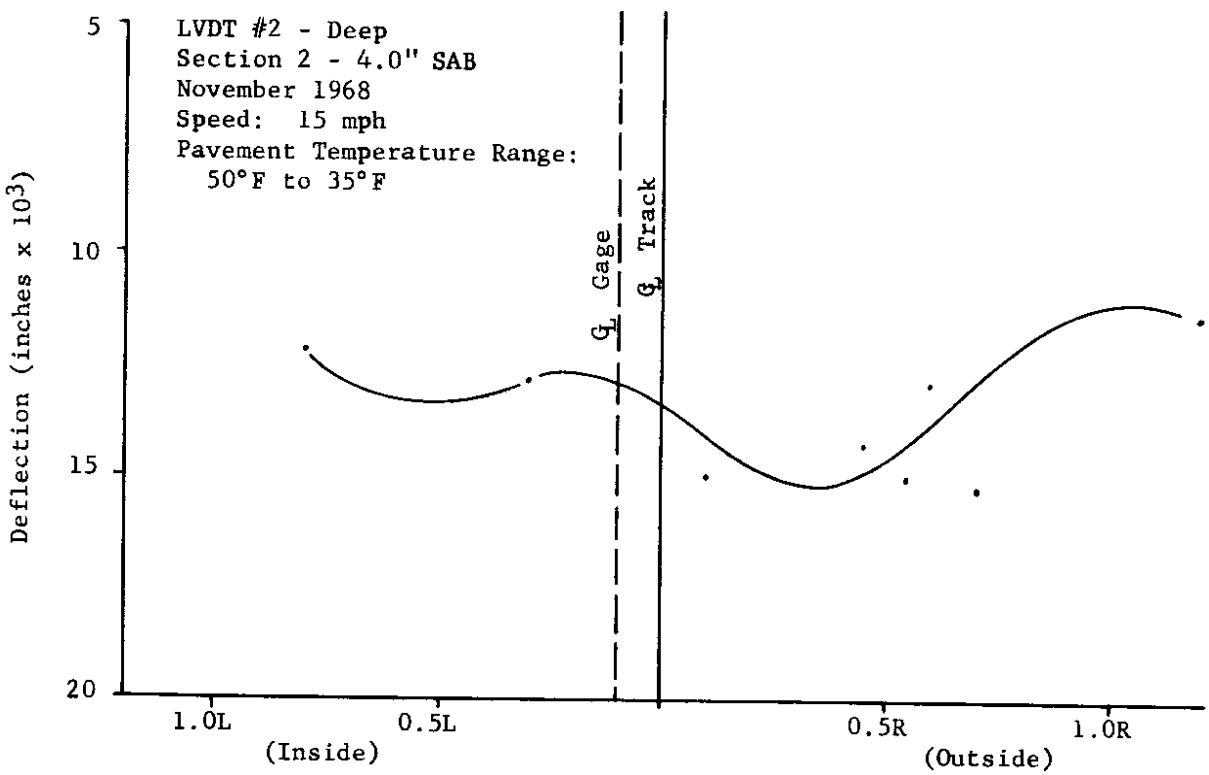

Distance to Duals (ft.)
LVDT #2
(Duration: November 4, 1968 to May 22, 1969)

FIGURE 90. DYNAMIC DEFLECTION VS. LATERAL DISTANCE

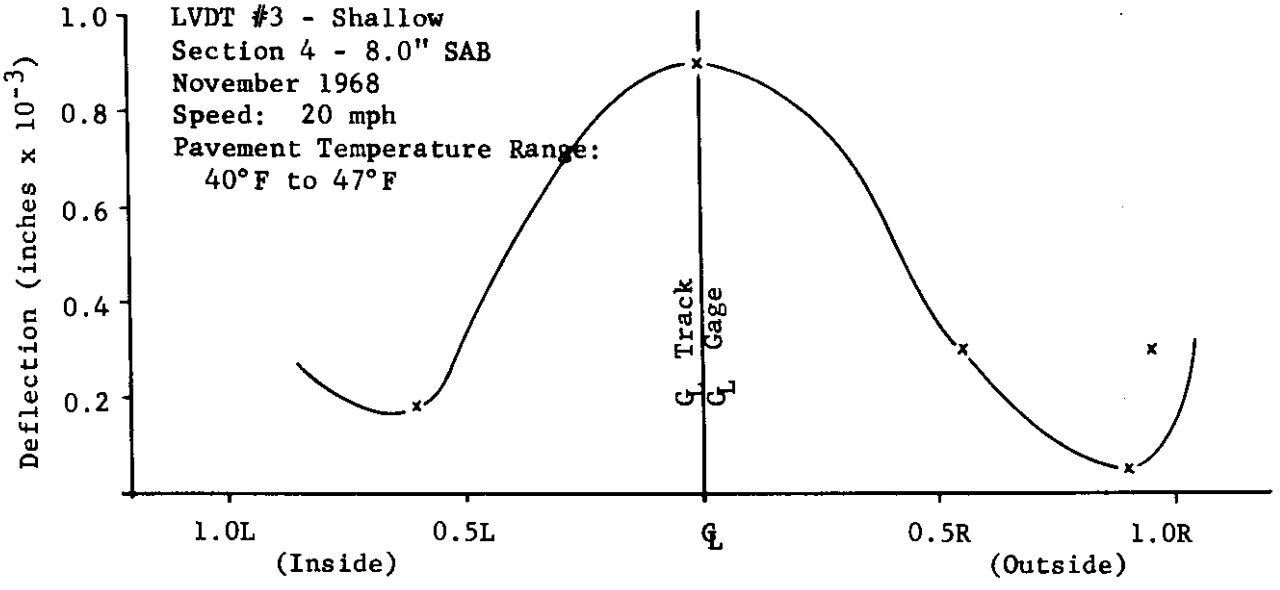

FIGURE 91. DYNAMIC DEFLECTION VS. LATERAL DISTANCE

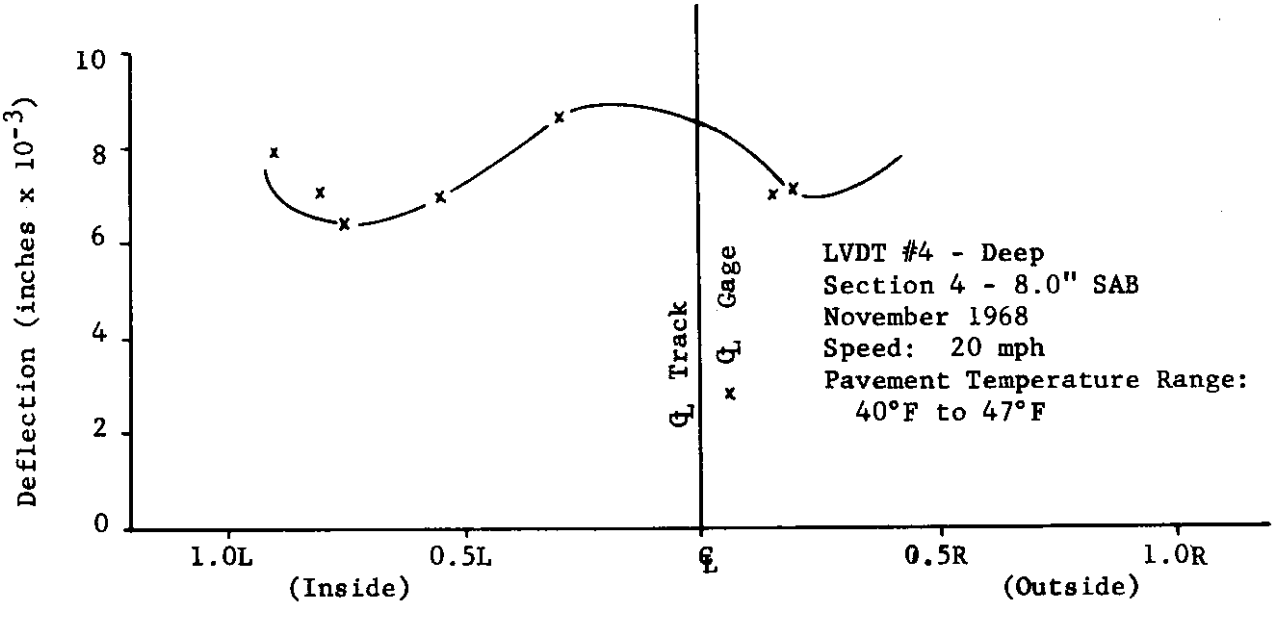

Legend:

Temperature	Symbol
40°F to 47°F	X

Note: Data from runs--wheel load effects were ignored.

FIGURE 92. DYNAMIC DEFLECTION VS. LATERAL DISTANCE
Ring #4 - Section 4 - 8.0" SAB
SPRING 1969

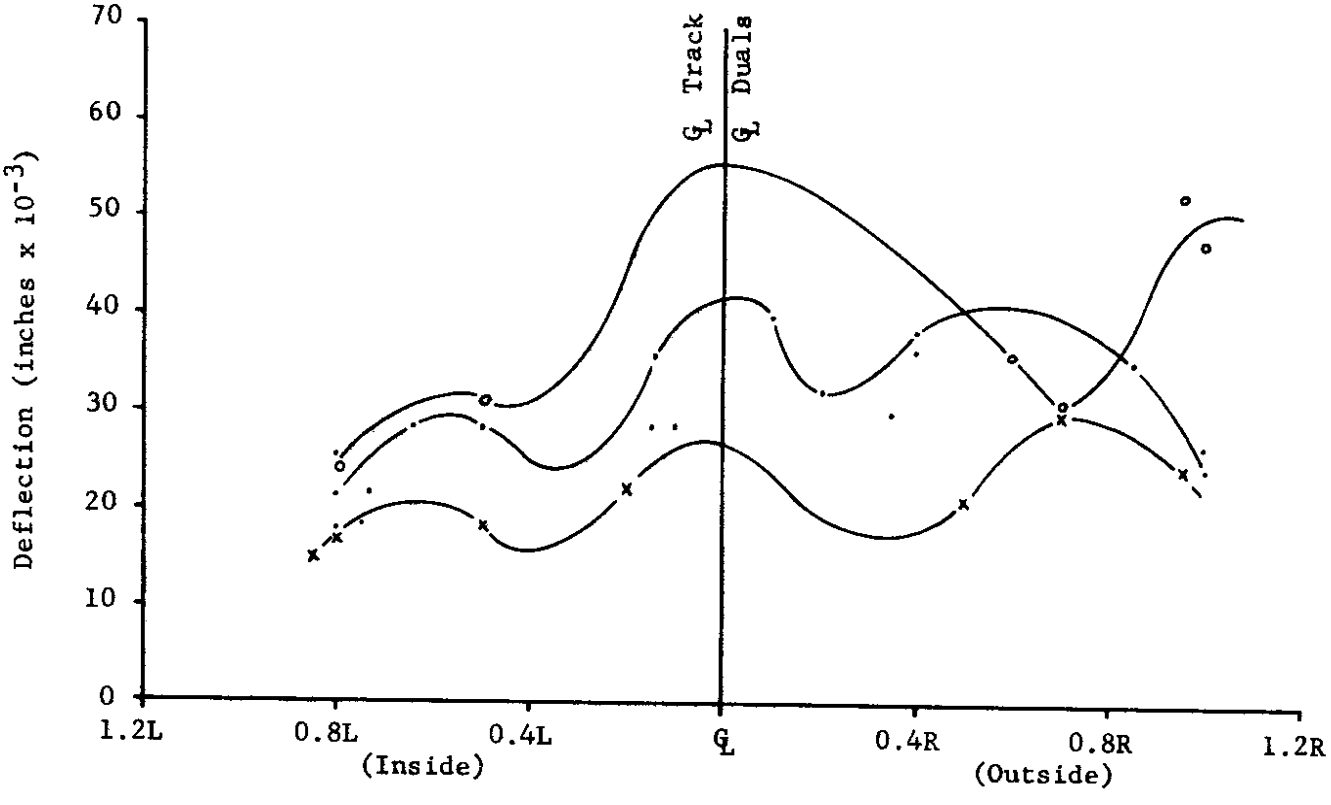

Legend:

Temperature	Symbol
48°F to 65°F	×
66°F to 85°F	·
86°F to 110°F	o

Speed: 6-10 mph

(Number of wheel loads disregarded)

FIGURE 93. DYNAMIC DEFLECTION VS. LATERAL DISTANCE

Ring #4 - Section 7 - 3.5" Cl "F" ACB

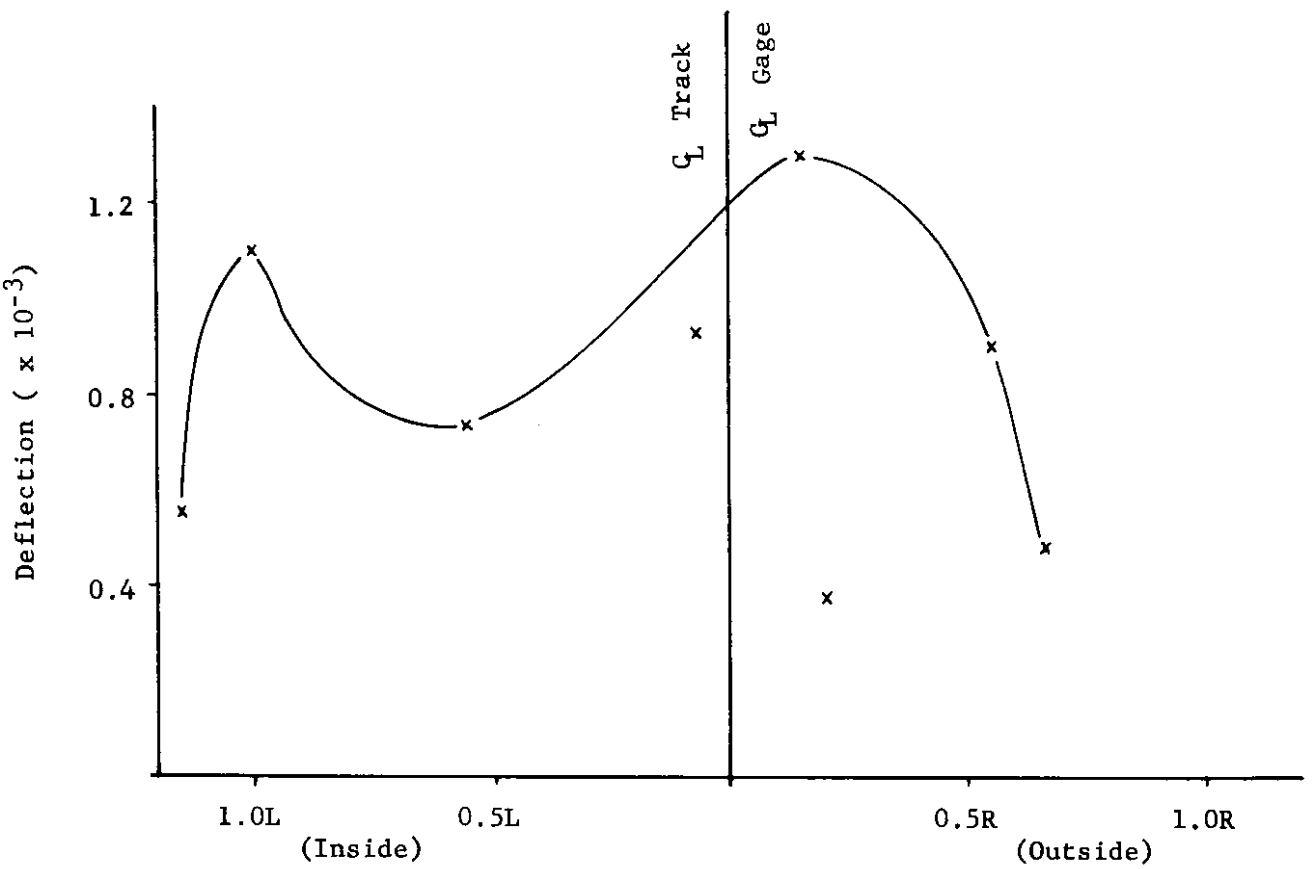

Distance to Duals (ft.)
LVDT #5 (Shallow)

Legend:

Temperature	Symbol
40°F to 47°F	X

Speed: 20 mph
November 1968

(Number of wheel loads disregarded)

FIGURE 94. DYNAMIC DEFLECTIONS VS. LATERAL DISTANCE

Ring #4 - Section 10 - 7.0" UTB

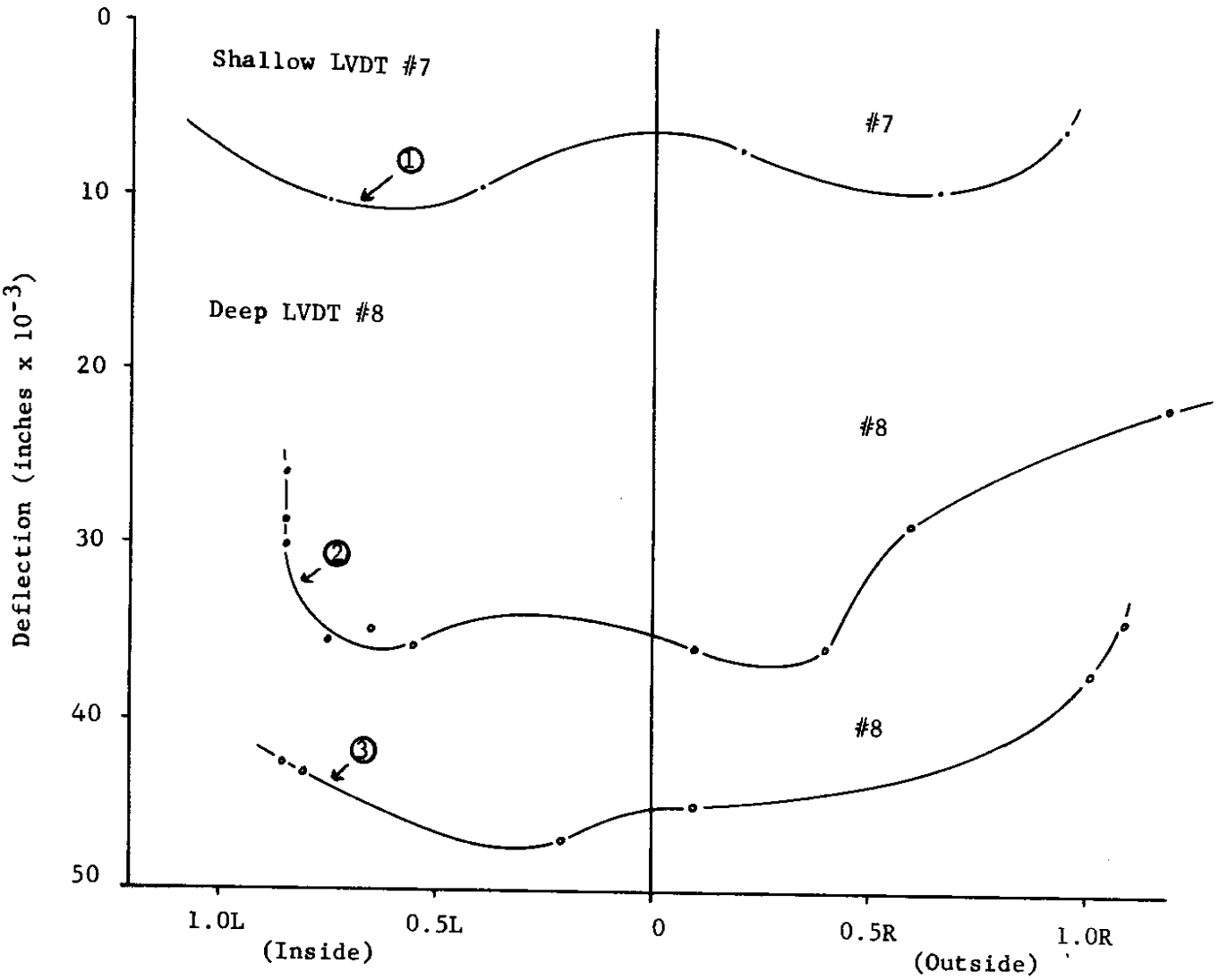

Legend:

November 7 - November 24, 1968
Run number 2 → 20
Speed: 20 mph for ① & ②
10-15 mph for ③

(Number of wheel loads disregarded)

Pavement Temperature Range:

①& ② 33°F to 40°F
③ Ave. 35°F

FIGURE 95. DYNAMIC DEFLECTIONS VS. LATERAL DISTANCE
(CONTINUOUS READINGS)

Ring #4 - Section 10 - 7.0" UTB

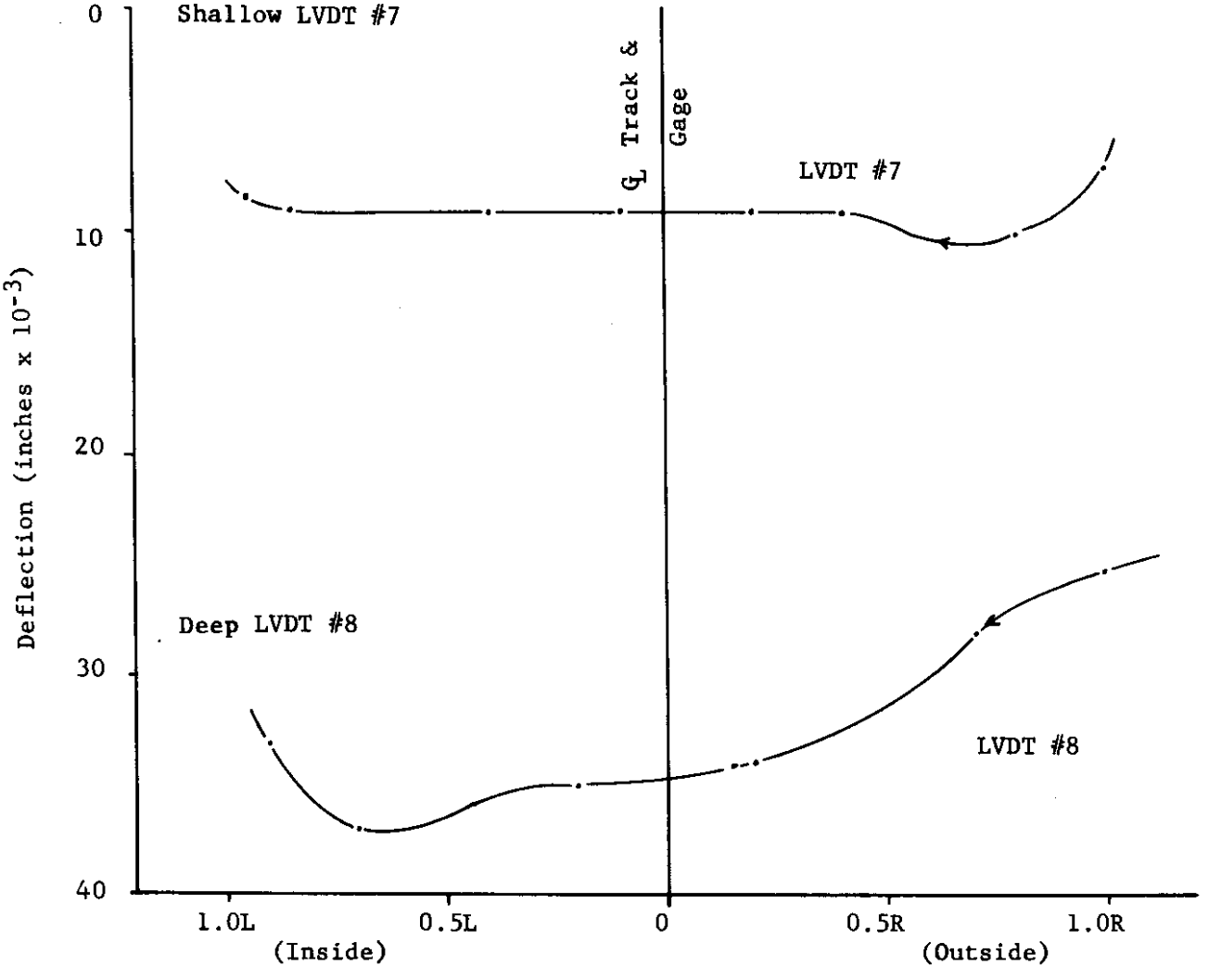

Legend:

7:30 pm - 12:00 mn
Ave. TC Temp. - 39°F to 37°F
Speed: 20 mph
November 15, 1968

(Number of wheel loads disregarded)

Deflections appear to have increased with wheel load repetitions. However, this may not be a function entirely due to wheel loads but to other factors such as the thickness and type of base, and most important, the changing environmental conditions. The latter, especially during the spring, caused a highly saturated subgrade condition which caused a decrease in both pavement and subgrade moduli and strength.

Although this was not examined, speed and temperature do affect the pavement deflection (22). Static deflections measured with a Benkelman beam usually are higher than those measured by LVDT gages under dynamic conditions. Figure 97 (p. 121) shows the effect of speed on dynamic deflections which increase as speed is decreased.

With time and wheel load applications, the pavement structure was called upon to take up more and more of the total pavement deflection. This is shown in Figure 96. This increase in dynamic deflection ratio indicates an increasing flexure in pavement structure thus inducing fatigue failure in the pavement. This is shown in Figures 62, 64, 73 and 74, in sections 2 and 3. Here one can see that base and pavement were deformed due to flexure and fatigue and that cracks started from the bottom.

Strain Gage Data

The strain gage data was plotted against lateral wheel placement by fall and spring periods whenever data was available. The data came from continuous readings (readings taken every half-hour or so during a 24-hour day or longer) and also from runs; that is, during a certain period of the day all the instruments were read. The combined data was frequently plotted together to be able to sort out the different variations due to temperature and lateral tire distance from the gage. The effects of accumulated wheel loads during

(Text continued on page 127.)

FIGURE 96. DYNAMIC DEFLECTION RATIO $\frac{(\text{SHALLOW})}{(\text{DEEP})}$ VS. WHEEL LOADS

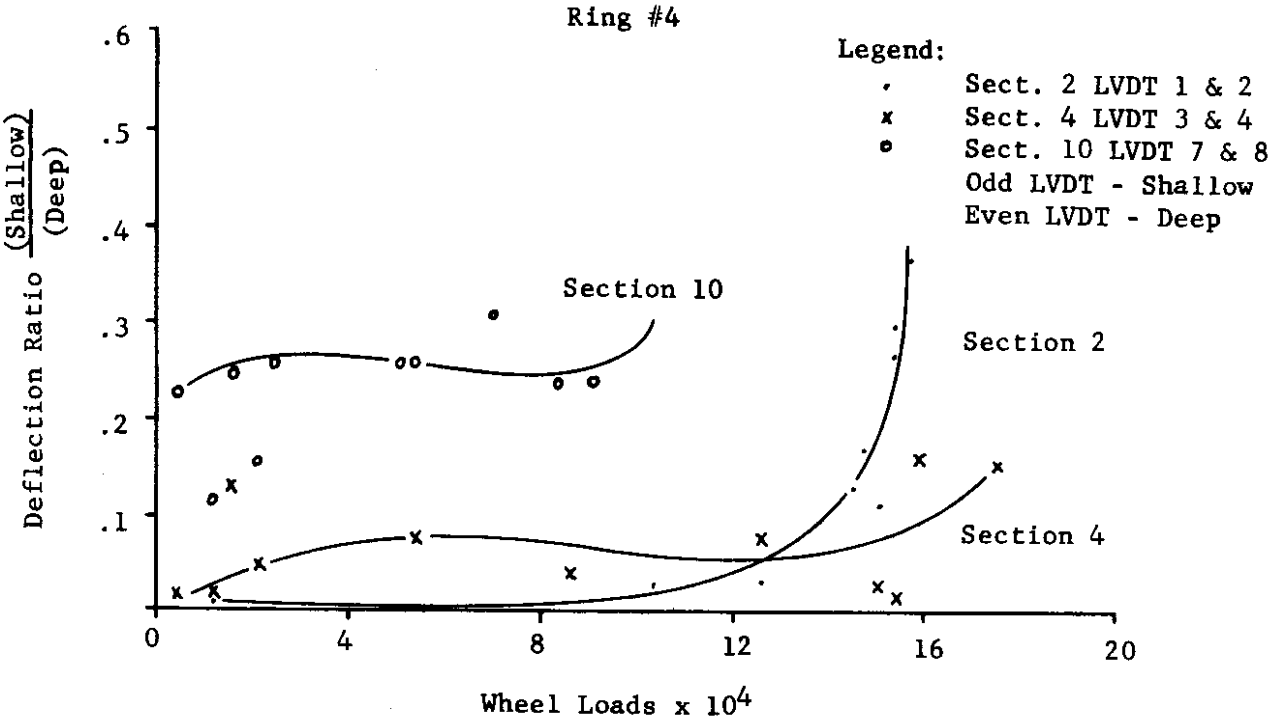

FIGURE 97. DYNAMIC DEFLECTION VS. SPEED FOR LVDT #4

Ring #4 - Section 4 - 8.0" SAB

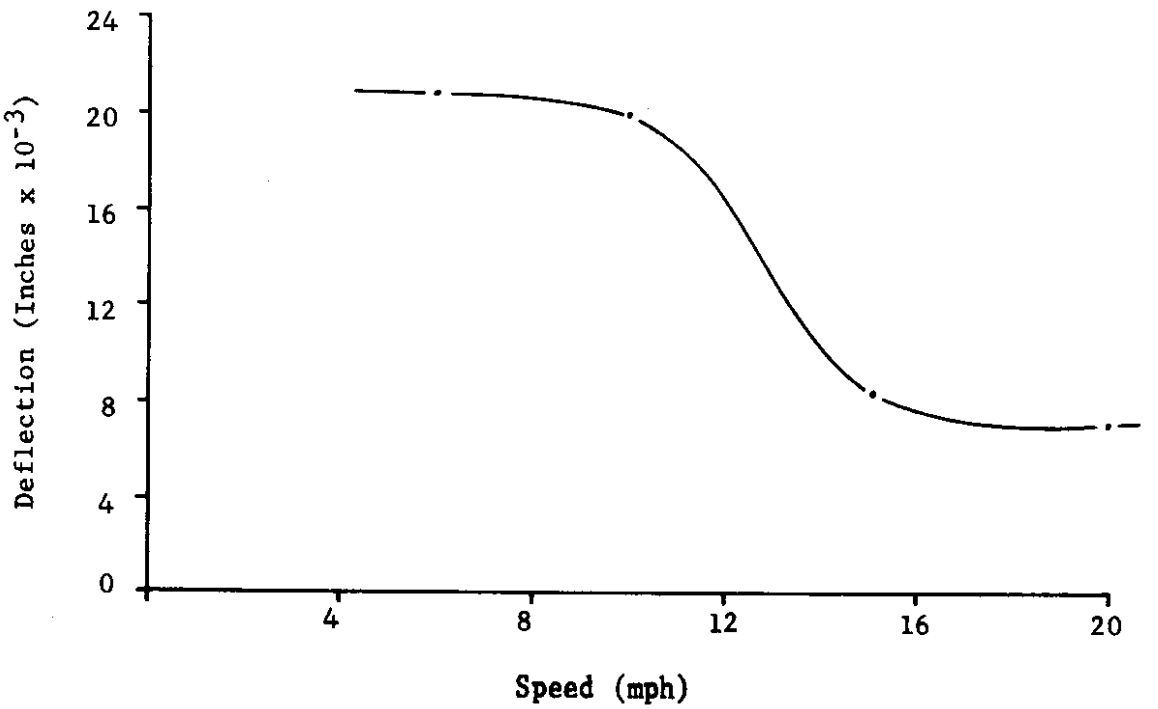

FIGURE 98. TRANSVERSE STRAINS VS. LATERAL DISTANCE
Ring #4 - Section 1 - 2.0" SAB

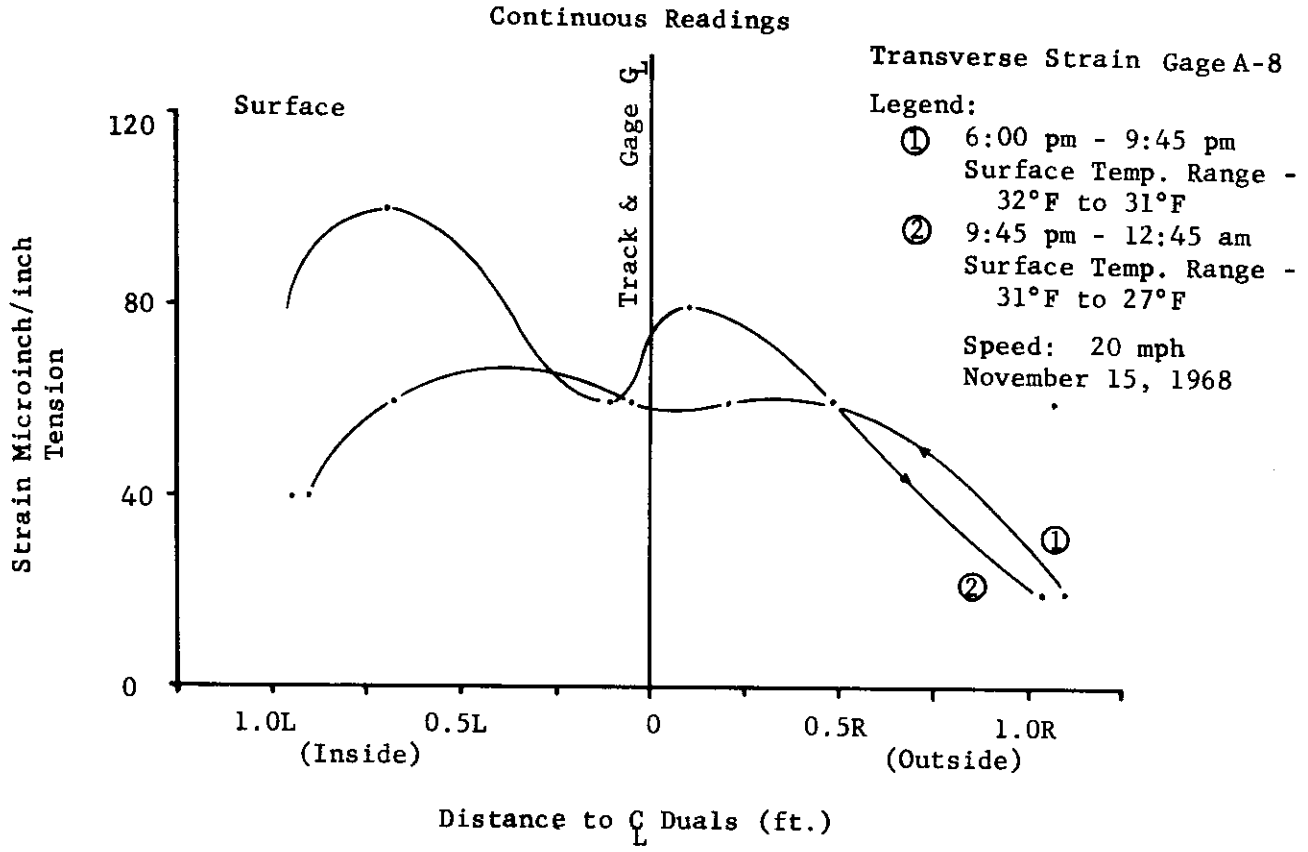

FIGURE 99. LONGITUDINAL STRAINS VS. LATERAL DISTANCE

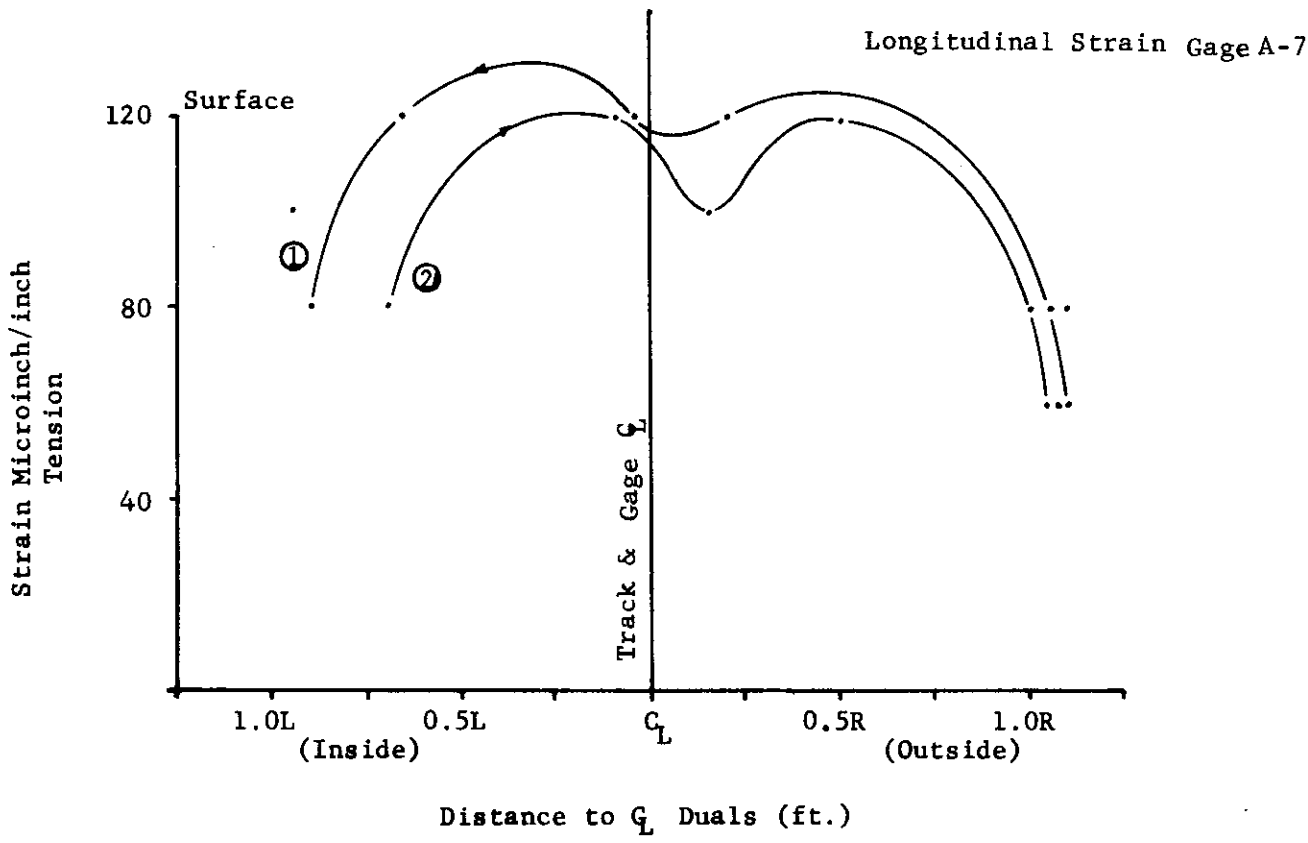

FIGURE 100. LONGITUDINAL STRAIN VS. LATERAL DISTANCE

Ring #4 - Section 2 - 4.0" SAB

Longitudinal Strain Gage *B-5

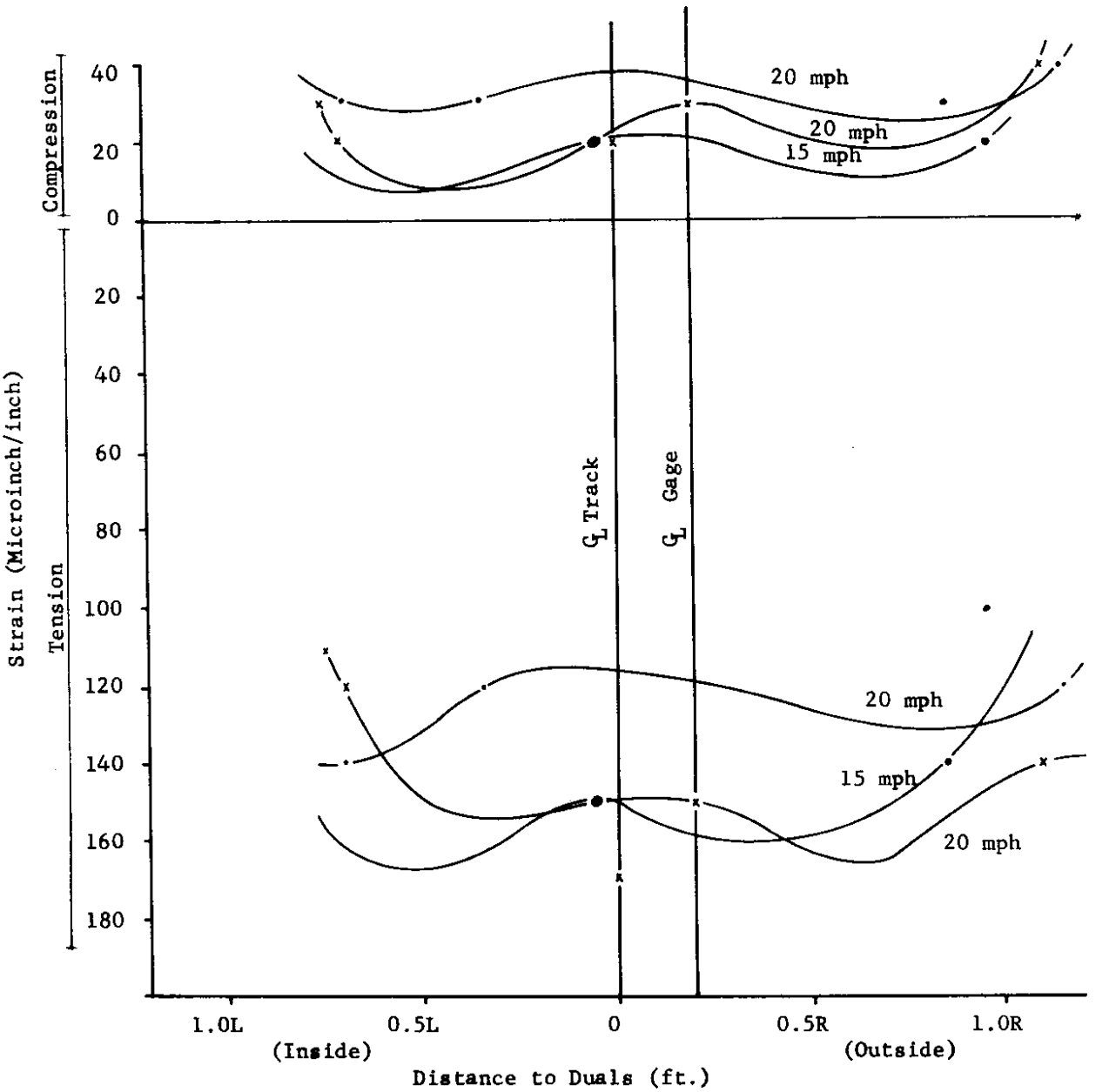

Legend:

Temperature	Symbol
30°F to 39°F	•
40°F to 46°F	x
Speed: 20 mph	—•—
15 mph	—•—

Location: Bottom of SAB
7.0" Depth
Asphalt Shingle
Mounted

November 1968

Wheel load deflection effect disregarded.

FIGURE 101. TRANSVERSE STRAIN VS. LATERAL DISTANCE
Ring #4 - Section 2 - 4.0" SAB

Transverse Strain Gage *B-6

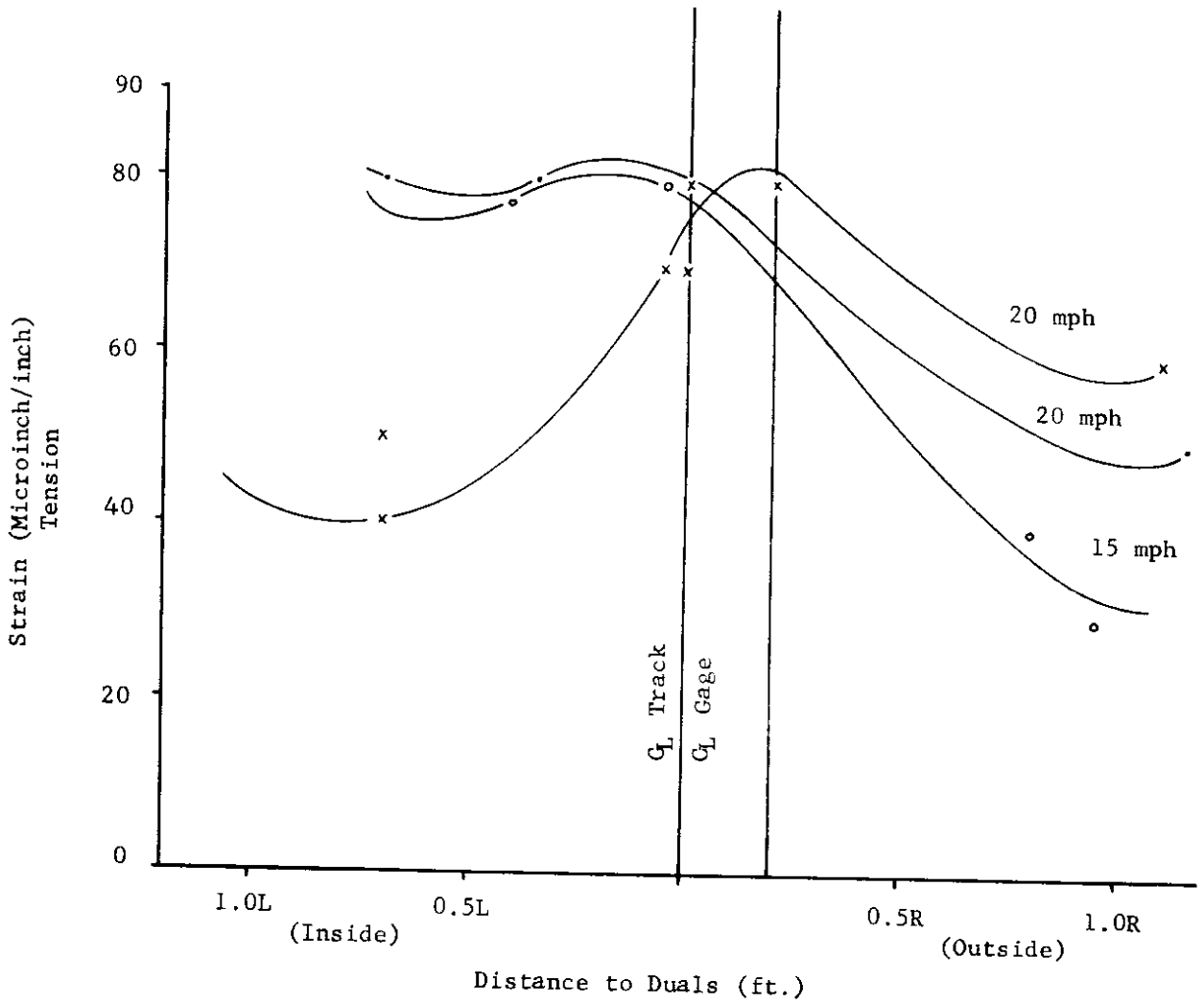

Legend:

Temperature	Symbol
30°F to 39°F	• •
40°F to 46°F	×
Speed: 20 mph	×—× ——
15 mph	•—•

Location: Bottom of SAB
7.0" Depth
Asphalt Shingle
Mounted
November 1968

Wheel load deflection effect disregarded.

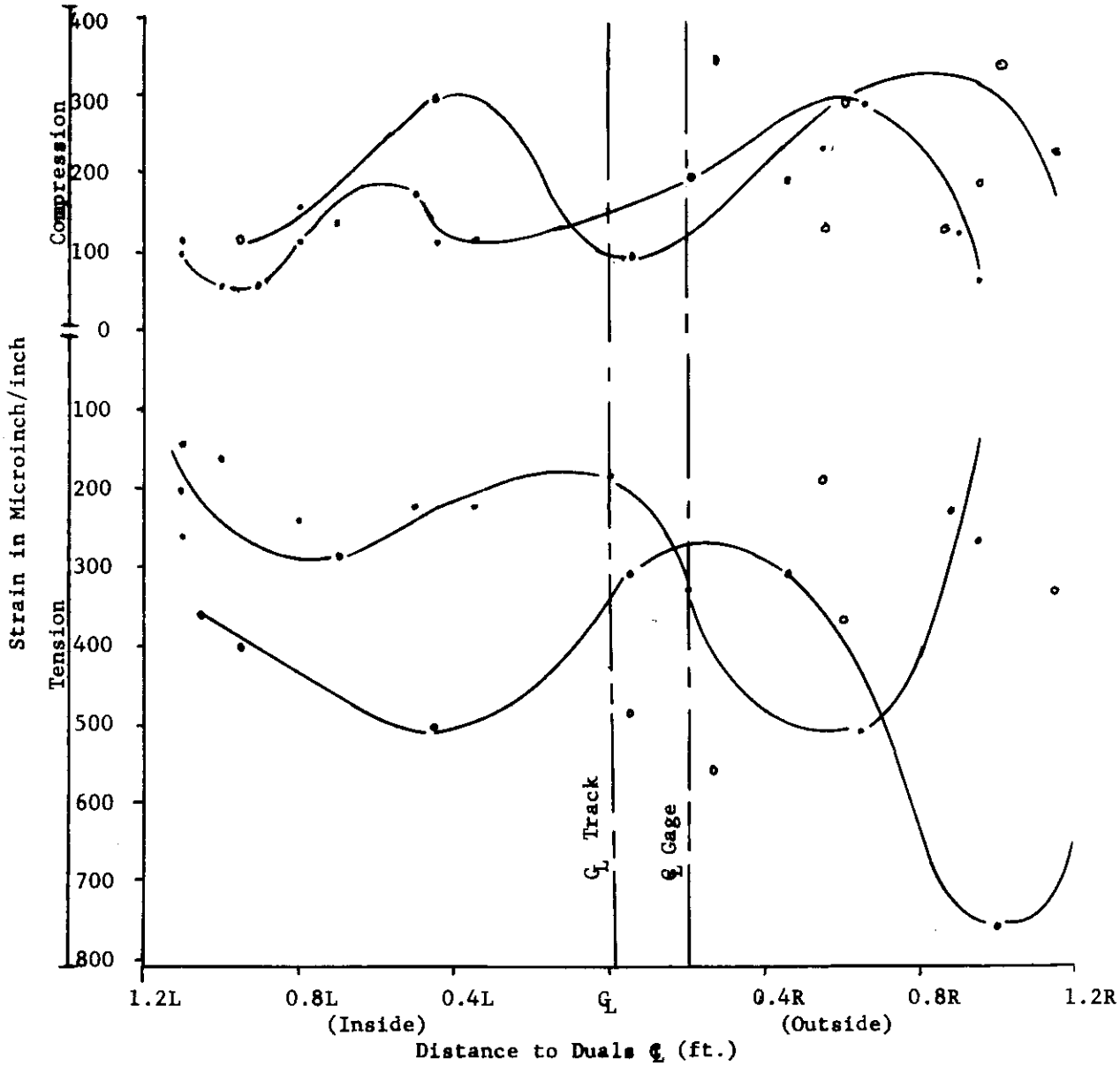

FIGURE 102. STRAIN VS. LATERAL DISTANCE
Section #2 - Ring #4 - 4.0" SAB
Surface Longitudinal Strain Gage *B-5-L
6-10 mph July-August 1969

Legend:

Temperature	Symbol
66-85°F	•
86-110°F	•

Bottom of SAB
Depth = 7.0"
Asphalt Shingle Mounted

FIGURE 103. STRAIN VS. WHEEL LOAD

Ring #4 - Section 2 - SG*B-5

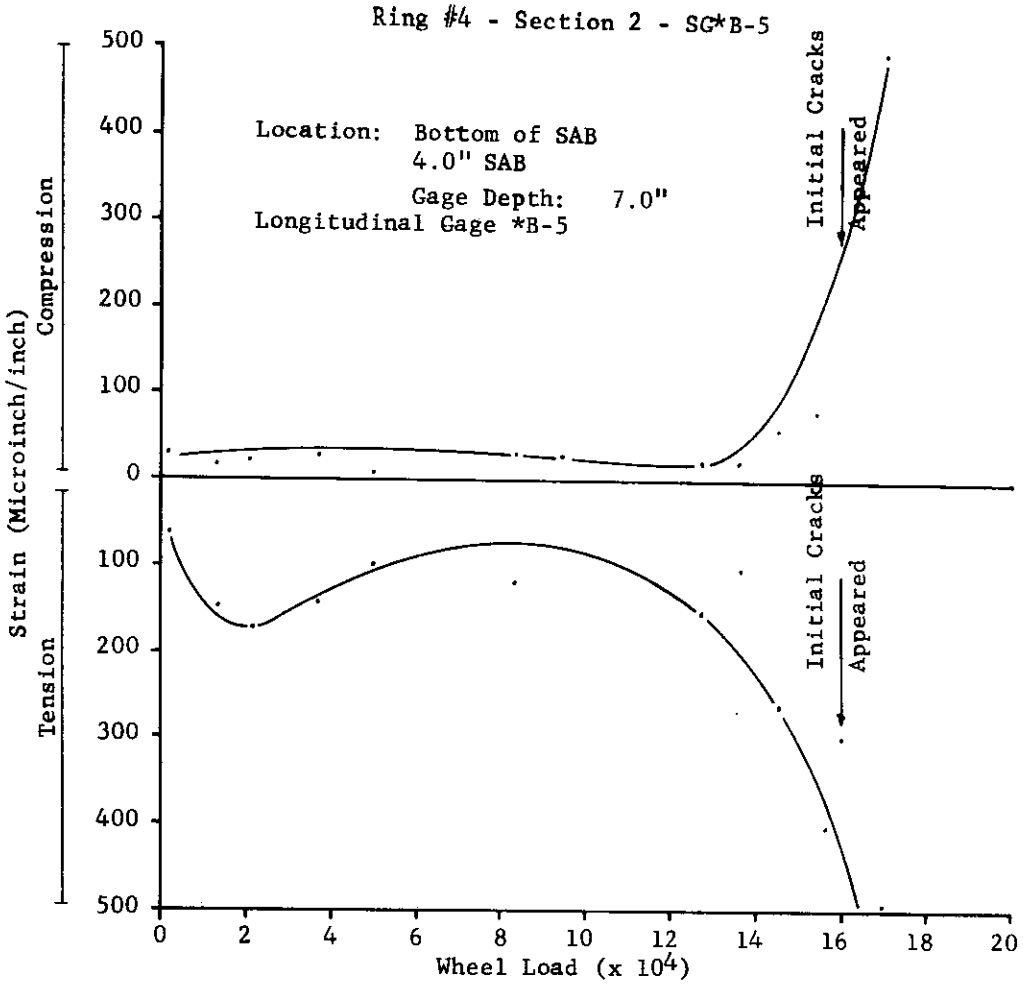

FIGURE 104. STRAIN VS. WHEEL LOAD

Ring #4 - Section 4 - SG D-5

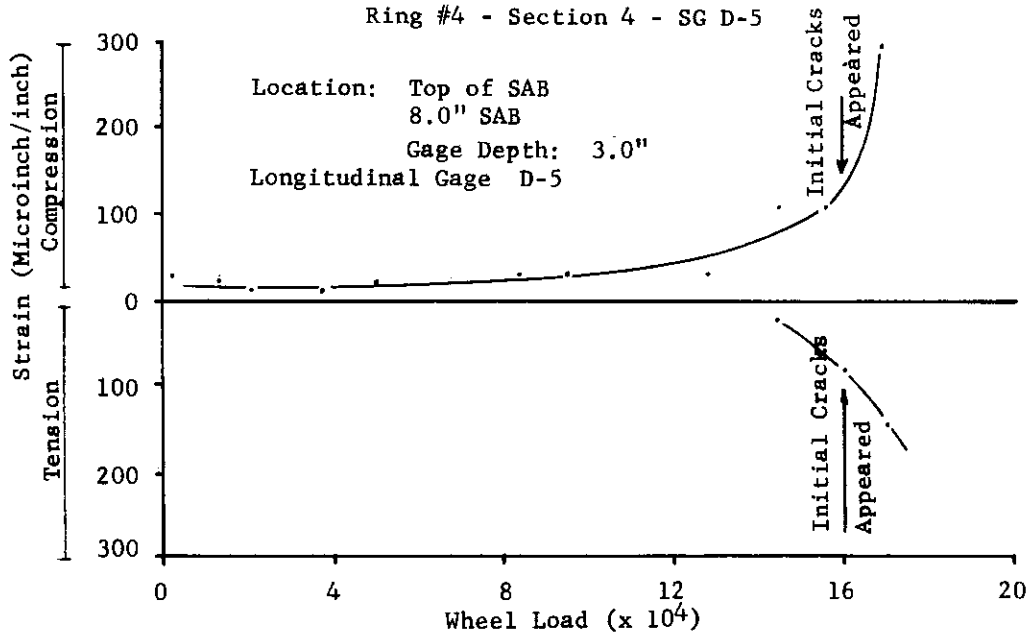

Note: Temperature effects were ignored.

the run were not considered. Operating speeds were 20 mph through November 24, 15 mph until the end of fall testing and then 6-10 mph during the spring testing period.

The maximum longitudinal transverse strains from runs are summarized in Table 27 (p. 128). The periods were divided into fall and spring. The table shows that the maximum strain readings occurred when one of the tires was over the strain gage. The table also shows that temperatures affected the strain values; low temperatures usually are associated with low strain readings and vice versa. Figures 115 and 116 seem to show that there is a correlation. Figure 116 (p. 136) suggests that for deep pavements temperature effects may not be as severe as for the thinner pavements. Table 27 also shows that the strains were usually higher during the spring period thus indicating that pavement conditions had changed.

Examination of the data and some of the figures reveals that strains usually increased dramatically prior to initial cracking. The high strain values in Table 27 are taken from run data prior to initial cracking, especially for the spring period. Tensile strain was greater in the longitudinal direction than in the transverse direction and frequently increased with depth. This may explain why transverse cracks appeared rather than longitudinal cracks, and why fatigue failure occurred and worked upward to the surface. Just before initial cracking occurred, strains (both in compression and tension) became very large and afterwards the gages became inoperational, perhaps indicating that the strain gage had reached its strain limit.

Comparison of strain values obtained from gages mounted on extensometers and on asphalt shingles indicates that the strains were higher from those mounted on the asphalt shingles than those mounted on the extensometers. Future evaluations may show that strain gages mounted on shingles may be more in keeping with calculated theoretical values.

TABLE 27: SUMMARY OF MAXIMUM LONGITUDINAL AND TRANSVERSE STRAIN GAGE MEASUREMENTS - RING #4[1]
(Readings are maximum values microinches/inch in longitudinal direction from runs only)

Section	Position	Period	Longitudinal Maximum Values				Pavement[3] Temp. °F		Transverse Maximum Values				Pavement[3] Temp. °F	
			Measurements		Lateral Pos.[2]				Measurements		Lateral Pos.[2]			
			C	T	C	T	C	T	C	T	C	T	C	T
1	Surface	Fall	190	50	U.T.	U.T.	45	45	190	-	U.T.	-	43	-
		Spring	950	300	P.T.	P.T.	73	73	220	100	P.T.	P.T.	73	73
2	Surface	Fall	120	120	B.T.	U.T.	42	39	100	40	℄	℄	49	49
		Spring	280	-	B.T.	-	72	72	160	40	B.T.	B.T.	72	72
	Base Bottom	Fall	40	170	℄	℄	42	43	10	90	B.T.	U.T.	44	42
		Spring	500	1400	U.T.	U.T.	116	116	400	600	P.T.	U.T.	100	116
3	Surface	Fall	160	1200	U.T. P.T.	U.T. P.T.	38	38	100	90	U.T.	P.T.	41	38
4	Surface	Fall	70	-	P.T.	-	44	-	150	450	U.T.	P.T.	46	37
		Spring	-	-	-	-	-	-	100	-	℄	-	71	-
	Base Top[4]	Fall	30	-	℄	-	46	-	-	-	-	-	-	-
		Spring	800	300	U.T.	P.T.	104	109	-	-	-	-	-	-
	Base Top[5]	Fall	50	10	U.T.	P.T.	41	36	30	70	℄	U.T.	50	41
		Spring	600	250	U.T.	U.T.	91	91	700	760	U.T.	U.T.	91	113
	Base Bottom[4]	Fall	20	100	P.T.	U.T.	45	43	-	90	-	U.T.	-	43
		Spring	160	480	U.T.	U.T.	98	98	180	560	P.T.	P.T.	109	109
	Base Bottom[5]	Fall	20	90	U.T.	U.T.	40	43	-	70	-	U.T.	-	43
		Spring	40	250	U.T.	U.T.	82	92	200	750	U.T.	U.T.	113	113
5	Surface	Fall	300	100	U.T.	P.T.	46	42	190	60	U.T.	U.T.	42	42
6	Surface	Fall	320	90	U.T.	U.T.	42	42	170	40	U.T.	U.T.	35	44
		Spring	100	-	U.T.	-	51	-	-	-	-	-	-	-
7	Surface	Fall	130	100	B.T.	P.T.	41	42	260	50	U.T.	P.T.	41	42
		Spring	140	30	P.T.	P.T.	71	71	20	20	P.T.	P.T.	71	71
	Base Top	Fall	40	10	℄	B.T.	50	43	40	10	B.T.	P.T.	45	35
		Spring	900	2100	U.T.	U.T.	112	112	500	800	U.T.	U.T.	112	112

TABLE 27 CONTINUED:

Section	Position	Period	Longitudinal Maximum Values				Pavement[3] Temp, °F		Transverse Maximum Values				Pavement[3] Temp, °F	
			Measurements		Lateral Pos.[2]				Measurements		Lateral Pos.[2]			
			C	T	C	T	C	T	C	T	C	T	C	T
7	Bottom Base[5]	Fall	-	-	-	-	-	-	-	140	-	U.T.	-	41
		Spring	-	-	-	-	-	-	-	1500	-	U.T.	-	112
8[8]	Surface	Fall	70	-	B.T.	-	43	-	-	100	-	U.T.	-	37
		Spring	70	30	U.T.	U.T.	71	71	-	-	-	-	-	-
9	Surface	Fall	280	100	℄	℄	53	53	150	60	U.T.	℄	43	53
10	Surface	Fall	360	230	U.T.	B.T.	43	43	340	30	U.T.	P.T.	43	44
	Base Top	Fall	70	120	U.T.	U.T.	41	40	-	-	-	-	-	-
		Fall	100	250	U.T.	B.T.	43	42	240	200	U.T.	U.T.	43	43
	Base Bottom[4]	Fall	130	280	U.T.	P.T.	43	46	260	230	P.T.	P.T.	43	46
	Base Bottom[5]	Fall	160	340	P.T.	P.T.	43	39	190	170	P.T.	P.T.	43	44
11	Surface	Fall	260	160	P.T.	U.T.	43	43	280	120	P.T.	U.T.	43	43
12	Surface	Fall	300	60	℄	℄	54	54	200	60	U.T.	P.T.	44	43
	Base Top[4]	Fall	140	480	U.T.	P.T.	32	42	130	300	P.T.	U.T.	32	42
		Spring	200	1200	P.T.	B.T.	73	106	140	700	B.T.	U.T.	106	111
	Base Top[5]	Fall	400	1500	U.T.	U.T.	42	42	230	230	P.T.	B.T.	39	34
		Spring	250	1500	U.T.	U.T.	71	73	350	500	U.T.	U.T.	108	73
	Base Bottom[4]	Fall	160	440	U.T.	U.T.	31	31	310	400	B.T.	U.T.	44	33
		Spring	160	240	P.T.	B.T.	42	106	-	-	-	-	-	-

[1] The speed up to November 24 was 20 mph; from November until end of fall testing, 15 mph; and for May onward the speed was 6-10 mph.

[2] U.T. means under tire, B.T. means beyond the inside or outside edge of tire with respect to gage, N.D. means not defined precisely but the gage is somewhere inside center line of duals, and ℄ means center line of duals is center line with gage. P.T. indicates that maximum reading occurred after wheels had traveled in a longitudinal direction forward beyond gage. Other references are to transverse orientation of wheels and gage.

[3] This is an average temperature of pavement surface, top of base and bottom base. In the UTB section, the temperature is an average of top and bottom of wearing course.

[4] Extensometer. [5] Asphalt shingle C means compression T means tension

The graphs show that transverse strain gage data was very complex and that the lateral position of the tires, the temperature, and depth greatly affected the magnitude, mode and reversal of the strains. The effect of the lateral position of the wheels was less for the longitudinally placed strain gages than for the transverse gages. However, the graphs do show that the lateral tire position affected the strains and also the mode.

Figures 98-99 show the values obtained from strain gages located on the surface of section 1, 2.0 inches of SAB. This was a continuous reading and it shows the complexity of the strains with lateral distance. Temperature effects are probably minimal due to extremely narrow surface temperature range. The hysteresis effect may be due to the lateral movement of the tires and perhaps uneven load displacement due to pavement roughness.

Figures 100-102 (p.123-125) show the strains obtained during the fall period at the bottom of the 4.0-inch SAB which is in section 2. Both temperature and speed effects are shown. Usually, lower speed results in higher readings. The figures seem to suggest the opposite effect. This may be due to temperature effects; that is, a combination of cold pavement temperatures with a low speed will not affect strains very much. The effects of speed may be more noticeable at higher temperatures. Figure 102 shows the strain values obtained in the spring which were 2 to 3 times higher than those measured in the fall. Figures 103 and 104 show that strains increased with accumulated wheel loads. Although this is true to a certain extent, other factors probably play a greater role in affecting strain values. Environmental conditions affect the whole pavement system, and wheel loads are but one factor among many which affect strains. The figures show that strain increased slowly prior to initial cracking and then increased rapidly.

Figures 105-117 show strain values measured in the various sub-systems of the 8.0-inch SAB, section 4. Figures 105-106 are values measured from the surface gages. Figures 107 and 108 show the values obtained at the 3.0-inch depth, top of the base, with two types of gage mounting. Figure 107 shows the readings obtained from gages mounted directly on top of the base while Figure 108 shows the values obtained from gages mounted on an asphalt shingle which was then attached to the top of the sand-asphalt base. The latter method seems to give higher average strain values although Table 27 shows that higher maximum values were measured from the first type of mounting. Figures 109-112 show the strain values obtained from the gages placed at the bottom of the sand-asphalt base for the fall period. The readings are similar. Figures 113 and 114 are for the same longitudinal gages as shown in Figures 109 and 111, except these show the strains measured in the spring. Values are about 2 times higher and gages mounted on asphalt shingles measured higher strains than those mounted on extensometers. This is due to the probability that the asphalt shingle modulus value is similar to that of the sand-asphalt base. Figures 115 and 116 are interesting in that they show the effect of temperature on compressive strain. The figures also show that effect of temperature variation is lessened on strain values for the deep pavements; the strain values do not change rapidly with depth. However, this may cause differential strains if temperature changes are extreme and may cause thermal effects which may lead to cracks (23, 25). Figure 117 shows strain values with depth for section 4. Tensile strains as measured are greater than compressive strains.

The strain values for section 5, 0.0 inches of base, are shown in Figures 118 and 119. These figures show how the lateral distance affected the values.

(Text continued on page 142.)

FIGURE 105. STRAIN VS. LATERAL DISTANCE

Ring #4 - Section 3 - 6.0" SAB

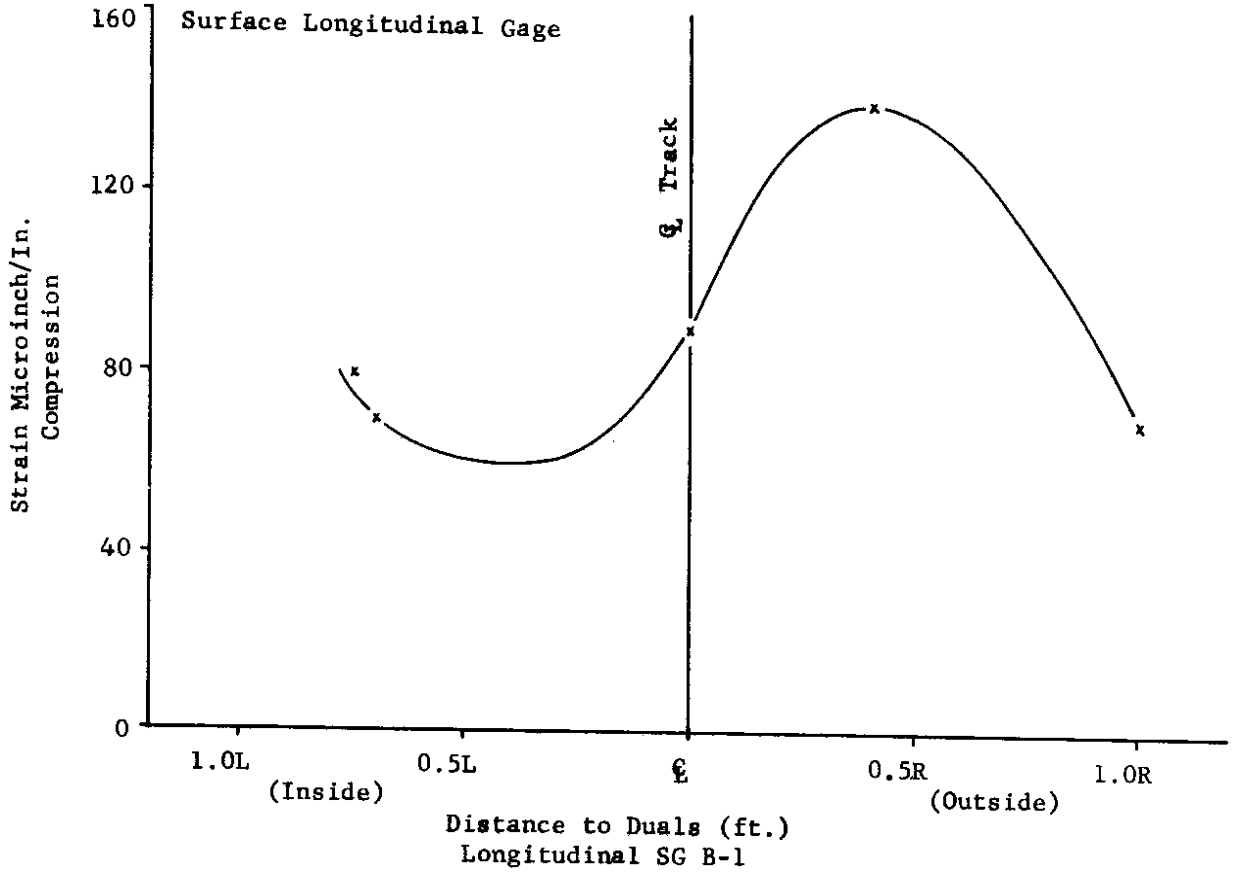

FIGURE 106. STRAIN VS. LATERAL DISTANCE

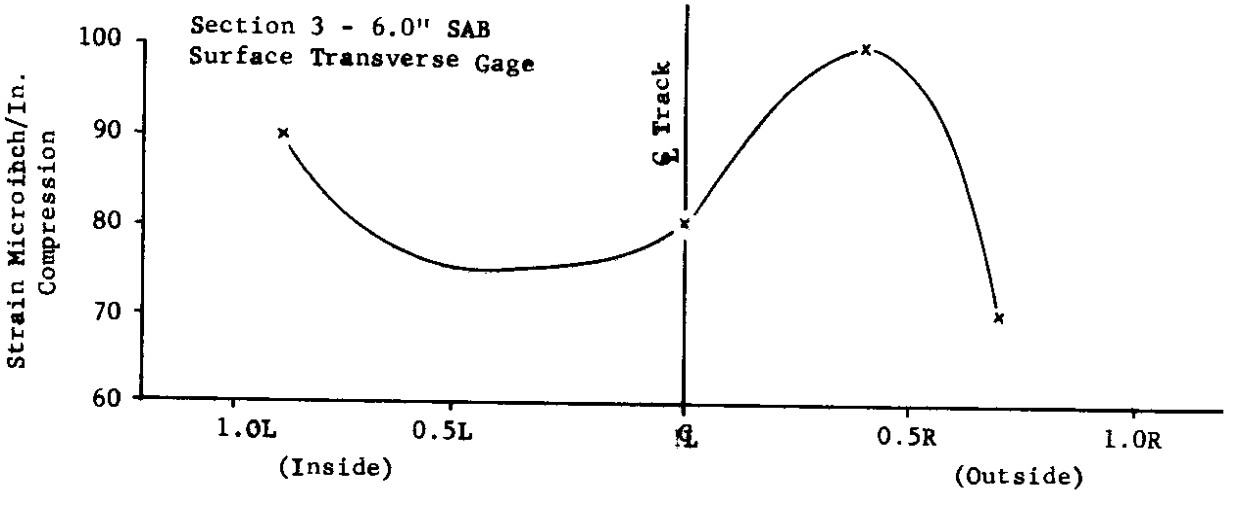

Legend:

Temp.: 40°F to 47°F
Speed: 20 MPH
November 1968

Symbol
X

Note: Data from runs--wheel load effects were ignored.

FIGURE 107. STRAIN VS. LATERAL DISTANCE

Ring #4 - Section 4

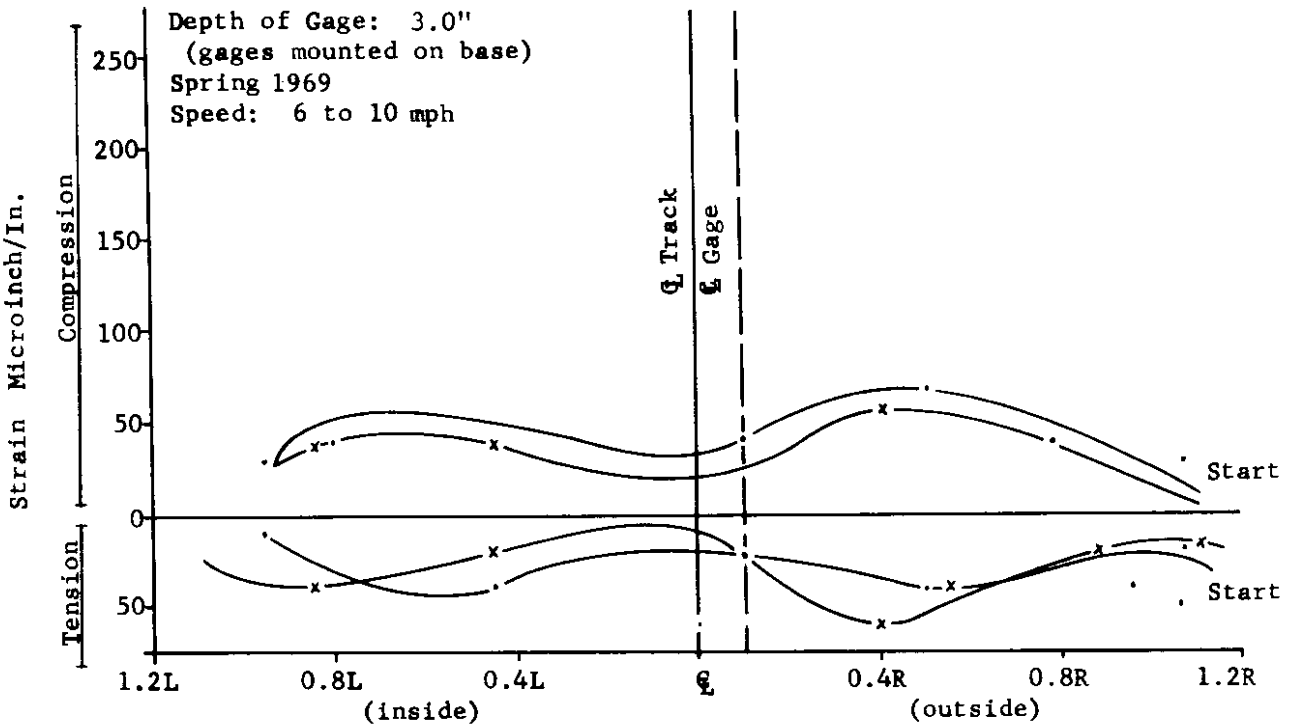

FIGURE 108. STRAIN VS. LATERAL DISTANCE

Ring #4 - Section 4

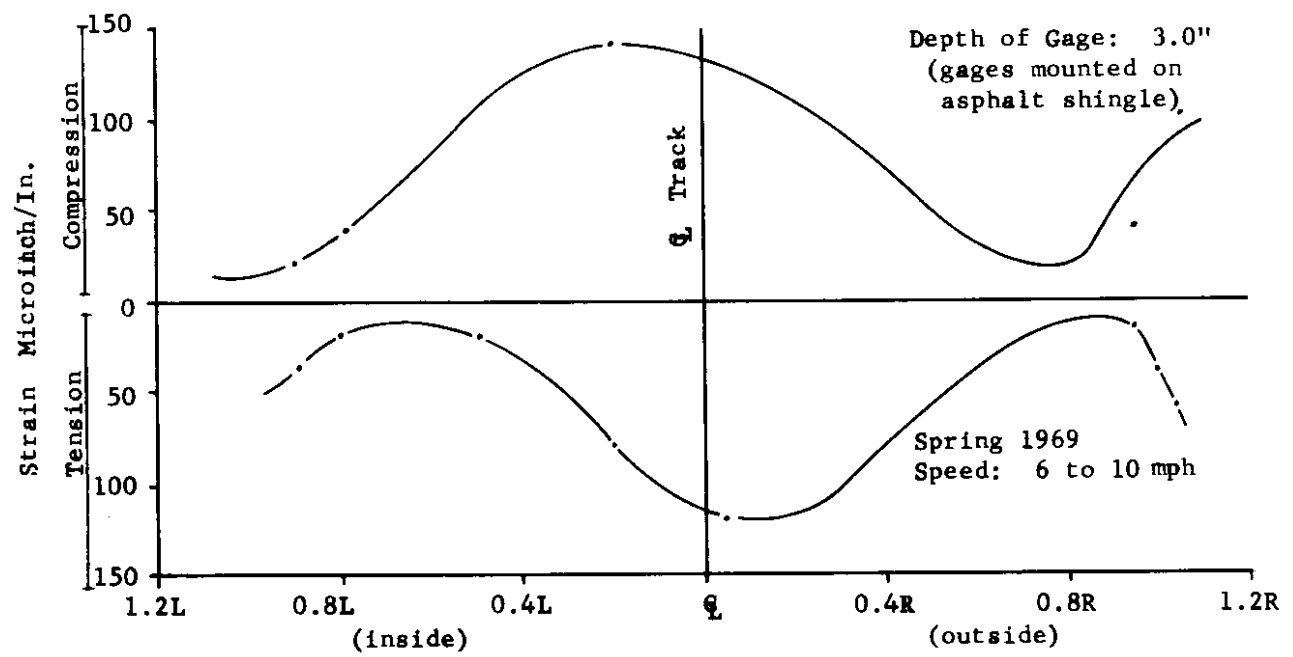

Legend:

Temperature	Symbol
48°F to 65°F	X
66°F to 85°F	.

FIGURE 109. STRAIN VS. LATERAL DISTANCE

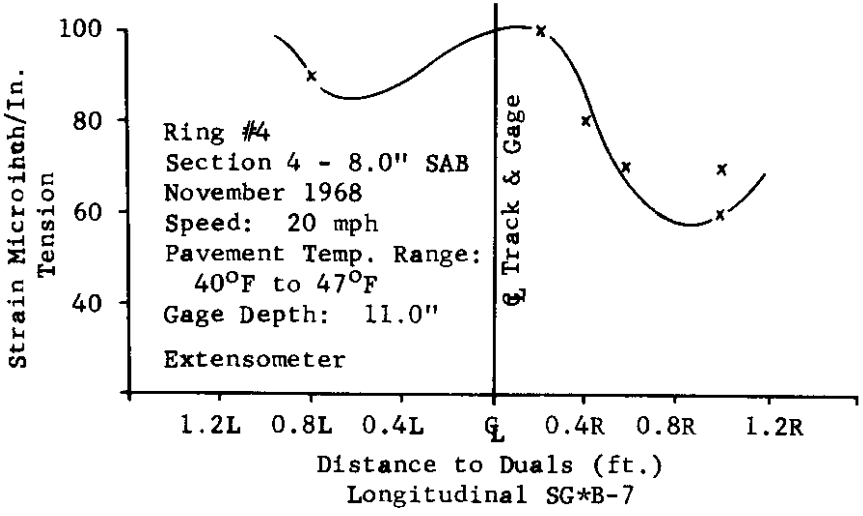

FIGURE 110. STRAIN VS. LATERAL DISTANCE

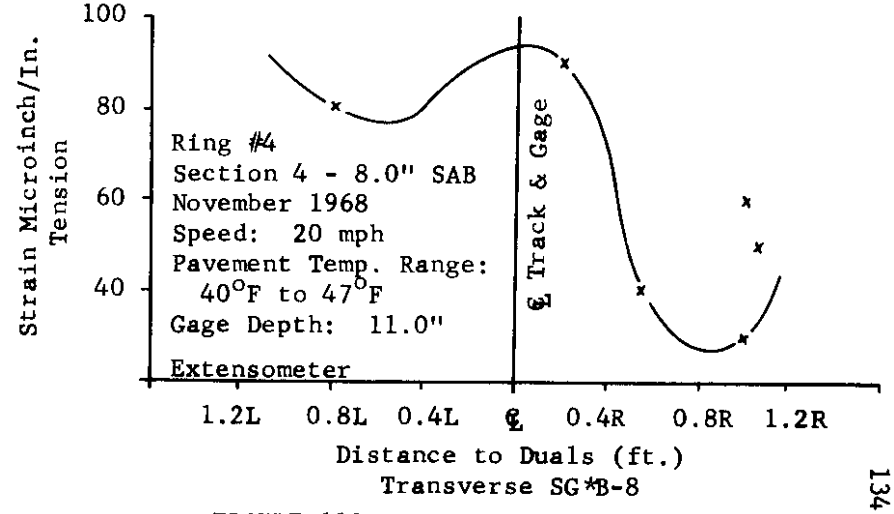

FIGURE 111. STRAIN VS. LATERAL DISTANCE

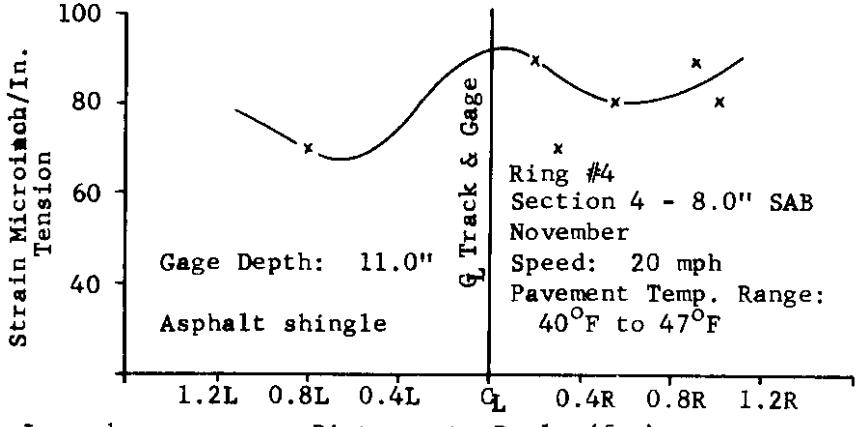

Legend:
Temperature:
40°F to 47°F
Symbol: X

FIGURE 112. STRAIN VS. LATERAL DISTANCE

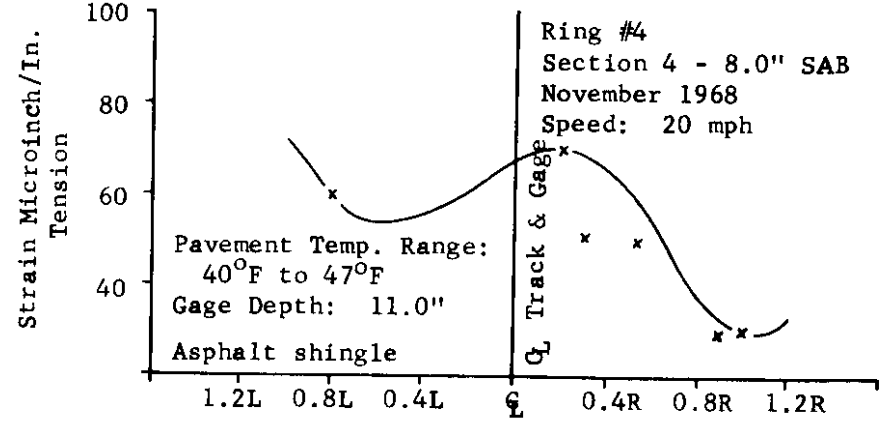

Note: Data from runs--wheel load effects were ignored.

FIGURE 113. STRAIN VS. LATERAL DISTANCE

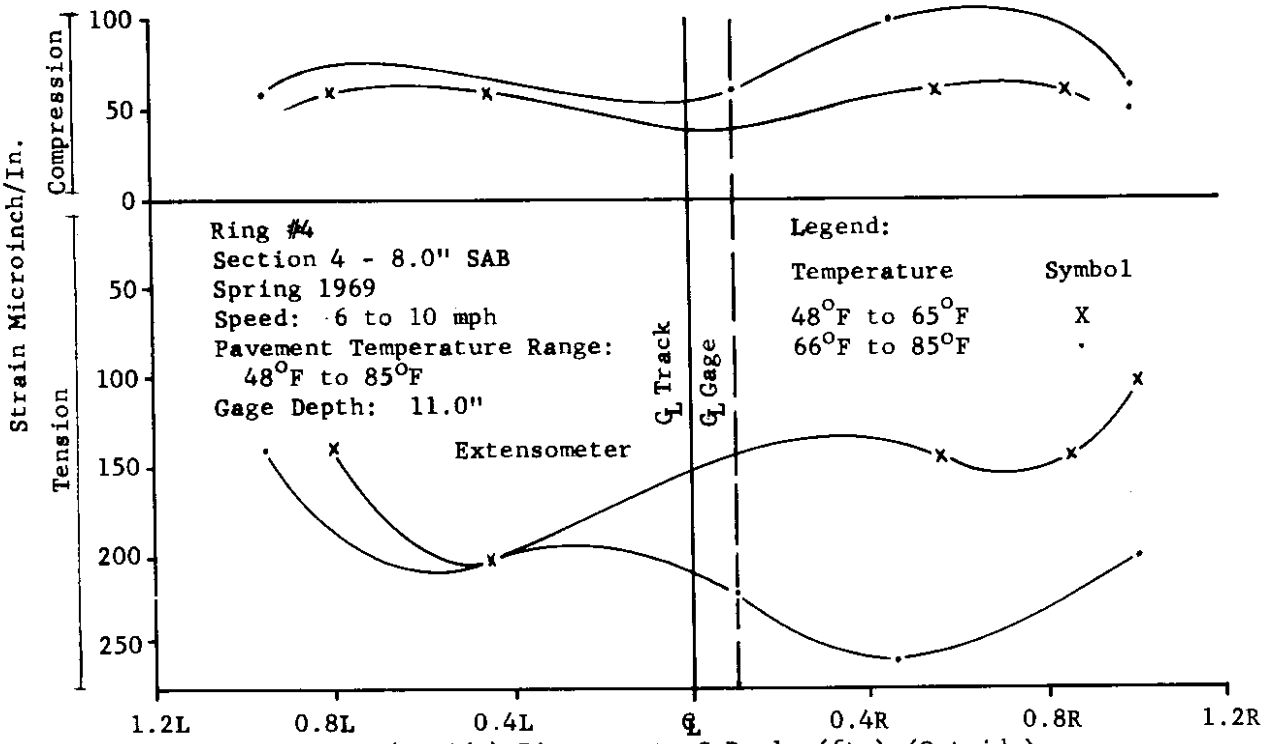

FIGURE 114. STRAIN VS. LATERAL DISTANCE

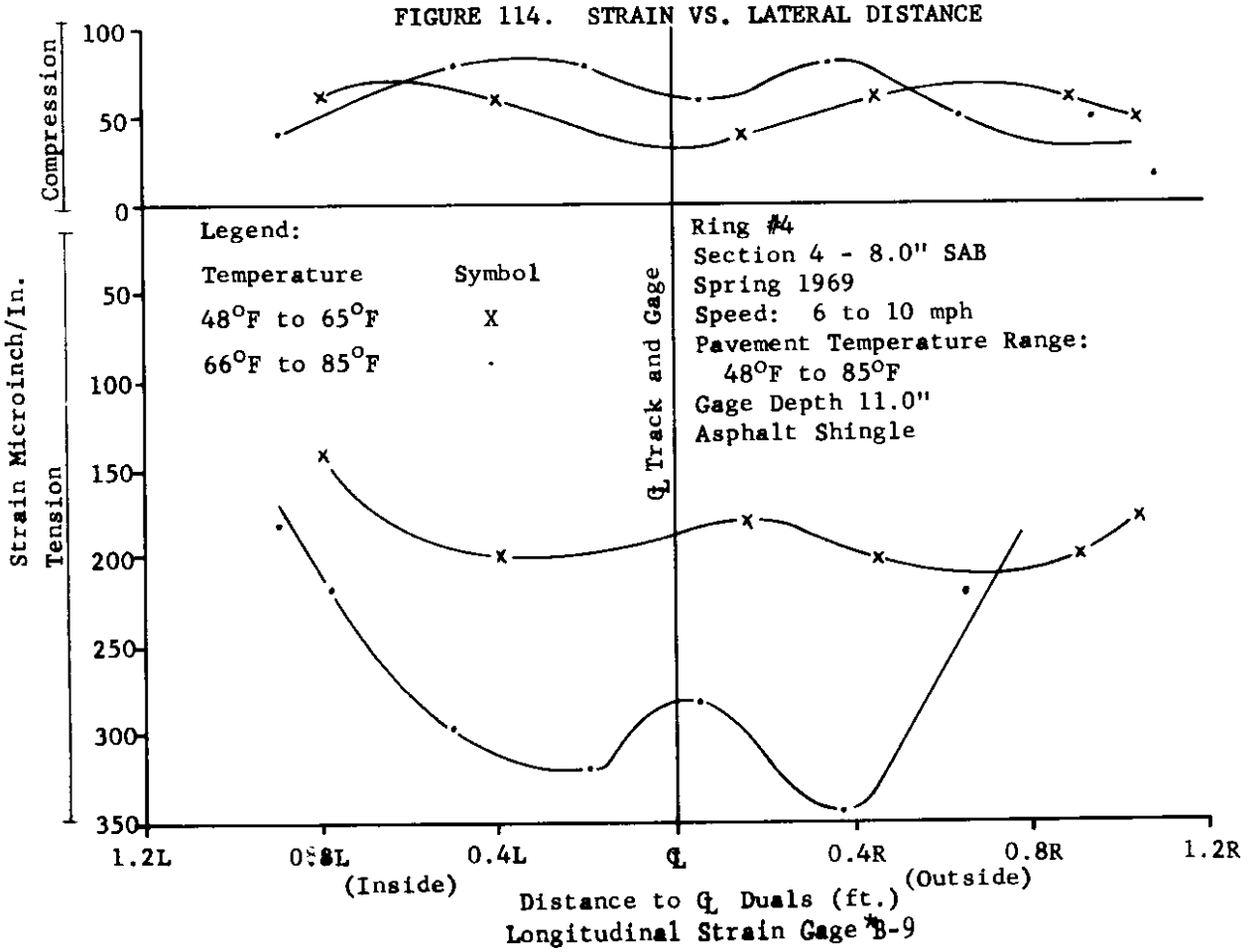

FIGURE 115. COMPRESSIVE STRAIN VS. TEMPERATURE

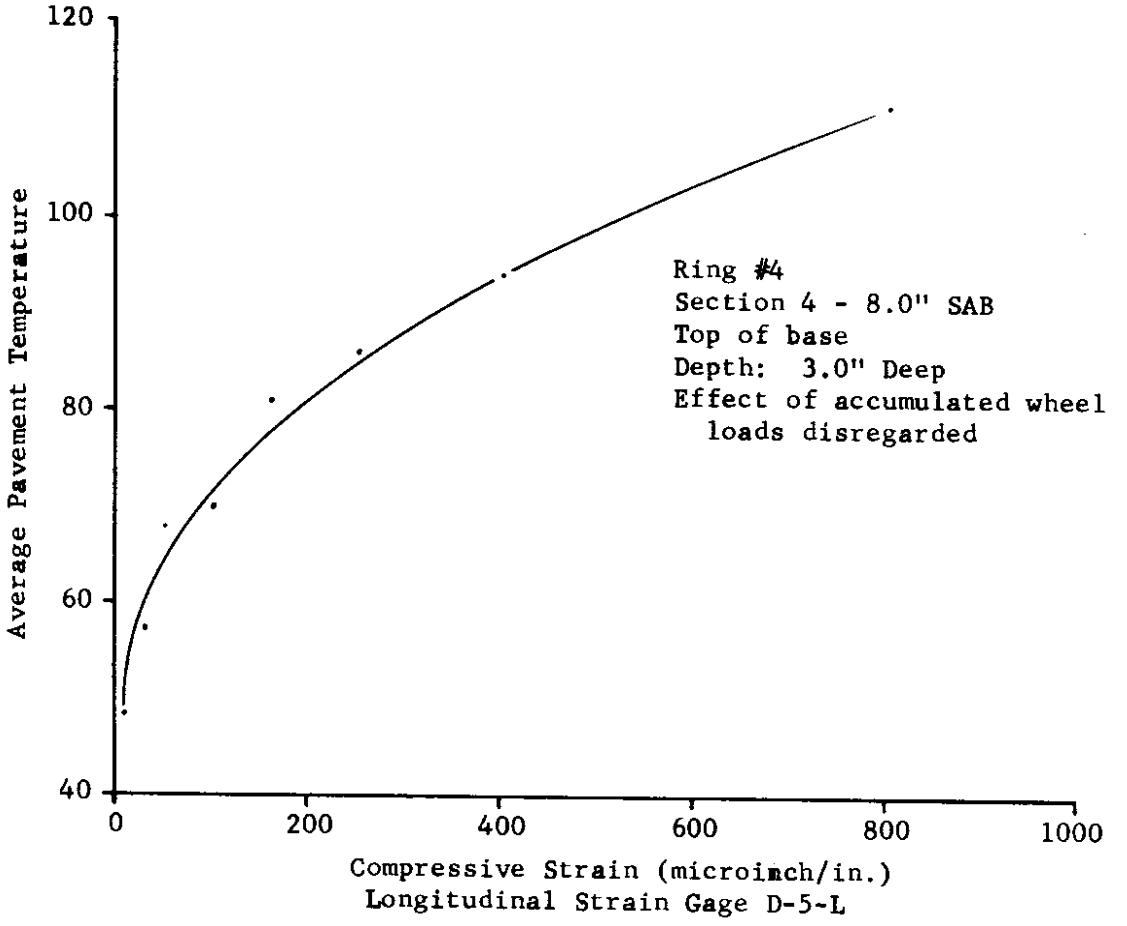

FIGURE 116. COMPRESSIVE STRAIN VS. TEMPERATURE

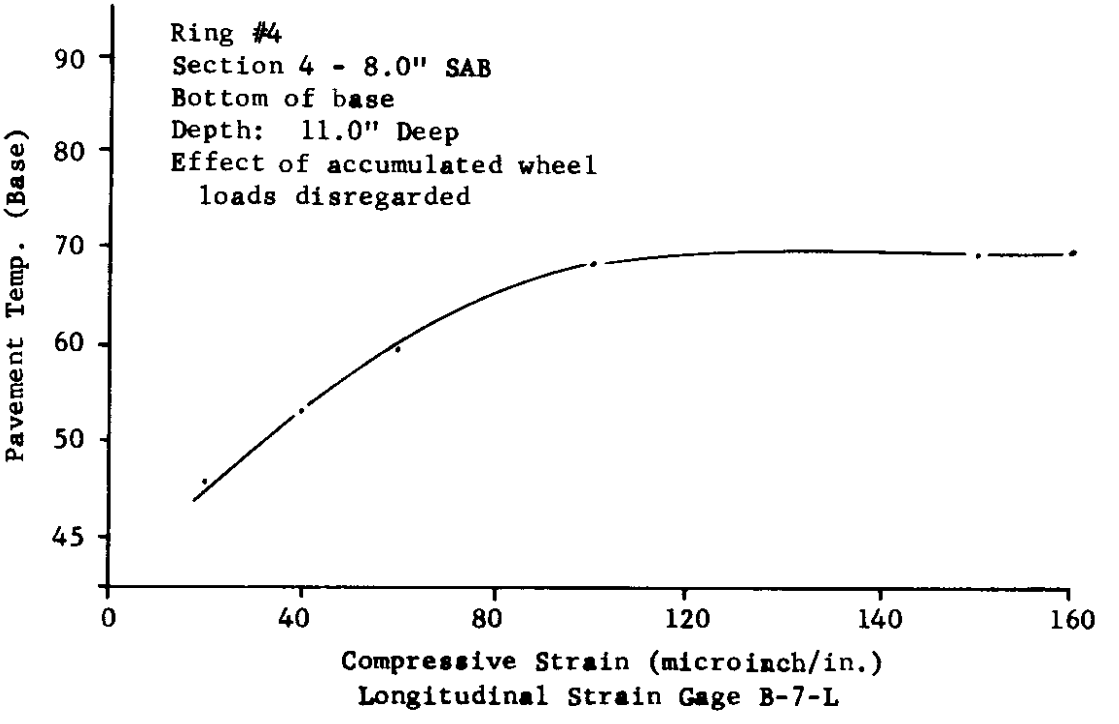

FIGURE 117. MAXIMUM STRAIN VS. DEPTH

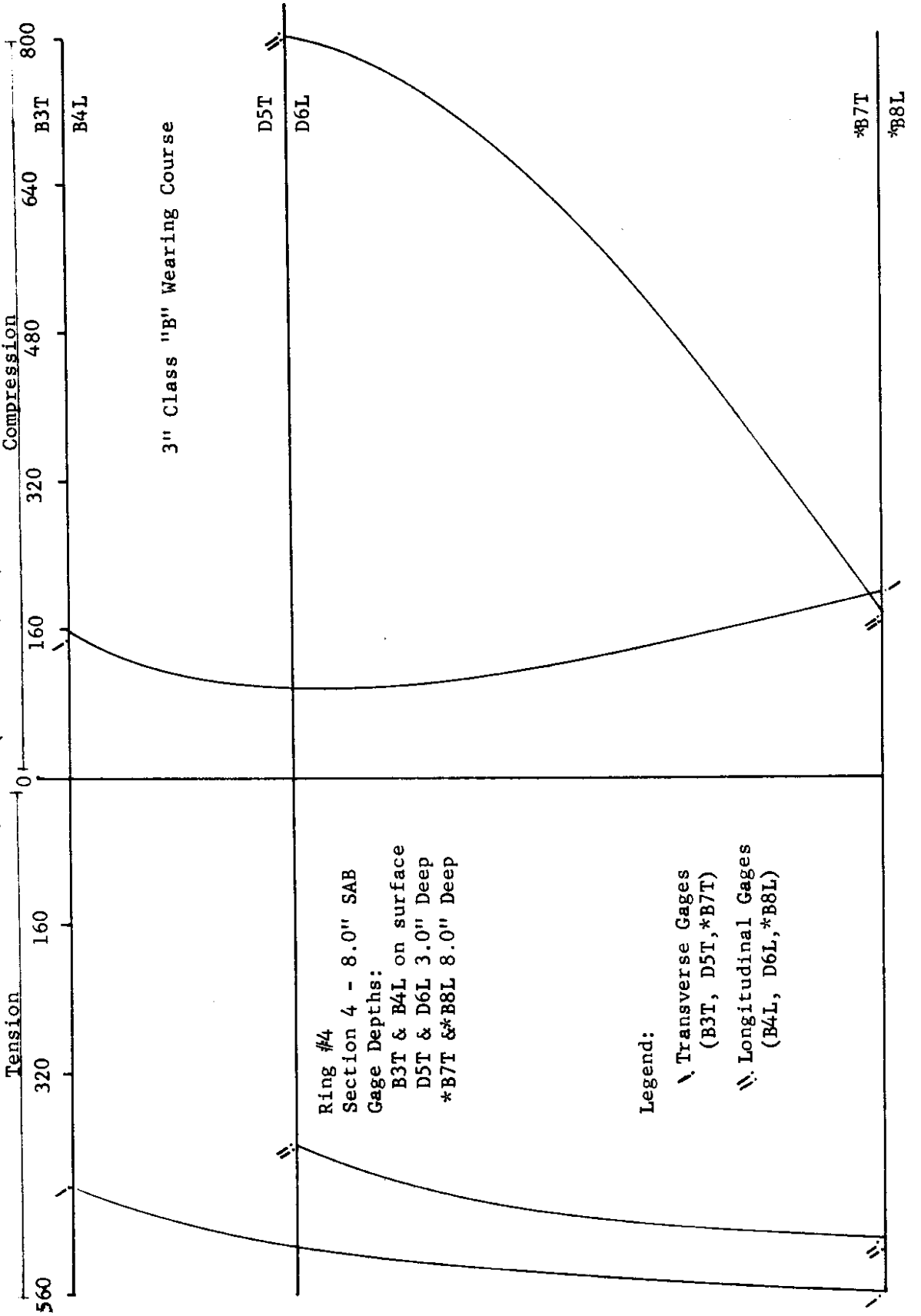

FIGURE 118. STRAIN VS. LATERAL DISTANCE

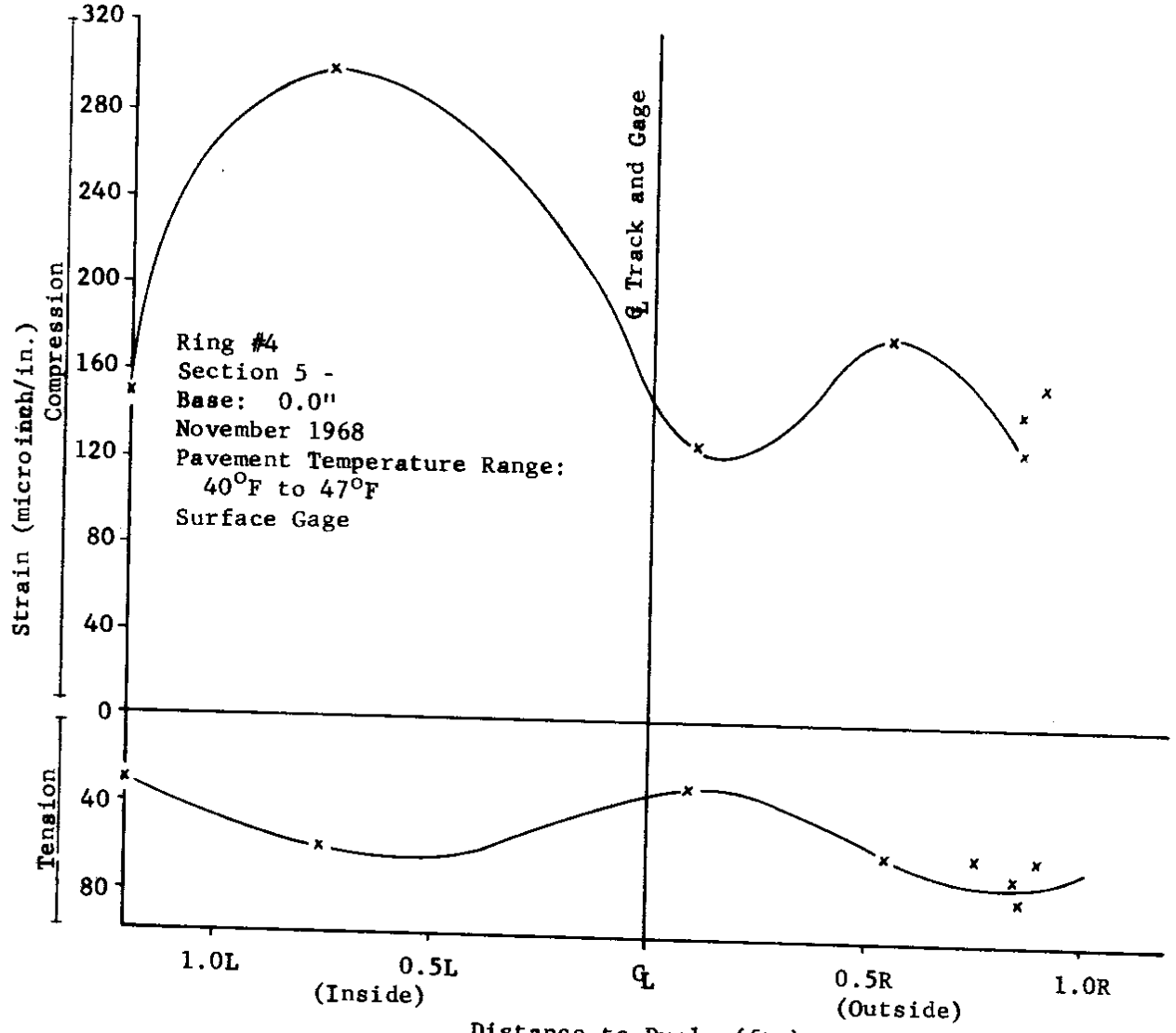

FIGURE 119. STRAIN VS. LATERAL DISTANCE

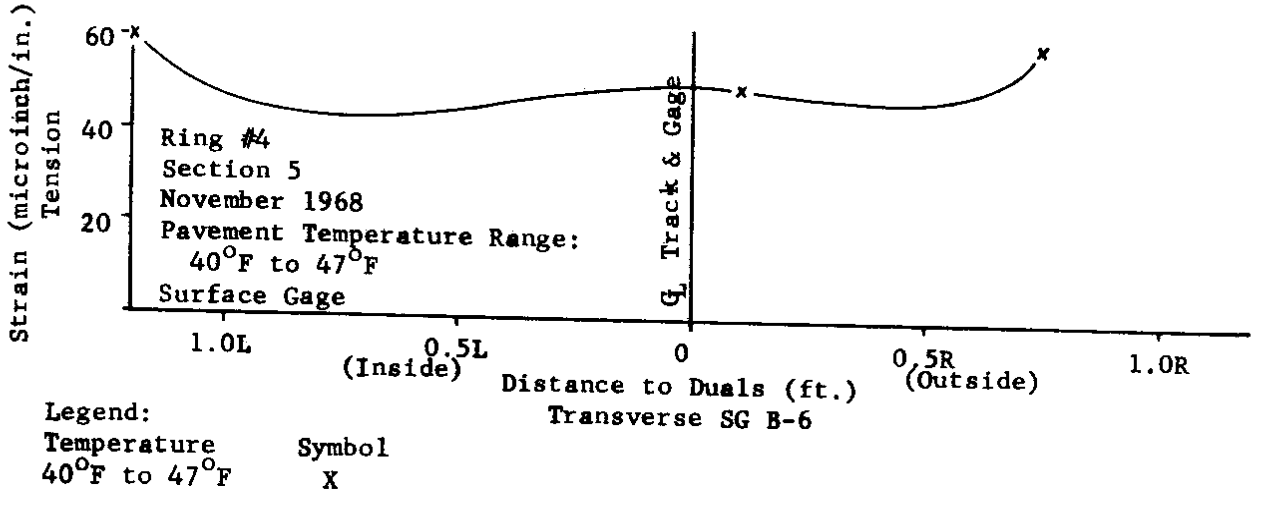

Legend:

Temperature	Symbol
40°F to 47°F	X

FIGURE 120. STRAIN VS. LATERAL DISTANCE

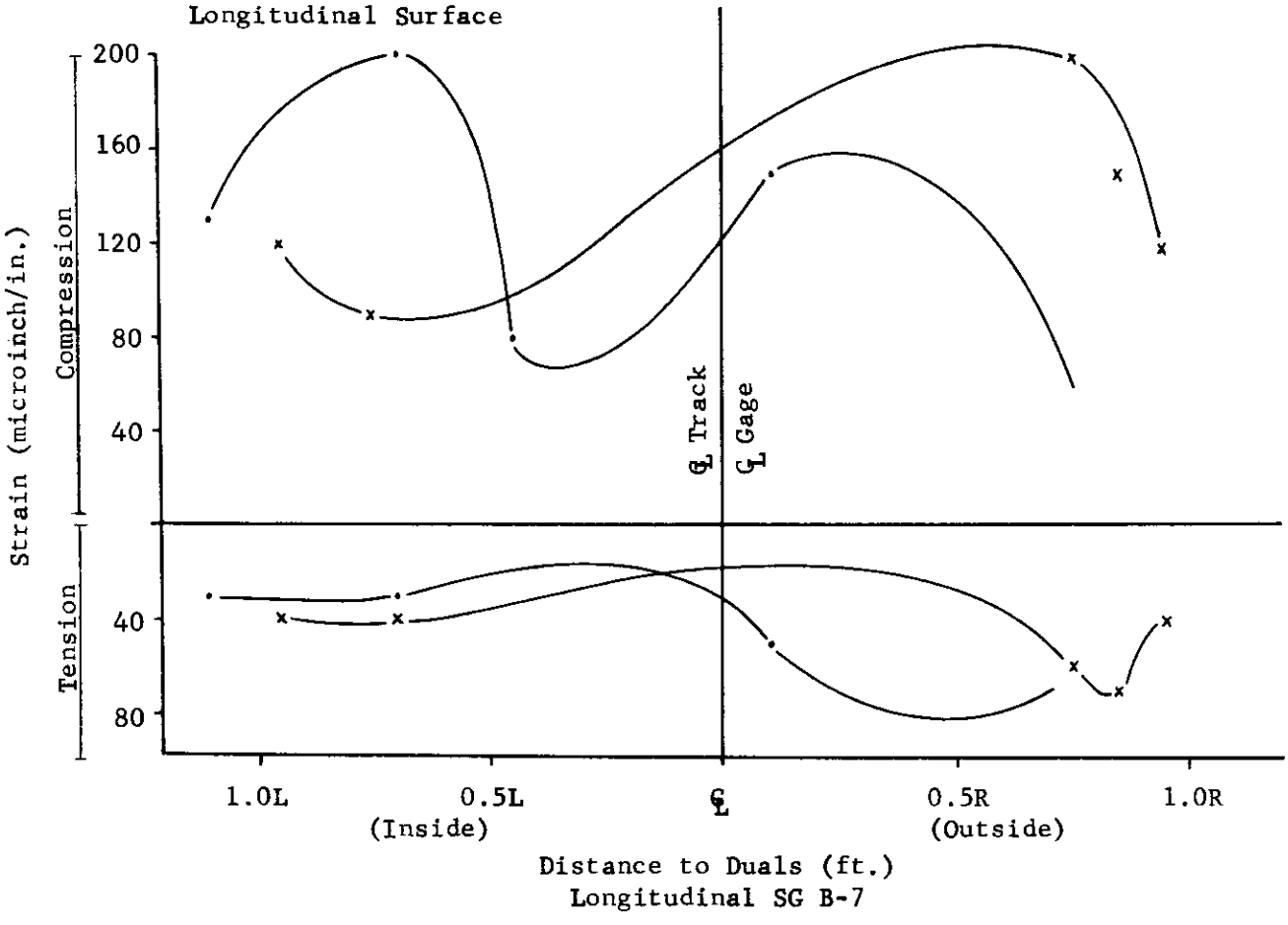

Ring #4
Section 6 - 2.0" CL "F" ACB
November 1968
Speed: 20 mph
Pavement Temperature Range:
30°F to 47°F

Legend:

Temperature	Symbol
30°F to 39°F	•
40°F to 47°F	x

FIGURE 121. STRAIN VS. LATERAL DISTANCE

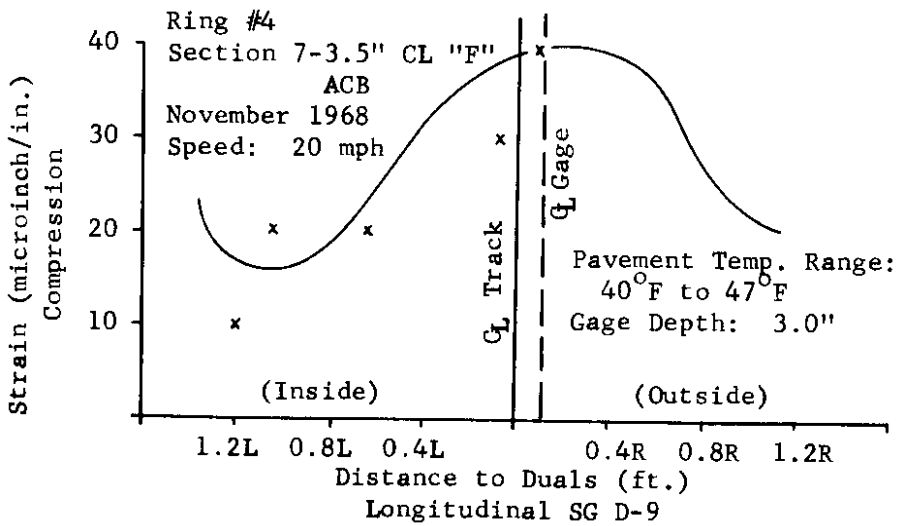

FIGURE 122. STRAIN VS. LATERAL DISTANCE

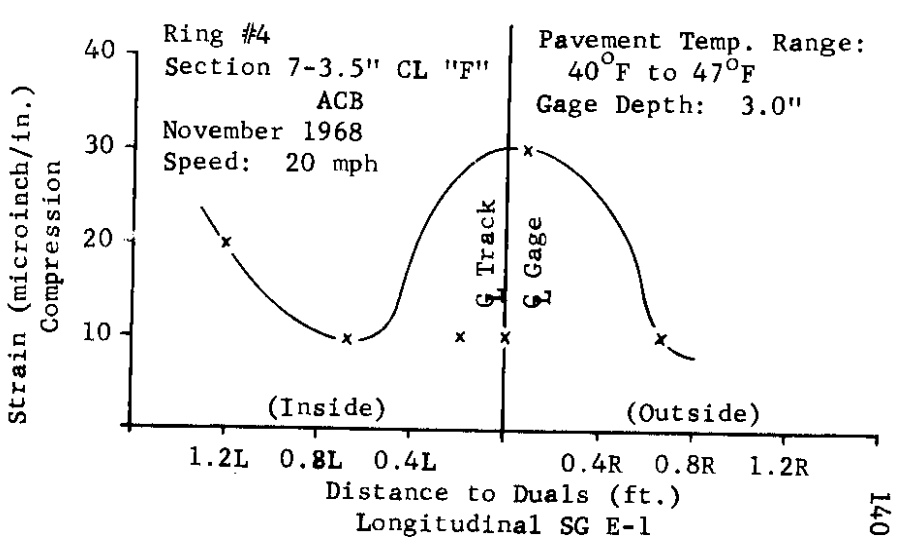

FIGURE 123. STRAIN VS. LATERAL DISTANCE

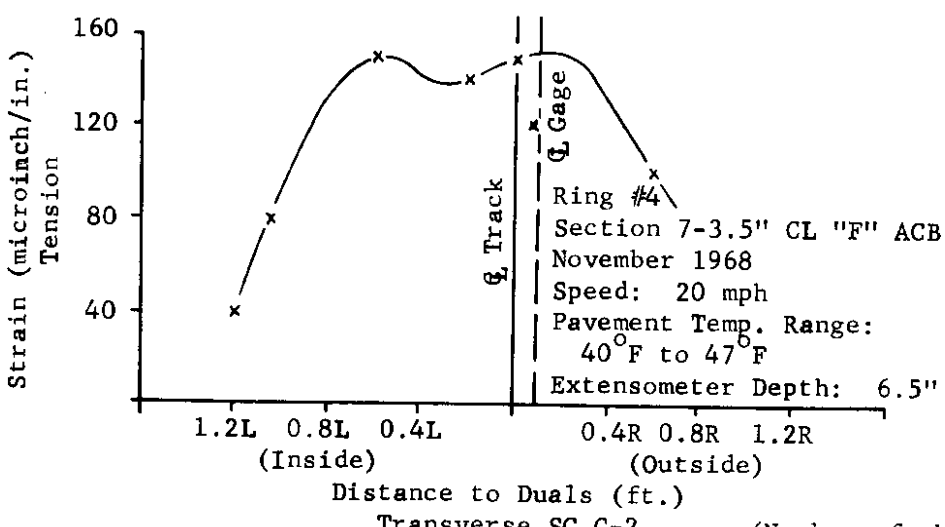

FIGURE 124. STRAIN VS. LATERAL DISTANCE

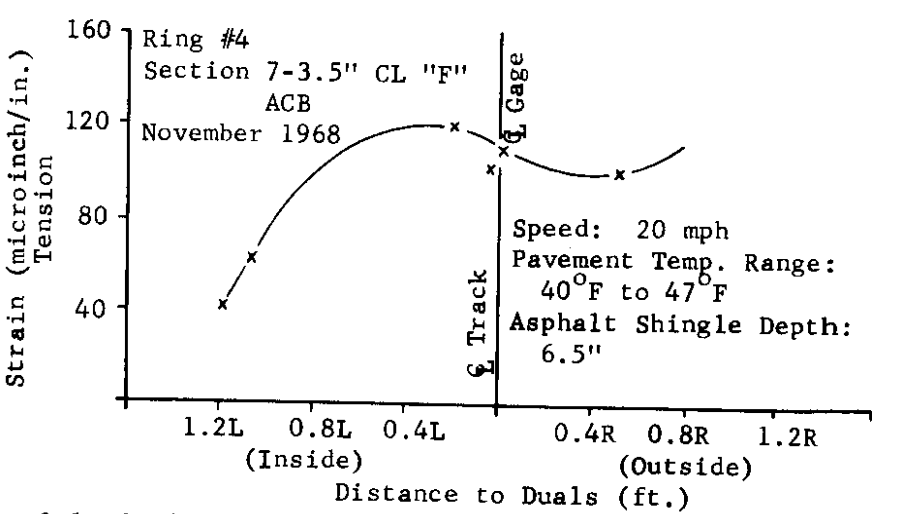

(Number of wheel loads disregarded)

FIGURE 125. STRAIN VS. WHEEL LOADS
SG D-10

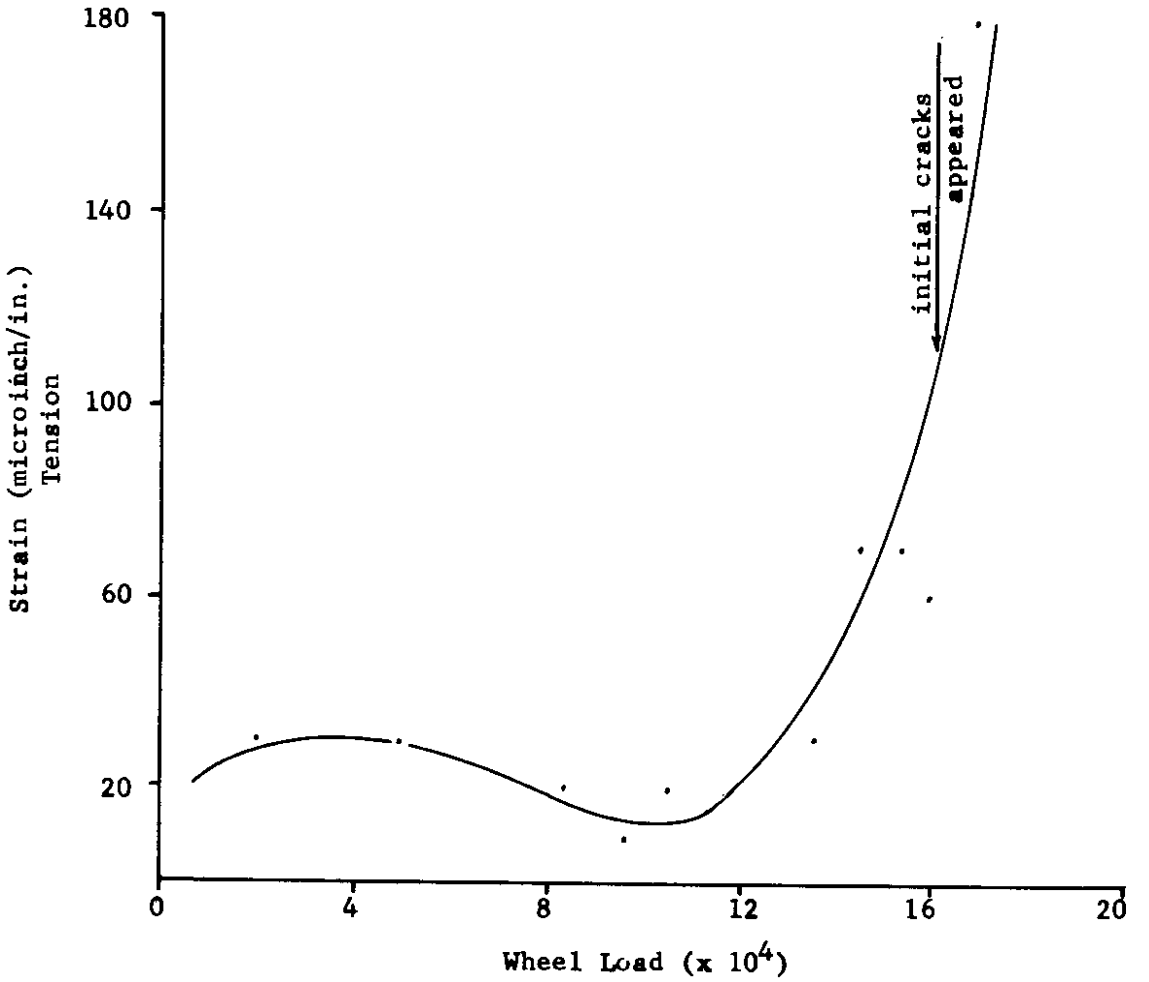

Ring #4
Section 7 - 3.5" CL "F" ACB
Gage Depth: 3.0"
Transverse Gage on Top of Base
Temperature effects are disregarded

Figure 120 shows the values of longitudinal strain values measured from the surface gage in the 2.0-inch Class "F" ACB, section 6. Some temperature effects are also shown. Strain values from section 5 seem to be higher than those measured from section 6. This difference may be due to the fact that the pavement flexed more with the wheel load.

Figures 121-124 (p. 140) show the strain values obtained from longitudinal and transverse gages at different depths of section 7, 3.5 inches of Class "F" ACB. Comparison of graphs 121 and 122 show that readings were not that much different at the top of the base. The same can be said for Figures 123 and 124. This may be due to low temperatures during the fall period. Figure 125 shows that tensile strain increased with accumulated wheel load. Again it should be mentioned that environmental conditions play a more important role in affecting the pavement system that accumulated wheel loads. The figure shows that strain increased prior to initial cracking and continued upward.

Figures 126 and 127 show the measured surface strain values obtained from section 9, 4.5 inches UTB. These are high, higher than those measured in sections 5 and 1. This was probably a prelude to the failure of section 9 which occurred in an extremely short time. Figures 128-131 show the strains measured at the bottom of the base in section 10. Figures 128-129 are those measured by gages mounted on extensometers while those strain values measured by gages on asphalt shingles are shown in Figures 130 and 131 (p. 145). Strains from extensometers seem to be higher, although maximum values were measured with gages mounted on asphalt shingles (Table 27) (p. 128).

Figures 132-138 show strain values measured in section 12, 12 inches of UTB, at various depths and locations and with extensometers and asphalt shingle-mounted gages. Figures 132 and 133 show the values of strain obtained with

extensometers at the top of the base during a continuous period. Temperature effects are probably negligible since the range was very narrow and it was quite cold. These readings were obtained just prior to cracking. Figures 134 and 135 show the values obtained at the same depth except with asphalt shingle-mounted gages during the same period and prior to cracking. The values are higher. Figures 136 and 137 show the strain values measured during the spring in the longitudinal and transverse positions at the bottom of the base. Tensile strains seem to be higher than in the fall, especially in the transverse direction. Figure 138 shows how the strains varied with depth in section 12. Tensile readings were high at the interface of the Class "B" pavement and the crushed base. Spring values seem to be lower than in the fall. This may be due to the fact that this section developed cracks in the fall and thereafter did not act as a continuous base but as individual entities.

Examination of the strains from the continuous strain gage data shows that strain readings were not always symmetrical. Some of this hysteresis effect may be due to temperature effects which caused strain changes and perhaps to the wheel loads. Another reason is that as the duals moved laterally the weight distribution may have changed due to transverse load displacement. The camber of the wheels was initially set to the slope of the pavement so that weight distribution on each wheel was equal; as the pavement became rougher, the load on each wheel may have shifted due to this camber thus causing some variations in strains, both in longitudinal and transverse directions. However, the continuous strain gage readings did show up the various patterns of reversals of strain with lateral distance and also showed the temperature effects.

FIGURE 126. STRAIN VS. LATERAL DISTANCE

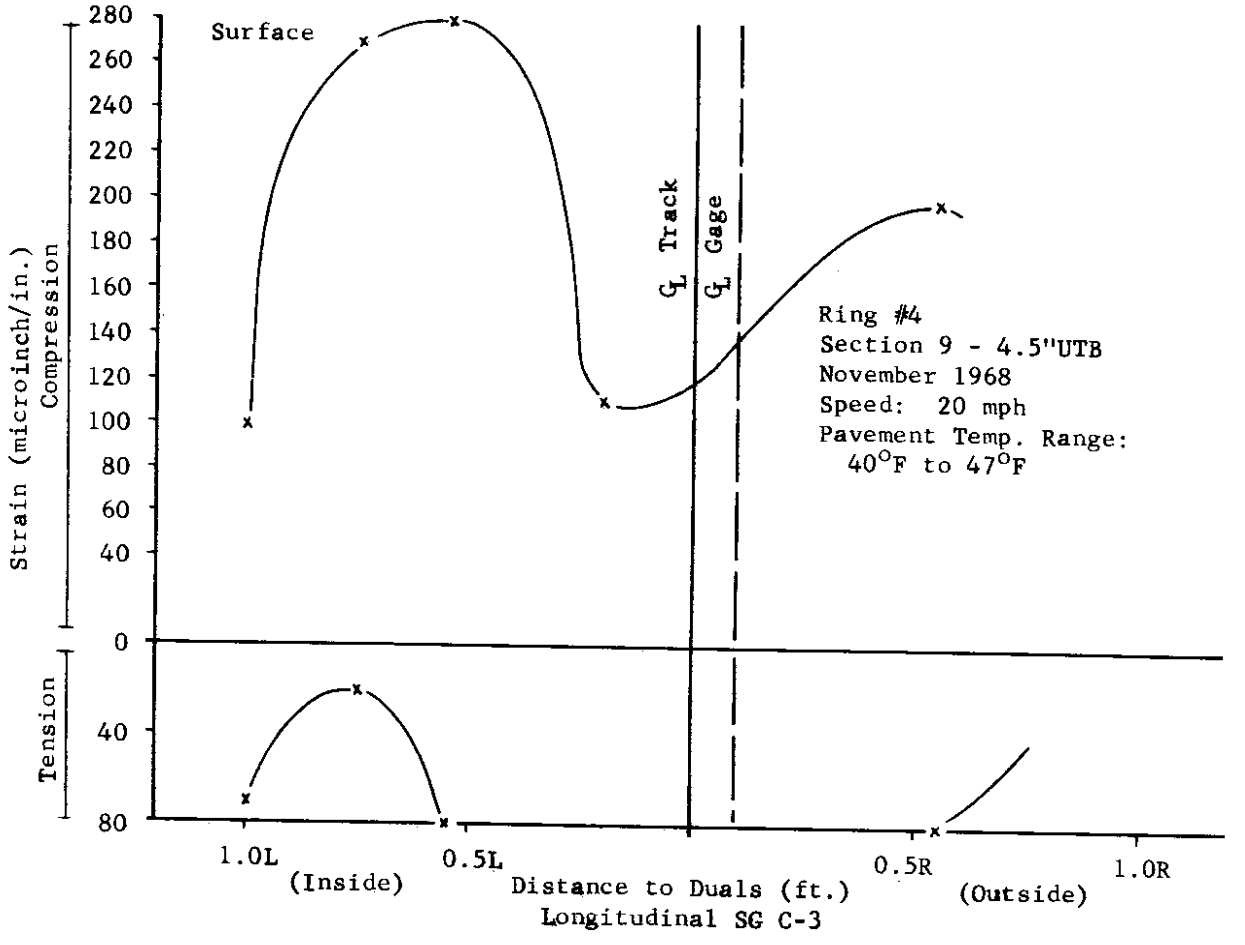

FIGURE 127. STRAIN VS. LATERAL DISTANCE

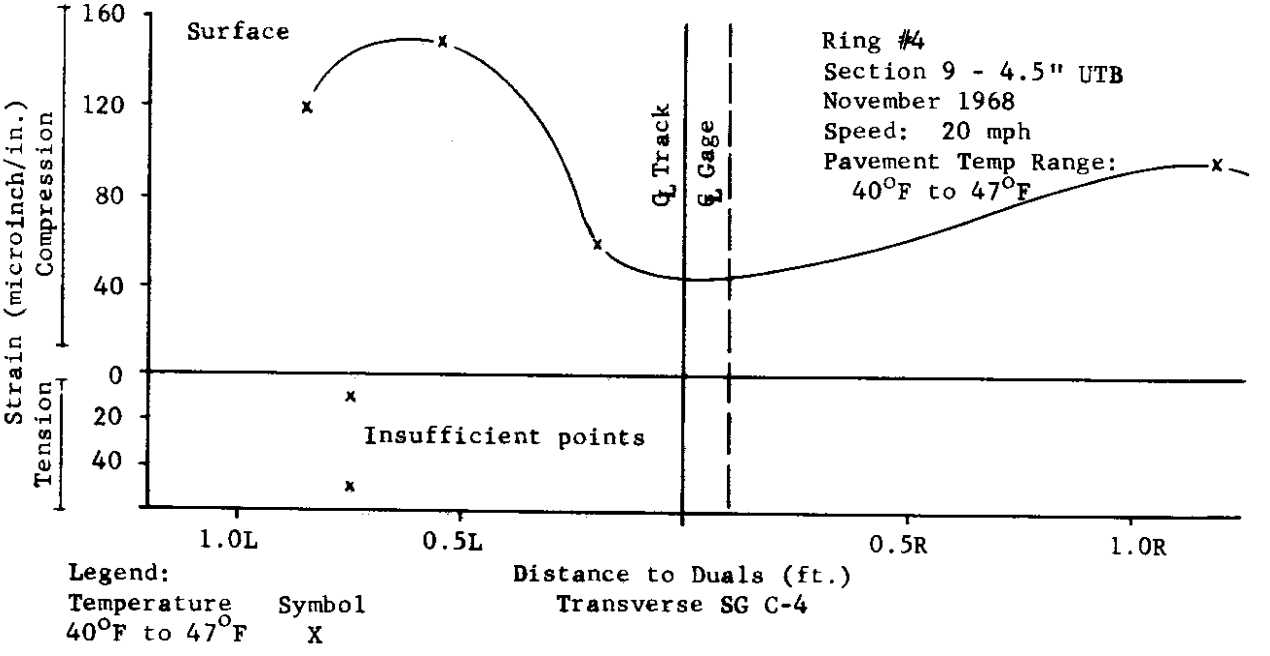

FIGURE 128. STRAIN VS. LATERAL DISTANCE

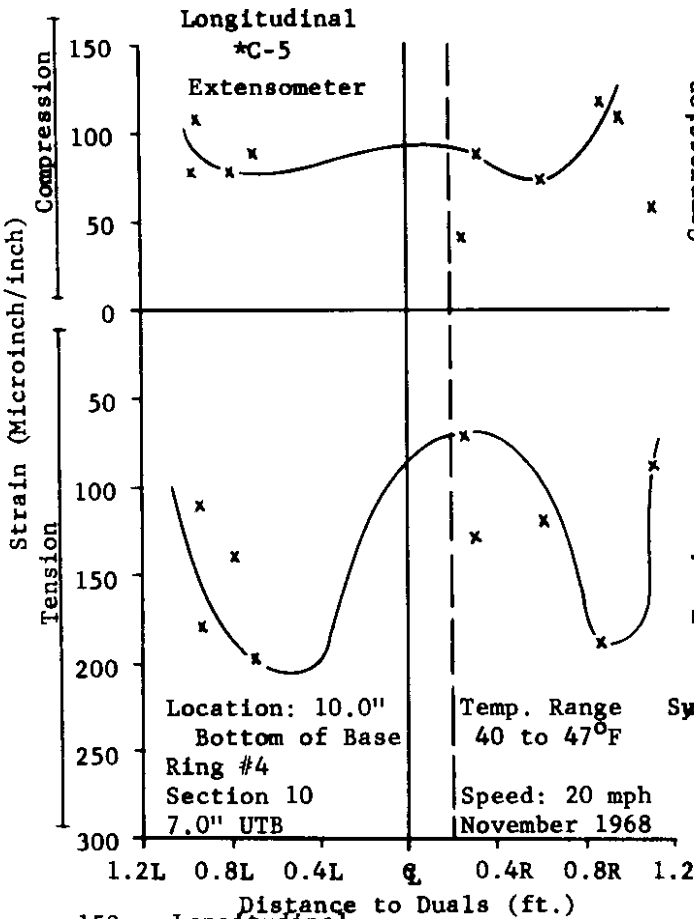

FIGURE 129. STRAIN VS. LATERAL DISTANCE

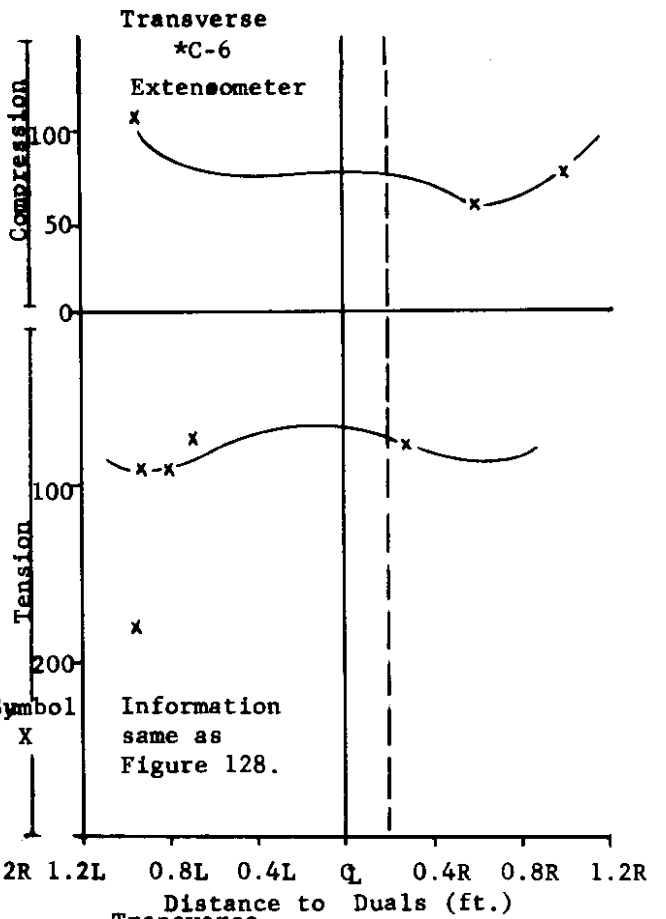

FIGURE 130. STRAIN VS. LATERAL DISTANCE

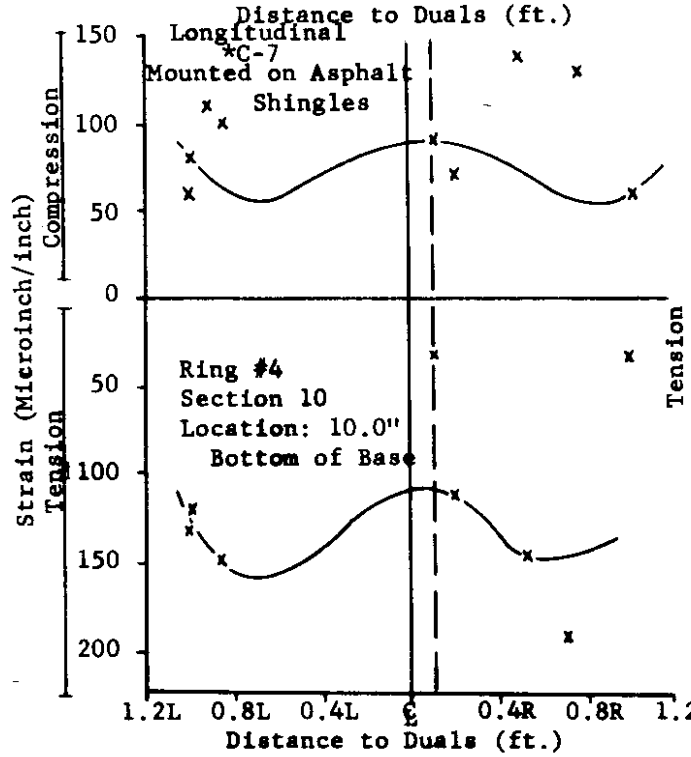

FIGURE 131. STRAIN VS. LATERAL DISTANCE

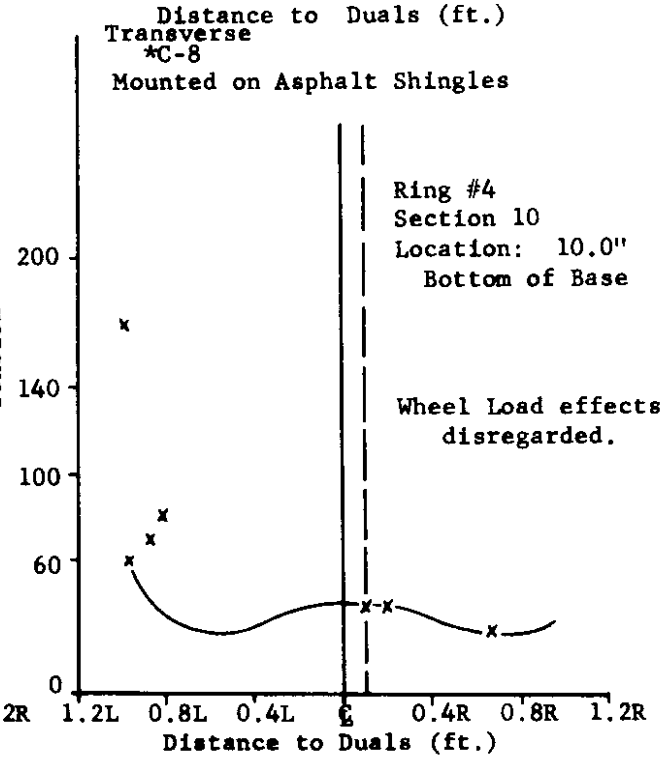

Rough comparison with maximum strains obtained from Rings #2 (2) and #3 (3) show that maximum strains for Ring #4 were reasonable if one examines the approximate temperature range and time period. Ring #4 experiment did not last as long as Ring #3, hence there was less data. The instruments did not last as long, and cold temperatures during November gave lower strain values than under higher temperature conditions. The maximum readings may give us better values for determination of initial strain values for design and failure with proper examination and evaluation.

Stress Data

Measurements of vertical stress were obtained from the WSU strain gage pressure cells and from the WSU hydraulic pressure cells taken on a continuous basis during a day or a period of days and also during runs along with other instrument readings. Unfortunately, operational difficulties with the WSU hydraulic pressure cells developed which resulted in insufficient data for inclusion in this report. All pressure cells were installed at the top of the subgrade in sections 2, 4, 7, 8 10 and 12; the cells in sections 2 and 12 failed to respond after installation. The WSU hydraulic cells were placed only in sections 7 and 8.

The maximum measured vertical stresses are summarized in Table 28 (p.153). Figures 139 to 144 (p.154-157) show the stress variations with lateral distance for the pressure cells in the different sections. Figures 139 and 141 are for the same cell in section 4 showing the difference in stresses during the two testing period. Stresses approximately doubled during the spring period. Figures 140 and 142 are for the same pressure cell in section 7, also taken during the fall and spring periods. Here, too, one can see that stresses with lateral distance and with temperature although these effects may not be so

(Text continued on page 158.)

FIGURE 132. STRAIN VS. LATERAL DISTANCE

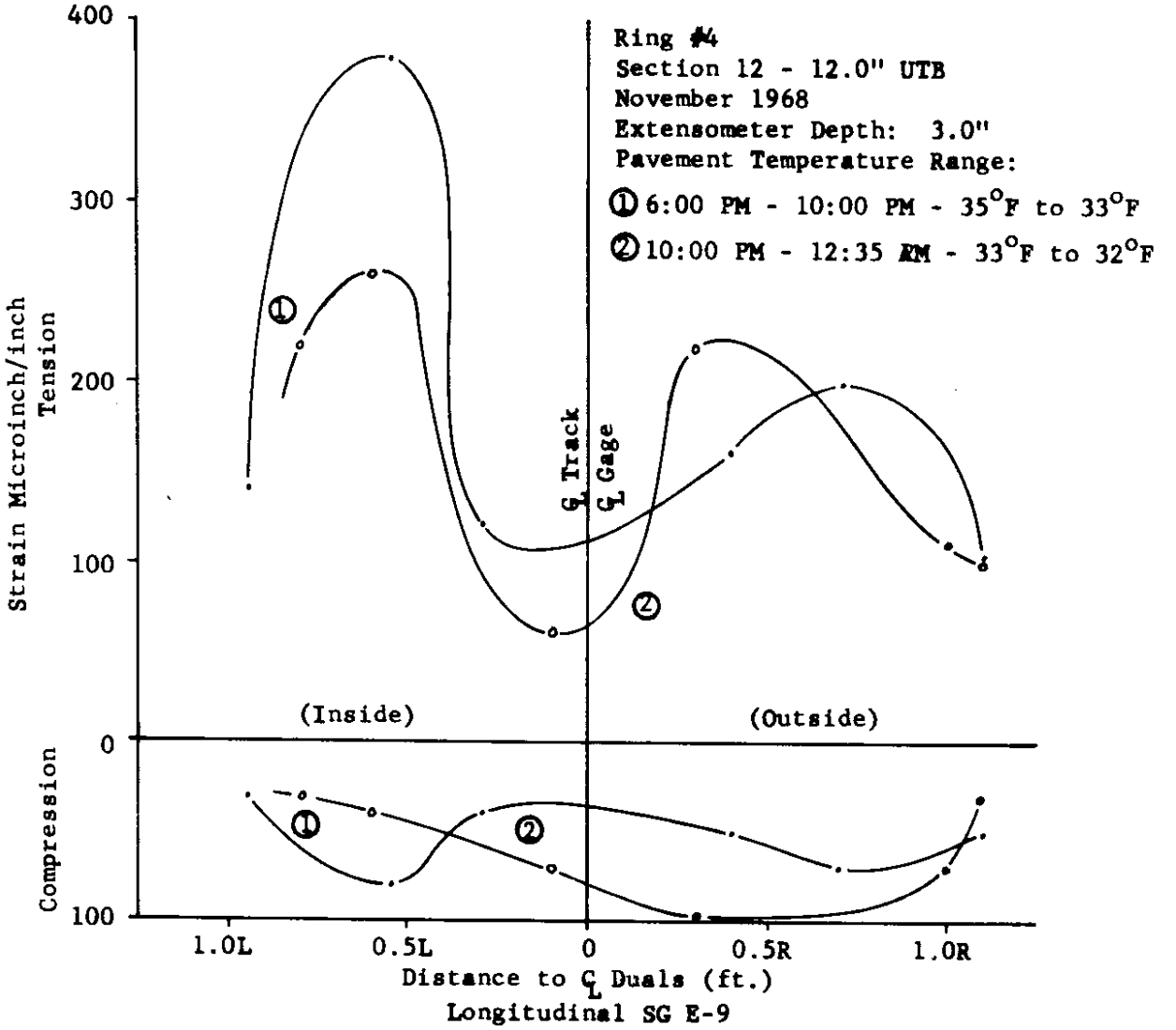

FIGURE 133. STRAIN VS. LATERAL DISTANCE

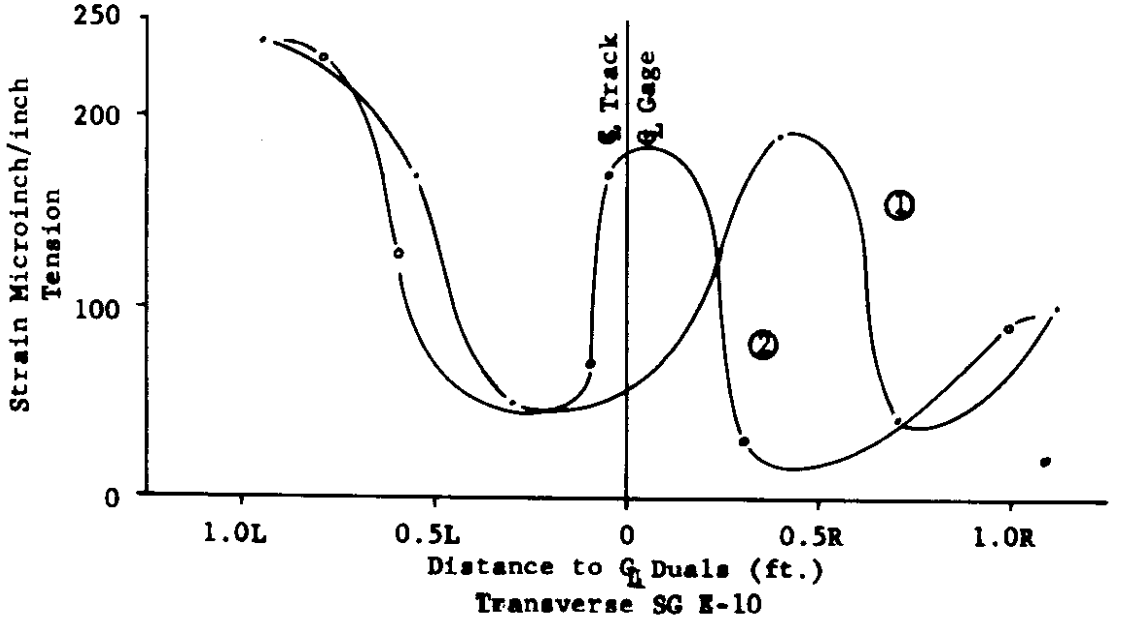

FIGURE 134. STRAIN VS. LATERAL DISTANCE

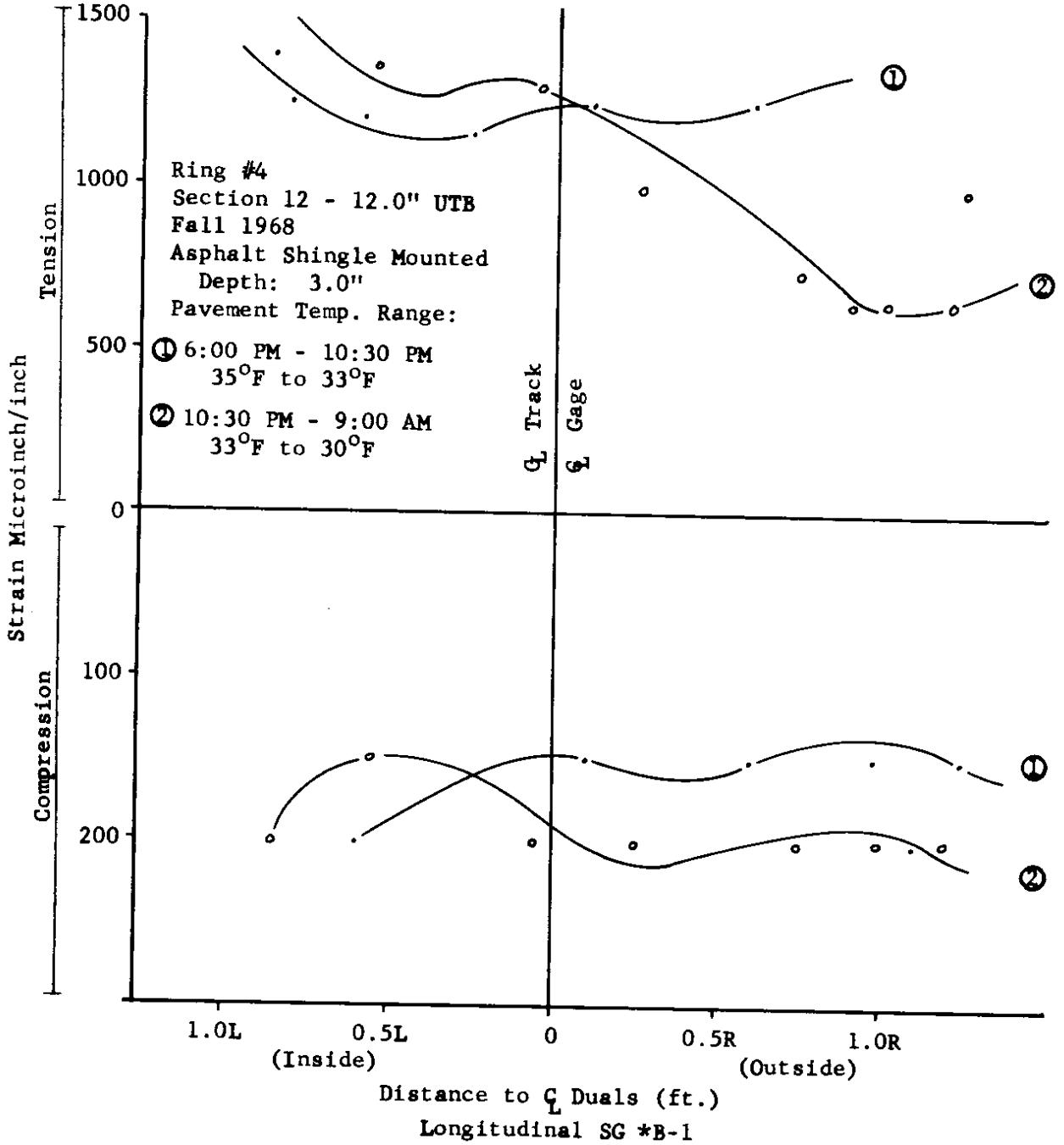

FIGURE 135. STRAIN VS. LATERAL DISTANCE

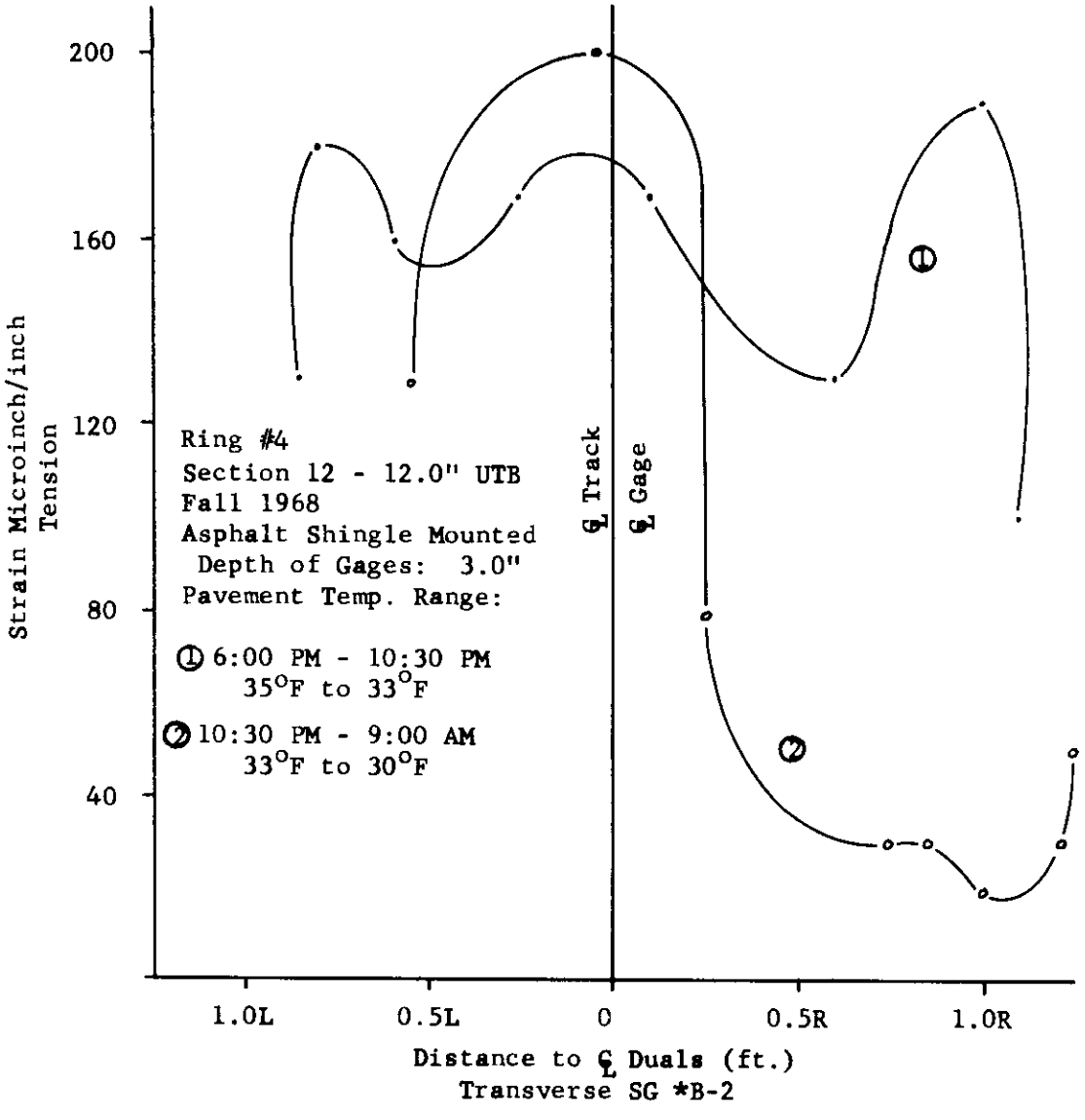

FIGURE 136. STRAIN VS. LATERAL DISTANCE

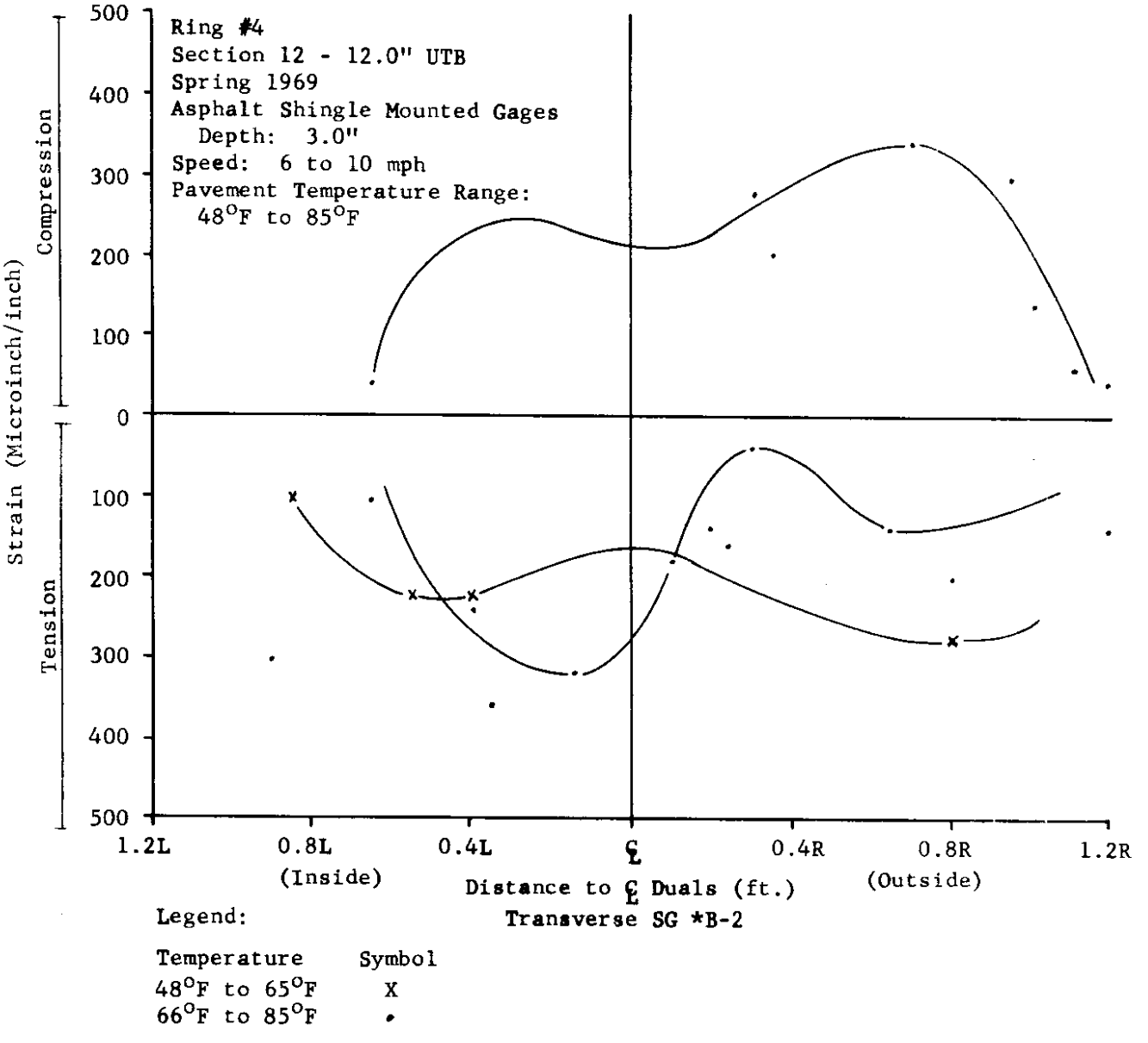

FIGURE 137. STRAIN VS. LATERAL DISTANCE

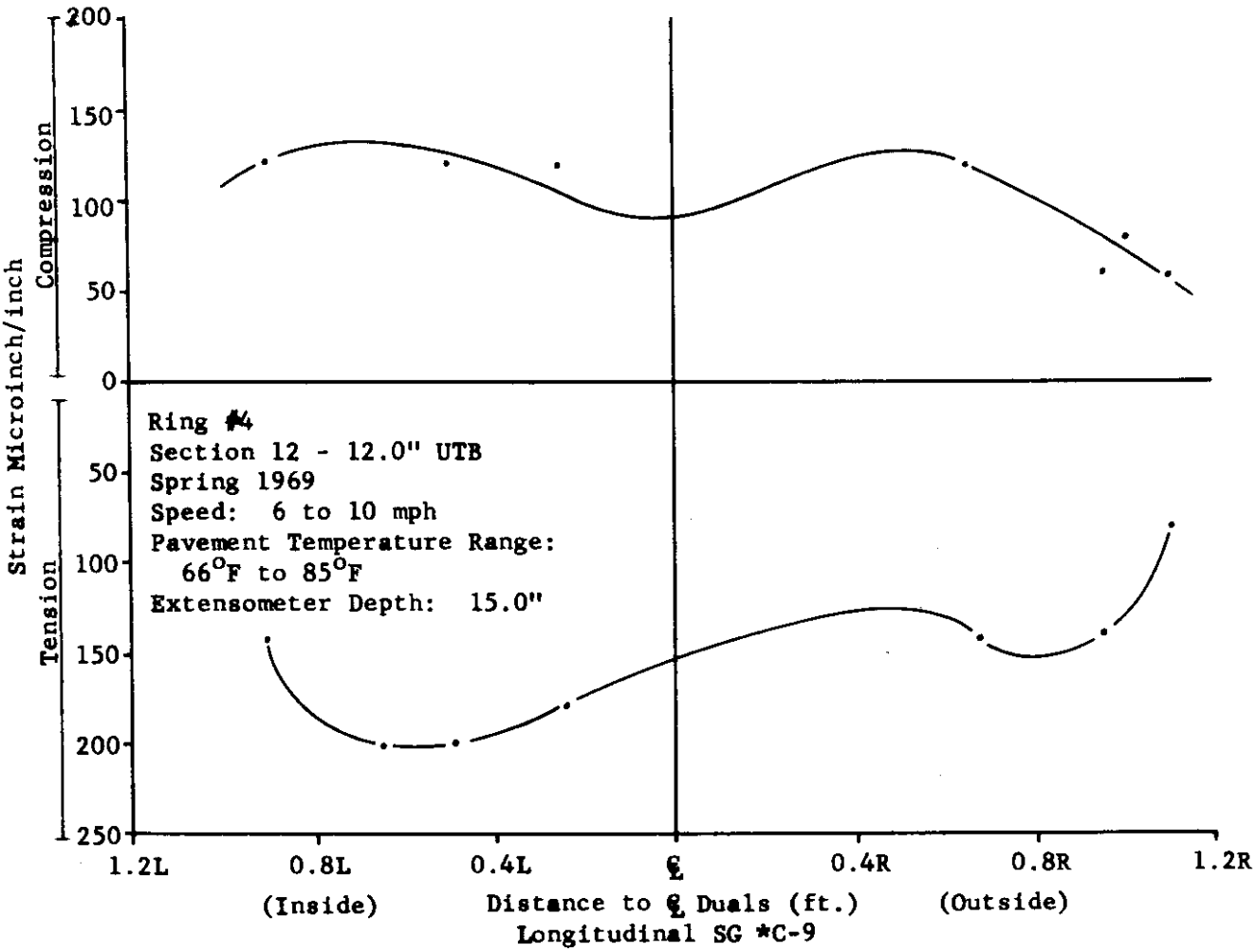

Legend:

Temperature	Symbol
66°F to 85°F	•

FIGURE 138. MAXIMUM STRAIN VS. DEPTH

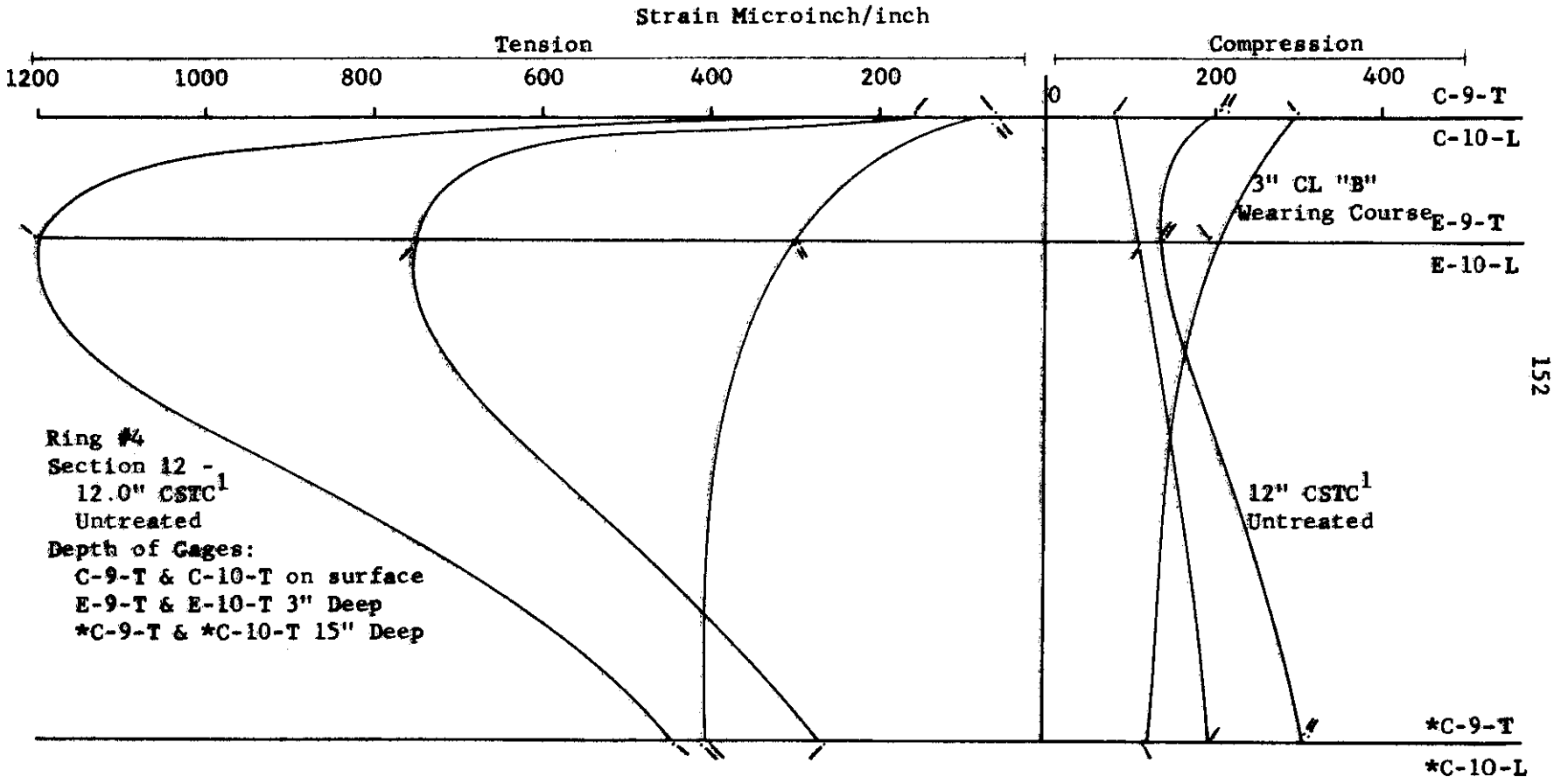

Legend:

\ Transverse Gages (C-9-T, E-9-T and *C-9-T) } Fall 1968

\\ Longitudinal Gages (C-10-L, E-10-L and *C-10-L) }

/ Transverse Gages (C-9-T, E-9-T and *C-9-T) Spring 1969

[1]CSTC - Crushed Surfacing Top Course

TABLE 28: SUMMARY OF MAXIMUM MEASURED VERTICAL STRESSES

Section	Period	Gage Depth Inches	Vertical Stresses PSI	Lateral Position to ℄ Duals (Feet)	Temp. at Gage °F	Speed MPH
2 - 4.0" SAB	Spring[7]	7.0	24.0	0.25L and 0.50R	65	10
4 - 8.0" SAB	Early Nov.[1]	11.0	11.8	0.05R	44	20
	Late Nov.[2]		6.0	0.75L	42	10
	Spring[3]		8.5	0.50L	75	6
	Summer[4]		16.0	0.40R	83	6
7 - 3.5" ACB	Early Nov.	6.5	6.0	0.15R	43	20
	Late Nov.		7.5	0.1R	41	20
	Spring[7]		16.5	1.1L	68	10
	Spring[8]		19.0	1.1L	81	8
	Summer[9]		34.0	0.35L	82	6
8 - 5.0" ACB	Early Nov.	8.0	9.0	℄	46	20
	Late Nov.		10.0	0.75R	40	10
	Spring		30.0	0.95R	78	10
	Summer		40.0	0.85L	86	6
10- 7.0" UTB[6]	Early Nov.	10.0	2.5	1.4L	44	20
	Late Nov.		2.0	0.4L	39	20

[1] To 11-16-68.
[2] From 11-16-68.
[3] Spring--April-May.
[4] Summer--June.
[5] R=Outside and L=Inside, ℄=Center of duals over gage.
[6] Readings seem to be too low; the pressure cell was probably defective.
[7] Prior to initial cracking.
[8] After cracking.
[9] At "ultimate" failure.

FIGURE 139. STRESS VS. LATERAL DISTANCE

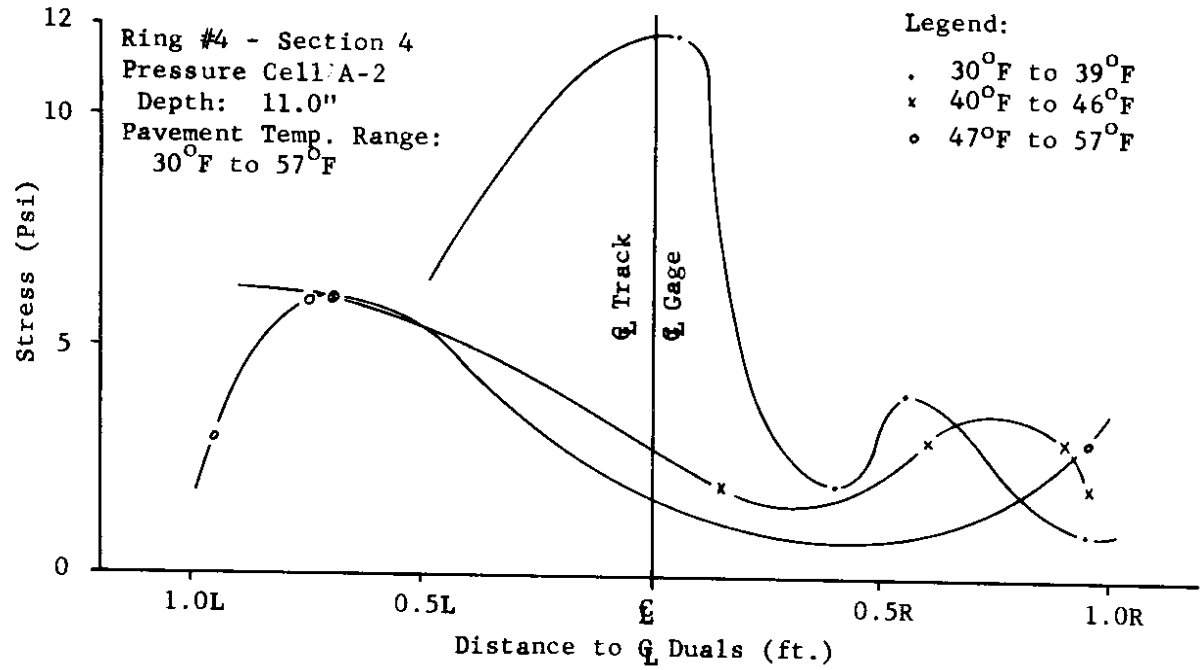

FIGURE 140. STRESS VS. LATERAL DISTANCE

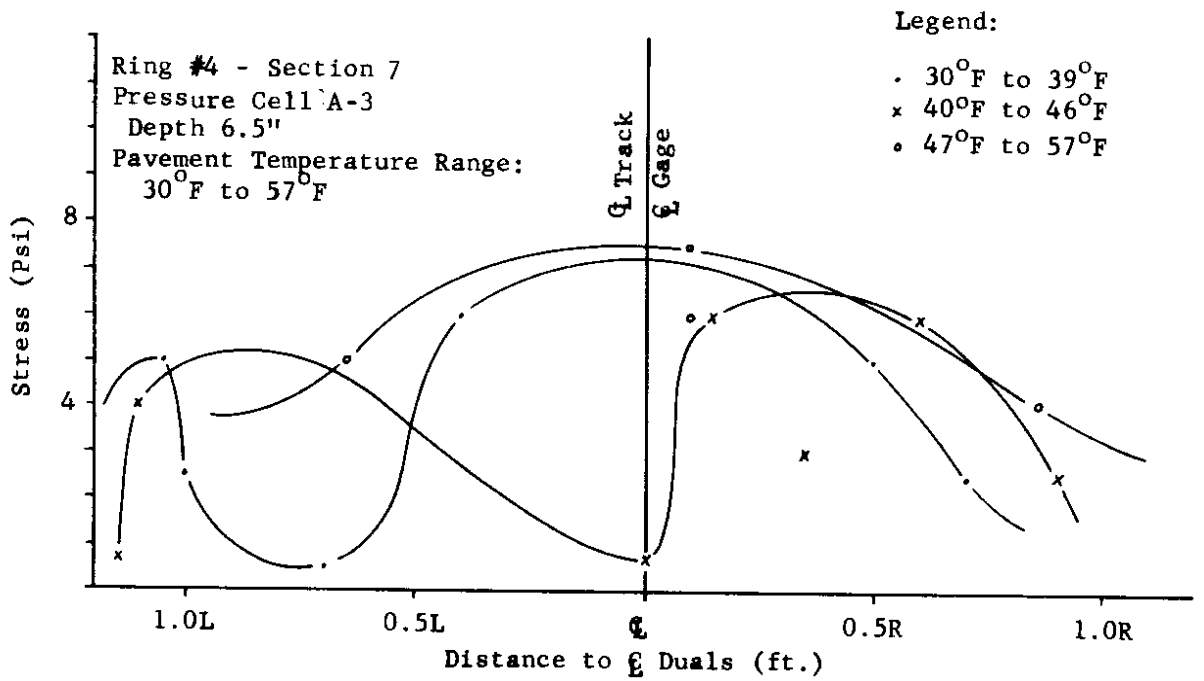

Note: Data taken from runs--wheel load effect disregarded.

FIGURE 141. STRESS VS. LATERAL DISTANCE

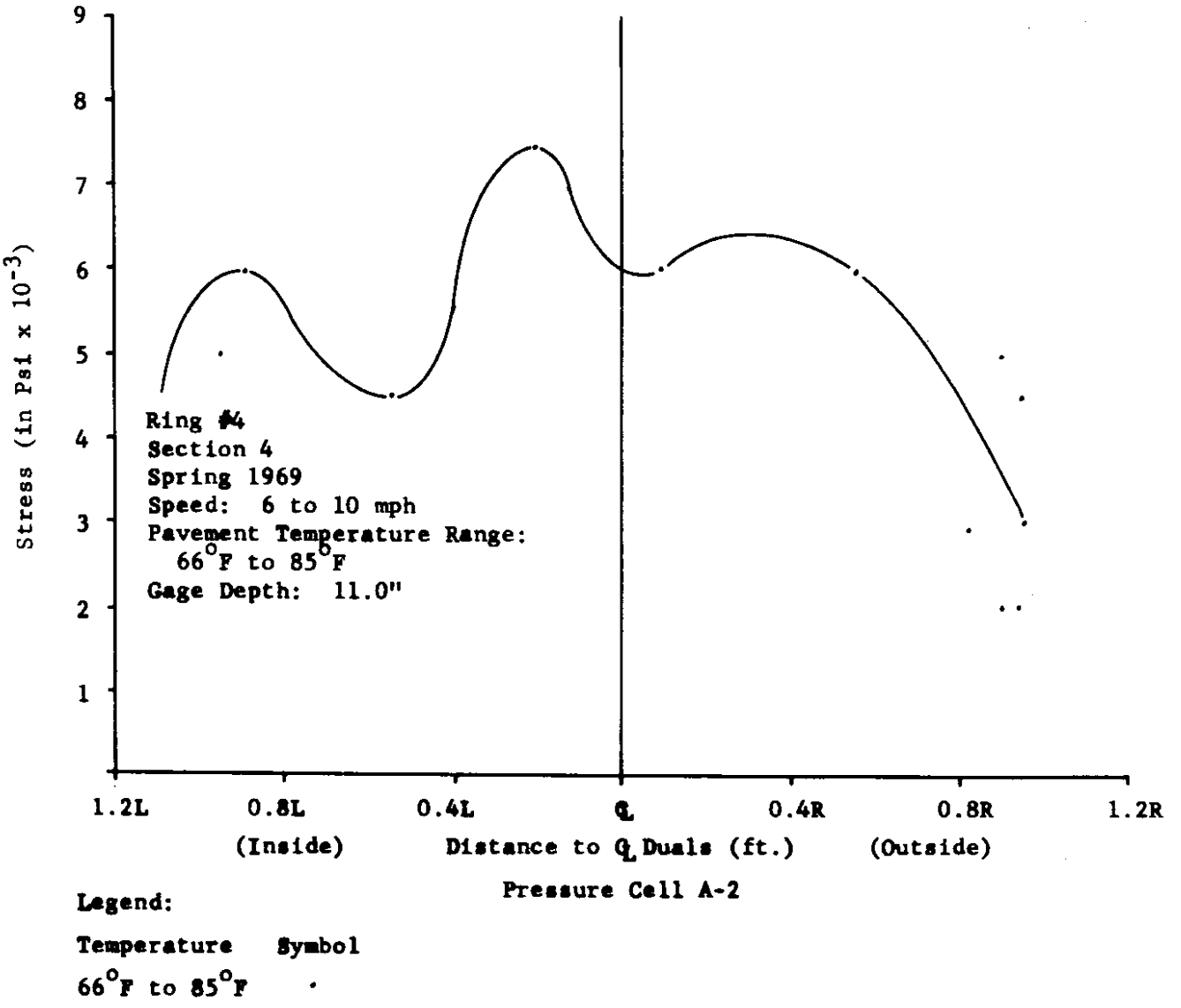

FIGURE 142. STRESS VS. LATERAL DISTANCE

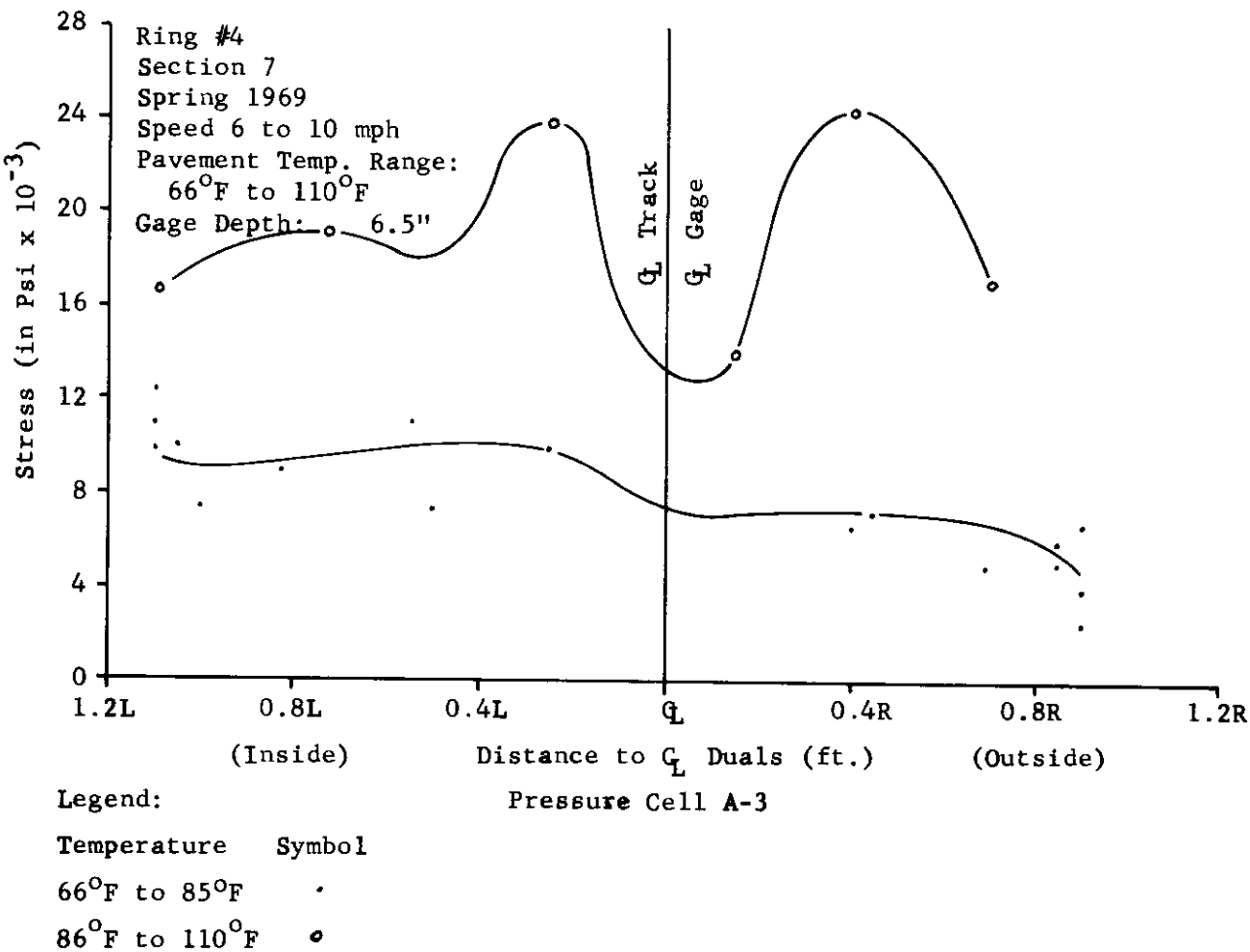

Legend:

Temperature	Symbol
66°F to 85°F	·
86°F to 110°F	o

FIGURE 143. STRESS VS. LATERAL DISTANCE

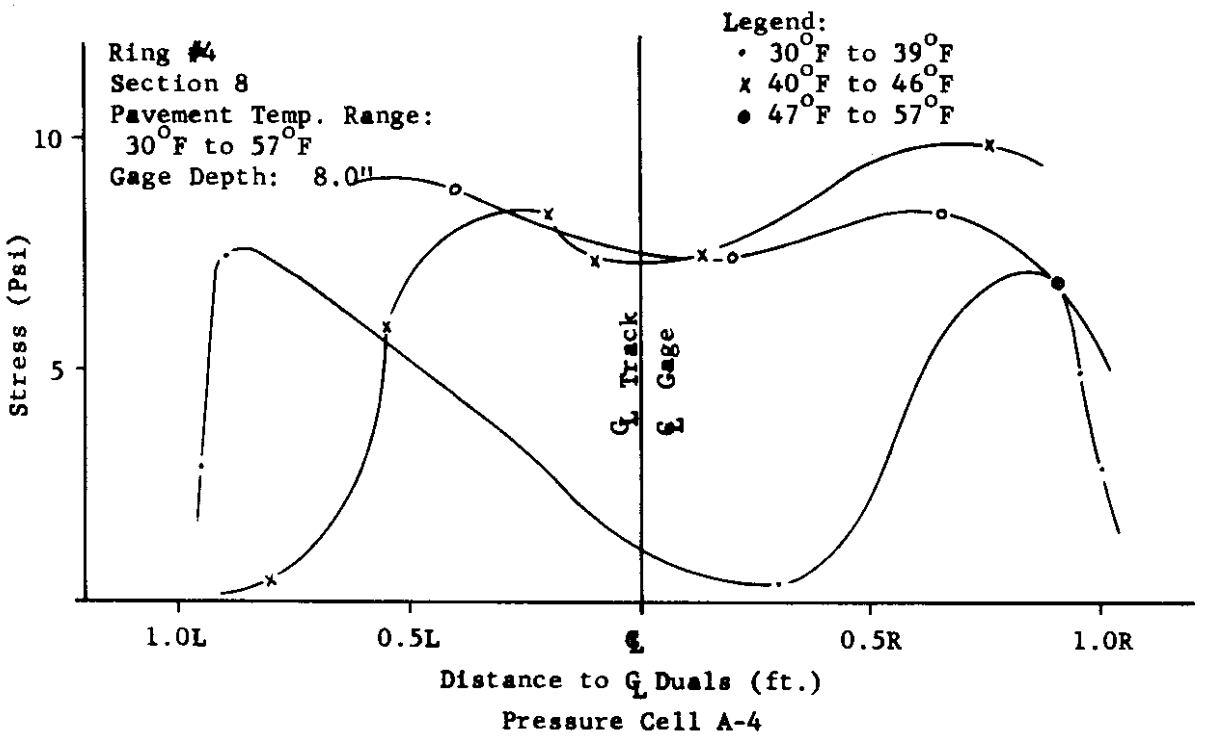

FIGURE 144. STRESS VS. LATERAL DISTANCE

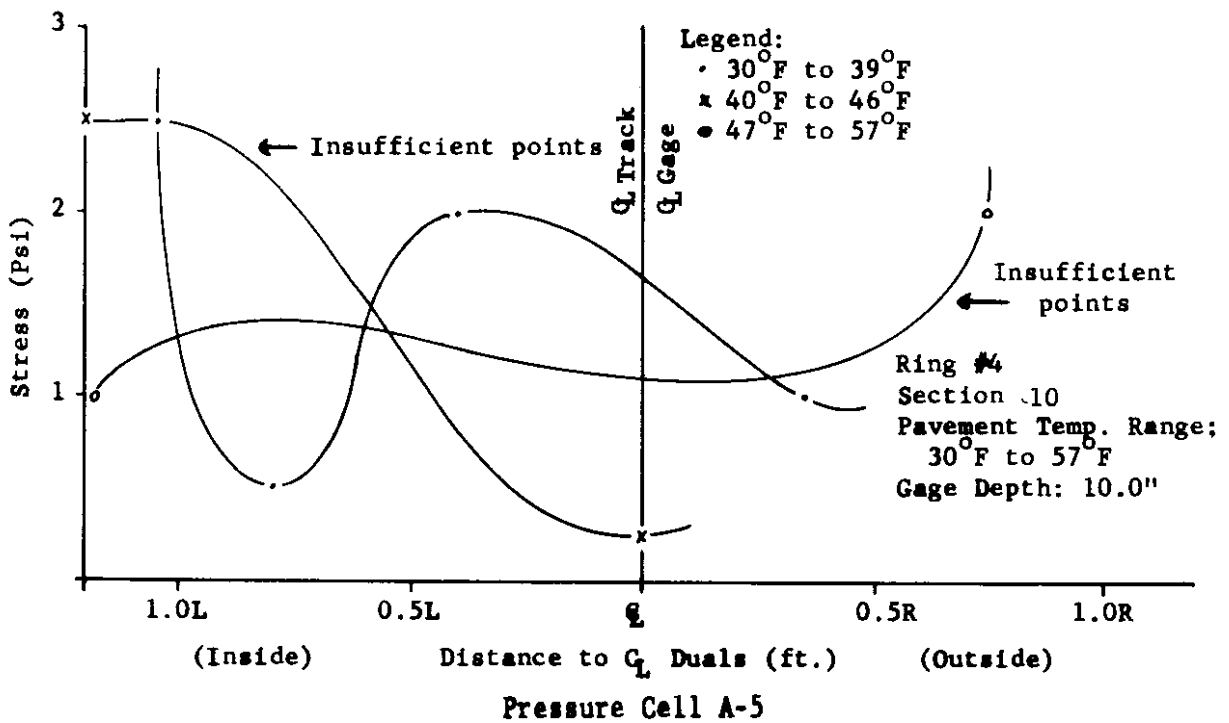

Wheel Load effect disregarded.

evident due to low temperature ranges present during the fall period. Generally, one can say that maximum stress values are found under the center line of the duals. Figures 143 and 144 (p. 175) show the stress values measured by pressure cells in sections 8 and 10. The stress levels in section 10 are too low; this may be due to a defective pressure cell.

According to Table 28 (p.153),the stress levels appear to be low. They were below the critical stress values of 9 to 11 psi mentioned by Vesic and Domaschuk (26) and obtained in the AASHO Road Test (22). These sections did not experience any distress during the fall. During the spring and summer, these critical values were exceeded with resulting distress in sections 1 and 2 and rutting in sections 4 and 8. The stress values measured in section 7 are valuable in that they point out that stress values increased prior to distress and then increased after cracking. This may be due to development of pressure points caused by individual slabs acting on the pressure cell rather than a continuous slab.

The higher stress values in the spring are an indication that conditions in the pavement had changed, and is an indication why different modes of failure occurred in spring as compared to the fall. As shown in Table 28, the critical stress values had been reached and exceeded. Since the stress values exceeded these values, rutting increased rapidly. Since the subgrade was weak due to high saturation levels and the thin pavement structure was strong, well-compacted, structural failure occurred mainly due to punching shear as shown in Figures 40, 48, 49, 55, 61, 69 and 70. All these sections showed well-developed rutting before "ultimate" failure occurred. This also occurred in Rings #2 (2) and #3 (3). Therefore, rutting is due to primarily compression and distortion of the subgrade soil. The thick sections 4 and 8 exhibited rutting but no

failure had developed due to cracking. The thickness of the pavement structure was probably able to overcome this punching failure phenomena. The fall stress values were below the critical values. The sections which failed had no pressure cells, hence no record of stress values exist. Probably critical stress values had been reached prior to initial cracking. Once that occurred, failure probably was due to other factors besides excessive vertical stresses. Environmental conditions such as excessive precipitation, lower temperatures and accumulated wheel loads on the sections may have been responsible for the different failure mode.

Discussion of Results

Two modes of failure were recognized as occurring in the sections of Ring #4. The failures in the fall were different from those in the spring.

The fall failures in the untreated base sections may have been due to a combination of thermal and environmental conditions coupled with mechanical distress. Environmental conditions during construction, prior to and during testing were adverse to say the least. The abnormal amount of precipitation with low temperatures added to the saturation of the subgrade. The crushed rock base may have also added to the saturation of the subgrade by acting as a reservoir, thus continuously adding moisture into the subgrade (Table 15) (p.89). Thermal distress may have occurred when the combination of temperature and environmental change caused differential stresses in the pavement structure. It is no coincidence that transverse cracks occurred in the thin section just after a period of cooling weather along with heavy rainfall and prior to snowfall. Transverse cracking due to thermal conditions has not been recognized as a major factor in local and Washington State pavement failures. Transverse cracking has been observed to be common in the colder states and in Canada (23). Investigators in Canada believe that transverse cracking can occur either with decreasing (24) temperatures or with sudden increases in temperature (25). The latter has been noted in the test track as the cracks usually appeared in the morning and afternoon rather than in the evening (27). It is possible that under slowly decreasing temperatures the pavement builds up enough strength to restrain cracking. It is therefore in a pre-tensioned condition with different stresses on the bottom and the top. Then when a warming spell occurs, the surface loses its strength because it is warmer than the sub-surface elements which are still pre-tensioned, and suddenly, a crack occurs at the bottom and works upward.

This will be accelerated by mechanical loading. Large daily variations in temperature, coupled with heavy wheel loading, could act as a loading device hence increasing the possibility of cracking occurring sooner than expected (28). The combined loading conditions due to thermal and mechanical loads probably caused distress in the thin sections of Ring #4 (27). Environmental changes undoubtedly accelerated this effect, especially in the untreated base sections.

Failures occurring during the spring testing period were spectacular and catastrophic. Deflections were very high--in excess of 0.080 inches. During this period the speed of the apparatus was 10 mph and because of the eccentric mechanism which is dependent upon the apparatus speed the wheels crossed the wheel path width slowly. Hence, there was a virtual concentration of wheel load on one part of the pavement. Winter conditions may have also elevated the pavement track (16). The first few heavy wheel loads probably caused considerable pavement deformation. This phenomena has been reported by the Canadian Good Roads Association (18). At this point longitudinal surface tension cracks occurred. The edge location of the observed failures may have been a factor as suggested by the WASHO Test Road Report (29) and reported by Meyerhoff (30). Examination of the subgrade after test completion showed that the subgrade was almost completely saturated. The degree of saturation of the subgrade affects the bearing capacity of flexible pavements as indicated by Broms (31). A reduction in relative density and an increase in degree of saturation which occurs during the spring thawing period reduces the subgrade bearing capacity greatly. The resilient modulus of the clay subgrade can be reduced by a factor of two due to the accumulation of moisture (32). This probably occurred in the sections that failed spectacularly in the spring. Rutting also occurred. Excavation made on Ring #3 (3) revealed that it

extended into the subgrade thus verifying the theories of Vesic and Domaschuk (26) which show that certain maximum vertical stress levels exist and remain constant, thus remaining within the pavement structure. Further excavation made on Ring #4 probably will bear this out. When stress levels are exceeded, and they were as measured by the pressure cells during the spring, rutting is extended into the subgrade. Another indication of a different mode of failure occurring during the spring was that LVDT and Benkelman beam deflections and strains were two to four times greater than in the fall. Since a relatively weak, compressible subgrade and a strong, well-compacted but thin pavement structure existed, structural failure occurred through punching shear. Therefore, one can say that different subgrade conditions occurred during the fall and spring testing periods causing different structural effects and different modes of failure.

Studies of the data obtained by instrumentation reveal definite trends. Lateral wheel placement did affect the measured values of stress, strain and deflection. This has been borne out by other studies (20, 22). Deflections occurring in the untreated bases show that about 40-60% of the movement occurred within the pavement and base structure and that this increased with wheel loads perhaps indicating a decrease in resilient modulus (32). Deflections increased with wheel loads indicating possible variations in the resilient characteristics of the subgrade due to environmental changes during the life of the pavement. This may be especially true during the spring when deflections increase two- to fourfold.

Strain readings below the pavement show that maximum strain occurred directly under the tire. Strains were higher in the spring than during the fall. Temperature also affects strain values. Tensile strain increased with depth while

compression decreased. Gusfeldt and Dempwold (33) and Klomp and Niesman (34) obtained strain results under controlled centered loading and with uniform top to bottom temperatures which were almost similar to that obtained at the test track. Some deviations were observed due to temperature differences between layers and different loading. Correlation of tensile strains with deflection data was not tried, but will be tried in the evaluation report. An effort to try to establish a criterion for measurement of fatigue failure as mentioned by Hong (35) will be tried. It is hoped that this may be possible as data from the last ring becomes available, along with this and the previous ring.

Work done by Sowers and Vesic (36) and Nijober (37) shows that vertical stress decreases with depth and is affected by the lateral positions of wheels. The different bases had a marked effect on the stress level. During the spring periods, stresses measured increased two to three times. The significance of this has been previously discussed. After distress occurred, high vertical stresses were measured indicating that perhaps pressure points may have been established as the pavement section began to act as separate entities.

The sand-asphalt bases performed very well. Despite their low stabilometer values, if put in properly these bases have a future in areas where sand is plentiful. The fine-grained matrix of sand-asphalt bases may permit more deformation than regular asphalt concrete mixes; the sand-asphalt bases may deform rather than develop cracking as compared to regular asphalt concrete bases. Other areas have found the performance of hot mix sand-asphalt bases to be satisfactory, especially on moderate and low traffic roads (38).

Another interesting development is the performance of the Class "B" asphalt concrete pavement with no base on the silt subgrade in both Rings #3 (2) and #4. The fact that these sections survived many wheel loads seems to

indicate that perhaps highways are being built too conservatively and that elimination of bases, especially for low traffic roads may be quite feasible and economical. It will be necessary to ensure good drainage and good compaction of subgrade to achieve maximum results.

The performance of the Class "F" asphalt treated bases shows that these bases are worthwhile and do add to the pavement system life. The tendency to use only the "best aggregate," even if it means transporting it at great distances, is questionable and engineers should look into the possibility of the best use of aggregates available (39).

Equivalencies based on fall and spring testing periods are shown in Tables 29 and 30 (p. 165) based on all three experimental rings. At the AASHO Road Test, one inch of bituminous surface was equivalent to 3 inches of crushed stone base or to 4 inches of sand-gravel subbase (22). Experience in Canada indicates that the ratio of the relative supporting capacity of bituminous concrete surface to granular base may be as low as 2 to 1 (40). Shook and Finn (41), using the AASHO Road Test data, showed that larger equivalencies of asphalt concrete surfacing in terms of crushed rock base ranged from 2 to 6.7 depending upon the criteria used. Equivalency values can be established using deflection data, strain gage and stress data (42). The values shown in Table 30 seem to be reasonable; these values were based on field tests which have shown repeatability during different time periods; for example, Rings #2 and #3. However, it should be noted that these equivalencies apply only to the materials used in this test and within the range and degree of this experiment and may be subject to modification as more evaluation on the data is done.

TABLE 29: EQUIVALENCIES BASED ON RINGS 2, 3 AND 4

Type of Base	Fall Period[1] Inches	Spring Period[2] Inches
Crushed Stone Base (UTB)	9.5	12.0
Emulsion Treated Crushed Stone (ETB)	3.0	9.0
Special Aggregate Asphalt Treated (ATB)[3]	2.0	5.0
Cl "F" Asphalt Concrete (ACB)[3]	2.0	5.0
Sand-Asphalt Base (SAB)[3]	2.0	8.0

[1] The thinnest sections which survived this period.
[2] The thickest sections which failed during this period.
[3] Hot mix.

TABLE 30: EQUIVALENCIES IN TERMS OF UTB

(3.0" of Cl "B" A.C. Wearing Course)

Base Type	Fall Period Inches	Spring Period Inches
UTB	1.00	1.00
ETB	0.32	0.75
ATB	0.21	0.42
ACB	0.21	0.42
SAB	0.21	0.67

Comparison With Other Rings

Tables 29 and 30 show the equivalencies obtained from all three rings. The results obtained are similar for the asphalt treated bases (SAB, ATB and ACB) for the fall period. Another similarity between the three rings is that the failures in the fall and spring were similar. All the untreated bases developed cracks in the fall for all three rings.

All three rings revealed that the thin sections will not survive the combination of thermal and mechanical loads past the fall period and that this will be accelerated by adverse environmental conditions as in Rings #2 and #4. In all three rings the untreated bases failed first, and the thin treated bases would not survive past the start of spring testing. In Rings #1, #3 and #4 the thick sections failed in rutting and not by cracking. The fact that modes of failure for the fall and spring were similar for three rings is an indication that the test track is capable of reproducing experimental results, and hence is a successful experimental tool.

Instrument measurements showed that the magnitude and modes of the measurements were similar. Some improvements in the instrumentation of Ring #4 may have given better results. The failure of some instruments indicates that this is still a weak point in pavement testing technology. Analysis by Terrel (15) and reported by Terrel and Krukar (21) show that the values obtained in the field from Ring #2 could be duplicated by laboratory and theoretical means. Similar analysis still has to be done on Rings #3 and #4. Rough comparisons with field data from the rings reveal the results are similar under certain conditions.

Both Rings #2 and #4 experienced similar environmental conditions of rain and cold temperatures with resulting rapid and sudden failures in the fall.

Ring #3 had ideal environmental conditions with the result that the experiment lasted 4 times as long. This points out that environmental factors should not be disregarded in the life and design of pavement structures. These factors may be the most important design parameters in pavement life.

Rings #3 and #4 show that the pavement laid directly on well compacted and drained subgrade may be useful for low traffic roads. All results show that properly treated low-grade aggregates have uses in highway pavements.

CONCLUSIONS

Major Conclusions

1. The Washington State University Test Track is a research tool capable of duplicating results. This was shown by comparison of results from Rings #2 and #3, by the distinctive failure modes for the different periods for all rings and by the failure of the untreated bases to survive cracking during the fall period in all three rings.
2. Equivalencies developed from all three rings are summarized in Table 30 (p.165). The fall equivalencies are based on the thinnest sections that survived, while the spring equivalencies are based on the thickest sections that failed in "ultimate" failure.
3. The modes of failure were different during the two testing periods. The fall failures were due to thermal and mechanical loads which were accelerated by adverse environmental conditions thus causing the thinnest sections to crack. The spring failures were caused by highly saturated subgrade conditions which resulted in a reduction in resilient modulus and thus a lack of bearing capacity.

4. On the basis of this and other tests, the aggregate which is not entirely fractured and when treated with asphalt seems to have superior load carrying performance ability as compared to sand-asphalt, emulsion treated and untreated crushed rock bases.
5. Sand-asphalt bases can be used with confidence on medium and low traffic roads. Although they have low stabilometer values, under proper construction techniques and design these sand-asphalt bases will give satisfactory performance.
6. The thickest sections had no surface cracks, but failed due to rutting. Examination will probably reveal that transverse cracks had started to develop on the bottom of the bases. It may be that for thick sections rutting may be a more valid criteria of failure that cracking.
7. A series of tables summarizing maximum values of static deflections, dynamic deflections, strains and stresses were developed. These could be used for the development of critical values needed for better rational pavement design.
8. The shortness of the testing of Ring #4 due to adverse environmental conditions points out that this may be one of the most important factors, if not the most important factor, in pavement structure life.

Minor Conclusions

1. The lateral position of the dual tires greatly affects the strain gage values and hence this is quite critical for obtaining accurate values of strain with respect to load location. Lateral position of tires also affects the stress and deflection values.

2. Temperature effects were noted on static and dynamic deflections, strains and stresses. Temperature effects, which were low, did not seem to be as critical in the fall as compared to the spring.
3. Continuous readings on the different gages were better able to establish the behavior patterns than readings taken over different periods of time. Temperature effects became quite noticeable during these tests. There is still need of an automatic system to obtain continuous data.
4. Problems developed with evaluation of data. Even with a manual system of obtaining data, a huge amount was generated which entailed much tabulation and evaluation. The operation of the automatic thermocouple recorder points out the fact that the need for rapid evaluation is critical. Data accumulation and assimilation caused delays in the evaluation of results.
5. Strain results revealed that tensile strains were greater in the longitudinal direction thus explaining the presence of transverse cracks. Pressure cells revealed that prior to cracking and rutting, the stress values exceeded the untreated stress values found at the AASHO Road Test (22) and by Vesic and Domaschuk (26).

PRACTICAL IMPLICATIONS FROM THE TEST RINGS TO DATE

The comparison of results obtained from all three rings show that the test track is capable of duplicating experimental results. The conclusion from this is that results can be used with some degree of confidence.

The equivalencies developed can now be used with assurance. This should be of some value to the pavement designer as he now has some values on the equivalent strength of the different materials tested.

Sand-asphalt bases, if properly designed, mixed and compacted, have a proper place where sand is available. Economies may be obtained in areas where these can be used. It should be emphasized that compaction is critical and that care has to be taken during construction.

The results from Rings #1 to #4 indicate that the use of fractured screened aggregate is not necessary. Bases constructed of non-fractured aggregate in varying percentages are apparently equal to many types and are probably superior to many others. The highway departments and contractors may be able to realize considerable savings by using these aggregates, especially where glacial and river deposits abound.

Thin pavements, laid directly on well compacted and drained subgrades, may be useful for low traffic roads. This may be of some benefit to counties and cities with low budgets. The possibility of such economizing should be investigated by application of this design and construction procedure.

The short operating time of Ring #4 points out the importance of environmental factors on pavement structure life. These should be considered in any kind of pavement design. Thermal loads should be considered, especially on thin pavements.

Rutting may be a better criterion of failure for thick sections than initial cracking and other cracking criteria. This has been shown by Rings #1, #3 and #4. Hence, the pavement serviceability index developed by AASHO (22) is probably a good index for evaluating pavement conditions.

Benkelman beam measurements can be used to predict where and to some extent when distress may occur. This was done in Rings #3 and #4. This would mean correlating deflections with pavement distress. This has practical implications for maintenance. As soon as one knows that a pavement has

reached a critical stage, an overlay can be planned. This would require studying deflections for all thicknesses and types of roads, and setting up deflection limits. When these limits are reached, the maintenance department would plan on laying an overlay. This would be economical in that overlays would not have to applied before necessary. Maximum life of existing pavements could then be achieved. Results from Rings #2, #3 and #4 should help in the development of critical deflection values for pavements of different materials.

Deflections, strains and stresses obtained from LVDT's strain gages and pressure cells will be useful in helping to evaluate strength parameters in pavements. Data from Rings #2, #3 and #4 showed some interesting trends which may be further clarified as the data from Rings #3 and #4 become evaluated and available. More analysis is needed on the data from Rings #3 and #4. This may lead to the development of critical values for pavement deflections, strains and stresses so that failure and design pavement theories can be formulated or substantiated. Ultimately and hopefully this will lead to better and more economical pavements.

REFERENCES

1. John C. Cook, G. A. Riedesel and Milan Krukar. Experimental Ring #1: A Study of Cement Treated and Asphaltic Treated Bases, Pavement Research at the Washington State University Test Track, Vol. 1, Report to the Washington Department of Highways on Research Project Y-651, Highway Research Section Publication H-28, Pullman, Washington, July, 1967.

2. Milan Krukar and J. C. Cook. Experimental Ring #2: A Study of Untreated, Emulsion Treated and Asphaltic-Cement Treated Bases, Pavement Research at the Washington State University Test Track, Vol. 2, Report to the Washington Department of Highways on Research Project Y-651, Highway Research Section Publication H-29, Pullman, Washington, July, 1968.

3. Milan Krukar and J. C. Cook. Experimental Ring #3: A Study of Untreated, Emulsion Treated and Asphaltic-Cement Treated Bases, Pavement Research at the Washington State University Test Track, Vol. 3, Report to the Washington Department of Highways on Research Project Y-993, Highway Research Publication H-30, Pullman, Washington, July, 1969.

4. Theodore W. Horner. Experimental Design and Analysis of Experiments for Comparison of Paving Materials, Engineering Analysis Section, The Asphalt Institute, Booz Allen Applied Research, Inc., August, 1965.

5. B. F. Kallas. "Summary of Asphalt Institute Laboratory Test Results," Interim Report, The Washington State University Test Track, Internal Asphalt Institute Report (Unpublished), May, 1968.

6. Standard Specifications for Road and Bridge Construction--1963, Washington State Highway Commission, Department of Highways, Olympia, Washington.

7. Specifications for Paving and Surfacing of Pavement Test Track, Rings Nos. 3 and 4, Washington State University, Project 918, April 28, 1967.

8. R. I. Kingham and T. C. Reseigh. "A Field Experiment of Asphalt-Treated Bases in Colorado," Second International Conference on the Structural Design of Asphalt Pavements Proceedings, University of Michigan, 1967; also Research Report 67-2, The Asphalt Institute, January, 1967.

9. Milan Krukar. Highway Test Track Research Project Y-993, Quarterly Report No. 6, Washington State University, September 30, 1968.

10. Milan Krukar. Highway Test Track Research Project Y-993, Quarterly Report No. 7, Washington State University, December 31, 1968.

11. The Asphalt Institute, Hot-Mix Sand-Asphalt Base, Misc-67-2, College Park, Maryland, March, 1967.

12. John C. Riley and J. F. Shook. "San Diego County Experimental Base Project: Design and Construction," Asphalt Institute Research Project 67-4, The Asphalt Institute, College Park, Maryland, June, 1967.

13. Pavement Instrumentation Studies for San Diego County Experimental Base Project, Report for the Asphalt Institute, Materials and Research Development (a division of Woodward, Clyde, Sherard and Associates), Oakland, California, February, 1966.

14. D. Croney and J. D. Coleman. "Pore Pressure and Suction in Soil," Proceedings, Pore Pressure and Suctions in Soils Conference, 1960, Buttersworth, 1961.

15. Ronald L. Terrel. Analysis of Ring No. 2 Washington State University Test Track, for The Asphalt Institute, University of Washington, Seattle, Washington, December, 1968.

16. Milan Krukar. Highway Test Track Research Project Y-993, Quarterly Report No. 9, Washington State University, June 30, 1969.

17. Milan Krukar. Highway Test Track Research Project Y-993, Quarterly Report No. 10, Washington State University, September 30, 1969.

18. "Pavement Evaluation Studies in Canada," Technical Publication No. 19, Canadian Goods Roads Association, Ottawa, Canada, September, 1963.

19. Report of the Director 1965-1966, Chapter on Materials, Design and Construction, British Road Research Laboratory, 1967.

20. "Three-Year Evaluation of Shell Avenue Test Road," Highway Research Record No. 147, Shell Avenue Test Road Committee, Highway Research Board, Washington, D. C., 1965.

21. R. L. Terrel and Milan Krukar. "Evaluation of Test Track Pavements," Proceedings of the Association of Asphalt Paving Technologists, Kansas City, Missouri, February, 1970.

22. "The AASHO Road Test, Report 5, Pavement Research," Special Report 61E, Highway Research Board, Washington, D. C., 1962.

23. R. Ian Kingham. "Prepared Discussion-Symposium on Non-Traffic Associated Cracking of Asphalt Pavements," Proceedings of the Association of Asphalt Paving Technologists, Minneapolis, Minnesota, February, 1966.

24. F. D. Young, I. Deme et al. "Ste-Anne Test Road: A Field Study of Transverse Crack Development in Asphalt Pavements--Construction Summary and Performance after Two Years Service," Proceedings, Canadian Technical Asphalt Association, Edmonton, Alberta, Canada, November, 1969.

25. B. P. Shields. "Discussion-Symposium on Non-Traffic Associated Cracking of Asphalt Pavements," Proceedings of the Association of Asphalt Paving Technologists, Minneapolis, Minnesota, February, 1966.

26. A. L. Vesic and L. Domaschuk. "Theoretical Analysis of Structural Behavior of Road Test Flexible Pavements," National Cooperative Highway Research Program Report 10, Highway Research Road, Washington, D. C., 1964.

27. Milan Krukar and John C. Cook. "Cracking of Asphaltic Pavements as a Function of Base Thickness and Environment under Controlled Loading Conditions at the WSU Test Track," Paper presented before the Western meeting of the Highway Research Board, Denver, Colorado on August 12-13, 1968.

28. Douglas Bynum, Jr. and R. N. Traxler. "Performance Requirements of High Quality Flexible Pavements," Research Report No. 127-1, Research Study no. 2-8-69-127, Texas Transportation Institute, Texas A & M University, College Station, Texas, August, 1969.

29. "The WASHO Road Test, Part 2 Test Data Analysis Findings," Special Report No. 22, Highway Research Board, Washington, D. C., 1955.

30. G. G. Meyerhoff. "Influence of Shoulders on Flexible Pavement Strength," Proceedings, Canadian Good Roads Association Meeting, 1960.

31. Bengt. B. Broms. "Effects of Degree of Saturation on Bearing Capacity of Flexible Pavements," Highway Research Record No. 71, Washington, D.C., 1965.

32. H. B. Seed, F. G. Mitry, C. L. Monismith, and C. K. Chan. "Prediction of Flexible Deflections from Laboratory-Repeated Load-Tests," National Cooperative Highway Research Program Report 35, Highway Research Board, Washington, D. C., 1967.

33. K. H. Gusfeldt and K. R. Dempwolff. "Stress and Strain Measurements in Experimental Road Sections Under Controlled Loading Conditions," Proceedings, Second International Conference on the Structural Design of Asphalt Pavements, University of Michigan, Ann Arbor, August, 1967.

34. A. J. G. Klomp and Th. W. Niesman. "Observed and Calculated Strains at Various Depths in Asphalt Pavements," Proceedings, Second International Conference on the Structural Design of Asphalt Pavements, University of Michigan, Ann Arbor, August, 1967.

35. Hyoungkey Hong. "Fatigue Characteristics of Flexible Pavement," Proceedings of the American Society of Civil Engineers, Journal of the Highway Division, April, 1967.

36. G. F. Sowers and A. B. Vesic. "Vertical Stresses in Subgrade Beneath Statically Loaded Flexible Pavements," Highway Research Board Bulletin 342, Washington, D. C., 1962.

37. L. W. Nijober. "Testing Flexible Pavements under Normal Traffic Loadings by Means of Measuring Some Physical Quantities Related to Design Theories," Proceedings, Second International Conference on the Structural Design of Asphalt Pavements, University of Michigan, Ann Arbor, August, 1967.

38. B. C. Hartronft. "Hot-Mixed Sand Asphalt Bases in Oklahoma," Proceedings, Second International Conference on the Structural Design of Asphalt Pavements, University of Michigan, Ann Arbor, August, 1967.

39. L. F. Loder, "Aspects of the Design and Construction of Rural Roads," Australian Road Research Board, Bulletin No. 6, Australia, March, 1970.

40. Report on AASHO Road Test, Canadian Good Roads Association, Ottawa, Canada, 1962.

41. J. F. Shook and F. N. Finn. "Thickness Design Relationships for Asphalt Pavements," Proceedings, First International Conference on the Structural Design of Asphalt Pavements, University of Michigan, Ann Arbor, August, 1962.

42. Bonner S. Coffman, George Ilves, and William Edwards. "Theoretical Asphaltic Concrete Equivalencies," Highway Research Record 239, Highway Research Board, Washington, D. C., 1968.

APPENDIX A

Daily Revolutions and Wheel Load Applications--Ring 4

Month	Day	Applications			
		Revolutions		Wheel Loads	
		Daily	Accumulated	Daily	Accumulated
November 1968	5	130		390	390
	6	996	1,126	2,988	3,378
	7	1,901	3,027	5,703	9,071
	8	4,371	7,398	13,133	22,194
	9	1,868	9,266	5,604	27,794
	10	2,961	12,227	8,883	36,681
	15	656	12,883	1,968	38,649
	16	8,210	21,093	24,630	63,279
	17	4,788	26,881	14,364	80,643
	18	3,343	30,224	10,029	90,672
	19	4,096	34,320	12,288	102,960
	20	409	34,729	1,227	104,187
	22	1,467	36,196	4,401	108,588
	23	897	37,093	2,691	111,279
	24	2,447	39,540	7,341	118,620
	25	1,413	41,953	4,239	125,859
	26	1,665	43,618	4,995	130,854
	27	408	44,026	1,224	132,078
	30	2,328	46,354	6,984	139,062
December 1968	1	943	47,297	2,829	141,891
	3	493	47,790	1,479	143,370
April 1969	2	22	47,812	66	143,436
	4	408	48,220	1,224	144,660
	28	535	48,755	1,605	146,265
	29	709	49,464	2,127	148,392
	30	648	50,112	1,944	150,336
May 1969	1	894	51,006	2,682	153,018
	9	269	51,275	807	153,825
	10	115	51,390	345	154,170
	19	837	52,227	2,511	156,681
	20	127	52,340	381	157,020
	22	405	52,745	1,215	158,235
	26	742	53,487	2,226	160,461
	27	598	54,085	1,794	162,255
	28	845	54,930	2,535	164,790

Month	Day	Applications			
		Revolutions		Wheel Loads	
		Daily	Accumulated	Daily	Accumulated
June 1969	2	674	55,604	2,022	166,812
	4	747	56,351	2,241	169,053
	6	705	57,056	2,115	171,168
	12	650	57,706	1,950	173,118
	13	589	58,295	1,767	174,885
	18	720	59,015	2,160	177,045
	19	152	59,167	456	177,501
	21	321	59,488	963	178,464
	23	757	60,245	2,271	180,735
	24	1,182	61,437	3,556	184,311
	25	1,345	62,882	4,035	188,646
	26	1,308	64,190	3,924	192,570
	27	769	64,949	2,307	194,877
	30	1,293	66,252	3,879	198,756
July 1969	1	890	67,142	2,670	201,426
	2	455	67,597	1,365	202,791
	11	812	68,409	2,436	205,227
	14	182	68,591	546	205,773
	15	486	69,077	1,458	207,231
	16	300	69,377	900	208,131
	17	978	70,335	2,934	211,065
	22	876	71,231	2,628	213,693
	23	836	72,067	2,508	216,201
	24	324	72,391	972	217,173
	25	722	73,113	2,166	219,339
	28	478	73,591	1,434	220,773
	29	852	74,443	2,556	223,329
	30	339	74,782	1,017	224,346
August 1969	1	917	75,699	2,751	227,097
	4	613	76,312	1,839	228,936
	5	1,348	77,660	4,044	232,980
	6	1,368	79,028	4,104	237,084
	7	856	79,884	2,568	239,652
	8	1,469	81,353	4,407	244,059
	9	1,023	82,376	3,069	247,128

Note: Missing dates indicate the track was not running.

APPENDIX B

Modified CGRA Benkelman Beam Rebound Procedure

Scope

This method of test covers a procedure for the determination of the static Benkelman beam rebound at a point on a flexible pavement under a standardized axle load, tire size, tire spacing and tire pressure for the Washington State University Test Track.

Equipment

The equipment shall include the following:

1. A Benkelman beam having the following dimensions:

	ft.	in.
a. Length of probe arm from pivot to probe point	8	0
b. Length of measurement arm from pivot to dial	4	0
c. Distance from pivot to front legs	0	10
d. Distance from pivot to rear legs	5	5½

2. A 5-ton truck is recommended as the reaction. The vehicle shall have an 18,000 pound rear axle load equally distributed on two wheels, each equipped with dual tires. WSU loading is fixed at a minimum of 10,800 pounds on each set of duals. This is directly equivalent to a 21,600 pound single rear axle load. The tires shall be 10.00 x 20, 12-ply, inflated to a pressure of 80 psi. WSU tire size is 11.00 x 22, 12-ply,tire pressure 80 psi. The use of tires with tubes and rig treads is recommended.

3. Tire pressure measuring gauge.

4. Thermometer (0-120°F.) with 1°divisions.

5. A mandrel for making a 1.75-inch-deep hole in the pavement for temperature measurement. The diameter of the hole at the surface shall be ½ inch. This equipment not used at WSU. Thermocouples are installed at time of construction as part of instrumentation.

Procedure

1. The point on the pavement to be tested is selected and marked. For highways, the points are located at specified distances from the edge of the pavement according to the width of the lane, as follows:

Land Width (feet)	Distance from Pavement Edge (feet)
9 or less	1.5
10	2.0
11	2.5
12 or more	3.0

2. The dual wheels of the truck are centered above the selected point. WSU readings are taken between the duals. The duals move laterally across the track; locations can be chosen or random.

3. The probe of the Benkelman beam is inserted between the duals and placed on the selected point.

4. The locking pin is removed from the beam and the legs adjusted so that the plunger of the beam is in contact with the stem of the dial gauge.

5. The dial gauge is set at approximately 0.4 inches. The initial reading is recorded when the rate of deformation of the pavement is equal to or less than 0.001 inches per minute (i.e., measurement dial rate is less than 0.005 inches per minute). The initial reading should be taken 3 minutes after positioning the beam if the rate of movement criteria is not satisfied.

6. The truck is slowly driven forward a distance of 8 feet 10 inches and stopped. WSU wheels are pulled to the desired distance through use of a pick-up truck.

7. An intermediate reading is recorded when the rate of recovery of the pavement is equal to or less than 0.001 inches per minute. The intermediate reading should be taken 3 minutes after positioning the wheels if the rate of movement criteria is not satisfied.

8. WSU wheels are pulled forward a further 30 feet.

9. The final reading is recorded when the rate of recovery of the pavement is equal to or less than 0.001 inches per minute. The final reading should be taken 3 minutes after positioning the wheels if the rate of movement criteria is not satisfied.

10. Pavement temperature is recorded at least once every hour, inserting the thermometer in the standard hole filled with water. At the same time the air temperature is recorded. WSU instrumentation eliminates this particular procedure.

11. The tire pressure is checked at 2- to 3-hour intervals during the day and adjusted to the standard if necessary.

Calculations

1. Subtract the final dial reading from the initial dial reading. Subtract the intermediate dial reading from the initial dial reading.

2. If the differential reading obtained compare within 0.001 inches the actual pavement rebound is the final differential reading for a direct-reading Benkelman beam.

3. If the differential readings obtained do not compare to 0.001 inches, the final differential dial reading represents the apparent pavement rebound.

4. Apparent rebounds for direct reading Benkelman beam are corrected by means of the following formula:

$$X_T = X_A + 0.9863Y$$

where X_T = true pavement rebound

X_A = apparent pavement rebound

Y = vertical movement of the front legs (i.e., the difference between the final and intermediate dial readings).